2015

Characterisation of SerpinB2 as a stress response modulator

Jodi Anne Lee
University of Wollongong

Characterisation of SerpinB2 as a stress response modulator

A thesis submitted in fulfilment of the requirements for the award of the degree

Doctor of Philosophy
from
University of Wollongong

By
Jodi Anne Lee
Bachelor of Science (Honours 1)

School of Biological Sciences
University of Wollongong
2015

Declaration

This thesis is submitted in accordance with the regulations of the University of Wollongong in fulfilment of the higher degree in research of Doctorate of Philosophy. It does not contain any material previously published by another person except where due reference is made in the text. The experimental work described in this thesis is original and has not been submitted for a degree at any other University.

Jodi Anne Lee

List of Publications

Lee JA, Yerbury JJ, Farrawell N, Shearer RF, Constantinescu P, Hatters DM, Schroder WA, Suhrbier A, Wilson MR, Saunders DN, Ranson, M. SerpinB2 (PAI-2) Modulates Proteostasis via Binding Misfolded Proteins and Promotion of Cytoprotective Inclusion Formation. PLoS One **2015;** 10(6). Epub 2015 June 18. PMC4470917.

Yerbury JJ, Gower D, Vanags L, Roberts K, **Lee JA**, Ecroyd H. The small heat shock proteins αB-crystallin and Hsp27 suppress SOD1 aggregation *in vitro*. Cell Stress Chaperones **2013** Mar; 18(2):251-7. Epub 2012 Sep 21. PMID: 22993064 PMCID: PMC3581626

Vine KL, Chandran VI, Locke JM, Matesic L, **Lee J**, Skropeta D, Bremner JB, Ranson M. Targeting urokinase and the transferrin receptor with novel, anti-mitotic N-alkylisatin cytotoxin conjugates causes selective cancer cell death and reduces tumor growth. Curr Cancer Drug Targets. **2012** Jan 1;12(1):64-73. PubMed PMID: 22111834.

Lee JA, Cochran BJ, Lobov S, Ranson M. Forty years later and the role of plasminogen activator inhibitor type 2/SERPINB2 is still an enigma. Semin Thromb Hemost. **2011** Jun;37(4):395-407. Epub 2011 Jul 30. Review. PubMed PMID: 21805446.

De Souza M, Matthews H, **Lee JA**, Ranson M, Kelso MJ. Small molecule antagonists of the urokinase (uPA): urokinase receptor (uPAR) interaction with high reported potencies show only weak effects in cell-based competition assays employing the native uPAR ligand. Bioorg Med Chem. **2011** Apr 15;19(8):2549-56. Epub 2011 Mar 12. PubMed PMID: 21454081.

Lee JA, Croucher DR, Ranson M. Differential endocytosis of tissue plasminogen activator by serpins SerpinE1 and SerpinB2 on human peripheral blood monocytes. Thromb Haemost. **2010** Dec;104(6):1133-42. Epub 2010 Sep 13. PubMed PMID: 20838737.

Cochran BJ, Gunawardhana LP, Vine KL, **Lee JA**, Lobov S, Ranson M. The CD-loop of SerpinB2 (SERPINB2) is redundant in the targeting, inhibition and clearance of cell surface uPA activity. BMC Biotechnol. **2009** May 14;9:43. PubMed PMID:19442270; PubMed Central PMCID: PMC2693429.

List of Presentations

Poster

Vine KL, Chandran VI, Locke JM, Matesic L, **Lee J**, Skropeta D, Bremner JB, and Ranson M. Targeting Urokinase and the Transferrin Receptor with Novel, Anti-Mitotic N-Alkylisatin Cytotoxin Conjugates Causes Selective Cancer Cell Death and Reduces Tumour Growth. 24th Lorne Cancer Conference, Lorne Victoria, Feb. 2012

Lee JA, Croucher DR and Ranson M.
Differential endocytosis of Tissue Plasminogen Activator by Serpins PAI-1 and PAI-2 on human peripheral blood monocytes. Australian Society for Medical Research (NSW) Scientific Meeting. The Powerhouse Museum, Ultimo. (2010)

Vine KL, Locke JM, **Lee JA**, Bremner, JB, and Ranson M. Synthesis and *in vitro* anticancer activity of a targeted plasminogen activator inhibitor type II (PAI-2) cytotoxin conjugate. 7th International Symposium On Targeted Anticancer Therapies, Amsterdam, The Netherlands, March 2009

Lee JA, Croucher DR and Ranson M
The Plasminogen Activation System in Monocytic Cell Differentiation and Proliferation: potential target for plasminogen activation inhibitor type 2 based therapeutics. XIth International Workshop on Molecular & Cellular Biology of Plasminogen Activation, Saltsjöbaden, Sweden. (2007)

Oral

Lee JA, Saunders DN, Schroder W, Wilson M, Yerbury JJ, Marie Ranson. SerpinB2 (PAI-2) modulates protective cellular responses to proteotoxic stress and processing of intracellular protein aggregates. Plasminogen Activation System in Pathology Workshop, Illawarra Medical Research Institute, University of Wollongong NSW Australia. (2012)

Lee JA, Croucher DR and Ranson M
Cell surface interactions of Tissue Plasminogen Activator with peripheral blood monocytes. XIIth International Workshop on Molecular & Cellular Biology of Plasminogen Activation, Cold Spring Habor Laboratory, Cold Spring Harbor, New York. (2009)

Acknowledgements

I would like to sincerely thank Professor Marie Ranson, Dr Justin Yerbury and Dr David Croucher (Chapters 2 and 3) for the formal supervision of the work within this thesis. I will be forever grateful for the contributions they have made to the projects undertaken and for all that they have taught me. I would like to acknowledge and thank Dr Darren Saunders, Professor Mark Wilson, Dr Andrew Aquilina and Associate Professor Heath Ecroyd for the many lengthy discussions on proteastasis networks and experimental advice given, without which I would not have gotten so far. I would also like to thank Dr Wayne Schroder for supporting the working hypothesis for a role of SerpinB2 as a molecular chaperone and providing the mouse embryonic fibroblasts used within the latter part of this thesis, in which to test it. I will be forever grateful to Professor Robert Medcalf for believing me when I approached him in New York to discuss this work, in its infancy. I would like to thank all fellow PhD students whom I have worked alongside for the contribution they made to my health and wellbeing. I wish you all the best science can offer.

Abstract

SerpinB2 [plasminogen activator inhibitor type-2 (PAI-2)] was first described as a placental protein, which regulated plasminogen activation via the inhibition of the urokinase (uPA) or tissue-type (tPA) plasminogen activators during pregnancy. Further work has confirmed that SerpinB2 is an efficient inhibitor of cell surface, receptor bound uPA and clearance of the serpin:protease complex occurs via members of the low density lipoprotein receptor (LDLR) family, specifically very low density lipoprotein receptor (VLDLR) and low density lipoprotein-related protein receptor (LRP). This property has allowed for the development of SerpinB2 drug conjugates for the selective targeting of uPA positive carcinoma cells. However, potential utility of SerpinB2 in haematological disorders, such as acute myeloid leukaemia (AML), as well as its role as a physiological inhibitor of tPA is not well characterised. To date biochemical analysis has shown that SerpinB2 is able to inhibit the two-chain (active) form of tPA. However, whether this inhibitory function occurs within the cellular context was unknown.

This thesis investigates the potential use of exogenous SerpinB2 as a delivery vehicle for the specific targeting of lymphoma or leukaemia, via cell surface uPA using the relatively low versus high uPA expressing, monocytic cell lines U-937 and THP-1, respectively, as disease models. We show here that uPA:SerpinB2 is internalised via the Low Density Lipoprotein Receptor (LDLR) family members, specifically Low Density Lipoprotein-Related Protein (LRP) and Very Low Density

Lipoprotein Receptor (VLDLR) in a uPA dependent manner and these findings are consistent with those previously reported for epithelial cancer cell lines.

In order to clarify the role of SerpinB2 in the inhibition and clearance of tPA from the cell surface of monocytes and macrophages, we next assessed the formation and endocytosis of tPA:SerpinB2 complexes at the cell surface of freshly isolated peripheral blood monocytes (PBM), as a non-transformed tPA-dependent/negligible uPA-expressing cellular model representing normal myeloid lineages. We demonstrated that while both SerpinE1 (PAI type-1) and SerpinB2 inhibit surface-bound tPA and are internalised predominately via LDLR family members, SerpinE1 enhanced the endocytosis of tPA, whereas SerpinB2 did not. Surface plasmon resonance biochemical analyses revealed differential binding affinities between VLDLR and tPA or tPA:SerpinE1 complexes in addition to those previously described for LRP. Moreover, tPA:SerpinB2 bound to both endocytosis receptors with similar kinetics to tPA. These differential biochemical interactions between tPA and the tPA:serpin complexes may underlie the observed differences in endocytosis mechanisms on the PBMs. This suggests that while SerpinE1 and SerpinB2 function similarly in the control of cellular plasmin generation by tPA, they may have disparate effects on the alternative functions of tPA via modulation of its engagement with endocytosis receptors in a physiological setting. Importantly, this work suggests that in the treatment of haematological disorders non-specific delivery of therapeutics via tPA using SerpinB2 would be negligible, thus contributing to the proof of concept for the use of SerpinB2 as a cancer targeting

molecule. However, assessment within an animal model of haematological disease is required to confirm this.

SerpinB2 has been reported to have a multitude of other activities including regulation of monocyte and keratinocyte proliferation and differentiation, inhibition of apoptosis and necrosis, modulation of immune responses and to display cytoprotective properties in neurons. Some of these activities for SerpinB2 are strongly associated with its classical serpin inhibitory function within the pericellular space as, apart from pregnancy, it can be detected at very high concentrations in body fluids associated with inflammation, infection and other pathophysiological conditions. In many of these circumstances however, SerpinB2 protein is retained primarily in intracellular pools. SerpinB2 has been reported to interact with a number of intracellular proteins including components of the autophagy-lysosomal and ubiquitin-proteasome systems. These appear to be independent of SerpinB2 protease inhibitory interactions, suggesting a novel non-serpin function for SerpinB2. It was thus postulated that SerpinB2 is one of the many intracellular proteins that maintain homeostasis during cellular damage or stress.

The latter chapters of this thesis investigated this putative function for intracellular SerpinB2 as a chaperone-like protein using a series of cellular and biochemical assays. Biochemical experiments revealed that SerpinB2 binds preferentially to misfolded proteins and is an efficient inhibitor of amorphous protein aggregation in some but not all models tested. SerpinB2 was also able to completely inhibit fibril

formation of amyloid-β 1-40 peptide ($A\beta_{1-40}$) and significantly delay fibril formation by $A\beta_{1-42}$. Incubation of SerpinB2 with Aβ was found to obstruct protease:SerpinB2 complex formation, suggesting that Aβ may bind within β-sheet-A, breach region, of the serpin. We further explored the potential for SerpinB2 as a modulator of cellular proteotoxic stress using a well-established huntingtin protein (Htt) aggregation model, comprising an exon 1 fragment fused to either 25 polyglutamine (Htt_{ex1}25Q-mCherry) or 46 (Htt_{ex1}46Q-mCherry) polyglutamine sequences. Wild-type or SerpinB2$^{-/-}$ mouse embryonic fibroblasts (MEF) were transiently transfected with expression vectors containing either Htt_{ex1}25Q-mCherry or Htt_{ex1}46Q-mCherry, and cellular processing of aberrant Htt-fusion protein was examined. These experiments revealed a clear difference in phenotype, whereby inclusion body formation was evident in the wild-type MEF controls and minimal in the absence of SerpinB2, where small foci predominated. The impaired inclusion body formation was found to correspond with a significant loss in cell viability for the SerpinB2$^{-/-}$ MEFs. Importantly, recovery of the wild-type MEF phenotype and cell viability was achieved in a human SerpinB2 knock-in MEF line. Given previous literature that suggests a possible role for SerpinB2 within both the autophagy-lysosomal and proteasome degradation pathways, we compared activity of each in the wild-type and SerpinB2$^{-/-}$ cell lines. Interestingly, both systems were found to be impaired in the absence of SerpinB2. It was thus concluded that intracellular SerpinB2 plays an important role in proteostasis as its loss leads to a proteotoxic phenotype associated with an inability to compartmentalize aggregating proteins. This represents a major contribution

towards understanding the otherwise elusive cytoprotective role of intracellular SerpinB2 and it is likely that further research will uncover therapeutic targets for neurodegenerative disorders, as well as in cancer.

Table of Contents

List of Figures

List of Tables

List of Abbreviations

3-MA	3-methyladenine
AIIt	Annexin 2 Heterotetramer
Aβ	Amyloid-β
AAT	Alpha(1)-antitrypsin
ACT	Alpha(1)-antichymotrypsin
AD	Alzheimer's disease
AID	Activity-regulated Inhibitor of Death
ALS	Amyloid lateral sclerosis
AML	Acute myeloid leukemia
AP-1	Activator protein-1
AP-2	Activator protein-2
apoE	Apolipoprotein E
APS	Ammonium Persulphate
ARE	AU-rich motif
ASC-1	Activating signal cointegrator-1
Atg	Autophage specific
BCL-2	B-cell lymphoma 2
BBB	Blood brain barrier
Bis-ANS	4,4′-Dianilino-1,1′-binaphthyl-5,5′-disulfonic acid dipotassium salt
BiFC	Biomolecular fluorescence complementation
BSA	Bovine Serum Albumin
C/EBP-β	CCAAT enhancer binding element
CPK	Creatine phosphokinase
CS	Citrate Synthase
CRE	cAMP response element
DNA	Deoxyribonucleic Acid
DTT	Dithiothreitol
DUBs	Deubiquitinating enzymes
ECL	Enhanced chemiluminescence
ECM	Extracellular Matrix
EDTA	Ethylene Diamine Tetraacetic Acid
ELISA	Enzyme Linked Immunosorbent Assay
FCS	Fetal calf serum
FITC	Flourescein Isothiocyanate
g	Gravity
G-CSF	Granulocyte colony stimulating factor
GFD	Growth Factor Domain
GFP	Green fluorescent protein
GM	Geometric Mean

GPI	Glycosylphosphatidylinositol
GST	Glutathione S-transferase
HD	Huntington Disease
HDC	Heat denatured casein
HEPES	4-(2-hydroxyethyl)-1-piperazineethanesulfonic acid
HFIP	Hexafluoroisopropanol
HRP	Horseradish Peroxidase
HSP	Heatshock protein
Htt	Huntingtin protein
HUVEC	Human umbilical vein endothelia cells
IAA	Iodoacetic acid
IB	Inclusion body
ICE	Interleukin-1β-converting enzyme
IgG	Immunoglobulin-G
IL	Interleukin
IP	Intraperitoneal
IPOD	Insoluble protein deposits
IPTG	Isopropyl β-D-1-thiogalactopyranoside
ISG15	Interferon-stimulated gene-15
JUNQ	Juxtanuclear quality control
kDa	Kilo Daltons
LDLR	Low Density Lipoprotein Receptor
LPS	Lipopolysaccharide
LRP	Low Density Lipoprotein Receptor-Related Protein
Mab	Monoclonal Antibody
MAZ	Myc-associated zinc finger protein
MBP	Mannose binding protein
M-CSF	Macrophage colony stimulating factor
MDR	Multiple drug resistence
MEF	Mouse embryonic fibroblast
MENT	Myeloid and erythroid nuclear termination stage-specific protein
MFI	Mean Flourescense Intensity
MIC	Matched Isotype control
MMP	Matrix Metalloproteinase
MNEI	Monocyte neutrophil elastase inhibitor
mRNA	messenger ribonucleic acid
MTS	[3-(4,5-dimethylthiazol-2-yl)-5-(3-carboxymethoxyphenyl)-2-(4-sulfophenyl)-2H-tetrazolium, inner salt]
NF-κβ	Nuclear factor-kappabeta
NK	Natural Killer

NLR3	NOD-like receptor-3
NMDA	N-methyl-D-aspartate
NO	Nitric Oxide
OPD	o-phenylenediamin dihydrochloride
OSB	Oxidative stress buffer
p36	Annexin II
PAGE	Polyacryamide Gel Electrophoresis
PA	Plasminogen activator
PAb	Polyclonal Antibody
PAI	Plasminogen activator inhibitor
PAI-1	Plasminogent activator inhibitor type-1
PAI-2	Plasminogent activator inhibitor type-2
PAR	Protease activation receptor
PFA	Paraformaldehyde
PDB	Protein data bank
PBM	Peripheral blood monocytes
PBS	Phosphate buffered saline
PG	Prostaglandins
PI	Propidium Iodide
PMA	Phorbol-myristate acetate
PMSF	alpha-toluenesulfonyl fluoride
PSMB1	Proteasome subunit beta type-1
PtdIns3K	Phosphatidylinositol 3-kinase
PVDF	polyvinylidene difluoride
RAP	Receptor Associated Protein
Rb	Retinoblastoma protein
RCL	Reactive Centre Loop
ROI	Reactive oxygen intermediate
RNA	Ribonucleic acid
Rt-PCR	Reverse-transcription polymerase chain reaction
(sc)-tPA	Single Chain tPA
(sc)-uPA	Single Chain uPA
suPAR	Soluble uPAR
SCCA	Squamous cell carcinoma antigen
SD	Standard Deviation
SDS	Sodium Dodecyl Sulfate
SEM	Standard error mean
SEM	Scanning electron microscopy
Serpin	Serine protease inhibitor
sHSP	Small heatshock protein
SOD	Superoxide dismutase
SPD	Serine Protease Domain
SPR	Surface Plasmon Resonance

(tc)-tPA	Two Chain tPA
(tc)-uPA	Two Chain uPA
TB	Terrific Broth
TBS	Tris-buffered saline
TBST	Tris-buffered saline 20% Tween
TEMED	NNN'N'-tetramethylethylenediamine
TFA	Trifluoroacetic acid
ThioT	Thioflavin-T
TLR	Toll-like receptor
TNF-α	Tumour Necrosis Factor-α
TPA	12-*O*-tetradecanoylphorbol-13-acetate
tPA	Tissue-type plasminogen activator
uPA	Urokinase-type plasminogen activator
uPAR	Urokinase-type plasminogen activator receptor
UPS	Ubiquitin-Proteasome System
VLDLR	Very Low Density Lipoprotein Receptor
WT	Wild-type

1. Introduction

1.1. Overview

SerpinB2 is a member of the Serine Protease Inhibitor super family and was originally isolated from placental tissue and described as an inhibitor of the serine proteinase urokinase-type plasminogen activator (uPA) (Kawano et al. 1968; Kawano et al. 1970). Subsequent investigations revealed that SerpinB2 was also able to inhibit the tissue-type plasminogen activator (tPA) (Astedt et al. 1985; Astedt et al. 1985; Thorsen et al. 1988). On this basis SerpinB2 was named plasminogen activator inhibitor type-2 (PAI-2) distinguishing it from PAI-type-1 (PAI-1) (referred to herein as SerpinE1), also a newly discovered inhibitor of plasminogen activators (PAs) (Loskutoff and Edgington 1977). Initial characterisation of SerpinB2 focussed on its role as an extracellular mediator of plasmin generation with frequent comparison to SerpinE1. With the finding that SerpinE1 was the faster acting inhibitor (Kruithof et al. 1995) and was present in normal and pregnancy plasma, whereas SerpinB2 was only detectable during late pregnancy (Kruithof et al. 1984), SerpinE1 was originally considered the primary physiological mediator of thrombosis and fibrinolysis. Increasing evidence supports a role for SerpinB2 as a physiological inhibitor of PAs however, consistently placing the serpin within the extracellular milieu of diseased tissue exhibiting localised inflammation and homeostatic imbalance (Kruithof et al. 1995; Croucher et al. 2008; Schroder et al. 2010; Siefert et al. 2014).

The highest concentration of SerpinB2 protein is found intracellularly, *in vitro,* within cells of the monocytic lineage (Kruithof et al. 1986; Genton et al. 1987).

However, an intracellular serine protease target for this serpin is yet to be defined. Furthermore, intracellular SerpinB2 seems to be promiscuous with many non-protease binding partners described over the years, since its discovery (Schroder et al. 2010). This combined with the finding that intracellular SerpinB2 up-regulation in response to inflammation, infection and other pathophysiological conditions, suggest a non-classical role for this serpin, independent of its protease inhibitory capabilities.

This review will focus on 1) the known roles of SerpinB2 as an extracellular protease inhibitor, specifically literature relating to inhibition of uPA and tPA; and 2) the putative roles of intracellular SerpinB2 which suggest it's possible placement as a pivotal protein functioning within proteostasis pathways.

1.2. Serine Protease Inhibitor Super Family

The Serine Protease Inhibitor (serpin) Super Family consists of a large group of multi-functional proteins with highly conserved structure and variable amino acid sequence homology, with exception of highly conserved residues within the breach and shutter regions (Fig.1.1.A) (Gettins 2002). Typically, serpins range between 330-500 amino acids, consist of three β sheets (A,B and C), 8-9 α helices (hA-hI) and a reactive centre loop (RCL) which contains the protease recognition site (Fig. 1.1.A). Formation of a serpin-protease complex involves a suicide substrate-like inhibitory mechanism, whereby the initial interaction results in an intermediate conformational change of the inhibitor from a stressed to relaxed state (Fig.1.1.B),

which allows the irreversible insertion of the RCL into β-sheet A of the serpin – initiating in the breach region - in a 1:1 covalently linked, stable conformation (Fig. 1.1.C) (Huntington et al. 2000). The rate and efficiency of complex formation between a serpin and its target protease is dependent on the complete insertion of the RCL into β-sheet A and partial inhibition or blocking of this step results in the substrate-like cleavage of the RCL, followed by serpin release (Fig.1.1.D) (Silverman et al. 2001). Whilst the suicide inhibitory mechanism of serpins is most typical, some serpins inhibit their target protease via the substrate mechanism, never forming an SDS-stable serpin:protease complex.

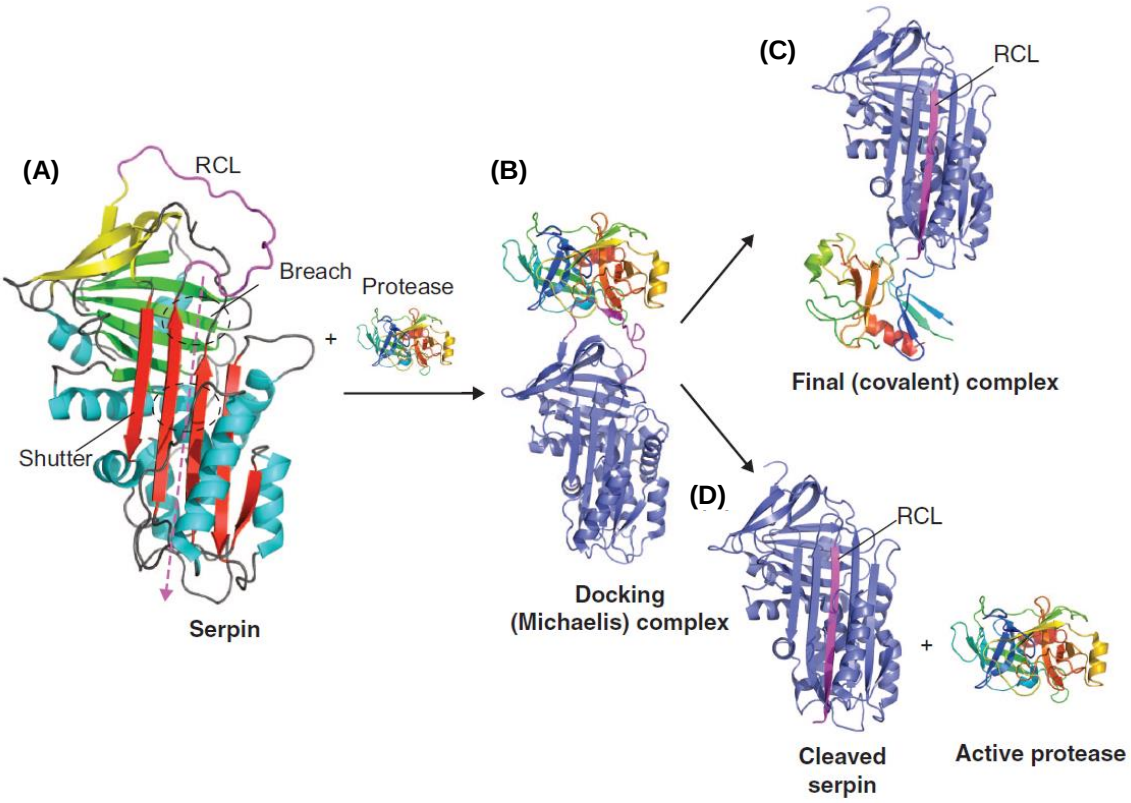

Figure 1.1: Highly conserved tertiary structure of Serpin Super Family. **(A)** Native serpin structure, represented by serpinA1 (Protein Data Bank (PDB) # 1QLP (Elliott et al. 1996)) showing A-β-sheet (red), B-β-sheet (green), C-β-sheet (yellow) and helices A-I (blue). Positioning of the reactive center loop (RCL) (magenta) in stressed (solid line) and relaxed (dashed line) confirmation. The breach and shutter regions are labelled. **(B)** Initial serpin:protease interaction via the RCL results in the intermediate Michaelis complex formation as represented by SerpinA1 and inactive trypsin (multicolours) (PDB # 1OPH (Ye et al. 2001)), which leads to either **(C)** the 1:1 covalently linked, stable serpin:protease complex (PDB # 1EZX (Huntington et al. 2000)) or **(D)** cleaved serpin in the relaxed and inactive confirmation (RCL insertion) (PDB code 7API (Loebermann et al. 1984)) and active protease. In this case the serpin has acted as a substrate for the protease. Adapted from Law et al. (2006)).

Serpin distribution is diverse with over 1000 members found across higher order plants, mammals, invertebrates, prokaryotes, archea, fungi and some viruses. Originally thought to only target serine proteases, some serpins have now been

shown to inhibit cysteine protease targets (Hook et al. 1993; Komiyama et al. 1994; Schick et al. 1998; Schick et al. 1998; Higgins et al. 2010; Kantyka et al. 2011), furthermore, non-inhibitory serpins have also been described, which function in hormone transport (Hammond et al. 1987; Pemberton et al. 1988) or stabilisation of structural support molecules (Tasab et al. 2000; Sauk et al. 2005). Given the diversity of serpins, they have been arranged into sub-families (Clades) based on their evolutionary relationships (Irving et al. 2000).

As the focus of this thesis is specifically SerpinB2, a member of the serpin clade B (see below), a full discussion of all other clades is beyond the scope of this chapter, however for comprehensive reviews see Gettins (2002), Irving et al. (2000), Silverman et al. (2010) and Whisstock et al. (2010).

1.3. Serpin Clade B

The ovalbumin-serpin sub family (serpin clade B) consists of 14 members, 13 of which are found within the human genome (Tab. 1.1) and classified as such, due to their similarity to ovalbumin (SerpinB14). All members of this clade feature: (i) a high degree of amino acid homology (~ 50%), (ii) a lack of N- and C- terminal extensions found in many other serpins, (iii) a similar gene organization, three of the 13 human serpins within this clade map to position 6p25 (B1, B6 and B9), whilst all others map to position 18q21.3, and (iv) the presence in several members of an inter-helical domain connecting helices C and D, encoded by an exon 3 (Remold-O'Donnell 1993; Scott et al. 1999).

Table 1.1: Members of the Serine Protease Inhibitor (serpin) Clade B; known function and expression profiles.

Clade-B Member	Alternative Names	Target Protease	Location/Cell specificity/functions (if known)	Reference
SerpinB1	Monocyte Neutrophil Elastase Inhibitor (MNEI)	Neutrophil Elastase Human granzyme H Proteinase3 Cathepsin G	Intracellular, immune Neutrophils, monocytes, macrophages, NK	(Remold-O'Donnell et al. 1992; Wang et al. 2013)
SerpinB2	Plasminogen Activator Inhibitor Type-2	Extracellular; Urokinase and Tissue Type Plasminogen Activators Intracellular; unknown	Extracellular; inhibition of plasminogen activators; immune modulator Intracellular inflammation response protein, immune modulator. (Refer Table 1.2 for list of cells which have been shown to express SerpinB2)	(Kruithof et al. 1984; Kruithof et al. 1995; Schroder et al. 2010) Reviewed in; (Croucher et al. 2008; Schroder et al. 2010; Medcalf 2011)
SerpinB3	Squamous cell carcinoma antigen-1 (SCCA-1)	Cathepsin K, L, & S papain and JNK1.	Intracellular; Squamous epithelial cells	(Takeda et al. 1995; Schick et al. 1998; Schick et al. 1998; Zheng et al. 2009)
SerpinB4	Squamous cell carcinoma antigen-2 (SCCA-2)	Cathepsin G, Mast Cell Chymase	Intracellular; Squamous epithelial cells	(Schick et al. 1997)
SerpinB5	Maspin	Non-inhibitory	Intracellular; tumour suppressor Hypothesized functions; Extracellular matrix remodeling via Rac and Cdc42 signaling. Pro-apoptotic mediator. Potential	(Odero-Marah et al. 2003; Liu et al. 2004; Bailey et al. 2005; Latha et al. 2005; Romani et al. 2006;

Clade-B Member	Alternative Names	Target Protease	Location/Cell specificity/functions (if known)	Reference
			involvement in cellular stress responses.	Shi et al. 2007; Teoh et al. 2010)
SerpinB6	Proteinase Inhibitor-6	Cathepsin G, kallikrein 2 and 8, neuropsin, Granzyme B, thrombin, trypsin, plasmin, urokinase, chymotrypsin.	Intracellular; nucleocytoplasm of neutrophils, cytotoxic T cells, keratinocytes, skeletal muscle, placenta, heart, lung, liver, kidney pancreas, inner ear hair cells, normal mast cells and by mast cells in mastocytoma lesions.	(Scott et al. 1999; Scarff et al. 2004; Zhang et al. 2006; Sirmaci et al. 2010)
SerpinB7	Megsin	Plasmin, metalloproteinase 2 and 9	Intracellular; Mesangial cells within the glomerulus (kidney). Involved in mesangial - cell proliferation and extracellular matrix expansion. Secretion of collagen type- IV	(Miyata et al. 1998; Miyata et al. 2002; Ohtomo et al. 2008; Xia et al. 2011)
SerpinB8	Proteinase Inhibitor-8	Furin. Trypsin-like serine proteinases.	Extracellular; released from platelets Intracellular; monocytes, platelets, squamous epithelial and neurocrine cells.	(Dahlen et al. 1998; Strik et al. 2002; Leblond et al. 2006)
SerpinB9	Proteinase Inhibitor-9	Cytotoxic lymphocyte protease granzyme B, subtilisin A, caspase-1, 4, 8 & 10	Intracellular; nucleocytoplasm of cytotoxic lymphocytes. Protects against granzyme B-mediated apoptosis.	(Sun et al. 1996; Bird et al. 1998; Bird et al. 2001; Hirst et al. 2003)
SerpinB10	Proteinase Inhibitor-10, Bomapin, MENT (Chicken ortholog)	Unknown. Trypsin-like serine proteinases.	Intracellular; monocytic cells. Chromatin remodeling protein (MENT).	(Riewald et al. 1998; Chuang and Schleef 1999; Springhetti et al. 2003)

Clade-B Member	Alternative Names	Target Protease	Location/Cell specificity/functions (if known)	Reference
SerpinB11	Epipin	Non-inhibitory (humans)	Unknown. Avian SerpinB11 expression is restricted to oviduct epithelial cells. Hoof wall structure in Connemara Ponies.	(Askew et al. 2007; Lim et al. 2011; Finno et al. 2015)
SerpinB12	Yukopin	Unknown. Trypsin-like serine proteinases	Unknown. Wide tissue distribution; brain, bone marrow, lymph node, heart, lung, liver, pancreas, testis, ovary and intestines	(Askew et al. 2001)
SerpinB13	Proteinase Inhibitor-13, Hurpin, Headpin	Lysosomal cathepsin L	Intracellular; Keratinocytes	(Jayakumar et al. 2003; Welss et al. 2003)
SerpinB14	Ovalbumin	Non-inhibitory	Storage/structural protein found in chicken eggs.	(Hunt and Dayhoff 1980)

Despite their sequence and structural similarities the independent Serpin clade B members appear to be quite diverse in cell distribution and specific protease targets and/or function (Table 1.1) whilst sharing common placement as either enhancers or suppressors of inflammation and tumorigenesis. Serpins within this clade can be either non-inhibitory, ie SerpinB5, B11 and B14 or have clearly defined protease targets (Table 1.1). Furthermore, some members are restricted to the cytoplasm, others localise within the nucleus, ie SerpinB2 and B10, whilst SerpinB8 (Leblond et al. 2006) and SerpinB2 are found within both the intracellular and extracellular environment.

1.4. SerpinB2

The *SERPINB2* gene is located between 18q21.3 – 18q22.1 (Webb et al. 1994), within the known serpin B-clade cluster on chromosome 18q (van Gent et al. 2003). SerpinB2 protein consists of 415 amino acids, and has a predicted molecular weight of 47 kDa. The conventional hydrophobic amino-terminal signal sequence, necessary for protein direction into the secretory pathway, is internally positioned within SerpinB2, resulting in inefficient processing down this classical pathway (von Heijne et al. 1991), whilst allowing for intra and extracellular distribution. SerpinB2 contains three potential N-linked glycosylation sites, at asn-75, asn-115 and asn-339 positions, and occupation of all three gives rise to the 60 kDa extracellular species of SerpinB2 (Ye et al. 1988). The RCL is positioned at P1 arg-380 and P1' thr-381 (Kiso et al. 1988) and the loop is disordered in structure (Harrop et al. 1999). In SerpinB2, the inter-helical domain between helices C and

D is called the CD-loop. The CD-loop is highly mobile structure and can translocate by approximately 40 Å between the side and the bottom of the molecule (Lobov et al. 2004). Due to this flexibility, the structure of the CD-loop has yet to be resolved, however the rest of SerpinB2 conforms to the general tertiary structure conserved across all known serpins (Harrop et al. 1999; Jankova et al. 2001) (Figure 1.1).

1.5. Expression of the SERPINB2 gene

Isolation and characterisation of the SerpinB2 promoter region has identified mechanisms by which transcription of SerpinB2 mRNA can be up-regulated by a wide range of activating molecules, within a variety of cell types (Table 1.2). The SerpinB2 promoter region contains a putative MAZ site (Almeida-Vega et al. 2009), an ASC-1 site (Almeida-Vega et al. 2009), two AP1-like binding sites (Cousin et al. 1991), an AP2-like binding site (Kruithof and Cousin 1988), CRE-like element (Cousin et al. 1991; Park et al. 2005) and a NF-κB binding site (Mahony et al. 1999; Park et al. 2005). Response elements to glucocorticoids (Schuster et al. 1993; Schuster et al. 1994), retinoic acid (Schuster et al. 1993; Schuster et al. 1994) and xenobiotics (Sutter et al. 1991) have also been localised to the 5' promoter region of SerpinB2. Recently, the transcription factor C/EBP-β has been shown to mediate constitutive and LPS-inducible transcription of murine SerpinB2 (Udofa et al. 2013) and an AP-1 element binds FosB which is necessary for PMA induced up-regulation of SerpinB2 expression in U937 cells (Stringer et al. 2012).

Table 1.2: The expression of SerpinB2 mRNA and/or protein can be regulated by a range of biological agents in a diverse set of cell types.

Agent	Expression mRNA	Expression Protein	Cell Type	Cell Line	Ref.
Pro-inflammatory Cytokines					
TNF-α	↑	↑	Fibroblast	HT-1080	(Medcalf et al. 1988)
	↑	ND	Fibroblast	HT1080	(Ong et al. 2000)
	↑	↑	Fibroblast	PC	(Pytel et al. 1990)
			Melanocyte	SK-MEL-109	
	↑	ND	Myeloid	U-937, PC	(Gyetko et al. 1992)
	↑	↑	Vascular SM	PC	(Jang et al. 2004)
	↑	↑	Keratinocyte	PC	(Wang and Jensen 1998)
Interferon-γ	↑	↑	Monocyte	U-937, PC	(Gyetko et al. 1992)
	ND	↑	Fibroblast (Bladder)	RT4, RT112, DAG-1, T24, J82S, TCCsup	(Champelovier et al. 2003)
IL-1β	ND	↑	Fibroblast (BM)	PC	(Hannocks et al. 1992)
	↑	ND	Monocyte	PC	(Gyetko et al. 1993)

	↑	↑	Fibroblast (Synovial)	PC	(Hamilton et al. 1993)
IL-2	↑	ND	Monocyte	PC	(Gyetko et al. 1993)
IL-13	↑	ND	Epithelial (Bronchial)	PC	(Woodruff et al. 2007)
G-CSF	↑	↑	Monocyte	PC	(Hamilton et al. 1993)
M-CSF	↑	↑	Monocyte	PC	(Hamilton et al. 1993)
Steroids/Growth Factors					
Gastrin	↑	ND	Epithelial (Gastric)	AGS	(Varro et al. 2002)
Epidermal Growth Factor (EGF)	↑	↑	Epithelial (Epidermal)	A-431	(George et al. 1990)
	↑	ND	Cumulus	PC	(Piquette et al. 1993)
			Granulosa-luteal	PC	
Glucocorticoids	↓	↓	Fibroblast	HT-1080	(Medcalf et al. 1988)
	↓	ND	Epithelial (Bronchial)	PC	(Woodruff et al. 2007)
Pathogenic Stimuli					
LPS	↑	↑	Monocyte	PC	(Schwartz and Bradshaw 1992)
	↑	ND	Macrophage	RAW-267, PC	(Costelloe et al. 1999)
	↑	ND	Monocyte	PC	(Suzuki et al. 2000)

	↑	↑	Fibroblast (Gingival)	PC	(Xiao and Bartold 2004)
Signalling mediators					
cAMP	↑	ND	Myeloid	PL-21	(Niiya et al. 1994)
Calcium	↑	↑	Keratinocytes	PC, HaCaT	(Wang and Jensen 1998; Seo et al. 2002)
	↑	ND	Neurons	PC	(Zhang et al. 2009)
Toxins					
Dioxin	↑	ND	Keratinocyte	SCC-12F	(Sutter et al. 1991)
	↑	ND	Epithelial (Breast)	M13SV1	(Ahn et al. 2005)
Kainate	↑	ND	Neuronal	Whole tissue	(Sharon et al. 2002)
Okadaic acids	↑	ND	Fibroblast	HT-1080	(Medcalf 1992)
			Myeloid	U-937	
Oxamflatin	↑	↑	Myeloid	U-937	(Dear and Medcalf 2000)
Tumour promoting agents					
PMA	↑	ND	Macrophage	RAW-267, PC	(Costelloe et al. 1999)
	↑	↑	Myeloid	U-937, THP-1, HL-60, K-562	(Genton et al. 1987; Schleuning et al. 1987; Schuster et al. 1993)

Vasculature effectors and regulators					
Angiotensin II	↑	ND	Aortic SM	PC	(Feener et al. 1995)
D-Dimer	ND	↑	Myeloid	NOMO-1	(Hamaguchi et al. 1991)
Factor VIIa	↑	ND	Keratinocytes	HaCaT	(Camerer et al. 2000)
Thrombin			Monocyte/Macrophage	U-937, PC	(Lundgren et al. 1994; Ritchie et al. 1995)
Other					
Lipoprotein-a	↑	↑	Monocyte	PC	(Buechler et al. 2001)
Retinoic acid	↑	↑	Myeloid	U-937, THP-1, HL-60, K562	(Schuster et al. 1993)
	↑	ND	Keratinocytes	PC	(Braungart et al. 2001)
	↑	↑	Monocyte	PC	(Montemurro et al. 1999)
VLDL and LDL	ND	↑	Monocyte	PC	(Wada et al. 1994)

ND: Not Determined
PC: Primary Culture
VLDL: Very low density lipoprotein
LDL: Low density lipoprotein

In addition to the promoters described above, the SerpinB2 gene contains at least two repressor regions in the 5' region of the SerpinB2 gene (positions,1859-1100 and 259-219) (Antalis et al. 1996). The latter site also contains a binding site for an as yet unidentified nuclear protein (Dear et al. 1996). A repressor motif termed PAUSE-1 (SerpinB2 upstream silencer element-1, sequence: 5'-CTCTCTAGAGAG-3') (Antalis et al. 1996) is located at position -1832 and binds a specific, ~ 67 kDa binding factor (Ogbourne and Antalis 2001). This region overlaps with the repressor described by Dear et al. (1996), suggesting that these studies may have described the same repressor region.

Full length SerpinB2 mRNA is unstable, with a half-life of approximately one h (Maurer et al. 1999). The best characterised mRNA degradation components are AU-rich regions in the 3' region of mRNAs. The 3'-untranslated region of SerpinB2 mRNA contains an AU-rich region which plays an important role in the degradation of SerpinB2 mRNA (Maurer and Medcalf 1996). Disruption of the nonameric motif UUAUUUAUU via mutagenesis led to an increase in SerpinB2 mRNA and protein expression levels (Maurer et al. 1999). Additionally, this motif is a binding site for HuR, which has been associated with mRNA decay (Maurer et al. 1999). Tristetraprolin, a CCCH tandem zinc finger protein that binds to ARE-containing transcripts, also interacts with the AU-rich region of the 3'-UTR and mediates SerpinB2 mRNA degradation (Yu et al. 2003). Exon 4 of SerpinB2 also contains an mRNA instability region, sharing homology with instability determinants of other mRNAs (Tierney and Medcalf 2001).

1.6. Polymorphisms

SerpinB2 has not, as yet, been linked to any ‘serpinopathies’, that is, diseases directly related to or caused by aberrant SerpinB2 function. However, there are numerous studies showing correlation between disease states and polymorphisms of the SerpinB2 gene. Two forms of SerpinB2 have been described, with variations in three amino acids (Antalis et al. 1988; van den Berg et al. 1990). These variations occur at positions 120, 404 and 413 with Asn, Asn and Ser in form A and Asp, Lys and Cys in form B. Each of these changes is the result of a single base change in each codon (120, Aat/Gat; 404, aaC/aaG; 413, tCc/tGc), however it appears that all three mutations are linked and do not exist in isolation. Whilst the functional consequences of these residue changes are unknown, a number of studies have linked SerpinB2 genotype and disease. Form A has been associated with lupus erythematosus and thrombotic pneumonia in patients with this condition (Palafox-Sanchez et al. 2009), anti-phospholipid syndrome (Vazquez-Del Mercado et al. 2007) and mycocardial infarction (Buyru et al. 2003; McCarthy et al. 2004; Corsetti et al. 2013), although Foy and Grant (1997) found no evidence of the link between SerpinB2 variants and mycocardial infarction. These disease states all relate to disorders in haemostasis, highlighting the role of SerpinB2 in this system. In addition, Shioji et al.(2005) showed an association between the A form and prostate cancer. SerpinB2 form B is linked to preterm birth in subjects later diagnosed with cerebral palsy (Gibson et al. 2007) and poor overall survival in patients with non-small cell lung cancer (Di Bernardo et al. 2009). Many serpinopathies described for other serpins, result from serpin polymerisation that

gives rise to protein aggregation diseases (Belorgey et al. 2007). In this context, SerpinB2 is unique.

1.7. Polymerisation of SerpinB2

SerpinB2 can spontaneously form polymers *in vitro* (concentration and temperature dependent) and also *in vivo* when directed to the cell secretory pathway (Mikus et al. 1993; Mikus and Ny 1996; Wilczynska et al. 2003). Most serpins require amino acid substitution(s) in key structural positions to provide the ability to polymerise as is the case for natural mutants of α1-antitrypsin, C1-inhibitor, α1-antichymotrypsin and neuroserpin (Stein and Carrell 1995; Davis et al. 1999). In these instances, serpin polymerisation underlines a variety of genetic disorders including emphysema (α1-antithrypsin deficiency), hereditary angioneurotic edema (C1-inhibitor deficiency), and dementia (neuroserpin mutations). In contrast, SerpinB2 does not require additional mutagenesis and wild type protein can exist in a highly polymerogenic conformation (Wilczynska et al. 2003). Polymerisation of SerpinB2 has not been linked with any pathological outcomes. Furthermore, the role of SerpinB2 polymers and their relative abundance compared to non-polymerised SerpinB2 in the organism remains unknown.

SerpinB2 can exist in two different monomeric and inhibitory active forms: the polymerogenic and the stable monomeric form (Wilczynska et al. 2003). The polymerogenic (prone to polymerisation) form is characterised by open β-sheet A

and is stabilised by a disulfide bond connecting C79 in SerpinB2 CD-loop to C161 at the bottom of the molecule (Mikus et al. 1993; Wilczynska et al. 2003; Lobov et al. 2004). Under reducing conditions, the di-sulfide bond is not formed and the CD-loop folds on the side of the molecule; in this form the β-sheet A is closed and the molecule remains as a monomer under physiological conditions providing the stable monomeric form of SerpinB2 (Mikus et al. 1993; Wilczynska et al. 2003; Lobov et al. 2004). The two forms are fully inter-changeable, depending on the redox status of the environment and thus reduction/oxidation of the di-sulfide bond determines whether SerpinB2 is present in the stable monomeric or the polymerogenic form (Lobov et al. 2004) or potentially, polymers. Interestingly, SerpinB2 seems to be able to form different types of polymers under different conditions. For example, polymers of recombinant SerpinB2 obtained upon incubation at 37 ^{o}C or induced by bis-ANS have no inhibitory activity (Wilczynska et al. 2003; Wilczynska et al. 2003), while polymers of SerpinB2 formed in the cell secretory pathway retain their inhibitory activity (Wilczynska et al. 2003). Different mechanisms for serpin polymers have been proposed, including the so called “loop-sheet” and “domain-swapping” polymers (Whisstock and Bottomley 2008). Interestingly however, SerpinB10 has also been shown to undergo redox sensitive conformational changes giving rise to polymers, similar to those described for SerpinB2 (Przygodzka et al. 2010). Whilst the functional significance of SerpinB10 is also unknown, it’s close homology to SerpinB2 and shared polymerisation characteristics give strength to the physiological relevance of redox sensitive

conformational changes. Thus, the mechanisms of SerpinB2 polymerisation and the activity of its different polymer types require further investigation.

1.8. Extracellular SerpinB2

The main physiological producers of SerpinB2 are activated monocytes and macrophages (Wohlwend et al. 1987; Hamilton et al. 1993; Ritchie et al. 1997). However, many other cell types including eosinophils (Swartz et al. 2004), adipocytes (Lijnen et al. 2007), microglia (Akiyama et al. 1993), neurons (Yamanaka et al. 2005; Zhang et al. 2009), astrocytes (Dietzmann et al. 2000), trophoblasts (Astedt et al. 1998) and mesothelial (Ivarsson et al. 1998) (in addition to those listed within Table 1.2), produce this serpin. It has been suggested that a non-classical secretory pathway for SerpinB2 exists due to the presence of both the 47 kDa and 60 kDa forms of SerpinB2 within the extracellular matrix in localised tissues and the detection of similar concentrations of both forms in the blood of pregnant women (Kruithof et al. 1987; Ritchie and Booth 1998). Indeed, recent studies show the secretion of 47 kDa SerpinB2, in response to inflammatory stimulus (LPS), via transport-like vesicles (Boncela et al. 2013). Furthermore, Schroder et al. (2014) have now shown SerpinB2 associated with micro-particles, which facilitate its secretion from metastatic murine B16 melanoma cells. Importantly, SerpinB2 was secreted as an active serpin, able to inhibit urokinase-type plasminogen activator (uPA) and therefore inhibit plasmin formation within the extracellular environment.

Plasmin is a broad-spectrum protease, which is derived from the circulating zymogen plasminogen, by activation via either tPA or uPA systems (Dano et al. 2005). The role of tPA is predominantly associated with fibrinolysis (clot dissolution) (Hoylaerts et al. 1982) and has more recently been identified in important neurobiological processes, discussed below in section 1.11 and reviewed in (Melchor and Strickland 2005). Conversely, uPA is generally implicated in pericellular proteolysis resulting in ECM degradation (Andreasen et al. 1997).

1.9. Urokinase Plasminogen Activator System

Controlled expression of the uPA system is associated with cell surface proteolysis and tissue remodelling during normal physiological conditions such as wound healing and embryogenesis (Andreasen et al. 2000; Dano et al. 2005). However, de-regulation of the uPA system is known to allow tumour invasion and metastasis through the proteolytic degradation of the ECM, effectively presenting a gateway for proximal and distal spread of malignant cells. It is now accepted that the role of uPA in cancer is broader than ECM degradation and incorporates non-proteolytic functions, including cell proliferation, cell migration and cell adhesion (Andreasen et al. 1997; Ranson and Andronicos 2003; Duffy 2004; Dano et al. 2005).

The uPA cascade is initiated by the high affinity binding of pro-uPA, the zymogen form of uPA, to the uPA receptor (uPAR) (discussed below) at the cell surface (Fig.

1.2) (Ellis et al. 1989; Andreasen et al. 1997). Pro-uPA is subsequently activated to form the serine protease uPA through cleavage of the peptide bond Lys_{158} - Ile_{159}, via a number of proteases, with plasmin being most common (Andreasen et al. 1997). It has been suggested that pro-uPA contains intrinsic activity and that this may, in part, contribute to the activation of the uPA cascade (Behrendt et al. 2003).

The binding of pro/uPA to its cell surface receptor uPAR via the *N*-terminal growth factor domain (GFD), results in the placement of the serine protease domain (SPD) within the extracellular matrix (Andreasen et al. 1997) (Fig. 1.2). As its substrate, plasminogen binds to co-localised receptors, e.g. Annexin II hetratetramer (AIIt) resulting in the accelerated activation of plasmin at the cell surface (Plesner et al. 1997) (Fig. 1.2).

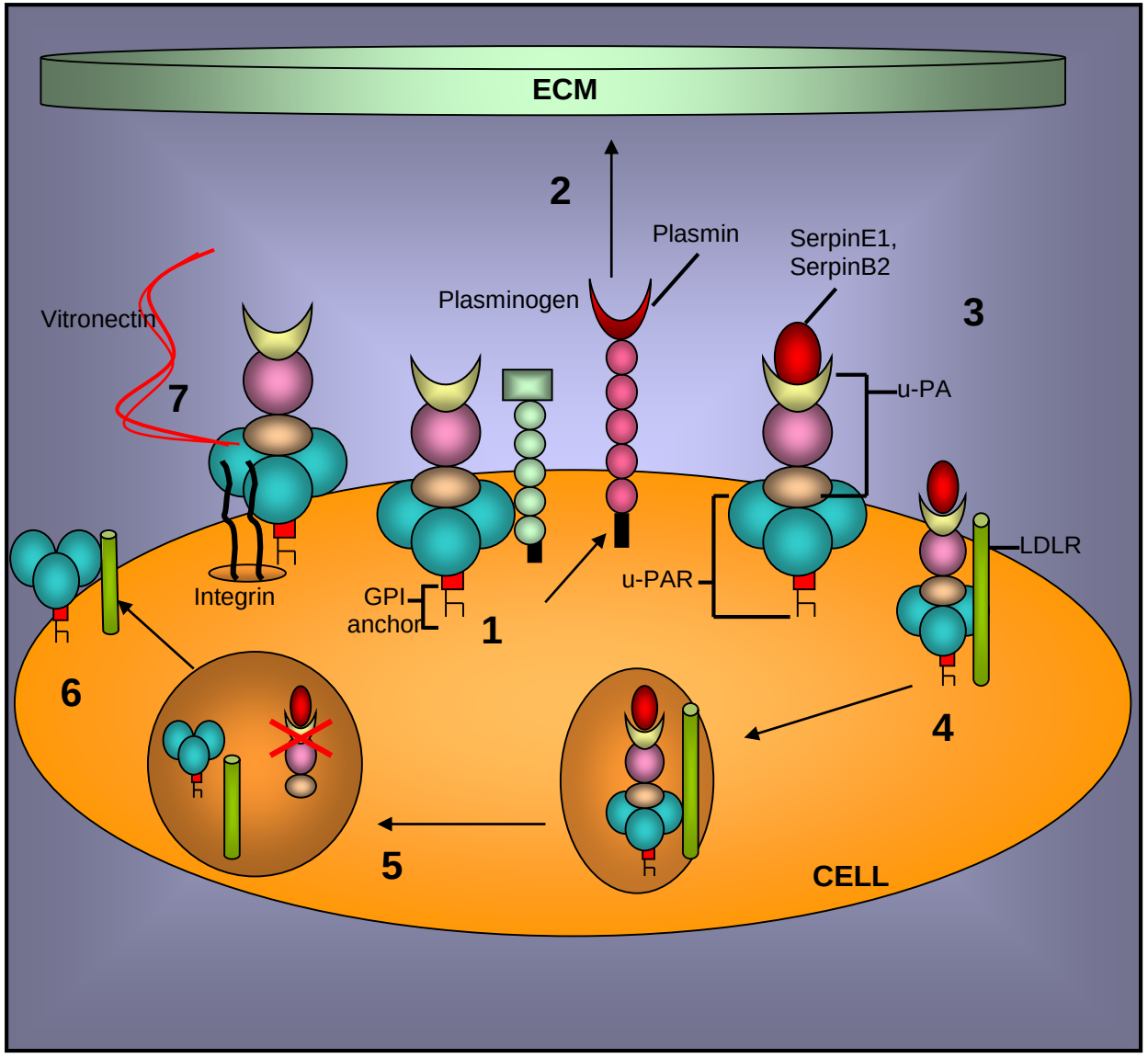

Figure 1.2: Components of the uPA system at the cell surface. 1. uPAR bound uPA is co-localised with plasminogen allowing proteolytic activation of plasminogen, at its C-terminal serine protease domain (SPD), to form plasmin. **2.** Plasmin directly breaks down the ECM through its SPD, or indirectly through activation of MMPs. **3**. The uPA system is inhibited by SerpinE1 (PAI-1) and SerpinB2 (PAI-2), which deactivates the SPD of uPA by direct binding. **4.** Binding of serpins to uPA allows interaction with LDLRs due to conformational changes and facilitates the accelerated clearance of uPAR:uPA:serpin complex from the cell surface. **5.** The complex and receptors are delivered to lysosomes via transport vesicles, where uPA:serpin complexes are enzymatically degraded. **6.** uPAR and the LDLRs are recycled to the cell surface. **7.** Non-proteolytic activity of uPA system; uPAR interactions with integrins result in cell signalling, uPAR interactions with vitronectin allows cell adhesion and migration.

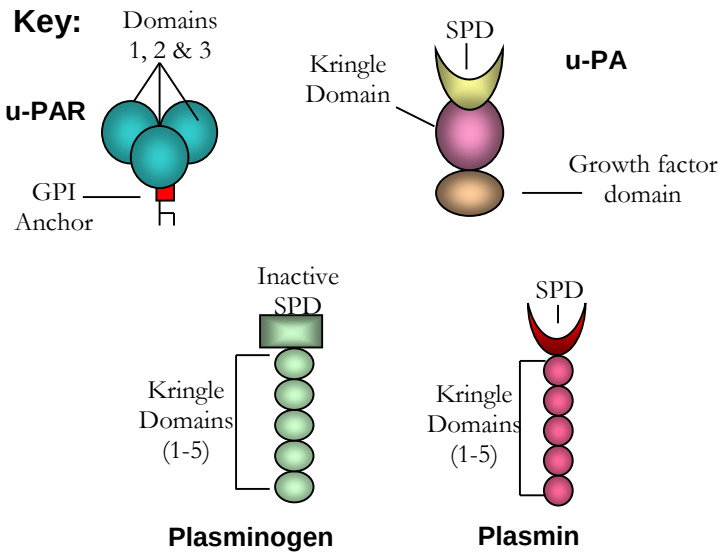

1.10. Urokinase Plasminogen Activator Receptor

The uPA receptor (uPAR) is a glycoprotein containing 283 amino acid residues and is bound to the cell surface through a carboxyl terminal glycosylphosphatidylinositol (GPI) anchor (Andreasen et al. 1997; Huai et al. 2006) (Fig. 1.2). The uPAR protein is comprised of three extracellular domains (D1 – D3) (Fig. 1.2) and whilst bound through the GPI anchor, does not contain an intracellular domain or membrane spanning peptide segment (Behrendt and Stephens 1998). Until recently it was widely accepted that D1 contained the binding domain for the growth factor region of (pro)-uPA, however using x-ray crystallography, Huai et al. (2006) have shown that all three domains are involved in binding interactions. The GFD within uPA contains an omega loop with residues critical for binding to D1, D2 and D3 of uPAR (Behrendt and Stephens 1998). Soluble forms of uPAR (suPAR) have also been identified within plasma and are thought to originate through the cleavage of the GPI anchor at the cell surface by plasmin (Hoyer-Hansen et al. 2001; Rasch et al. 2008). Whilst SerpinE1 binding to uPA interrupts the vitronectin interactions (Andreasen et al. 1997), it also facilitates the internalisation of uPAR and associated integrins (Czekay et al. 2001). As SerpinE1 can also bind to vitronectin it is able to inhibit uPAR/vitronectin interactions from re-occurring and these two processes lead to cell detachment (Degryse et al. 2004).

1.11. Tissue Type Plasminogen Activator

The tissue type plasminogen activation system was predominantly associated with fibrinolysis and under normal physiological conditions plasma tPA concentration is ~ 0.1 nM (Dano et al. 1985). However, it is now known that tPA is not restricted to maintaining homeostasis of coagulation and fibrinolysis. For example, tPA has been shown to play a role in angiogenesis via cell surface interactions with annexin II (p36) (Ling et al. 2004) and has emerged as a key component of neurobiology with a vast number of roles described such as; effector of learning and memory (Seeds et al. 2003; Obiang et al. 2012; Li et al. 2013); stress, as a modulator, via stabilisation of the NMDA (N-methyl-D-aspartate) receptor during stress and participating in behavioral changes and synaptic plasticity via NMDA signaling within the hippocampus (Norris and Strickland 2007). Furthermore, links to protection against neuronal degeneration have been found, whereby tPA has been shown to degrade amyloid-β (Aβ) *in vivo*, within two different mouse models of Alzheimer's disease (Melchor et al. 2003) and has recently been shown to neutralise Alzheimer's disease progression (Oh et al. 2014). Of interest however is the role plasminogen activators play in monocyte biology, given that cells of myeloid lineage interchangeably express tPA, uPA and SerpinB2/SerpinE1, specifically during activation or differentiation processes (McWilliam et al. 1998; Missen et al. 2006), although the physiological implications of this flexibility requires further investigation.

Many cells secrete tPA such as; melanocytes (Rijken and Collen 1981), endothelial cells (Ljungner et al. 1983; Larsson and Astedt 1985) and peripheral blood monocytes (Hart et al. 1989; Hart et al. 1989; Soo et al. 1996). As a single chain polypeptide, tPA is a glycosylated protein with molecular weight ~ 72 kDa (Rijken and Collen 1981; Dano et al. 1985; Vassalli et al. 1992). Cleavage of sc-tPA, via hydrolysis of the Arg_{275}-Ile_{276} peptide bond, produces the 62.9 KDa two chain (tc) tPA conformation (Rijken and Collen 1981; Collen and Lijnen 2004). Linked by one disulfide bridge, chain A and chain B have Mr ~ 33 kDa and 39 kDa, respectively (Rijken and Collen 1981; Pennica et al. 1983). The basic structure of the tPA molecule contains 4 domains; i) the *N*-terminal region of 47 residues comprising the finger domain (F Domain), which is homologous with the finger domain of fibronectin, ii) an epidermal growth factor domain (E-domain) residues 50-87, iii) two kringle domains, residues 87-176 (K1), and 176-256 (K2), which share similar amino sequences to the five kringle domains within plasminogen and iv) the serine protease domain within the *C*-terminus, containing the active sites His_{322}, Asp_{371} and Ser_{478} (Pennica et al. 1983). Domains 1-3 are found in the A chain of activated tPA, whilst the protease domain is located within the B chain (Pennica et al. 1983). The high affinity binding of tPA to fibrin is mediated by the finger domain and lysine sites within the kringle domains of tPA (Hoylaerts et al. 1982; van Zonneveld et al. 1986; Kaczmarek et al. 1993). Furthermore, the regions of homology identified within the kringle domains of plasminogen and tPA enable the co-localisation of these proteins via fibrin on the clot surface, which in turn facilitates the accelerated production of plasmin (Hoylaerts et al. 1982).

Soluble tPA is cleared from circulation via parenchymal and endothelial cells in the liver (Kuiper et al. 1988; Nguyen et al. 1992; Simon et al. 1995), whilst cell bound inactivated tPA is internalised via endocytosis and degraded in lysosomes (Camani et al. 1994; Hardy et al. 1997). The characterisation of a tPA receptor on the cell surface of human umbilical vein endothelial cells (HUVEC) by Hajjar and Hamel (1990) identified the annexin II heterotetramer (AIIt) (Cesarman et al. 1994; Hajjar et al. 1994) as an important binding site for both tPA and plasminogen. In addition, high density - low affinity binding sites for tPA have also been described for HUVECs, the U-937 and THP-1 monocytic cell lines and peripheral blood monocytes (Felez et al. 1991). Investigation of the role of glycosaminoglycans in cell surface tPA interactions by Camani et al. (2000) concluded that these receptor types are not involved.

Little is understood about the role of SerpinB2 as a physiological inhibitor of tPA due to limited reports of tPA:SerpinB2 complexes identified *in vivo* (Kruithof et al. 1995). Yet, co-expression of tPA and SerpinB2 has been shown in normal bone marrow (McWilliam et al. 1998), skin (Chen et al. 1993), saliva and salivary gland tissue (Virtanen et al. 2006), gingival fluid (Brown et al. 1995; Kinnby 2002), as well as during pregnancy (Astedt et al. 1998), and SerpinB2 is able to inhibit cell surface bound tc-tPA *in vitro* (Lobov et al. 2008). Furthermore, enhanced expression of both tPA and SerpinB2 by epithelial cells is indicative of some disease states, e.g. periodontal disease (Kinnby 2002), psoriasis and

pre/eclampsia (Kruithof et al. 1995), strongly suggesting a role for SerpinB2 in the control of tPA activity at sites of localised inflammation and warrants further investigation.

1.12. Inhibition of uPA or tPA

SerpinB2 is an efficient inhibitor of soluble and receptor bound, activated (two-chain) tc-uPA and soluble activated (two-chain) tc-tPA (Thorsen et al. 1988; Kruithof et al. 1995) (Table 1.3). While SerpinB2 can inhibit the soluble pro-enzyme (single-chain) sc-uPA, albeit less efficiently than tc-uPA, it cannot form stable covalent complexes with the former (Schwartz 1994). Since sc-uPA has some intrinsic plasminogen activation capacity, but is inefficiently inhibited by SerpinB2 (Table 1.3) (or SerpinE1), it has been suggested that this may allow initiation of cell surface proteolysis in PAI rich environments (Schwartz 1994). Once sufficient tc-uPA activity is formed, SerpinB2 can then efficiently inhibit further plasmin formation. It is important to note here that since most of the uPA in plasma/fluids appears to be in the sc-uPA form (Wojta et al. 1989), only cell surface associated activity is thus of relevance when considering the inhibitory effects of PAIs on uPA. This is supported by the findings of Siefert et al. (2014) that the absence of SerpinB2, not SerpinE1 coincided with an increase in uPA activity and faster venous thrombus resolution using a deep vein thrombosis model within wild-type C57BL/6, SerpinB2($^{-/-}$) , and SerpinE1($^{-/-}$) mice.

Table 1.3: Inhibition kinetics of SerpinB2 for uPA and tPA (adapted from (Lee et al. 2011)).

Plasminogen Activator	Solution phase	Receptor bound
sc-tPA	(4.6±0.6) x 10^3 $M^{-1}s^{-1}$ * (Thorsen et al. 1988)	-
tc-tPA	(2.0± 0.02) x 10^5 $M^{-1}s^{-1}$ (Thorsen et al. 1988)	-
	-	2.5 pM †‡ (Leung et al. 1987)
sc-uPA	ND	ND
tc-uPA	(2.1± 0.2) x 10^6 $M^{-1}s^{-1}$ (Thorsen et al. 1988)	-
	5.3 x 10^5 $M^{-1}s^{-1}$ (Ellis et al. 1990)	3.3 x 10^5 $M^{-1}s^{-1}$ ¥ (Ellis et al. 1990)
	~ 20 pM ‡ (Leung et al. 1987)	60 - 80 pM ‡∞ (Al-Ejeh et al. 2004)

* 2^{nd} order rate constant
† Bound to poly-D-lysine
‡ Inactivation constant K_i
¥ Bound to human monocytoid cell lines
∞ Bound to human carcinoma cell lines
ND – not determined

SerpinB2 is also a poor inhibitor of free circulating (single chain) sc-tPA (in contrast to SerpinE1) (Thorsen et al. 1988; Kruithof et al. 1995) (Table 1.3). The ability of SerpinB2 to inhibit bound tc-tPA appears to depend on the type of tPA binding interaction. For example, fibrin-bound tPA is protected from inhibition by SerpinB2 (Leung et al. 1987) (although SerpinB2 crosslinked to fibrin can inhibit tPA (Ritchie et al. 2001)), while poly-D-lysine-bound-tPA is not protected (Leung et al. 1987) (Table 1.3). SerpinB2 has also been shown to inhibit tc-tPA bound to various cell types *in vitro* and to purified AIIt (Lobov et al. 2008). Where studied, SerpinB2 has poor inhibitory activity against other serine proteases (reviewed in (Kruithof et al. 1995)).

1.13. Intracellular SerpinB2

A new focus into SerpinB2 research was invoked when it became apparent that unlike SerpinE1, the highest expression levels of SerpinB2 are found intracellularly within monocytes and macrophages *in vitro* (Kruithof et al. 1986; Genton et al. 1987). The potential roles described for intracellular SerpinB2 have typically not been associated with a classical inhibitory serpin function but rather with a variety of potential functions ranging from signal transduction (Antalis et al. 1998) to inhibition of apoptosis in some cell models (Dickinson et al. 1995) but not others (Fish and Kruithof 2006). Whilst a definitive function for intracellular SerpinB2 has not been forthcoming, it has become clear that SerpinB2 is an immune modulator (Schroder et al. 2010; Zhao et al. 2013; Shea-Donohue et al. 2014). This role is supported by the subsequent reports showing up-regulation of SerpinB2 in response to a barrage of inflammatory stimuli within these and other cell types (Table. 1.2).

1.14. Inflammation and Pathogenesis

The role of SerpinB2 in response to inflammatory mediators is well studied and a strong association between IL-1β suppression and SerpinB2 has been formed using *in vivo* mouse and *in vitro* cell models (Bystrom et al. 2004; Park et al. 2005; Greten et al. 2007; Sekine et al. 2009). The initial hypothesis for how SerpinB2 controlled IL-1β activation, rotated around the inhibition of caspase-1 (interleukin-1β-converting enzyme [ICE]) by SerpinB2 (Jensen et al. 1999). Whilst this has never been proven, it is now known that SerpinB2 gene expression is regulated by

transcription factor NF-κβ under inflammatory conditions and the up-stream mediators of NF-κβ (i.e. IKKβ) are thought to be responsible for the control of IL-1β secretion (Greten et al. 2007). This is supported by a study in which Schroder et al. (2010) were unable to detect any difference in IL-1β secretion when comparing resting peritoneal macrophages isolated from the SerpinB2$^{-/-}$ mouse model (Dougherty et al. 1999), to littermates (SerpinB2$^{+/+}$). Importantly, this study reinforced the link between SerpinB2 expression and adaptive immunity, with the finding that SerpinB2 appears to function in the suppression of TH1-promoting cytokine production (Schroder et al. 2010). The mechanisms associated with this are currently unclear. Of interest however, is the recent finding that SerpinB2 depletion in macrophages induces caspase-1 activation and IL-1β production in response to TLR agonists and *Escherichia coli* (Chuang et al. 2013). Furthermore, interactions between SerpinB2 and Beclin 1 lead to an increase in autophagy, which coincided with decreased IL-1β maturation. Thus providing possible insight into the functional mechanisms of SerpinB2 as an immune modulator and inflammatory mediator.

The link between SerpinB2 with immune function is not new and up-regulation of SerpinB2 by monocytes and macrophages in response to a variety of pathogens such as Dengue Virus (Krishnamurti and Alving 1989; Krishnamurti et al. 1989), *Legionella pneumophilia* (Losick and Isberg 2006), *Borrelia burgdorferi* (Haile et al. 2006) and *Mycobacterium avium* infection (Gan et al. 1995) has been reported. Also, elevated SerpinB2 mRNA in eosinophilic leukocytes has been linked to

protection from parasitic organisms, inflammation and asthma (Swartz et al. 2004). In asthma patients, SerpinB2 levels are suppressed by anti-inflammatory steroids such as glucocorticoids (Table. 1.3). More recently, elevated SerpinB2 expression has been observed in monocytes co-cultured with *Aspergillus fumigatus*, a fungi infecting immuno-compromised patients (Loeffler et al. 2009). Whilst the expression profiles for SerpinB2 in response to inflammation and pathogenesis are consistent, the function of SerpinB2 has not been defined, although the hypothesis that SerpinB2 protects against apoptosis within these environments appears to be supported in some cell models, but not others.

1.14.1. Apoptosis

The hypothesis that intracellular SerpinB2 may play a role in protection against apoptosis arose due to the chromosomal co-localisation of a potent inhibitor of apoptosis bcl-2 (B-cell lymphoma) and SerpinB2 genes, along with their co-expression during cellular stress (Silverman et al. 1991). Early work conducted using the HT1080 fibro sarcoma cell line transfected with SerpinB2 reported delayed apoptotic responses within these cells following TNF-α challenge, when compared to controls (Kumar and Baglioni 1991; Dickinson et al. 1995). Furthermore, SerpinB2 was found to protect primary cultures of human macrophages from apoptosis following *in vitro* infection with *Mycobacterium avium* and treatment with indomethacin (Gan et al. 1995). Therefore the hypothesis that SerpinB2 may inhibit an undefined intracellular protease was formed. This was supported by the identification a cleaved 33 kDa intracellular SerpinB2 species in

NB_4 leukaemia cells following induction of apoptosis with okadaic acid, calyculin A and the protein synthesis inhibitor cycloheximide (Jensen et al. 1994). It was suggested SerpinB2 may undergo intracellular processing during apoptosis resulting in a cleaved yet active inhibitor, given the detection of cleaved SerpinB2 in complex with uPA. Indeed, Jensen et al. (1999) found that SerpinB2 cleavage occurred within the first two hs of okadaic acid or camptothecin induced apoptosis in the HL-60 pro-myeloid cell line and that this occurrence was negated by the inhibition of caspase-1 using the peptide inhibitor YVAD-cmk. However, an *in vitro* assay revealed that SerpinB2 was not a substrate for caspase-1 or caspase-3. The functional mechanisms, significance and protease/s involved in the production of the 33 kDa species of SerpinB2 during early apoptosis are still unknown.

Interestingly, transfection of HeLa cells with the SerpinB2-ΔC-D interhelical loop mutant did not replicate the protective effect of wild-type SerpinB2 against TNF-α/cycloheximide induced apoptosis, indicating a functional role for the unique C-D loop (Dickinson et al. 1998). The identification of Gln residues at positions 83,84 and 86 as substrate sites for transglutaminase within the C-D interhelical loop (Jensen et al. 1994) and subsequent characterisation of SerpinB2 in complex with members of the transmembrane annexin family (annexins I, II, IV and V) (Jensen et al. 1996) suggests a role for stabilisation of the apoptotic envelope during early apoptosis. This is supported by the observation of SerpinB2 incorporation into the cornified envelope of differentiated keratinocytes (Jensen et al. 1995), possibly

through transglutaminase cross-linking. It is thought that SerpinB2 may help to maintain membrane structure and integrity within keratinocytes.

The epidermis is a high SerpinB2 expressing environment, under normal physiological conditions (Hibino et al. 1988). Therefore the role of SerpinB2 in keratinocyte biology presents another area of interest to researchers. A link between reduced proliferation and SerpinB2 expression in keratinocytes was reported by Hibino et al. (1999). Shortly after, Zhou et al. (2001) found that basal keratinocytes over expressing SerpinB2 in a transgenic mouse model, were highly susceptible to chemically induced cutaneous papilloma formation. Repeated application of 12-*O*-tetradecanoylphorbol-13-acetate (TPA) to the skin of the mice resulted in lesion formation on 97% of the transgenic mice versus 65% in the control group. Furthermore, the papilloma lesions observed on the skin of control mice were found to regress as a result of apoptosis once treatment was withdrawn, whilst those of the transgenic mice persisted. The authors reported very low detection of apoptotic cells within the papillomas of the transgenic mice compared to controls. It is important to note that the control mice were SerpinB2 positive and therefore representative of a normal expression profile, which was below detectable levels. However, taken together the persistence of the papilloma lesions on the skin of the transgenic mice contributes to the idea that in this context at least, SerpinB2 protects against commitment to cell death. Indeed, this is in line with the recent characterisation of Annexin I and SerpinB2 high molecular weight complexes extracted from cell lysates of human macrophages undergoing

apoptosis following *in vitro* infection with *Mycobacterium avium* (Gan et al. 2008) and corroborates the earlier works of Jensen et al. (1994) and Jensen et al. (1996).

However, despite the accumulated support for SerpinB2 as an anti-apoptotic agent the specific function and mechanisms associated with this proposed role have not been identified or fully characterised. Recently Fish and Kruithof et al. (2006) conducted a thorough investigation of SerpinB2 in the prevention of TNF-α induced apoptosis using HeLa, Isreco-1 and HT1080 cell lines. The study compared the effect of wild-type SerpinB2, SerpinB2-Δ-C-D interhelical loop and reactive centre (R380A) mutants; SerpinB2 null, SerpinB2 expressing and SerpinB2 over-expressing cell models in addition to the application of exogenous SerpinB2 to cultures. Despite this, however, they were unable to replicate any of the earlier work showing a protective role for SerpinB2 in apoptosis. Unlike earlier works, these investigators used a lenti-viral transfection system which may explain the contrast in results between their findings and others works. Furthermore, overexpression of SerpinB2 in pulmonary arterial smooth muscle cells was recently shown to enhance apoptosis whilst suppressing proliferation and migration (Zhang et al. 2015). Knockdown of SerpinB2 was then shown to suppress apoptosis and enhance proliferation and cell migration, suggesting possible cell context differences.

1.14.2. Other intracellular binding partners of SerpinB2

Irrespective of the conflicting results supporting a role for SerpinB2 in apoptosis, a protease binding partner for intracellular SerpinB2 remains to be identified. The distribution of SerpinB2 within the nucleus, cytoplasm and the extracellular environment suggests alternate functions, independent of its role as a serpin, which may be dependent on the previously described binding sites within the C-D interhelical loop.

The C-D interhelical loop contains three transglutaminase sites previously mentioned, a cysteine at position 79 (C79) which is functional in the polymerisation of SerpinB2 (Mikus and Ny 1996; Wilczynska et al. 2003; Lobov et al. 2004) (discussed in section 1.7), and a PENF motif: in addition, asparagine at position 75 (N75) is glycosylated in extracellular SerpinB2. It is not surprising therefore that non-serpin related interactions, most of which are dependent on the C-D interhelical loop of SerpinB2 have been reported and include; Interferon regulatory factor-3 (Zhang et al. 2003), PSMB1 (Fan et al. 2004; Schroder et al. 2010; O'Hara et al. 2013), Annexin I, II, IV and V (Jensen et al. 1996; Gan et al. 2008) and retinoblastoma protein (Rb) (Darnell et al. 2003).

The tumour suppressor, Rb protein, was identified as a binding partner for SerpinB2, by Darnell et al. (2003). Stable transfection of the HeLa cervical carcinoma cell line with SerpinB2 resulted in an increase in Rb protein levels compared to control cells. This was supported by the detection of increased Rb

expression and stability in the Jurkat cell line when transfected with SerpinB2. Furthermore, co-localisation of SerpinB2 with Rb in the nucleus of HeLa and other cell lines, was observed.

HeLa cells are positive for human papilloma virus (HPV) – 18 oncoproteins, of which, E6 and E7 fusion proteins are responsible for the degradation of Rb (Scheffner et al. 1992; Boyer et al. 1996). Interestingly the authors reported a decrease in mRNA for E6/E7 within the SerpinB2 positive HeLa cells. Taken together it was hypothesised that SerpinB2 was acting to inhibit degradation of Rb protein by an undefined cellular protease, recently hypothesised to be calpain (Tonnetti et al. 2008), and in the case of HPV-18 positive cells, through the suppression of E6/E7 mRNA expression. Further investigation by Darnell et al. suggested that SerpinB2 suppresses HPV oncogenes by stabilisation of Rb, which subsequently silences the HPV-18 up-stream regulatory region (URR) responsible for E6 and E7 transcription (Darnell et al. 2005).

Whilst this represented the first solid indication of a role for intracellular SerpinB2, Fish et al. (2006) were unable to detect any difference in Rb expression when comparing IS-1 and HT1080 cell lines transfected with wild-type SerpinB2 or inactive SerpinB2 (R380A), relative to controls and between transfected cells. They did however; report a slight elevation of Rb protein within transduced HeLa cells compared to control cells, although there was no difference in Rb detection between wild-type SerpinB2 or inactive SerpinB2. In a recent study, no correlation

between SerpinB2 expression and prognostic outcomes could be found following assessment of 225 cervical biopsy specimens. SerpinB2 expression did however increase with lesion grade (Syrjanen et al. 2009).

1.14.3. Neurology

Very little is known about the role of SerpinB2 within neurobiology, however astrocytes (Dietzmann et al. 2000) and neurons (Yamanaka et al. 2005) have been reported to synthesise this protein. Furthermore, an early study conducted by Akiyama et al. (1993) reported high SerpinB2 deposition within microglia, which surrounded the senile plaques associated with Alzheimer's Disease (AD) and much lower antigen detection in control tissue. The authors surmised that SerpinB2 was inhibiting proteolysis within the localised extracellular environment and therefore contributing to the prevalence of the disease. Importantly, AD lesions represent high inflammatory environments (McGeer and McGeer 2002) and microglial cells are the macrophage equivalent within the central nervous system. Therefore, up-regulation of SerpinB2 by microglia in AD is most likely due to the inflammatory environment of AD lesions, which is in-line with the many cell models showing increases of SerpinB2 mRNA and/or antigen in response to pro-inflammatory cytokines (Table. 1.2). Recently, SerpinB2 was identified as a binding partner for the cell adhesion molecule CHL1 which promotes CHL1-induced neurite outgrowth and neuronal migration in mice (Katic et al. 2014). Whilst, Zhang et al. (2009) have identified SerpinB2 as one of nine key neuronal protective proteins expressed in response to brain trauma, that are required for survival of

cultured hippocampal neurons suggesting that SerpinB2 may be important in controlling haemostasis within the central nervous system also. SerpinB2 is highly expressed within micro-environments undergoing acute and chronic homeostatic imbalances which suggest a broader function as an inflammation modulator, not limited to immune response pathways. Most of the early *in vivo* studies utilised immunohistochemisty to assess expression of SerpinB2 in-conjunction with other aspects of the PA system and while this confirmed the presence of SerpinB2 within the tissue examined, it has not contributed to the development of functional role/s. Furthermore, it is difficult to accurately discern the location of SerpinB2 antigen as either intracellular or extracellular within the earlier immunohistochemistry works. Therefore, this line of investigation is warranted given the earlier reports of SerpinB2 deposition within amyloid plaques of Alzheimer's patients and more recent associations with Amyloid Lateral Sclerosis (ALS) animal model and oxidative stress induced expression of SerpinB2 (Boutahar et al. 2011).

1.15. Rationale and Specific Aims of the Thesis

This thesis aims to examine; 1) the role of SerpinB2 within the extracellular environment as a plasminogen activator inhibitor in monocytes and 2) the role of SerpinB2 within the intracellular environment as a stress response protein.

There have been many studies conducted which have defined and supported the role of SerpinB2 as a classical inhibitory serpin, at a biochemical level. More recent studies have clearly shown that SerpinB2 facilitates the rapid endocytosis of

uPA:uPAR complexes from the cell surface of PC-3 (Croucher et al. 2006) and MCF-7 (Croucher et al. 2007; Cochran et al. 2011) cell lines, via members of the Low Density Lipoprotein Receptor (LDLR) family. However, these findings contradict those described using the THP-1 monocytic cell line by Ragno et al. (1995). This inconsistency within the published literature led us to examine, using similar techniques to those described for the above mentioned breast and prostate cells, the role SerpinB2 may or may not play in uPA clearance from the surface of monocytic cell lines. Furthermore, the role of either SerpinE1 or SerpinB2 in the inhibition and endocytosis of tPA at the cell surface is unclear. Given that the main producers of SerpinB2 are monocytes and macrophages the control of plasmin generation via uPA or tPA, by SerpinB2 at the cell surface warrants further investigation.

Therefore, the aims of chapter 2 were to investigate the inhibition of cell surface uPA by SerpinB2 and characterise the endocytosis pathways facilitating clearance of uPA:SerpinB2 complexes, once formed at the surface of monocytic cell lines. Confirmation of similar endocytosis pathways to those described by Croucher et al. (2006) and Croucher et al. (2007), will aid in establishing a robust model for SerpinB2 and contribute towards establishing its role as a physiological inhibitor of uPA. An additional aim addressed in chapter 2 was to assess the potential for use of SerpinB2 based therapeutics in the treatment of acute myeloid leukaemia (AML).

The specific aims of chapter 3 were to examine inhibition of tPA by SerpinB2 and characterise the role of LRP and VLDLR as potential endocytosis receptors for tPA and tPA:PAI complexes on these cells. Cell profiling of the U-937 and THP-1 cell line in addition to PBMs was undertaken to ascertain the basal PA levels present on the surface of malignant versus healthy myeloid cells with the aim of assessing the potential impact SerpinB2 directed therapeutics may have through non-uPA facilitated endocytosis pathways.

Up-regulation of intracellular SerpinB2 in response to acute and chronic homeostatic imbalances suggests a potential function within cellular stress response pathways. This hypothesis is supported by the lack of an intracellular protease target for SerpinB2, suggesting a non-inhibitory role. Of interest is the finding that some non-inhibitory serpins appear to function as transport chaperones/molecules, cytoskeleton support molecules or heat shock proteins, all with very specific targets or niches (Hammond et al. 1987; Pemberton et al. 1988; Tasab et al. 2000; Sauk et al. 2005; Finno et al. 2015). In this context, SerpinB2 presents as a co/chaperone or shuttle protein given the promiscuity of described binding interactions with many partners and no known associated function, despite 40 years of research. Importantly, promiscuity is a common characteristic associated with molecular chaperones (Hartl et al. 2011). Therefore the specific aims of chapter 4 were to assess the possible chaperone-like activity of SerpinB2, using an array of amorphous and fibril forming substrate models.

The specific aims of chapter 5 were to gauge a better understanding of the cellular pathways in which SerpinB2 may function as a stress response protein. The intracellular processing of aberrant protein trafficking was assessed using wild-type and SERPINB2$^{-/-}$ murine embryonic fibroblasts and a transient huntingtin expression model.

2. Investigation of SerpinB2 as a potential therapy delivery mechanism for the treatment of acute myeloid leukaemia.

2.1. Abstract

The high prevalence of drug resistance in Acute Myeloid Leukaemia (AML) has led to the development of toxin-fusion-proteins for the treatment of this disease. Here we report the preliminary investigation of SerpinB2 as a potential toxin delivery and internalisation mechanism in the treatment of AML. The U-937 and THP-1 cell lines were found to endocytose SerpinB2 via the urokinase plasminogen activation system (uPA) and low density lipoprotein receptor (LDLR) family pathways. This work indicates the potential for use of SerpinB2 based therapeutics in the treatment of AML.

2.2. Introduction

Acute myeloid leukaemia (AML) originates from the myeloid stem cells within the bone marrow and has traditionally been sub-typed based on morphology with respect to their stage of myeloid differentiation (Meshinchi and Arceci 2007). Despite the advances in therapy development for the treatment of AML, this disease accounts for more than half of the leukaemia related deaths in paediatric patients (Meshinchi and Arceci 2007). This appears to be linked to the high occurrence of multiple drug resistance (MDR) within this patient cohort (Meshinchi and Arceci 2007). Due to the problematic treatment of AML patients with MDR, research focus is growing in the development of targeted toxin-fusion protein therapies.

Of particular interest as a potential cell surface targeted antigen in AML patients is the urokinase plasminogen activation (uPA) system, which is associated with pericellular proteolysis via the conversion of plasminogen to plasmin (Ellis et al. 1990). Elevated expression of the uPA system by leukaemic cells has been widely documented and is thought to contribute to excessive bleeding and poor prognosis of patients (Wada et al. 1993; Hildenbrand et al. 1999; Scherrer et al. 1999; Graf et al. 2005; Ohba et al. 2005). Control of cell surface plasmin generation may be mediated through the inhibitory functions of the serpins plasminogen activator inhibitors (PAI) type 1 (SerpinE1) and 2 (SerpinB2) (Ellis et al. 1990). Inhibition of receptor bound uPA at the cell surface facilitates the rapid endocytosis of the inhibited complex via the family of low density lipoprotein receptors (LDLR) (Croucher et al. 2006). Pre-clinical evaluations conducted using human breast and prostate carcinoma xenograft murine models, have shown that systemic (i.p.) administration of ^{213}Bi-SerpinB2 causes tumour growth inhibition in a dose-dependent manner (Allen et al. 2003; Stutchbury et al. 2007). Furthermore, the delivery pathway was found to be uPA dependant (Al-Ejeh et al. 2004; Croucher et al. 2006; Croucher et al. 2007). Whilst SerpinB2 shows promise as a delivery mechanism for anti-cancer therapy directed at solid tumours, it's suitability for use in the treatment of haematological malignancies has not been investigated.

2.2.1. Specific Aims

The aims of this study were to investigate the inhibition of cell surface uPA by SerpinB2 and characterise the endocytosis pathways facilitating clearance of

uPA:SerpinB2 complexes once formed at the surface of monocytic cell lines. Using a fluorescence quenching internalisation assay and inhibitory antibodies (Al-Ejeh et al. 2004), we show that SerpinB2 is endocytosed by the histocytic lymphoma U-937 cell line and the AML cell line THP-1, in a uPA and LDLR family dependent manner indicating that further development of SerpinB2 based therapies is warranted for the treatment of AML.

2.3. Experimental Procedures

2.3.1. Proteins, Antibodies and Reagents

Recombinant human SerpinB2 (47 kDa form) was provided by SerpinB2 Pty Ltd (Sydney, Australia). Purified human receptor associated protein (RAP) was from Molecular Innovations (MD, USA). Monoclonal murine anti-human uPA B-chain IgG_1 (#394), monoclonal murine anti-human uPAR IgG_{2a} (#3936) and monoclonal murine anti-human LRP α-chain IgG_1 (#3402) were from American Diagnostica Inc. (USA). Polyclonal rabbit anti-human VLDLR IgG was from Santa Cruz Biotechnology, Inc. Polyclonal goat anti-rabbit FITC conjugate IgG (whole molecule), goat anti-mouse IgG (Fab specific) FITC conjugate, propidium iodide (PI), Hanks balanced salt modified and non-modified and bovine serum albumin (BSA) were from Sigma-Aldrich. Anti-DNP rabbit polyclonal isotype control was from DakoCytomation (Glostrup, Denmark). Alexa-488 labeling kit and Alexa-488 quenching polyclonal antibody were from Molecular Probes (OR, USA). RPMI-1640 powder and foetal calf serum were from Trace Bioscientific (NSW, Australia). The rabbit anti-human LRP polyclonal and murine anti-human VLDLR monoclonal

antibodies 1H5, 5H3 and 1H10 were a kind gift from Professor Dudley Strickland, USA (Ruiz et al. 2005; Croucher et al. 2006).

2.3.2. Cell Lines and Tissue Culture Conditions

The monocyte like U-937 histocytic lymphoma and THP-1 human monocytic leukaemic cell lines were used for all experiments. Cells were maintained in medium consisting of RPMI-1640, 5% (U-937) or 10% (THP-1) heat inactivated fetal calf serum and 2 mM glutamine at 37 °C and 5% CO_2 enriched humidified air.

2.3.3. Immunofluorescence Assays

Cell surface antigens were measured by dual colour immunofluorescence and flow cytometry as previously described (Al-Ejeh et al. 2004). Internalisation assays were conducted using the fluorescence quenching internalisation assay as described previously (Al-Ejeh et al. 2004; Croucher et al. 2006). Briefly, cells were incubated at 37 °C for 1 h in the absence (control) of presence of 10 nM $SerpinB2_{Alexa488}$ in Hanks buffer. The cells were next washed twice and incubated on ice for 30 min with 4 $\mu g.mL^{-1}$ Alexa488 quenching antibody (quenches any remaining cell surface fluorescence and is thus a measure of internalised ligand) in ice cold Hanks buffer. Finally, the cells were washed twice with ice cold PBS and analysed using flow cytometry as described above. All assays were conducted in triplicate and appropriate background controls subtracted.

2.3.4. Plasmin Generation Assays

Briefly, cells were harvested, washed twice and resuspended at $1x10^6$ cells.mL^{-1} in Tris-buffered saline (TBS) (50 mM Tris HCl, 150 mM NaCl, pH 7.4). Cells were pre-incubated in the absence or presence of 10 nM uPA on ice for 30 min, washed twice in TBS and then resuspended in 100 µL TBS in the presence of 10 µg plasminogen. Following 15 min pre-incubation at room temperature, 100 uL of Spectrozyme PL substrate was added to a final concentration of 0.25 mM. Substrate conversion by plasmin was measured kinetically at 405 nm over a 2 h period at 37 °C in a Molecular Devices SpectraMax 250 plate reader, and analysed using SoftMax® Pro software (Molecular Devices, USA). Negative controls contained TBS buffer and either 0.25 mM Spectrozyme PL or whole cell suspension made to a final volume of 200 µL with TBS buffer. Positive control consisted of 1 µg uPA, 10 µg plasminogen in 100 µL TBS and 100 µL 0.5 mM Spectrozyme Pl. All assays were conducted in triplicate and appropriate background controls subtracted.

2.3.5. Statistical analysis

Students paired t-tests were performed using Graphpad Prism (USA) to determine statistical significance $p<0.05$.

2.4. Results

To confirm basal cell surface expression levels of the uPA and uPAR by the U-937 and THP-1 cell lines, immunofluorescence assays were undertaken using flow cytometry. Both components were detected at the cell surface of both cell lines, but compared to the U-937 cell line, the THP-1 cell line showed 7 and 16.5 fold higher levels of uPAR and uPA antigens, respectively (Fig. 2.1).

Previous studies have shown that the rapid endocytosis of uPA:SerpinB2 complexes on human carcinoma cell lines are facilitated by interactions with LRP (Croucher et al. 2006) and VLDLR (Croucher et al. 2007). Therefore LRP and VLDLR were considered the most probable LDLR candidates for the endocytosis of uPA:SerpinB2 complexes on the U-937 and THP-1 cell lines. Indeed VLDLR and LRP were detectable on both cell lines (Fig. 2.1). While low on both cell lines the expression level of LRP was 2-fold higher on the THP-1 cell line compared to the U-937 cell line (Fig. 2.1). Both cell lines displayed distinctly measurable VLDLR, with the THP-1 cell line displaying a 6-fold increase in VLDLR expression compared to the U-937 cell line (Fig. 2.1).

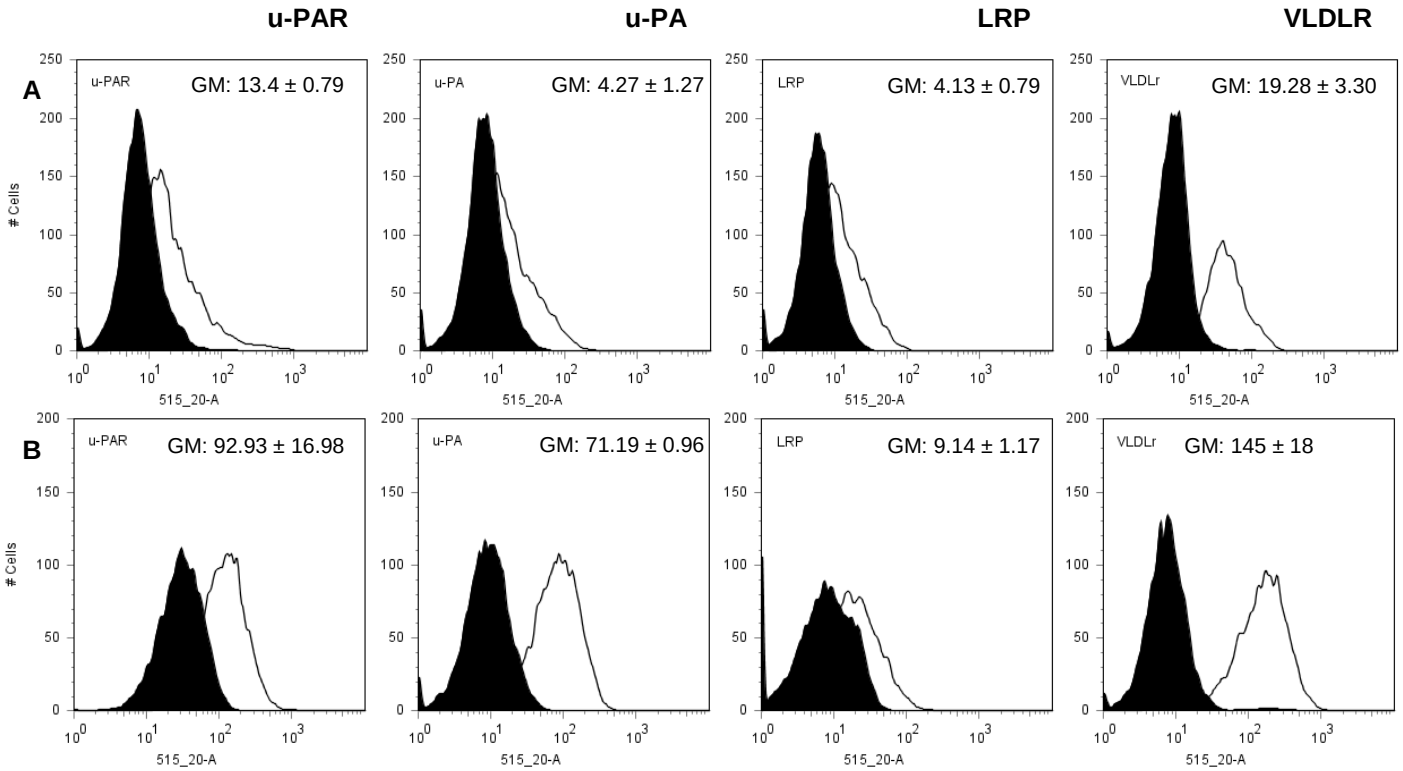

Figure 2.1: Histogram plots showing cell surface expression levels of u-PAR, u-PA, LRP and VLDLR, on the **(A)** U-937 and **(B)** THP-1 monocytic cell lines. Cells were assayed using indirect immunofluorescence and flow cytometry. Geometric means (GM) indicate fluorescence intensity values for specific antibodies (unfilled) with isotype-matched control antibody (filled) values subtracted, ± SD, (n=3).

To obtain a quantitative indication of the cell surface plasminogen activation potential of U-937 and THP-1 cell lines and to compare the SerpinB2 inhibitory capacity, whole cell plasmin generation assays were conducted. Low levels of intrinsic plasmin generation by the U-937 (Fig. 2.2) cell line was detected which is indicative of low endogenous uPA, or indeed tPA levels (refer Fig.2.1). While still low, the THP-1 cell line had higher levels of endogenous plasmin generation than the U-937 cell line (Fig. 2.2), reflecting higher levels of uPA on these cells. Importantly this activity was found to be inhibited in the presence of SerpinB2 (Fig. 2.2), confirming previous studies (Ellis et al. 1990). Pre-treatment with 10 nM uPA significantly increased the plasminogen activating potential of both cell lines (Fig. 2.2), indicating that a portion of the uPAR detected at the cell surface was unoccupied in both cell lines. In both cases SerpinB2 significantly abrogated this activity to below levels in the absence of added uPA (Fig. 2.2).

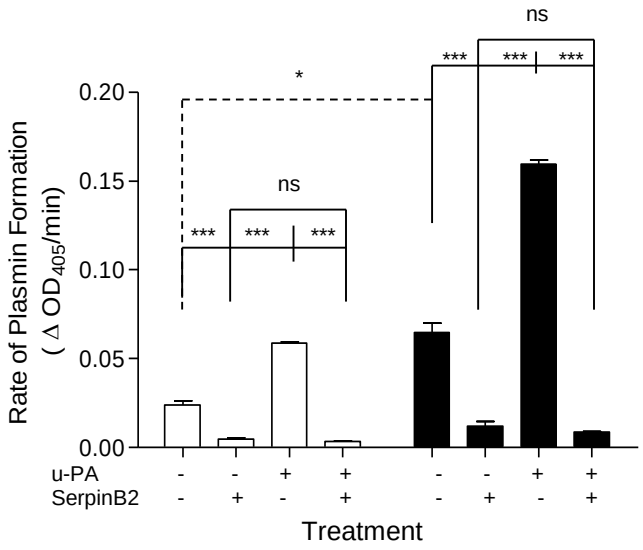

Figure 2.2: Inhibition of cellular plasminogen activation by SerpinB2. U-937 (unfilled bars) and THP-1 (filled bars) cells were pre-treated in the absence or presence of 10 nM u-PA and 10 nM SerpinB2 as indicated. Then glu-plasminogen was added at a final concentration of 0.25 μM and the rate of plasmin formation in the absence or presence of 10 nM SerpinB2 where indicated was analysed using Spectrozyme PL substrate (ADI). Assays were conducted over 2 hs at 37°C. Data represents mean ± SEM, (n=3), background (cells only) subtracted. Statistical analysis by 2-way ANOVA (solid lines) or t-test (dotted line) * = $p<0.05$, *** = $p<0.001$, ns = not significantly different.

uPA:SerpinB2 complex clearance pathways were investigated. Inhibition in the presence of RAP, a commonly used antagonist of ligand binding specific to the LDLR family, significantly inhibited SerpinB2 internalisation seen in both the U-937 and THP-1 cell lines (Fig. 2.3A). The dependence of uPA was demonstrated using a monoclonal antibody specific for the catalytic domain of uPA that, at the concentration used, is known to block SerpinB2 complex formation with uPA at the cell surface of other cell lines (Al-Ejeh et al. 2004). SerpinB2 internalisation was significantly reduced by the MAb in both the U-937 (20%) and THP-1 (80%) cell

lines (Fig. 2.3B). Again, this effect was more pronounced in the THP-1 cell line which expresses significantly greater levels of endogenous uPA and uPAR compared to the U-937 cell line. Taken together these results confirmed the role of receptor bound uPA and LDLRs in the endocytosis of uPA:SerpinB2 by monocytic cell types and that the effect was dependent on endogenous uPA expression.

The involvement of VLDLR and LRP in the endocytosis of SerpinB2 was investigated further using inhibitory antibodies. Anti-VLDLR monoclonal antibodies 1H5 and 1H10 were reported to be effective inhibitors of binding interactions with VLDLR and apolipoprotein E (apoE) (Ruiz et al. 2005) and uPA:SerpinB2 complexes in the MCF-7 cell line (Croucher et al. 2007). Therefore an antibody cocktail comprising of 1H5, 1H10 and 5F3 was used to inhibit uPA:SerpinB2 complex interactions with VLDLR. Although 5F3 alone was not found to efficiently inhibit apoE:VLDLR interactions this monoclonal epitope is specific for the ligand binding repeats within VLDLR (Ruiz et al. 2005) suggesting it may efficiently inhibit the uPA:SerpinB2 complex interactions. As expected, the application of the antibody cocktail inhibited a proportion of SerpinB2 internalisation showing some VLDLR dependence in the endocytosis of SerpinB2 by the U-937 and THP-1 cell lines (Fig. 2.3C). Higher concentrations of the antibody cocktail gave similar results. Consistent with this, the rabbit anti-LRP polyclonal antibody previously found to inhibit uPA:SerpinB2 complexes (Croucher et al. 2006) was also able to block SerpinB2 internalisation in the U-937 cell line

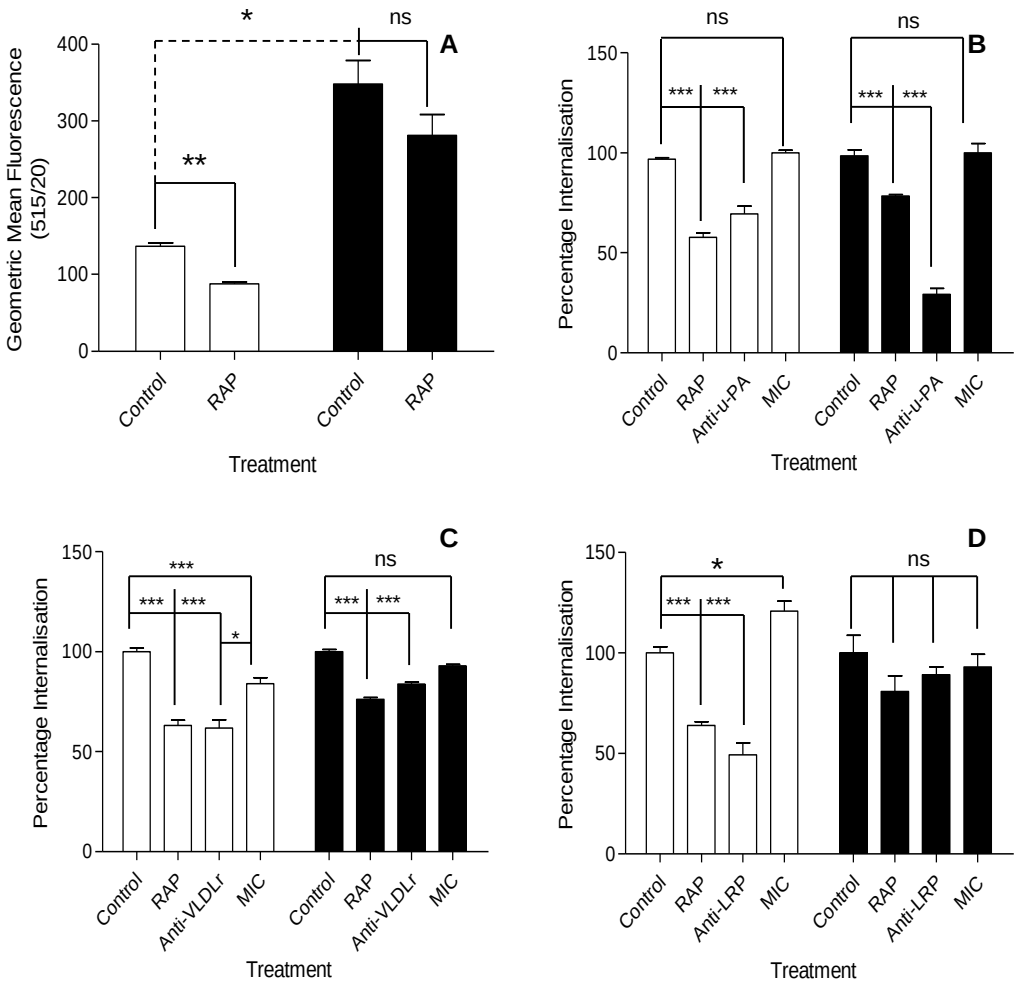

Figure 2.3: Internalisation of SerpinB2:Alexa488 by U-937 (unfilled) and THP-1 (filled) cell lines. **(A)** Representative data shows SerpinB2 internalisation signal pattern. Assays were conducted in the absence (control) or presence of 200 nM RAP and either **(B)** 20 $\mu g.mL^{-1}$ anti-uPA monoclonal antibody or 20 $\mu g.mL^{-1}$ matched isotype control (MIC) where indicated, or **(C)** 15 $\mu g.mL^{-1}$ anti-VLDLR monoclonal antibodies (5H1, 5F3, and 1H10, 5 $\mu g.mL^{-1}$ each) or 15 $\mu g.mL^{-1}$ MIC where indicated or **(D)** 50 $\mu g.mL^{-1}$ anti-LRP polyclonal antibody or 50 $\mu g.mL^{-1}$ MIC. Cells were cultured for 1 h at 37 °C in the presence of 10 nM SerpinB2:Alexa488, surface bound SerpinB2:Alexa488 was quenched by incubating cells with 4 $\mu g.mL^{-1}$ anti-Alexa488 monoclonal antibody for 30 min prior to analysis by flow cytometry. All values shown are means ± SEM (n=3). For panels B-D values are normalised to the control (representing no inhibitory antibody and therefore total internalised SerpinB2) for each cell line. Statistical analysis by 2-way ANOVA (solid lines) or t-test (dotted line) * = $p<0.05$, *** = $p<0.001$, ns = not significantly different.

but not in the THP-1 cell line (Fig. 2.3D). The difference in antibody blocking efficiency between the cell lines may be a result of substantially more VLDLR and LRP on the THP-1 cell line (refer Fig. 2.1.B) and therefore less efficient inhibition.

2.5. Discussion

In this study, we confirmed the presence of uPA, uPAR and LDLR family members at the surface of U-937 and THP-1 monocytic cell lines. The basal levels of uPAR and uPA detected at the cell surface were higher on the THP-1 cell line compared to the U-937 cell line. This is likely due to their differences in maturation along the myeloid differentiation lineage. However, it is important to note that the THP-1 cell line is a naturally occurring SerpinB2 null model, in that the SerpinB2 mRNA is truncated and the translation product inactive (Gross and Sitrin 1990; Katsikis et al. 2000). Therefore the lack of endogenous SerpinB2 in the THP-1 cell line may also contribute to the higher uPA levels detected, compared to the U-937 cell line. Importantly, the differences in detectable uPA and uPAR expression levels observed between these cell lines was supported by the clear difference in plasminogen activation potential, therefore presenting two distinctive cell models for the examination of uPA facilitated SerpinB2 internalisation. The data presented here is consistent with previous studies on carcinoma cell lines (Croucher et al. 2006; Croucher et al. 2007), using similar techniques and reagents. However, this contradicts the work of Ragno et al (1995), who reported that the majority of preformed uPA:SerpinB2 complexes added to THP-1 cells were cleaved and released into the supernatant as a 70 KDa species rather than being internalised.

Conditioned supernatants were not examined within our study, therefore the presence of a 70 KDa species representing cleaved uPA complexed with SerpinB2 cannot be ruled out, however distinct differences in methodology may explain the conflicting results. Specifically, Ragno et al (1995) used widely accepted acid stripping techniques to remove uPAR bound uPA from the cell surface, prior to incubation with pre-formed uPA:SerpinB2 or uPA:SerpinE1 complexes. The method described here (and as per (Croucher et al. 2006)) did not require harsh pre-treatment of the cell line, which could compromise the balance of membrane associated proteases, thus leading to premature degradation of the uPA:SerpinB2 complex. Furthermore, we pre-loaded uPAR with uPA, prior to addition of SerpinB2 which is therefore indicative of mechanisms associated with cell surface inhibition of uPA, which may alter endocytosis dynamics, specific to the THP-1 cell line, or indeed myeloid cells. Regardless, our results clearly show the involvement of VLDLR and LRP in the endocytosis of SerpinB2 via a uPA dependant mechanism by both the U937 and THP-1 cell lines.

Thorough investigation of expression for both antigens by malignant haemopoietic cell types has revealed a correlation between differentiation and uPAR expression. AML - M0 subtype displays low levels of uPAR expression compared to M5 subtype, whilst all AML subtypes have been found to express uPA (Lanza et al. 1998; Scherrer et al. 1999). Importantly, uPA is the predominant plasminogen activator in leukemic marrow, a characteristic not found in healthy marrow (McWilliam et al. 1998; Scherrer et al. 1999), therefore SerpinB2 targeted

therapeutics may prove successful in eradicating MDR leukaemic blasts and stem cells within the marrow of patients. As SerpinB2 interaction with uPA at the cell surface facilitates the rapid endocytosis of the uPA:SerpinB2 complexes (Croucher et al. 2006) this allows for fast uptake of therapeutics. The use of ^{213}Bi-SerpinB2 directed at solid tumours in preclinical trials has shown that SerpinB2 can target uPA and deliver attached cytotoxins (Stutchbury et al. 2007), it is therefore hypothesised that SerpinB2 directed therapies may be as effective for the treatment of haematological malignancies expressing uPA if not more so due to the enhanced cell surface accessibility of single cell malignancies.

Furthermore, as the endocytosis of uPA:SerpinB2 complexes is in part VLDLR and LRP dependent in the U-937 and THP-1 cell lines, utilisation of this specific endocytosis process in the design of fusion toxins will allow increased specificity for SerpinB2 directed therapeutics, giving potential for tailoring to the individual. This is of particular importance given the potential for alternative endocytosis pathways for internalisation of SerpinB2, as indicated by this work. Whereby, complete inhibition of SerpinB2 internalisation using either RAP or LDLR inhibitory antibodies was not possible. Investigation of the role scavenger receptors may play is therefore required to further the development of SerpinB2 directed therapeutics.

Current treatment regimes for AML comprise of intensive combination induction therapies and in some cases stem cell transplantations, despite this at least half of paediatric patients who reach complete remission will relapse with poor

prognostic outcomes (Meshinchi and Arceci 2007). For patients exhibiting high uPA expression, SerpinB2:toxins may prove successful in targeting residual leukaemic cells post-induction therapy, therefore reducing the cases of disease relapse.

The preliminary work presented here contributed towards the proof of concept data for the use of SerpinB2:cytotoxin targeting of the U-937 and THP-1 cell line. Importantly, further work within our research group has since shown successful uPA specific targeting of these cell lines (Vine et al. 2012).

3. Differential Endocytosis of Tissue Plasminogen Activator by Serpin E1 and SerpinB2 on Human Peripheral Blood Monocytes

3.1. Abstract

Generation of the broad spectrum protease plasmin is facilitated by the tissue (tPA) and urokinase (uPA) plasminogen activators, within multiple physiological and disease states. Finely tuned control of this proteolytic cascade is exerted by the plasminogen activator inhibitors type-1 (PAI-1/SerpinE1) and 2 (PAI-2/SerpinB2). Expression of this network of activators and inhibitors by cells of myeloid lineage appears to be highly interchangeable between physiological environments, and whilst the role of SerpinE1 and SerpinB2 in regulating uPA-dependent functions is well established, the interaction between tPA and SerpinB2 on myeloid cell types is poorly characterised. To this end, we used freshly isolated peripheral blood monocytes (PBM) as a model of a tPA-dependent cellular environment. We demonstrate that while both SerpinE1 and SerpinB2 could inhibit surface-bound tPA and are internalised predominately via low density lipoprotein receptor family members, SerpinE1 enhanced the endocytosis of tPA, whereas SerpinB2 did not. Surface plasmon resonance analyses revealed differential binding affinities between the very low density lipoprotein receptor (VLDLR) and tPA and tPA:SerpinE1 complexes in addition to those previously described with low density lipoprotein receptor-related protein (LRP). Moreover, tPA:SerpinB2 bound to both endocytosis receptors with similar kinetics to tPA. These differential biochemical interactions between tPA and the tPA:PAI complexes may underlie the observed differences in endocytosis mechanisms on the PBMs. This suggests that while SerpinE1 and SerpinB2 function similarly in the control of cellular plasmin

generation by tPA, they may have disparate effects on the alternative functions of tPA via modulation of its engagement with endocytosis receptors.

3.2. Introduction

The tissue plasminogen activator (tPA) converts plasminogen to plasmin, which is involved in fibrinolysis, tissue remodelling and cell migration (Kruithof et al. 1995). tPA is secreted as a single chain (sc-tPA), 72 kDa glycosylated protein, by peripheral blood monocytes (Hart et al. 1989) and endothelial cells (Hajjar 1993). Cleavage of sc-tPA produces the 62.9 kDa two chain (tc-tPA) conformation (Rijken and Collen 1981). Both sc-tPA and tc-tPA display enzymatic activity towards plasminogen, which is enhanced when they are bound to fibrin (Hoylaerts et al. 1982). In addition to fibrin interactions, both forms of tPA also bind and efficiently activate plasminogen at the cell surface of monocyte (Felez et al. 1991; Felez et al. 1996), macrophage (Noorman et al. 1995), endothelial (Ljungner et al. 1983) and human tumour (Lobov et al. 2008) cell lines.

Control of plasmin generation by either form *in vivo* is thought to be mediated predominantly through the inhibitory functions of the plasminogen activator inhibitor type 1 (PAI-1/SerpinE1) and potentially to a lesser extent by plasminogen activator inhibitor type 2 (PAI-2/SerpinB2) (Jorgensen et al. 1987). Both SerpinE1 and SerpinB2 efficiently inhibit tc-tPA in solution phase with second order rate constants of ~10^7 and 10^5 $M^{-1}.s^{-1}$, respectively, and both are inefficient inhibitors of fibrin bound tPA (Thorsen et al. 1988; Ritchie et al. 1999). Therefore tPA:PAI complexes are typically formed after tPA dissociates from the fibrin clot. However,

SerpinE1 is considered the primary inhibitor of tPA as it is able to form serpin-protease complexes with both sc-tPA and tc-tPA and is found in normal human plasma at concentrations ranging from 140 pM to 1.9 nM (Estelles et al. 1989). SerpinB2 is only detected within plasma during late stage pregnancy but, with concentrations ranging between 100-250 ng/mL (Kruithof et al. 1987; Hunt et al. 2009). A role in maintaining placental integrity has been described for SerpinB2, as a regulator of fibrinolysis in normal pregnancy (Astedt et al. 1998), however, little is understood about the potential of SerpinB2 as a physiological inhibitor of tPA due to limited reports of tPA:SerpinB2 complexes identified *in vivo* (Kruithof et al. 1995). Yet, co-expression of tPA and SerpinB2 has been shown in normal bone marrow (McWilliam et al. 1998), skin (Chen et al. 1993), saliva and salivary gland tissue (Virtanen et al. 2006), gingival fluid (Brown et al. 1995; Kinnby 2002), as well during pregnancy (Astedt et al. 1998), and SerpinB2 is able to inhibit cell surface bound tc-tPA *in vitro* (Lobov et al. 2008). Furthermore, enhanced expression of both tPA and SerpinB2 by epithelial cells is indicative of some disease states, e.g. periodontal disease (Kinnby 2002), psoriasis and pre/eclampsia (Kruithof et al. 1995), strongly suggesting that SerpinB2 may control tPA activity at sites of localised inflammation.

Whilst SerpinB2 expression can be up-regulated by a variety of cell types under stress conditions, the predominant physiological producers of SerpinB2 are monocytes and macrophages (Kruithof et al. 1995). Monocytes also express and secrete tPA (Hart et al. 1989) which has been shown to bind to the surface of these

cells via numerous and varied receptors (Felez et al. 1991; Otter et al. 1991; Noorman et al. 1995). Furthermore, Ritchie et al. (1995) reported the up-regulation of SerpinB2 expression by monocytes cultured in the presence of thrombin. This suggests a potential role for SerpinB2 in the homeostatic balance between thrombosis and fibrinolysis at local sites of inflammation or during wound healing processes, possibly through the inhibition and clearance of tc-tPA from the pericellular environment.

Clearance of tPA and tPA:SerpinE1 from the circulation via endocytic processes in the liver is well characterised (Wing et al. 1991; Nguyen et al. 1992). The mechanisms for endocytosis of these ligands have been shown to be dependent on members of the low density lipoprotein receptor (LDLR) family, specifically LRP (Bu et al. 1992; Orth et al. 1992) and scavenger receptors such as the mannose receptor (CD206) (Otter et al. 1991). The rate of endocytosis of SerpinE1-inhibited tPA was shown to be accelerated compared to tPA only, on rat hepatoma cells (Camani et al. 1994). This acceleration in clearance was found to be due to the increased affinity of tPA:SerpinE1 complexes for LRP (Horn et al. 1998). Interestingly, Camani et al. (2000) found that Novikoff rat hepatoma cells, MEF-1 mouse embryonic fibroblasts, HT1080 fibroblasts and COS African green monkey kidney cells were all able to degrade [^{125}I]tPA and [^{125}I]tPA:SerpinE1 via LRP-mediated uptake, whilst the THP-1 and U-937 monocytic cell lines were not. The authors suggested that a co-receptor, absent on the THP-1 and U-937 cell lines, may be required for these ligands to interact with LDLRs. However, tPA was shown

to specifically bind to the surface of freshly isolated peripheral blood monocytes (PBM), THP-1 and U-937 cell lines (Felez et al. 1991). Macrophages derived from human PBMs were shown to take up and degrade [^{125}I]tPA via the mannose receptor (Noorman et al. 1995). Furthermore, Simon et al. (1995) showed LDLR-family dependant endocytosis and degradation of [^{125}I]tPA:SerpinE1 by the THP-1 cell line. Thus, the potential function of SerpinE1 or SerpinB2 in the inhibition and enhanced endocytosis of tPA bound to myeloid cell types remains unclear.

3.2.1. Specific Aims

In order to clarify and compare the role of these serpins as regulators of cellular tPA, freshly isolated PBMs were utilised as a non-transformed tPA-dependent cellular model representing myeloid lineages (McWilliam et al. 1998). The specific aims of this chapter were to examine inhibition of tPA by SerpinB2 and characterise the role of LRP and VLDLR as potential endocytosis receptors for tPA and tPA:PAI complexes on these cells. Cell profiling of the U-937 and THP-1 cell line in addition to PBMs were undertaken to ascertain basal PA levels present on the surface of malignant versus healthy myeloid cells with the aim of assessing the potential impact, if any SerpinB2 directed therapeutics may have through non-uPA facilitated endocytosis pathways.

3.3. Methods

3.3.1. Materials

Recombinant human SerpinB2 (47 kDa form) was provided by SerpinB2 Pty Ltd (Sydney, Australia). Purified human receptor associated protein (RAP), recombinant human serpinE1 (stable mutant) and human tc-tPA were obtained from Molecular Innovations (MD, USA). Spectrozyme PL substrate, murine anti-human uPA B-chain IgG_1 (#394), murine anti-human tPA IgG_1 (#E-4) and murine anti-human LRP α-chain IgG_1 (#3402) were supplied by American Diagnostica Inc. (USA). Rabbit anti-human VLDLR IgG and rabbit anti-annexin II (p36) were from Santa Cruz Biotechnology, Inc. Goat anti-S100A10 (p11) was from R&D Systems. Goat anti-rabbit FITC conjugate IgG (whole molecule), goat anti-mouse IgG (Fab specific) FITC conjugate, rabbit anti-goat IgG (whole molecule) FITC conjugate, goat IgG, propidium iodide (PI), Hanks balanced salt modified and non-modified, bovine serum albumin (BSA), human fibrin, D-phenylalanyl-L-prolyl-L-arginine chloromethyl keytone (PPACK) and OptiPrep^{TM} density gradient medium were from Sigma-Aldrich. Alexa 488 protein labelling kit and Alexa 488 quenching polyclonal antibody were from Molecular Probes (OR, USA). Murine α-CD14-texas red conjugated monoclonal antibody was purchased from Invitrogen (USA). Murine α-CD206 monoclonal antibody was purchased from Hycult-biotech (Netherlands). Recombinant human tPA (Actylise, a mixture of sc and tc-tPA) was a kind gift from Boehringer-Ingelheim, Australia.

3.3.2. Isolation of Human Peripheral Blood Monocytes

Peripheral venous blood was collected from donors into EDTA vacuum tubes (BD Biosciences, Nth Ryde, Australia) under controlled conditions by a trained phlebotomist at the University of Wollongong (UOW) (protocol approved by UOW, Human Ethics Committee, approval number HE00/221). Buffy coats were prepared by centrifuging whole blood samples at 1300 g for 30 min. White blood cells were removed under sterile conditions and monocytes isolated using OptiPrep™ as per the manufacturer's instructions. This methodology yielded cell preparations containing 60 to 80% CD14 positive (monocyte) cells as determined by flow cytometry. Freshly isolated PBMs were used immediately for all experiments.

3.3.3. Plasminogen Activation Assays

Cells were washed and resuspended at $1x10^6$ cells.mL^{-1} in Tris Buffered Saline (TBS) (50 mM Tris, 150 mM NaCl, pH 7.4), incubated on ice in the absence or presence of 100 nM tPA for 40 min and then washed twice in TBS to remove excess unbound protein. Triplicate 50 µL cell suspensions were then aliquoted into 96-well microtitre plates and incubated for 15 min at room temperature, in the absence or presence of increasing concentrations of serpinE1, SerpinB2 and 10 µg.mL^{-1} plasminogen made up to a final volume of 100 µL with TBS buffer. Spectrozyme PL substrate (100 µL) was then added to a final concentration of 0.25 mM and substrate conversion by plasmin measured kinetically at 405 nm over 2 h at 37 °C using a SpectraMax 250 plate reader; data was recorded using SoftMax® Pro software (Molecular Devices, USA). Negative controls contained cells alone

(no tPA or plasminogen). Other controls consisted of tPA (100 nM) in the absence or presence of 1.4 μM fibrin, plasminogen (10 μg.mL^{-1}) and Spectrozyme PL (0.25 mM), as previously described (Lobov et al. 2008). Background absorbance (buffer only wells) was subtracted from all data.

3.3.4. Flow Cytometry Analysis

3.3.4.1. Cell surface antigen detection

Membrane bound antigens were detected using indirect immunofluorescence assays, essentially as previously described (Ranson et al. 1998). Briefly, cells were suspended at a final concentration of 1x10^6 cells.mL^{-1} in ice cold binding buffer (phenol red-free Hanks buffered salt solution, pH 7.4, containing 1 mM $CaCl_2$, 1 mM $MgCl_2$ and 0.1% BSA) containing 10 μg.mL^{-1} of primary antibody and incubated on ice for 40 min. After washing steps, the cells were resuspended with ice-cold binding buffer containing 1:100 dilution of FITC conjugated secondary antibody, followed by incubation with 10 μg.mL^{-1} α-CD14-texas red conjugated antibody (for identification of PBMs). Cells were then washed prior to analysis by flow cytometry, with viable cell populations selected through propidium iodide (PI) exclusion. Isotype matched control antibodies were used to assess non-specific binding due to the primary antibody. All data obtained was analysed using FLOJO software version 7.1 (Treestar, Inc) and was restricted to CD14 positive/PI negative cells. All geometric mean fluorescence values reported represent mean fluorescence intensity for specific binding ± SEM. All assays were conducted in triplicate.

3.3.4.2. Ligand binding assay

Cell surface binding analyses were conducted by incubating cells on ice in binding buffer containing increasing amounts of Alexa488-labelled tPA ($tPA_{Alexa488}$) or BSA ($BSA_{Alexa488}$) (negative control) for 40 min. This was done in order to allow maximal cell surface binding by also minimising internalisation of tPA. Cells were then washed twice with ice cold PBS and analysed using flow cytometry as described above.

3.3.4.3. Internalisation assays

This assay has previously been utilised to characterise the clearance pathways of uPA:SerpinB2 complexes on PC-3 cells (Croucher et al. 2006) and was therefore adapted for characterisation of Actylise-tPA:$_{Alexa488}$ clearance pathways in this study. Briefly, cells were incubated for 40 min at $1x10^6$ cells.mL^{-1} in binding buffer, containing 0 (control) or 100 nM tPA or $tPA_{Alexa488}$, on ice to minimise internalisation. After washing to remove excess unbound tPA, cells were incubated with either SerpinB2 or $SerpinB2_{Alexa488}$ (where stated), SerpinE1 or no additions and incubated at 37 °C for the time periods indicated. All subsequent steps were performed at 4 °C. The cells were next washed twice and incubated for 30 min with 4 μg.mL^{-1} Alexa488 quenching antibody (quenches any remaining cell surface fluorescence and is thus a measure of internalised ligand). Then, after washing, the cells were incubated for 40 min with 10 μg.mL^{-1} α-CD14 monoclonal antibody. Finally, the cells were washed twice with ice cold PBS and analysed using flow cytometry as described above.

3.3.5. Surface Plasmon Resonance Assays

Kinetic analysis was performed using a BIAcore 2000 (BIAcore AB, Uppsala, Sweden). LRP or VLDLR was immobilised on to a CM5 BIAcore chip according to the manufacturer's instructions. Briefly, the chip was activated using a 1:1 mixture of 0.2 M *N*-ethyl-*N'*-(3-dimethylaminopropyl)carbodi-imide and 0.05 M *N*-hydroxysuccimide. LRP or VLDLR was coated on to the chip at 40 $\mu g.mL^{-1}$ in 10 mM sodium acetate buffer (pH 3) for 7 min at 5 $\mu L.min^{-1}$, as previously described (Croucher et al. 2007), to a level of 2000 response units (VLDLR) or 2000 to 10000 response units (LRP). The un-occupied binding sites were blocked using 1 M ethanolamine, pH 8.5. Analytes (tPA, tPA:PAI) were buffer exchanged into running buffer (10 mM HEPES (pH 7.4), 140 mM NaCl, 1 mM $CaCl_2$, 0.05% v/v Tween-20) before applying to the BIAcore chip at 20 $\mu L.min^{-1}$. A serial dilution of analytes ranging from 500 – 15 nM were used to allow kinetic analyses. tPA:PAI complexes were prepared by incubating tPA with SerpinE1 (1:1 molar ratio) or SerpinB2 (1:3 molar ratio) for 60 min at 37 ˚C. An excess of SerpinB2 could be used and not removed from the tPA:SerpinB2 solutions as un-reacted SerpinB2 does not bind LRP or VLDLR (Croucher et al. 2006; Croucher et al. 2007; Cochran et al. 2009; Cochran et al. 2011). SDS-PAGE confirmed the presence of tPA:SerpinE1 or tPA:SerpinB2 complexes with minimal/negligible residual free tPA or SerpinE1 (Fig. 3.1). In all cases the analyte concentration refers to the concentration of tPA present. Regeneration of the chip was achieved using 100 mM H_3PSO_4. All buffers were filtered and degassed before use. For kinetic analysis, a blank cell was used

as the reference cell and data was analysed using BIAevaluation software (Version 3).

Figure 3.1: Representative gel showing preformed tPA:PAI complexes. Stock solutions were prepared by incubating tPA with SerpinE1 (1:1 molar ratio) or SerpinB2 (1:3 molar ratio) for 60 min at 37 ˚C and used for comparison of kinetic interactions with LRP and VLDLR using Surface Plasmon Resonance. Excess PAI-2 could be utilised to make the complexes as residual (free) PAI-2 does not interact with LRP or VLDLR (Croucher et al. 2006; Croucher et al. 2007; Cochran et al. 2011).

3.3.6. Statistical Analysis

Statistical significance was determined using Students t-test and was performed using GraphPad Prism version 5.00 for Windows, GraphPad Software, San Diego California USA (***www.graphpad.com***).

3.4. Results

3.4.1. Cell surface expression profiles of tPA, uPA and potential receptors on U-937, THP-1 and Peripheral Blood Monocytes.

To ascertain basal cell surface expression levels of the plasminogen activation systems by the U-937, THP-1 cell lines compared to peripheral blood monocytes (PBMs), immunofluorescence assays were undertaken on all cells using flow cytometry. As described in chapter 2, the uPA system was detected at the cell surface of both cell lines, with highest expression observed on the THP-1 cell line corresponding to a 17 and 39 fold increase in specific fluorescence intensity compared to the U-937 and PBMs respectively (Tab. 3.1). Conversely, surface bound tPA was detectable on PBMs whilst absent from both monocytic cell lines (Tab. 3.1).

Table 3.1: Ligand expression profiles of plasminogen activators and associated receptors.

	U-937 Cell Line	THP-1 Cell Line	Peripheral Blood Monocytes
Ligand	Relative MFI ± SEM		
uPA	4.27 ± 1.27	71.19 ± 0.96	1.82 ± 0.5
tPA	ND	ND	5 ± 0.9
LRP	5.0 ± 0.8	9.14 ± 1.17	15.7 ± 1.3
VLDLR	19.4 ± 3.2	145 ± 18	70.5 ± 0.8
Annexin 2A (P36)	67.0 ± 4.6	43 ± 4	68.78 ± 5.9
S100A10 (P11)	ND	18 ± 9	ND
Mannose Receptor (CD206)	ND	ND	ND

Data represents mean fluorescence intensity (MFI), with relevant matched isotype control values subtracted (n=3, ± SEM). ND = not detected.

Both LRP and VLDLR were detected on all cell types. The PBMs exhibited the highest LRP expression with 1.7 and 3 fold higher mean fluorescence intensity compared to the THP-1 and U-937 cell lines, respectively (Tab. 3.1). The THP-1 cell line was found to have the highest VLDLR cell surface level with 2 and 7.5 fold higher mean fluorescence intensity compared to the PBMs and U-937 cells, respectively (Tab. 3.1). As tPA is reported to also bind the mannose receptor and the annexin II heterotetramer (AIIt), cell surface profiles for these antigens were undertaken. All cell types expressed detectable levels of annexin 2A (p36) with comparable expression between the U-937 cell line and PBMs, whilst the THP-1 cell line exhibited 1/3 less detectable P36 (Tab. 3.1). Interestingly the THP-1 cell line was found to also express p11, the second component of the AIIt, whilst it was not detectable on the surface of either the U-937s or the PBMs. It was not possible to detect the mannose receptor (CD206) on any cells (Tab. 3.1).

3.4.2. Tissue Plasminogen Activator; cell surface binding potential (exogenous protein addition)

Since at least one known tPA receptor, p36, was detected, we tested the binding of exogenous tPA to PBMs. When incubated on ice to minimise internalisation and/or proteolytic activity, the binding of tPA to PBMs was saturable within 40 min, showing maximum binding at about 200 nM (Fig. 3.2A). A negative control BSA-Alexa488 did not bind to the cell surface at the highest equivalent tPA concentration (Fig.3.2B). We next tested the contribution of LDLRs to the direct binding of tPA to PBMs. Pre-incubation of the cells with RAP significantly reduced cell surface binding of exogenous tPA to PBMs (Fig. 3.2C) by 30%. This level of

inhibition was consistent with previous studies using human umbilical vein endothelial cells (Mulder et al. 1997), indicating that LDLR family members are functional cell surface receptors for tPA in addition to the potentially numerous other receptors represented by the non-RAP inhibitable binding interactions. Furthermore, tPA bound only to the CD14-positive stained (i.e. PBM) cells within the cell suspension, indicating that the other blood cell types present did not bind measurable amounts of tPA (Fig. 3.2D).

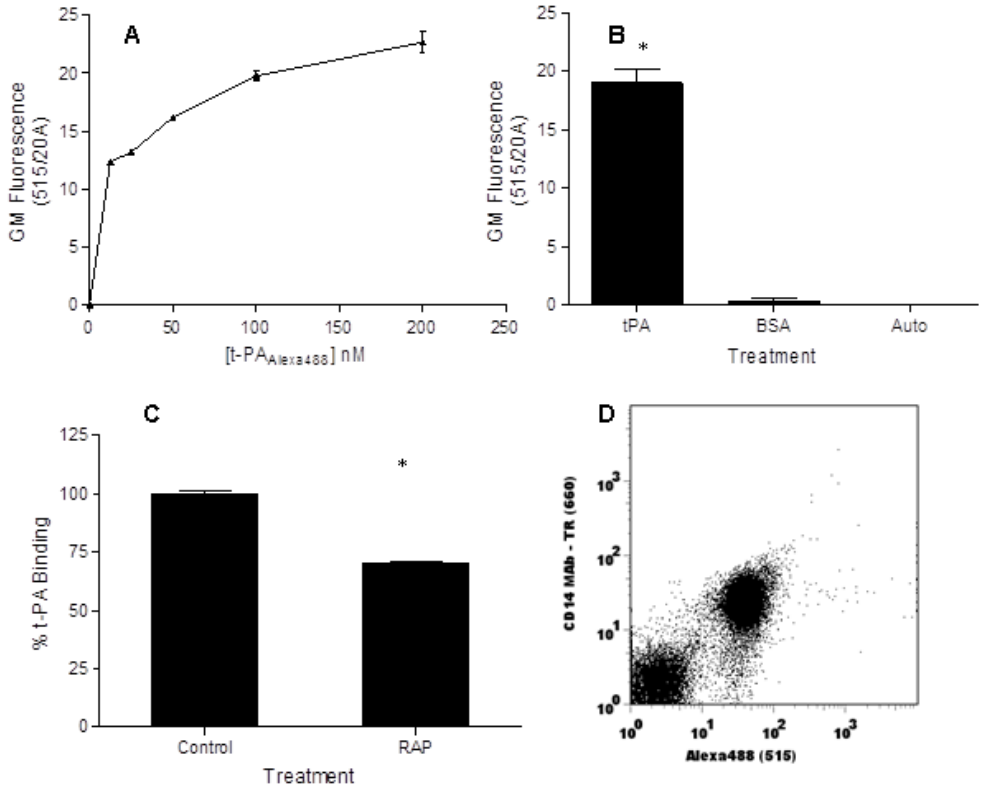

Figure 3.2: Characterisation of Actylise-tPA binding to PBMs. (A) Plot showing the concentration dependence of the binding of Alexa488-labelled Actylise-tPA to the surface of PBM. **(B)** Binding of 200 nM Alexa488-labelled Actylise-tPA or Alexa488-BSA (control) to the cell surface of PBM. **(C)** Plot showing the effects of RAP on cell surface binding of Alexa488-labelled Actylise-tPA using flow cytometry. Data within A, B and C plots, represents the geometric mean (GM) fluorescence, corrected for auto-fluorescence, n=3 ± SEM. **(D)** Two dimensional flow cytometry dot plot showing Alexa488-labelled Actylise-tPA binding (515 nm) to CD14 positive (660 nm) cell population.

Of note, significantly more Actylise-tPA:$_{Alexa488}$ bound to the PBMs (> 4 fold at 100 nM or 200 nM) compared to the U-937 and THP-1 cell lines which bound comparable levels (Fig. 3.3A). The specificity of tPA binding to the U-937 cell lines was confirmed using the negative control, BSA-Alexa488, which did not bind to the cell surface at the highest equivalent tPA concentration (Fig.3.3B). Non-specific binding of Actylise-tPA was not tested for the THP-1 cell line and therefore cannot be ruled out.

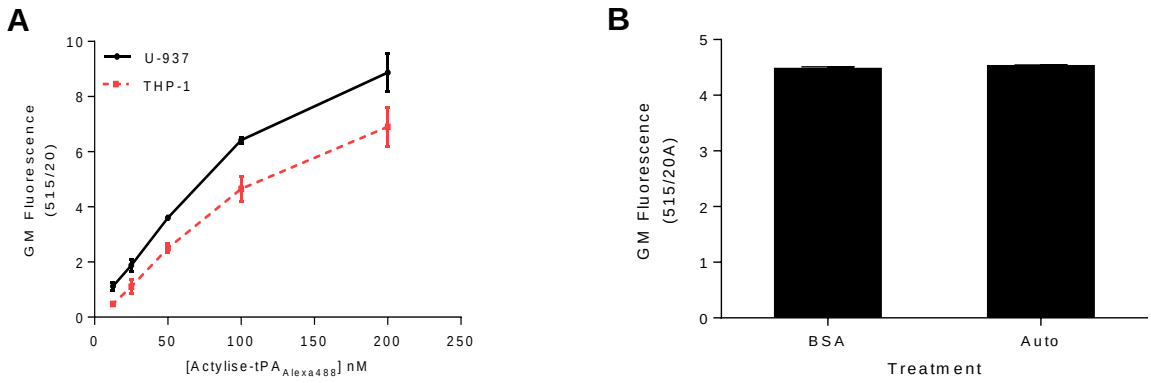

Figure 3.3: Exogenous tPA b**inding potential of cell models. A)** The U-937 and THP-1 monocytic cell lines were incubated on ice for 40 min in the absence (auto fluorescence) or presence of Actylise-tPA$_{Alexa488}$ at concentrations indicated. Unbound Actylise-tPA$_{Alexa488}$ was then removed via centrifugation and cell surface bound Actylise-tPA$_{Alexa488}$ measured using flow cytometry. **B)** Specificity of Actylise-tPA binding to the U-937 cell line was confirmed using 100 nM BSA$_{Alexa488}$ under the same conditions. Data represents the geometric mean (GM) fluorescence (panel A and B) with background (auto fluorescence) removed (panel A only), n=3 ± SEM.

3.4.3. tc-tPA mediated cell surface plasmin generation

To obtain a quantitative indication of the cell surface plasminogen activation potential, whole cell plasmin generation assays were conducted. Saturation of the

cell surface with exogenous tc-tPA caused a significant increase in cellular plasmin activity (Fig. 3.4). As expected from previous work showing inhibition of cell surface tPA by SerpinB2 on the MCF-7 and HeLa cell lines (Lobov et al. 2008), SerpinB2 was also able to inhibit cell surface tc-tPA on PBMs at similar concentrations (Fig. 3.4). SerpinE1 was overall more efficient at inhibiting plasmin formation compared to SerpinB2, resulting in 95 - 100% inhibition at all concentrations used (Fig. 3.4). However, at 50 nM SerpinB2 inhibited about 80% of plasmin formation while at 200 nM both serpins inhibited plasmin formation by > 90%.

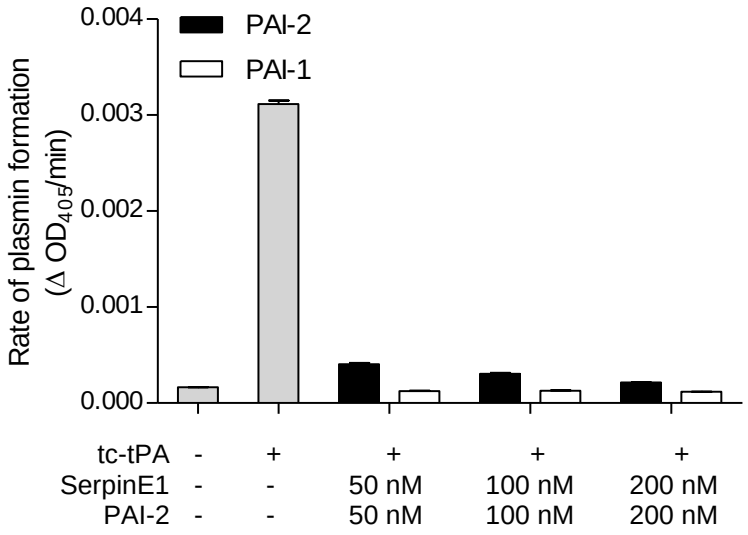

Figure 3.4: Plot showing inhibition of PBM-mediated plasminogen activation by exogenous SerpinE1 and SerpinB2. Freshly isolated PBMs were pre-incubated in the absence or presence of 100 nM tc-tPA where indicated. Then glu-plasminogen was added at a final concentration of 0.25 μM and the rate of plasmin formation in the absence (grey) or presence of either SerpinE1 or SerpinB2 (50, 100, 200 nM), was analysed using Spectrozyme PL substrate (ADI). Assays were conducted over 2 hs at 37 °C. Data represents mean ± SEM, (n=3), background (cells only) value subtracted.

Investigation of plasmin formation at the cell surface in the absence or presence of SerpinB2 was also conducted using the U-937 and THP-1 cell lines. Low levels of intrinsic plasmin generation were detected (Fig.3.5), which is indicative of low to negligible endogenous of either tPA or uPA levels on these cell lines (see Table 3.1). The addition of tc-tPA resulted in a significant enhancement of cell surface plasmin activity on both cell lines (Fig 3.5) reflecting the ability if these cells to specifically bind exogenous tPA (see Fig 3.3). At tc-tPA to SerpinB2 concentration ratios of 2:1, 1:1 and 1:2, SerpinB2 was able to inhibit the rate of plasmin formation on the U-937 cell line by 60%, 70% and 80%, respectively when compared to no SerpinB2 control (Fig. 3.5). Importantly, these results were consistent with those obtained using freshly isolated PBMs (Fig. 3.4). Conversely at the same concentration ratios SerpinB2 was only able to inhibit the rate of plasmin generation on THP-1 cells by 18%, 30% and 43%, respectively (Fig 3.5). It is important to note that the THP-1 cell line was shown to have significantly more surface bound endogenous uPA compared to the U-937 cell line and PBMs (Table 3.1). Furthermore, pro-uPA is activated by plasmin, therefore addition of exogenous tc-tPA may also increase uPA activity. Therefore the reduced efficiency of SerpinB2 to inhibit plasmin generation at the cell surface of the THP-1 cell line may be attributed to the variability in ratios of SerpinB2 to total plasminogen activator potential, at the cell surface.

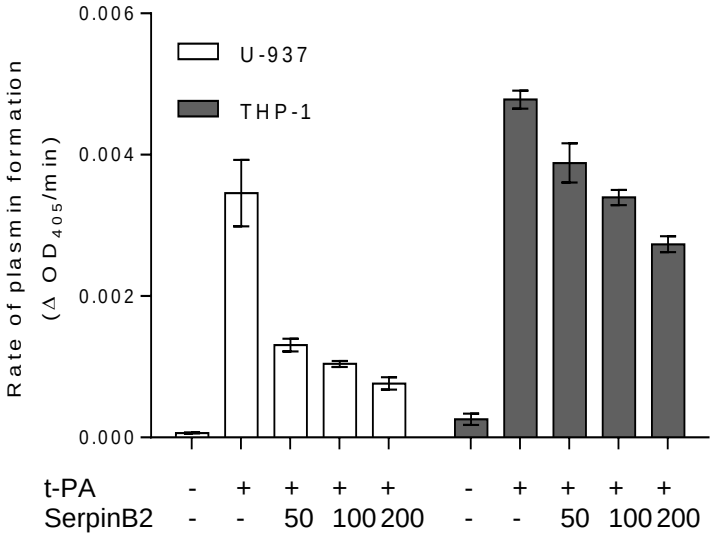

Figure 3.5: Inhibition of cellular plasminogen activation by SerpinB2. U-937 (un-filled) and THP-1 (filled) cells were pre-treated in the absence or presence of 100 nM tc-tPA where indicated. Then glu-plasminogen was added at a final concentration of 0.25 μM and the rate of plasmin formation in the absence or presence of SerpinB2 (50, 100, 200 nM), was analysed using Spectrozyme PL substrate (ADI). Assays were conducted over 2 hs at 37 °C. Data represents mean ± SEM, (n=3), background (cells only) subtracted.

3.4.4. Endocytosis of Tissue Plasminogen Activator by Monocytic Cell Lines and Peripheral Blood Monocytes

As tPA bound to the cell surface generated plasmin and this activity was inhibited by SerpinB2 we next examined the internalisation of Actylise-tPA:SerpinB2 complexes by the U-937 and THP-1 cell lines. A moderate but significant increase in $SerpinB2_{Alexa488}$ internalisation was observed for both cell lines upon pre-incubation with 50 nM Actylise-tPA compared to no exogenous Actylise-tPA controls (Fig. 3.6). As these cells were incubated on ice in the absence (control) or presence of Actylise-tPA to facilitate binding of exogenous tPA prior to

incubation at 37 °C with SerpinB2$_{Alexa488}$ this data represents internalisation of tPA:SerpinB2 complexes formed at the cell surface.

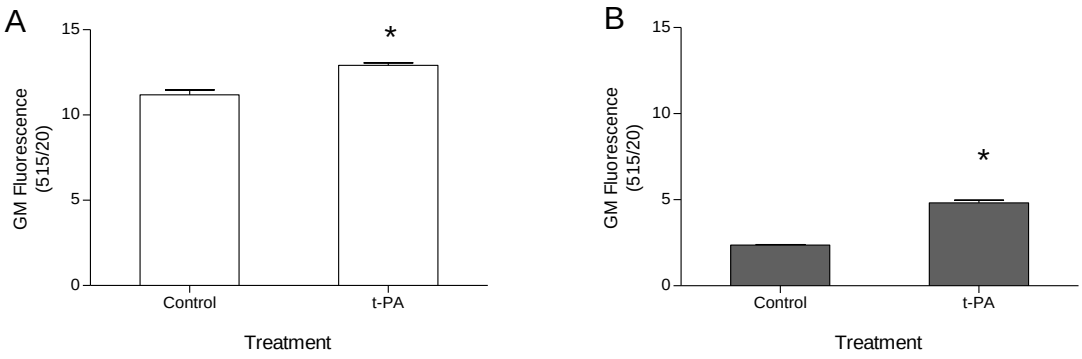

Figure 3.6: Tissue Plasminogen Activator facilitated internalisation of SerpinB2:$_{Alexa488}$ by the (A) U-937 and (B) THP-1 monocytic cell lines. Cells were incubated in the absence (control) or presence of 50 nM exogenous Actylise-tPA on ice for 40 min. Excess Actylise-tPA was removed by centrifugation, the cells were then resuspended in 10 nM SerpinB2:$_{Alexa488}$ and incubated at 37°C for 1 h. Surface bound SerpinB2:$_{Alexa488}$ was quenched on ice for 30 min with 4 μg.mL^{-1} rabbit-α-Alexa488 prior to analysis using flow cytometry. Data represents geometric mean (GM) fluorescence with background (auto-fluorescence) removed, n=3 ± SEM. * $p<0.05$ significantly different from cell line control.

We next investigated the internalisation of Actylise-tPA complexes by freshly isolated PBMs in the absence or presence of either SerpinB2 or SerpinE1. Blood samples were collected and cells isolated using OptiPrep^{TM} for immediate use in flow cytometry experiments and PBMs selected for, using anti-CD14 antibodies (Fig 3.7).

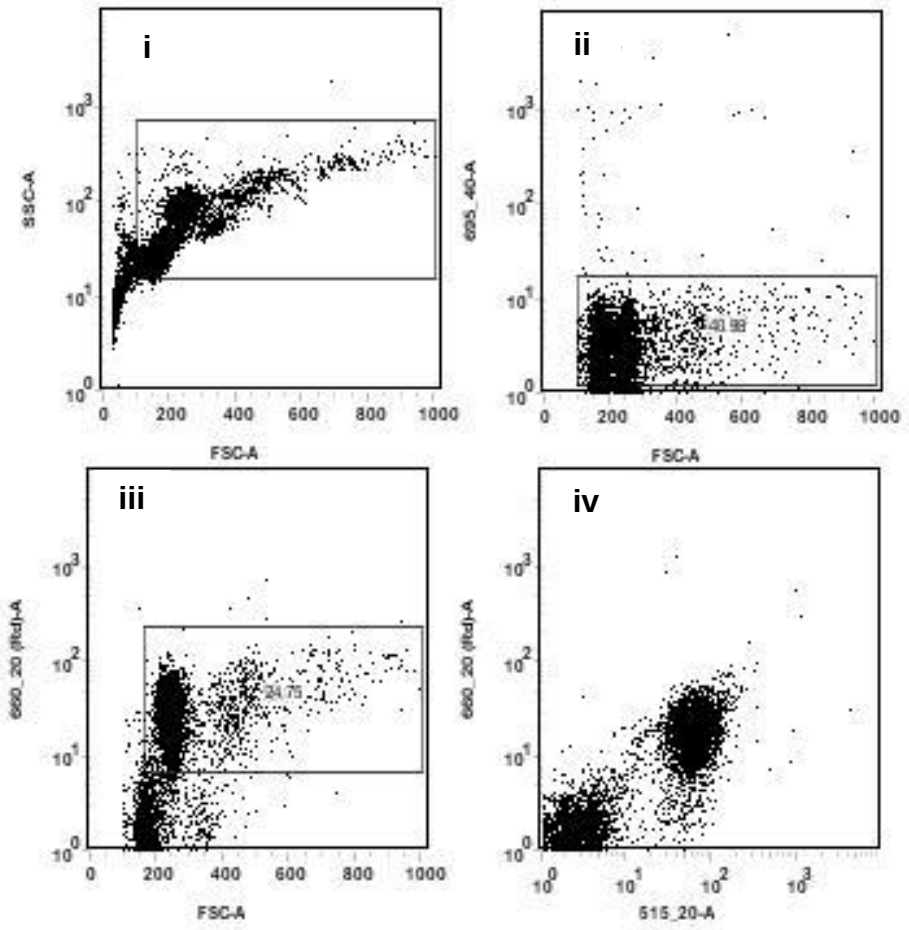

Figure 3.7: Identification of Peripheral Blood Monocytes. Freshly isolated blood monocytes where initially gated for based on side and forward scatter (i) then viable cells within this gate where selected using propidium iodide exclusion (695/40A) (ii) Cells where pre-stained with α-CD14 MAb, detected using α-mouse:Alexa633 and positive cells gated further for analysis (iii). Actylise-tPA:Serpin complex internalisation was therefore assessed on PI negative, α-CD14 positive cells and quantitated on Alexa488 positive fluorescence intensity (iv).

PBMs were found to endocytose both Actylise-tPA$_{Alexa488}$ and Actylise-tPA$_{Alexa488}$:Serpin complexes using a quenching internalisation assay (Fig. 3.8). Cells were pre-treated with 100 nM Actylise-tPA:$_{Alexa488}$ and excess unbound protein removed prior to addition of either SerpinE1 or SerpinB2, therefore

complexes cleared in this assay were those formed at the cell surface. Comparison of clearance efficiency between Actylise-tPA only, Actylise-tPA:SerpinB2 and Actylise-tPA:SerpinE1 was assessed at 37 °C, over a 30 min period. In the absence of serpins, increasing levels of Actylise-tPA:$_{Alexa488}$ were internalised over the time course (Fig. 3.8). Interestingly, SerpinE1 was found to enhance Actylise-tPA uptake from the cell surface after 20-30 min incubation time whilst SerpinB2 did not (Fig. 3.8). At the 20 min time point SerpinB2 treated cells exhibited a slight, but significant ($p = 0.023$, $n=3$) increase in tPA clearance compared to tPA alone, however this was not sustained and at 30 min the amount of tPA only was comparable to tPA:SerpinB2 (Fig. 3.8).

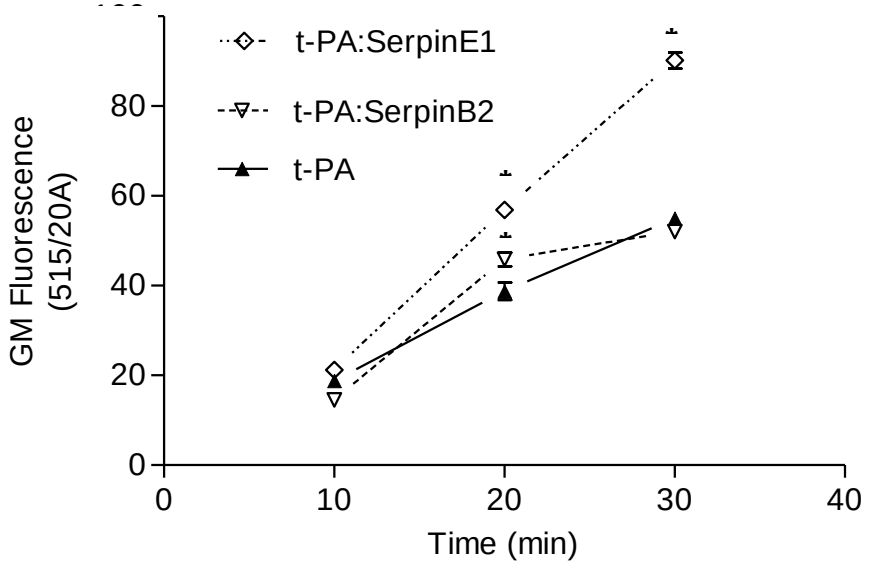

Figure 3.8: Internalisation of Actylise-tPA$_{Alexa488}$ by PBMs. Cells were incubated on ice for 40 min in the absence (auto-fluorescence) or presence of 100 nM Actylise-tPA$_{Alexa488}$ after which, excess protein was removed by centrifugation. Cells were then resuspended in binding buffer in the absence (tPA only) or presence of 100 nM SerpinB2 or SerpinE1, where indicated and incubated at 37 °C for 10, 20 or 30 min. Remaining cell surface bound Actylise-tPA$_{Alexa488}$ was then quenched by addition of 4 µg.mL^{-1} rabbit-α-Alexa488 and incubated on ice for 30 min with 10 µg.mL α-CD14 MAb. Indirect detection of CD14 was performed by a further 30 min incubation on ice in the presence of α-mouse:Alexa633 prior to analysis using flow cytometry. Data represents geometric mean (GM) fluorescence with background (auto-fluorescence) removed, n=3, ± SEM. * $p<0.05$ significantly different from tPA only control.

This differential effect on tPA endocytosis by SerpinB2 and SerpinE1 was surprising as SerpinB2 has previously been shown to enhance the uptake of uPA from the surface of prostate cancer cells, albeit not to the same extent as SerpinE1 (Croucher et al. 2007). As these experiments were conducted using Alexa488 labelled Actylise, which contains a mixture of sc and tc-tPA the significant but modest increase in tPA:SerpinB2 internalisation at the 20 min time point may be

indicative of tc-tPA clearance only, as SerpinB2 does not efficiently inhibit sc-tPA. This is supported by the 2-fold difference in internalisation of Actylise-tPA:SerpinE1 after 30 min as SerpinE1 is known to be an efficient inhibitor of both sc and tc-tPA (Thorsen et al. 1988).

To address this and confirm that SerpinB2 not only inhibited (i.e., bound) to cell surface tPA but was itself subsequently endocytosed as a tPA:Serpinb2 complex, internalisation assays using SerpinB2$_{Alexa488}$ and exogenous active-tPA or PPACK-inactivated tPA were performed. Furthermore comparison of SerpinB2$_{Alexa488}$ internalisation via Actylise-tPA and tc-tPA was undertaken. Cell surface bound PPACK-inactivated Actylise-tPA significantly reduced the internalisation of SerpinB2 by 25% compared to the active control (Fig 3.9A) whilst inactivation of tc-tPA reduced internalisation of SerpinB2 by 90% (Fig. 3.9B), indicating that SerpinB2 bound at the PBM cell surface was subsequently endocytosed as a tc-tPA:SerpinB2 complex.

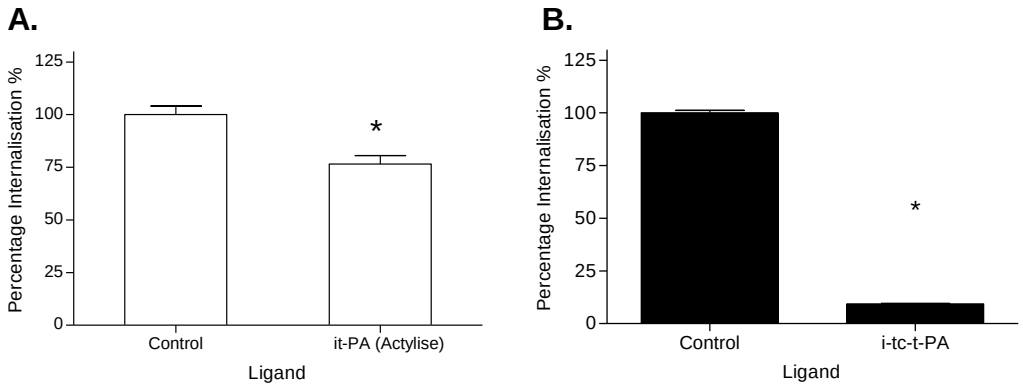

Figure 3.9: Actylise and tc-tPA dependent internalisation of SerpinB2. **(A)** Freshly isolated PBM were incubated on ice for 40 min in the absence (auto-fluorescence) or presence of 100 nM Actylise-tPA. Excess Actylise-tPA was then removed by centrifugation and cells were incubated for a further 15 min on ice in the absence (control) or presence of 100 μM PPACK (itPA). SerpinB2$_{Alexa488}$ was then added at a final concentration of 10 μM and the cells incubated for 1 h at 37 °C. Cell bound SerpinB2$_{Alexa488}$ was quenched using 4 μg.mL^{-1} rabbbit-α-Alexa488 for 30 min on ice prior to analysis using flow cytometry. **(B)** Freshly isolated PBMs were prepared as per (A), substituting 100nM purified tc-tPA for 100 nM Actylise-tPA. Data represents normalised (to control), geometric mean (GM) fluorescence with background (auto-fluorescence) removed, n=3, ± SEM. * $p<0.05$ significantly different from control.

In order to characterise the mechanisms involved in the clearance of tPA and tPA:serpin complexes from the cell surface of PBM the roles of scavenger proteins and the LDL receptor family were investigated. Where previous internalisation assays had been conducted on pre-treated (addition of exogenous Actylise-tPA) cells, pre-formed complexes were used to characterise internalisation pathways allowing for pre-treatment with inhibitors, followed by addition of Actylise-tPA. RAP, a commonly used antagonist of ligand binding specific to the LDLR family, significantly inhibited Actylise-tPA:$_{Alexa488}$/complex internalisation by 80 to 90% in all cases (Fig. 3.10). Furthermore the use of fucoidin, which is known to block

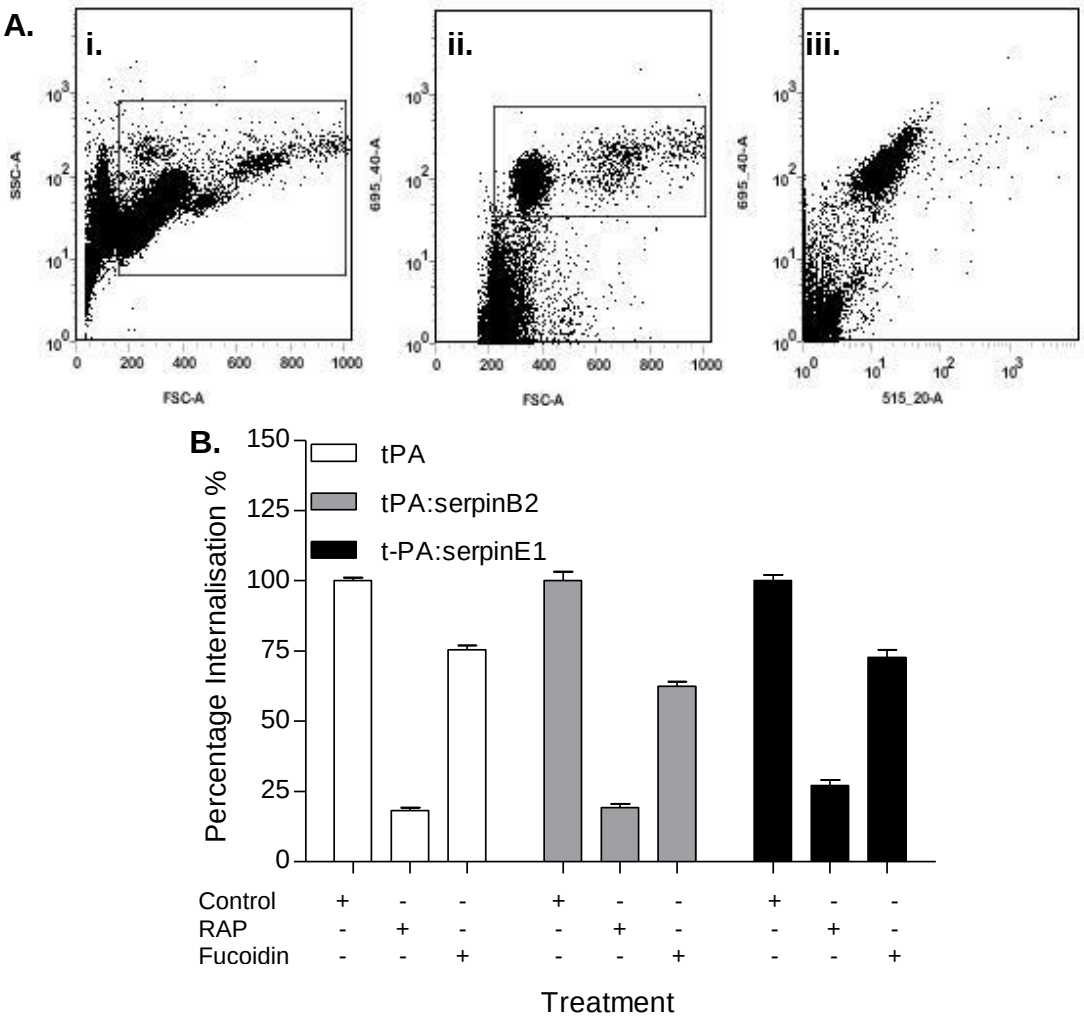

Figure 3.10: Role of LDLR family and scavenger receptors in the endocytosis of tPA. **(A)** Freshly isolated PBMs where initially gated on side and forward scatter, selecting viable cells based on morphology **(i)** Cells where pre-stained with α-CD14:PE-TR MAb and positive cells gated for analysis **(ii)**. Actylise-tPA:serpin complex internalisation was therefore assessed α-CD14 positive cells and quantitated on Alexa488 positive fluorescence intensity **(iii)**. **(B)** Freshly isolated PBMs were incubated for 15 min at 37 °C in the absence (control) or presence of either 300 nM RAP or 300 μg.mL^{-1} Fucoidin, after which 100 nM $tPA_{Alexa488}$ or $tPA_{Alexa488}$:serpin complexes were added and the cells incubated for a further 20 min at 37 °C. Cell bound $tPA_{Alexa488}$ and complexes were quenched using 4 μg.mL^{-1} rabbbit-α-Alexa488 for 30 min on ice prior to analysis using flow cytometry. Data represents normalised (to control) geometric mean (GM) fluorescence with background (auto-fluorescence) removed, n=3, ± SEM. * $p<0.05$ significantly different from control.

scavenger receptors was also able to inhibit internalisation, however to a much lesser extent then RAP with 20 – 10 % inhibition observed. Importantly, the combined percentage of inhibition for RAP and Fucoidin in the endocytosis of Actylise-tPA$_{Alexa488}$, Actylise-tPA$_{Alexa488}$:SerpinB2 or Actylise-tPA$_{Alexa488}$:SerpinE1 totalled 94%, 83% and 99% respectively (Fig. 3.10).

This finding indicates that the LDLR family plays a predominant role in the clearance of tPA and tPA:serpin complexes from the cell surface of PBMs whilst scavenger receptors contribute a minor role. As tPA clearance is reported to be facilitated via the mannose receptor by liver cells (Kuiper et al. 1988; Otter et al. 1991; Nguyen et al. 1992) and expression of the mannose receptor has been reported for primary macrophages (Noorman et al. 1995) immunofluorescence assays were conducted to assess cell surface expression of the mannose receptor (CD206) by the peripheral blood monocytes used in these experiments. There were no detectable levels of the mannose receptor found within three independent assays indicating that this receptor was not involved in the fucoidin dependent clearance of tPA or tPA:serpin complexes by the PBMs (see Table. 3.1).

Given the dominance of the LDLR family of endocytosis receptors in cell surface tPA clearance we next investigated their role in direct binding of tPA to PBM's. Cells were pre-incubated in the absence (control) or presence of RAP for 15 min prior to the addition of tPA$_{Alexa488}$ followed by further 30 min incubation on ice.

Under these conditions RAP was able to reduce cell surface binding of $tPA_{Alexa488}$ by 30 % (Fig. 3.11), confirming previous studies (Mulder et al. 1997).

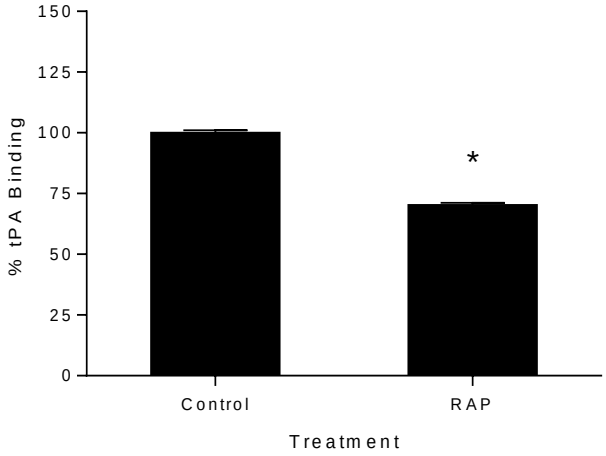

Figure 3.11: Role of LDLR family in the cell surface binding of Actylise-tPA. Freshly isolated PBMs were incubated for 15 min on ice in the absence (control) or presence of 300 nM RAP after which 100 nM $tPA_{Alexa488}$ was added and the cells incubated for a further 40 min on ice. Cell bound $tPA_{Alexa488}$ was then analysis using flow cytometry. Data represents normalised (to control) geometric mean (GM) fluorescence with background (auto-fluorescence) removed, n=3, ± SEM. * $p<0.05$ significantly different from control.

3.4.5. Surface plasmon resonance analysis of tc-tPA and tc-tPA:PAI complexes with LDLR members.

To obtain a more quantitative analysis of the role of LRP and VLDLR in the cell surface interactions of tPA and tPA:serpin complexes the kinetics of binding of these ligands to immobilized LRP and VLDLR were analysed using surface plasmon resonance (SPR). Initial specificity analyses using overlay plots of sensorgrams indicated that tPA:SerpinE1 bound more strongly to LRP than tPA alone or in complex with SerpinB2 (Fig. 3.12A). This effect was less obvious with VLDLR (Fig. 3.12B). For kinetic analyses a serial dilution of ligands were used,

which revealed dose dependent binding for all of the analytes (Fig. 3.12) and complex binding interactions of tc-tPA:SerpinE1 to both LRP and VLDLR. Nevertheless, in both cases, the data best fit competitive heterogeneous analyte models, suggesting the presence of a relatively low and a high affinity binding site within the complex for both LRP (K_{D1} ~ 21.2 nM, K_{D2} ~ 0.95 nM, respectively) and VLDLR (K_{D1} ~ 139 nM; K_{D2} ~ 23 nM) (Table 3.2). tc-tPA and tc-tPA:SerpinB2 also bound to LRP and VLDLR. However, these data were best fit by a one-binding site model with tc-tPA and tc-tPA:SerpinB2 binding with very similar, moderate affinities to LRP (K_D 67 – 57 nM) and VLDR (K_D 124 – 98 nM), respectively. The higher affinity binding (K_{D2}) of tPA:SerpinE1 to both LRP and VLDLR was due to a substantial (100 to 16 fold, respectively) decrease in the dissociation rate constant, indicating much slower dissociation of the complex (Table 3.2). The binding affinity of tc-tPA and tc-tPA:PAI complexes for LRP was generally higher than that obtained with VLDLR (Table 3.2). To our knowledge, there is no previously published data describing the binding of tc-tPA:SerpinB2 to LRP and VLDLR however the affinities reported here for the binding of tc-tPA and tPA:SerpinE1 to LRP are comparable to those obtained by others using SPR (Gliemann et al. 2004).

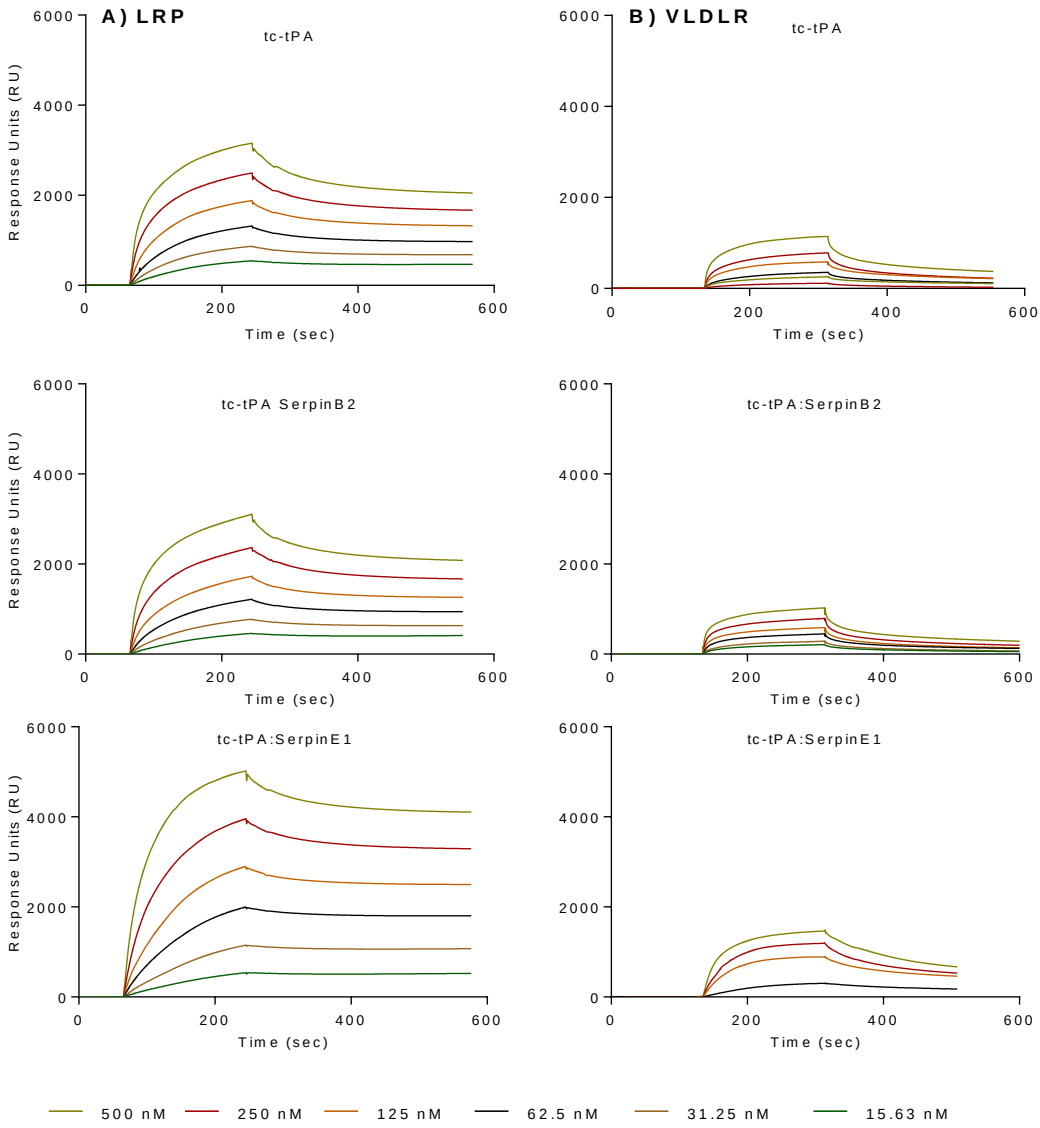

Figure 3.12: Surface plasmon resonance analysis of the interaction between tc-tPA, tc-tPA:SerpinB2 and tc-tPA:SerpinE1 and VLDLR or LRP. Sensorgrams showing the does dependent binding of analytes (15-500 nM) to either **(A)** LRP or **(B)** VLDLR. Data shown are representative of at least 3 separate experiments.

Table 3.2: Surface Plasmon Resonance kinetic analysis of the interaction between LDLRs and tc-tPA or tc-tPA:serpin complexes.

			LRP		
Analyte	**Model**	**ka (1/Ms)**	**kd (1/s)**	**KD (nM)**	χ^2
tPA	1:1	5.22×10^5	3.51×10^{-3}	**67**	1.52
tPA:SerpinB2	1:1	9.19×10^5	51.9×10^{-3}	**57**	1.24
tPA:serpinE1	Heterogeneous analyte - competing	2.21×10^5	4.69×10^{-3}	**21.2**	5.61
		4.62×10^4	4.38×10^{-5}	**0.95**	
			VLDLR		
tPA	1:1	4.18×10^5	51.7×10^{-3}	**124**	2.55
tPA:SerpinB2	1:1	4.16×10^5	54.4×10^{-3}	**98**	2.23
tPA:serpinE1	Heterogeneous analyte - competing	5.37×10^5	74.8×10^{-3}	**139**	5.07
		2.00×10^5	4.60×10^{-3}	**23.0**	

Binding data was fitted to normalised sensorgrams using the BIAevaluation 3.0 software. The binding model chosen represents that with the lowest χ^2 value.

3.5. Discussion

The results presented here show that both SerpinB2 and SerpinE1 inhibit the enzymatic activity of cell surface bound tPA and that tPA:serpin complexes formed at the cell surface are subsequently endocytosed, predominantly via an LDLR dependent pathway. While both tPA:serpin complexes are internalised, only inhibition by SerpinE1 accelerates tPA endocytosis. The differences in endocytosis of these ligands may be explained by the kinetic data obtained for the binding of tPA and tPA:SerpinE1 to LRP and VLDLR using SPR. The formation of complexes between SerpinE1 and either tPA or uPA are thought to cause a conformational change within SerpinE1 resulting in it exposing a high affinity binding site for LRP (Horn et al. 1998; Stefansson et al. 1998) or potentially VLDLR, which contributes directly to the enhanced endocytosis of tPA:SerpinE1 or uPA:SerpinE1 complexes from the cell surface. Indeed work by Cochran et al.

(2011) showed the importance of an LDLR minimal binding motif present in the α-helix D of SerpinE1 but not SerpinB2 that is responsible for the higher affinity interaction and enhanced endocytosis of uPA:SerpinE1 complexes.

Both LRP (Strickland et al. 2002; Croucher et al. 2006) and VLDLR (Strickland et al. 2002; Croucher et al. 2007) play a pivotal role in the rapid clearance of surface bound uPA:SerpinE1 and uPA:SerpinB2 complexes. Like SerpinE1, SerpinB2 has been shown to accelerate uPA internalisation due to an increased affinity of uPA:SerpinB2 for LRP and VLDLR compared to uPA alone (Croucher et al. 2006; Croucher et al. 2007). It is possible that formation of the uPA:SerpinB2 complex results in a conformational change within uPA as SerpinB2 does not bind to either LRP or VLDLR (Croucher et al. 2006; Croucher et al. 2007). Importantly, tc-tPA alone and tc-tPA:SerpinB2 show almost identical one-site binding affinities for LRP and VLDLR, suggesting that complex formation does not significantly alter the binding interaction of tc-tPA to LRP or VLDLR. Furthermore, especially in regards to VLDLR binding, the similar K_D values obtained for the lower affinity binding interactions of tPA:SerpinE1 compared to those observed for tPA or tPA:SerpinB2 (Table 3.2) suggests that no functional conformational change occurs within the tc-tPA molecule upon complex formation. Therefore it is likely that the differences in K_D values for LRP and VLDLR observed between tc-tPA:SerpinE1 and tc-tPA or tc-tPA:SerpinB2 are related to exposure of the high affinity cryptic binding site within SerpinE1. Of note, comparison of the binding affinities of tc-tPA and tc-tPA:serpin for LRP and VLDLR reveals a preference of these ligands for LRP

(Table 3.3). In contrast, uPA and uPA:serpin appear to bind with higher affinities to VLDLR compared to LRP (Table 3.3). However, the significance of these differences is unclear at this stage.

Table 3.3: Comparison of tc-tPA/tc-tPA:PAI to uPA/uPA:PAI affinities for LRP and VLDLR

	LRP	VLDLR
Analyte	**KD (nM)**	**KD (nM)**
tPA	67	124
tPA:SerpinB2	66	131
tPA:SerpinE1	21	139
	0.95	23
uPA	200 *	31.2 ^
uPA:SerpinB2	32.6 *	4.68 ^
uPA:SerpinE1	0.226 €	1.6 €
		84.8 ^
		1.51 ^

Previously published data: * (Croucher et al. 2006), ^ (Croucher et al. 2007), € (Skeldal et al. 2006)

Interestingly, RAP inhibited the direct binding of Actylise-tPA to the PBM cell surface by approximately 30%. This observation is similar to that reported by Mulder et al. (1997), where pre-treatment with RAP resulted in a 25% reduction of tPA binding to the cell surface of HUVECs. The identities of other receptors responsible for the remaining proportion of tPA binding are potentially numerous, of which p36 may partially contribute to total tPA binding on these cells, as previously published (Brownstein et al. 2004). The absence of the mannose receptor on our freshly isolated PBMs cells was not surprising as it is indicative of a monocyte versus a differentiated macrophage phenotype (Noorman et al. 1995). That fucoidin inhibited the clearance of tPA and tPA:serpin complexes from the surface of PBMs by about 10 – 20%, suggests that other scavenger receptors

present on PBMs play a minor role in the binding and subsequent endocytosis of these ligands.

The traditional role of tPA in fibrinolysis and of SerpinE1 as a regulator of tPA is well characterised. However in recent years it has become increasingly clear that tPA is not restricted to maintaining homeostasis of coagulation and fibrinolysis within the vasculature. tPA has been found to induce matrix metalloproteinase-9 gene expression in rat kidney interstitial fibroblast and promote activation of murine myofibroblasts (Hu et al. 2007), control permeability of the blood brain barrier (Yepes et al. 2003), facilitate migration of monocytes across the BBB into the central nervous system (Reijerkerk et al. 2008) and coordinate macrophage migration under inflammatory conditions (Cao et al. 2006). Interestingly, this diversity in function appears to be dependent on tPA interaction with LRP, which initiates activation of signalling cascades, whilst not always requiring the proteolytic activity of tPA. Expression of both tPA and SerpinB2 by monocytes, macrophages and myeloid progenitors within normal bone marrow (McWilliam et al. 1998), suggests a physiological role for SerpinB2 as an inhibitor of tPA associated with derivatives of the myeloid stem cells. The differential endocytosis mechanisms identified in our work suggest that while SerpinE1 and SerpinB2 both function similarly in the control of plasmin generation by tPA at the cell surface, they may have opposing effects on the non-classical roles of tPA and activation of signalling cascades via LRP or indeed VLDLR.

The molecular mechanisms and biological significance of a role for VLDLR in the endocytosis of tPA or tPA:PAI complexes are poorly understood. VLDLR is not found within the liver, however it is expressed at varied levels throughout the body (Strickland et al. 2002). Therefore, whilst the SPR analyses indicated that tPA and tPA:PAI bound to VLDLR with approximately 2-fold lower binding affinities than to LRP (Table 3.2), it is plausible that VLDLR may also play an important role in local clearance of tPA and tPA:PAI complexes. This could be through removal of proteolytic activity and/or potentiation of downstream signalling cascades through cell surface interactions with these ligands.

4. Biochemical analysis of SerpinB2 reveals chaperone-like activity.

4.1. Abstract

SerpinB2 exists primarily as a non-glycosylated 47 kDa intracellular protein and is significantly up-regulated during cellular stress responses, differentiation, proliferation and innate immunity. However, a defined serine protease binding partner for intracellular SerpinB2 has not yet been described, suggesting additional functions for this protein, independent of its role as a serpin. The distribution of SerpinB2 within the nucleus and cytosol, combined with high expression during cellular stress is consistent with a role in cellular pathways associated with stress responses. Molecular chaperones are classical stress response proteins, which act to stabilise unfolded proteins and can promote refolding and/or degradation of misfolded proteins (Hartl et al. 2011). Therefore, we have investigated a potential role for SerpinB2 in functional activities classically associated with intracellular protein stress responses by assessing its function as a molecular chaperone. As molecular chaperones have been shown to bind specifically to misfolded or aggregated proteins via hydrophobic interactions (Hartl et al. 2011), we conducted ELISA based binding assays and found that SerpinB2 preferentially binds misfolded proteins. SerpinB2 was also found to be an efficient inhibitor of amorphous aggregation in some but not all models tested and an efficient inhibitor of amyloid beta peptide aggregation measured in real-time. Our results indicate that while SerpinB2 binds specifically to misfolded proteins the interaction does not promiscuously shield inappropriate protein-protein interactions. This suggests that whilst not a universal chaperone, SerpinB2 does exhibit chaperone-like activity, which may contribute to its cytoprotective functions in vivo.

4.2. Introduction

SerpinB2 is a member of the Serine Protease Inhibitor super family and exists within the extracellular or intracellular environment. Secreted as a 47 kDa or glycosylated 60 kDa protein, extracellular SerpinB2 is thought to function as an inhibitor of the urokinase plasminogen activator and to a lesser extent, tissue-type plasminogen activator (Kruithof et al. 1995) (Lobov et al. 2008; Lee et al. 2010). However, the majority of SerpinB2 is found within the intracellular environment, as a 47 kDa protein. Whilst the 47kDa SerpinB2 maintains its inhibitory activity (Al-Ejeh et al. 2004), a target intracellular protease has not yet been defined, which suggests a role independent of the classical inhibitory mechanisms, characteristic of Serpins (Law et al. 2006). Importantly, SerpinB2 expression appears to be associated with inflammation and cellular stress (recently reviewed in (Schroder et al. 2010; Lee et al. 2011; Medcalf 2011)).

The main physiological producers of SerpinB2 are cells of the myeloid lineage, i.e monocytes and macrophages (Kruithof et al. 1995). It is not surprising then, that high SerpinB2 expression profiles have been described for activated microglial aggregates, co-localised with senile plaques in brain sections from Alzheimer's disease patients (Akiyama et al. 1993; Walker et al. 2006). More recently however, an association of SerpinB2 with Amyloid Lateral Sclerosis (ALS) was described, whereby, primary cultures of cortical neurons isolated from the SOD1 (G93A mutation) transgenic animal model, incubated under oxidative stress conditions, showed an 8 fold increase in SerpinB2 mRNA expression, relative to non-

transgenic control models, cultured under the same conditions (Boutahar et al. 2011). Furthermore, SerpinB2 was recently identified as one of the 9 core "Activity-regulated Inhibitor of Death (AID)" genes that mediate neuroprotection by *N*-methyl-D-aspartate (NMDA) receptor-induced calcium signalling. Within 3 h after injection of other glutamate analogues, such as kainic acid, into the brain SerpinB2 expression is increased by greater than 1800-fold (Zhang et al. 2009). Whilst adenoviral over-expression of SerpinB2 in the brain was protective against this insult (Zhang et al. 2009), the functional mechanism was not defined. Taken together these results suggest a potential role for SerpinB2 at sites of inflammation within the CNS.

Importantly, disruption of normal protein homeostasis (proteotoxic stress) is integral to the pathophysiology of both acute injury associated inflammation, neuronal dysfunction and age related neurodegeneration. Therefore, cellular quality control systems, such as the molecular chaperone network, are essential for maintaining proteostasis (Morimoto 2008). Chaperones are traditionally defined as molecules which interact with other proteins undergoing folding or unfolding conformational changes, specifically stabilizing intermediate non-native forms and either facilitating their conformational arrangement into a functional native state (foldases) or preventing aggregate formation between misfolded intermediates (holdases) (reviewed in (Tyedmers et al. 2010; Hartl et al. 2011)). Aberrant protein conformations are problematic in that they may become cytotoxic either through loss or gain of function and as such, form the basis of disease (Carrell and Lomas

1997). Furthermore, overloading of the chaperone network in response to cellular stress gives rise to protein aggregates which accumulate and may also become cytotoxic (Bucciantini et al. 2002).

As alluded to above SerpinB2 is one of the most up-regulated proteins in neurons and cells of the myeloid lineage in response to infections and inflammatory mediators, representing up to 1% of total intracellular protein following cellular stress (Schroder et al. 2010; Lee et al. 2011; Medcalf 2011). However, the relationship between the up-regulated expression, protein interactions, and the putative cytoprotective role of SerpinB2 is unclear. Of interest, chaperone activity has been described for other members of the serpin super family, such as sHsp47 (SerpinH1/H2 (Gettins 2002)) (Sauk et al. 2005), which is a collagen binding/carrier molecule and human alpha(1)-antitrypsin (AAT) (SerpinA1), which has been shown to inhibit protein aggregation using a variety of common substrate models (Zsila 2010). More recently, chaperone functions have also come to include macro-complex assembly, protein transport and direction of deleterious protein conformations into proteolytic degradation pathways, in addition to their protein folding functions (Hartl et al. 2011). In this context, some extracellular, non-inhibitory serpins function as transport proteins, for example; SerpinA6 is a major transporter of glucocorticoids and progestins within blood (Westphal 1986; Hammond et al. 1987; Pemberton et al. 1988; Hammond 1990) and SerpinA7 is a thyroxine transporter (Pemberton et al. 1988). Therefore, given the precedent

within the literature we hypothesised that SerpinB2 may also function within cellular pathways as a chaperone.

4.2.1. Specific Aims

A defining characteristic of chaperones is their ability to bind to misfolded or unfolded proteins (substrates), via hydrophobic residues which are normally buried within the three-dimensional structure of the native protein (Feder and Hofmann 1999; Schroder and Kaufman 2005; Nardai et al. 2006; Korcsmaros et al. 2007). Protein aggregation is also driven by hydrophobic forces and primarily results in amorphous protein structures or highly ordered fibrillar aggregates (termed amyloid), which are defined by β-strands that run perpendicular to the long fibril axis (cross-β structure) (Westermark et al. 2007; Eichner et al. 2011). Importantly, the latter is characteristic of neurodegenerative disorders such as Alzheimer's disease, Huntington disease, Parkinson's disease and ALS (Muchowski and Wacker 2005). Therefore, the specific aims of this chapter were to investigate the possibility that SerpinB2 could act as a chaperone using *in vitro* biochemical analysis of these key characteristics. Specifically, an ELISA based assay was utilised to examine the binding of SerpinB2 to misfolded substrates. We then assessed the ability of SerpinB2 to inhibit amorphous forming aggregation models in real-time using a light scattering microplate based assay. Finally, we aimed to investigate the ability of SerpinB2 to inhibit fibrillar aggregation, using the aggregation prone amyloid-β 1-40 amino acid peptide, or the rapidly aggregating

amyloid-β 1-42 amino acid peptide, associated with Alzheimer's disease, within real-time assays using Thioflavin-T as a reporter for fibril formation.

4.3. Methods

4.3.1. Materials

Recombinant human SerpinB2 (47 kDa form) was provided by SerpinB2 Pty Ltd (Sydney, Australia). Bovine serum albumin (BSA), bovine Cu/Zn superoxide dismutase (SOD1), Rabbit muscle creatine phosphokinase (CPK), dithiothreitol (DTT), iodoacetic acid, monoclonal antibody against ovalbumin, o-phenylenediamine dihydrochloride (OPD), ovalbumin (SerpinB14), porcine citrate synthase (CS), Thioflavin-T, casein, thimerosal, protease inhibitor cocktail and urokinase plasminogen activator from human urine (uPA) were all from Sigma-Aldrich. were from Bio-Rad Laboratories, Inc. Human recombinant αB-crystallin was a kind gift from Dr Heath Ecroyd (University of Wollongong) (Horwitz et al. 1998). Monoclonal antibody against human SerpinB2 (#3750) was from American Diagnostica Inc. Microtitre 96 and 384 well plates were from Greiner. Tissue culture supernatant containing antibody against human clusterin from the hybridoma clone "G7" (5-10 ug.mL-1) (Humphreys et al. 1999) and purified human clusterin from whole blood were a kind gift from Professor Mark Wilson (University of Wollongong). Amyloid-beta peptide 1-40 ($A\beta_{1-40}$) and NH_4OH was from Anaspec. Amyloid-beta 1-42 ($A\beta_{1-42}$) was from Biopeptide, USA. Millex syringe filters (0.45 µm) were from Millipore. The concentration of protein in solution was estimated

using the BioRad Dc Protein Assay kit, according to the manufacturer's instructions, using BSA as the standard.

4.3.2. Expression and Purification of Recombinant SerpinB2

Wild-type human SerpinB2 (47 kDa) was purified from *E. coli* (M15) using the pREP4/pQE-9 expression system, followed by a secondary purification using anion exchange chromatography. Briefly, purified pQE9/SERPINB2 vectors were transformed into electro-competent M15 [pREP4] cells using standard methods. Cells were cultured overnight at 37 °C with shaking in TB containing 100 µg/mL ampicillin and 25 µg/mL kanamycin. A 20 mL aliquot of this starter culture was added to 1 L TB and grown to an OD_{600} of ~0.6. Expression of SerpinB2 was induced by the addition of 0.5 mM IPTG and the culture incubated overnight at 18°C. Cells were collected by centrifugation at 10,000 *g* for 10 min. Pelleted cells were resuspended in 15 mL of ice-cold loading buffer (50 mM NaH_2PO_4, 300 mM NaCl, pH 7.0, containing protease inhibitor cocktail) and lysed using a French press (Thermo, USA). The cell lysate (~20 mL) was then incubated with 2.5 µg of DNase for 30 min on ice and cell debris pelleted by centrifugation at 17,000 *g* for 30 min. The supernatant was loaded onto 3 mL equilibrated TALON metal affinity resin at a rate of 1 mL/min. Unbound proteins were removed using 20 column volumes of loading buffer. Bound protein was eluted from the column using elution buffer (50 mM NaH_2PO_4, 300 mM NaCl, 150 mM imidazole, pH 7.0). Samples were buffer exchanged into 20 mM Tris, pH 8 using PD10 column and then loaded onto a mono-Q (5/50 GL) anion

exchange column (GE Healthcare) at room temperature. The column was then washed with 20 bed volumes of 20 mM Tris, pH 8 prior to elution of bound protein by a NaCl gradient with salting buffer (20 mM Tris, 1 M NaCl, pH 8), increasing NaCl concentration from 0 to 80% over 2 h, with flow rate at 1 $mL.min^{-1}$. Purified SerpinB2 was then buffer exchanged by dialysis, PD10 columns or Amicon Ultra-4 centrifugal filter units (MWCO 10 KDa) into PBS (140 mM NaCl, 2.7 mM KCl, 10 mM Na_2HPO_4, 1.4 mM KH_2PO_4, 0.02% NaN_3 pH 7.4). Purity and integrity of the recombinant protein was assessed by SDS PAGE (Fig. 4.1). Purified protein was stored at 4 °C until required.

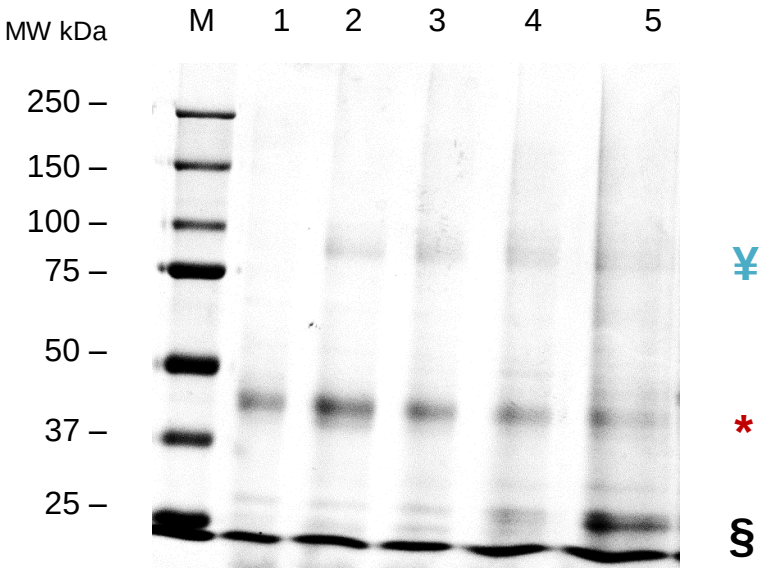

Figure 4.1: Representative gel showing visualisation of recombinant SerpinB2 protein following anion exchange chromatography. Fractions (Lanes 1-5) (20 µL) were prepared using non-reducing sample buffer and resolved by 10% SDS PAGE (see section 4.3.8). Purified monomeric SerpinB2 (*) and polymerised SerpinB2 (¥) was recovered with minimal low molecular weight impurities (§) and lanes 1-4 pooled for use in experiments. Precision dual colour prestained markers (M) (Biorad) were used.

Recombinant SerpinB2 made in house was used interchangeably with recombinant SerpinB2 from SerpinB2 Pty Ltd/Biotech Australia (Sydney, Australia), with comparable results.

4.3.3. Heat denatured Casein (HDC)

PBS was heated to 70 ºC and 1 % w/v casein added followed by continuous stirring for 2-3 h at 70 ºC. The solution was then cooled prior to the addition of 0.01% w/v Thimerosal and pH adjusted to 7.4.

4.3.4. End-point binding assays

Protein substrates in PBS were incubated overnight in 96 well microplates as follows: BSA (1 $mg.mL^{-1}$) was incubated at 37 °C in the absence (control) or presence of 20 mM DTT (reducing misfolded); creatine phosphokinase or citrate synthase (250 $\mu g.mL^{-1}$) were incubated at 4 °C (control) or 43 °C (heat denaturing); (lysozyme 1 $mg.mL^{-1}$) was incubated overnight at 37 °C in the absence (control) or presence of oxidative stress buffer (OSB) (100 µM $CuSO_4$, 4 mM H_2O_2). Unbound protein was removed by 2 x 5 min washes with wash buffer (1 x PBS, 0.1% triton-X100). Plates were then incubated for 1 h with blocking buffer (1 x PBS containing 0.02% (w/v) NaN_3 and 1% BSA). Unless otherwise stated wells were then incubated with 5 mM iodoacetic acid (IAA) in PBS at 37 °C for 1 h to acetylate free sulphydryl groups of cysteine residues. Prepared plates were then incubated with either a serial dilution (6.25 - 250 $\mu g.mL^{-1}$, 1.3 nM – 5.3 µM) or fixed concentration of SerpinB2 (100 $\mu g.mL^{-1}$), SerpinB14 (ovalbumin) (250 $\mu g.mL^{-1}$, 5.5

μM; negative control) or clusterin (50 μg.mL^{-1}, 800 nM; positive control) for 1.5 h at 37 °C. The plates were then washed 3 times with wash buffer and incubated with blocking buffer for 1 h at 37 °C prior to the addition of primary monoclonal antibodies to either SerpinB2 (1:1000), SerpinB14 (1:30000), or clusterin (25 μL.well^{-1} hybridoma culture supernatant) and incubated at 37 °C for 1.5 h. Wash and blocking steps with heat misfolded casein (HDC 1% w/v in PBS, containing 0.04 % thimerosal) were repeated prior to the addition of HRP conjugated secondary antibody (1:2000) in HDC/PBS. After 1 h at 37 °C the plates were washed 3 x 10 min with TBS-T buffer (50 mM Tris, 150 mM NaCl, 0.05% v/v Tween-20) followed by 3 x 10 min washes with TBS (50 mM Tris, 150 mM NaCl). Bound antigens were detected using 2.5 mg.ml^{-1} ortho-phenylenediamine (OPD) substrate in citrate buffer (50 mM citric acid, 100 mM Na_2HPO_4, pH 5) containing 0.03% H_2O_2 and absorbance at 490 nm was measured after 10 min using a Spectramax® 250 plate reader (Molecular Devices, USA) and Softmax Pro® software. Unless otherwise stated, the volume per well for all protein solutions and buffers was 100 μL. All incubation and wash steps were conducted at 37 °C with gentle agitation. Assays were conducted in triplicate and data analysed in GraphPad Prism (version 5.00 for Windows, GraphPad Software, San Diego California USA, www.graphpad.com), with background controls subtracted.

4.3.5. Light Scattering Assays

4.3.5.1. Heat Denaturing Stress:

Working solutions of CS (706 nM) in the absence or presence of an equimolar ratio of either SerpinB2, αB-crystallin (positive control) or SOD1 (negative control) were prepared in filtered 40 mM HEPES-KOH Buffer, pH 7.5 then aliquoted into wells of a 384 well microplate and incubated at 43 °C for 4 h. Turbidity measurements (absorbance at 360 nm, A^{360}) were acquired at 5 min intervals using a FLUOstar Optima plate reader (BMG Labtech, Germany).

4.3.5.2. Reducing Stress:

BSA (15 µM) or BSA with either SerpinB2 (21 µM), αB-crystallin (50 µM) (positive control) or SerpinB14 (22 µM) (negative control) were prepared giving 1:1 weight/weight ratios in filtered reducing buffer (PBS, 20 mM DTT, 0.02% NaN_3, pH 7.4) then aliquoted into wells of a 96 well microplate in triplicate and incubated at 37 °C overnight. Turbidity measurements (absorbance at 360 nm, A^{360}) were acquired at 5 min intervals using a FLUOstar Optima plate reader (BMG Labtech, Germany).

4.3.5.3. Oxidative Stress:

Working solutions of lysozyme only or lysozyme and SerpinB2, α-crystallin or SerpinB14 (negative control) at 20:1 molar ratios (French et al. 2008), were prepared in filtered PBS then aliquoted into wells of a 384 well microplate and 10 x oxidative stress buffer (OSB: Filtered PBS, 1 mM $CuSO_4$, 40 mM H_2O_2, 0.02%

NaN_3) added to all wells just prior to plate incubation at 37 °C for 4 h. Absorbance readings (360 nm) were acquired at 5 min intervals using a FLUOstar Optima plate reader (BMG Labtech, Germany).

4.3.6. Fibril formation - Amyloid-β:

4.3.6.1. Amyloid-β 1-40 Peptide

Prior to use amyloid-β 1-40 peptide ($Aβ_{1-40}$) was resuspended in 20 mM NH_4OH to a final concentration of 1 mM, then diluted to 500 µM with milli-Q H_2O. The samples were then aliquoted and frozen at -80 °C until required, as recommended by the supplier. This preparation step was conducted by Dr Heath Ecroyd (University of Wollongong) who generously supplied this reagent as a gift for use on this project.

On the day of the experiment an aliquot was diluted to 50 µM with ice cold phosphate buffer (0.45 µm filtered 50 mM NaH_2PO_4, 100 mM NaCl, pH 7.4). Working solutions of $Aβ_{1-40}$ (25 µM) in the absence or presence of 2.5 µM SerpinB2, αB-crystallin and SOD1 (negative control) were prepared on ice in phosphate buffer. Aggregation of the $Aβ_{1-40}$ peptide was monitored in real time by following thioflavin-T fluorescence. 10 µM thioflavin-T (thio-T) was added and solutions immediately transferred to wells of a 384 well microplate and incubated for 12 h at 37 °C. Samples were excited at 440 nm and fluorescence intensity (emission 485+/-10 nm) was acquired at 5 min intervals using a FLUOstar Optima plate reader (BMG Labtech, Germany). Assays were conducted in duplicate, repeated twice and data analysed in GraphPad Prism version 5.00 for Windows,

GraphPad Software, San Diego California USA, www.graphpad.com, with background controls (buffer containing 10 µM thio-T) subtracted.

4.3.6.2. Amyloid-β 1-42 Peptide

Given the propensity of amyloid-β (Aβ) to aggregate, stock solutions were prepared as previously described (Bolognesi et al. 2010). Prior to use amyloid-β 1-42 peptide ($A\beta_{1-42}$) was dissolved at 1 $mg.mL^{-1}$ in trifluoroacetic acid (TFA) followed by sonification for 30 s. TFA was then removed over night by lyophilisation and the $A\beta_{1-42}$ was then redissolved in 1 mL hexafluoroisopropanol (HFIP), aliquoted and HFIP removed by speed-vac. Samples were then frozen at -20 °C until required. All preparation steps were carried out at 4 °C with pre-chilled reagents. On the day of the experiment an aliquot was resuspended on ice in filtered Milli-Q H_2O, mixed using a sample oscillator (Millipore) for 60 s and immediately placed back on ice. 10 x PBS was then added to give a 250 µM $A\beta_{1-42}$ working stock in PBS and the sample placed in an ice cold sonication bath for 30 s prior to use. These solutions of $A\beta_{1-42}$ were then used in thio-T assays at 25 µM, final concentration, as described for $A\beta_{1-40}$ (section 4.4.5.1) with the following exception in method; aggregation of $A\beta_{1-42}$ was monitored in real time by adding 25 µM thio-T.

4.3.6.3. Scanning electron microscopy (SEM)

$A\beta_{1-42}$ peptide (25 µM) was incubated for 12 h at 37 °C in the absence or presence of 2.5 µM SerpinB2, αB-crystallin or SOD1. Samples from each reaction were

resuspended at a total protein concentration of 0.1 mg/mL in PBS and 2 µL of each sample was blotted onto carbon coated nickel 400 mesh grids covered in formvar resin (Gilder TEM grids, Proscitech, Townsville, Australia), incubated for 5 min at RT, washed three times with filtered dH_2O and negatively stained with 1% uranyl acetate in milli-Q dH_2O. The specimens were then visualised using a JSM7500FA cold Field Emission Gun Scanning Electron Microscope (JEOL) with an acceleration voltage of 20.0 kV and a working distance of 8 mm (spot size setting of 8). The detector used was a transmission electron detector (TED) mounted beneath the specimen platform. Secondary electron images were taken with a semi in-lens detector at a working distance of 8.0 mm. SEM imaging was kindly conducted by Patrick Constantinescu (University of Wollongong).

4.3.7. Protease:Serpin complex formation

End-point samples were taken from thio-t assays, as described in section 4.3.5.2. Briefly, SerpinB2 (2.5 µM) was incubated for 12 h at 37 °C in the absence (control) or presence of 25 µM $A\beta_{1-42}$ and 25 µM thio-T. Samples from each reaction were then taken and incubated in the absence or presence of uPA (1.25 µM) for 30 min at 37 °C. Formation of protease:SerpinB2 complexes were then assessed by western blotting. Briefly, samples were resolved by 10 % SDS PAGE and transferred onto Immobilom^{TM}-P PVDF (Millipore, USA) membrane, using a Bio-Rad Mini Trans-Blot system. The membrane was prepared and protein blotting apparatus was assembled according to the manufactures instructions with electrophoresis conducted at 4^{o}C for one h at 100 V. Once the transfer was complete (ensured by complete transfer of pre-stained markers (BioRad,

Australia)), blots were blocked with 10% skim milk powder in Tris-buffered saline (TBS) with 0.05% (v/v) Tween-20 (TBST) overnight at 4^{o}C. The blots were then rinsed three times with TBST for 5 min per wash. Rabbit α-uPA polyclonal antibody (1:500) or mouse α-SerpinB2 monoclonal antibody (1:1000) were applied in 2% milk/TBST and blots were incubated for 2 h, at RT on a shaker. The membrane was washed with TBST for 10 min, followed by three 5 min rinses with TBST. The blot was then re-blocked with 6% milk/TBST for 30 min at RT followed by one rinse with TBST for 5 min. Detection of bound primary antibody was conducted using the appropriate horse radish peroxidise (HRP) labelled secondary antibody, which was applied at a final concentration of 1:5000 in 2% milk/TBST for 1 h, at RT. Three 5 min rinses with TBST were conducted to remove unbound secondary antibody followed by three 5 min rinses with TBS.

Protein detection was visualised by an enhanced chemiluminescence (ECL) reaction using SuperSignal® Substrate for Western Blotting as per manufacturer's instructions (Progen, Australia). The membranes were exposed to X-ray film in a X-Omatic Cassette (Kodak) for 5 to 30 min depending on the strength of the signal. The film was then placed in Developer solution (Kodak) for 2 min, rinsed in water and placed in Fixer solution (Kodak) for 2 min. The film was rinsed in water and analysed.

4.3.8. Protein Concentration Assay

Unless otherwise specified, the concentration of protein in solution was estimated using the BioRad D_C Protein Assay kit, according to the manufacturer's instructions, using BSA as the standard. Absorbance was measured at 750 nm using a Molecular Devices SpectraMax 250 plate reader, and SoftMax® Pro software (Molecular Devices, USA).

4.3.9. Sodium Dodecyl Sulphate – Polyacrylamide Gel Electrophoresis (SDS-PAGE)

All SDS PAGE analysis was conducted using 10% polyacrylamide resolving gel and 4% polyacrylamide stacking gel in a Bio-Rad Mini Protean Gel system (Bio-Rad, Australia). Samples of 30 µL were prepared with 5 x non-reducing sample buffer and boiled for 5 min prior to loading. Electrophoresis was run at 160 V for 2 h in 1 x SDS running buffer. Bio-Rad low molecular weight markers were used to determine approximate protein size.

4.4. Statistical analysis

Statistical significance was determined by Students t-tests using GraphPad Prism version 5.00 for Windows, GraphPad Software, San Diego California USA (***www.graphpad.com***). *P* values less than 0.05 were considered significant.

4.5. Results

4.5.1. End-point binding assays

The ability of SerpinB2 to interact with native or misfolded client proteins, routinely used in the biochemical analysis of chaperone activity, was first determined using an ELISA approach. SerpinB2 was found to bind preferentially, in a saturable manner, to reduction (DTT)-stressed BSA (Fig 4.2A), oxidised lysozyme (Fig 4.2B), and heat-stressed CPK (Fig 4.2C), as negligible binding to native proteins was detected. Analysis of specific binding affinities, determined by non-linear fit with one-site binding model (Y=Bmax*x/(Kd+x)), between SerpinB2 and reduction-stressed BSA or heat-stressed CPK were similar with apparent K_D of 0.705 µM (± 0.131 µM SEM) and 0.818 µM (± 0.114 µM SEM), respectively, whilst the apparent K_D between SerpinB2 and oxidative-stressed lysozyme was 1.927 µM (± 0.323 µM SEM) (Tab 4.2). In contrast, SerpinB2 bound at low levels to both native and heat-stressed CS (Fig. 4.2D).

Low levels of SerpinB14 (ovalbumin) (negative control) were also found to interact preferentially with reduction-stressed BSA (Fig.4.2.E) and oxidised lysozyme (Fig.4.2.F). However, comparison of fold increases in binding interaction observed for each Serpin shows a 285 fold increase for SerpinB2 interaction with misfolded BSA – relative to native BSA - compared to 17.5 fold increase observed for SerpinB14 (Fig.4.2.E). Furthermore an 8-fold increase in SerpinB2 interaction with oxidised-lysozyme was observed – relative to native lysozyme - compared to a 3

fold increase in SerpinB14 (Fig.4.2F). In contrast, SerpinB2 binding interaction with heat misfolded CPK increased 5-fold – relative to control CPK- whilst there was no detectable interaction observed between SerpinB14 and either native or heat-stressed CPK (Fig.4.2G); nor native or heat-stressed CS (Fig.4.2H), which corresponded to a non-significant fold increase in binding.

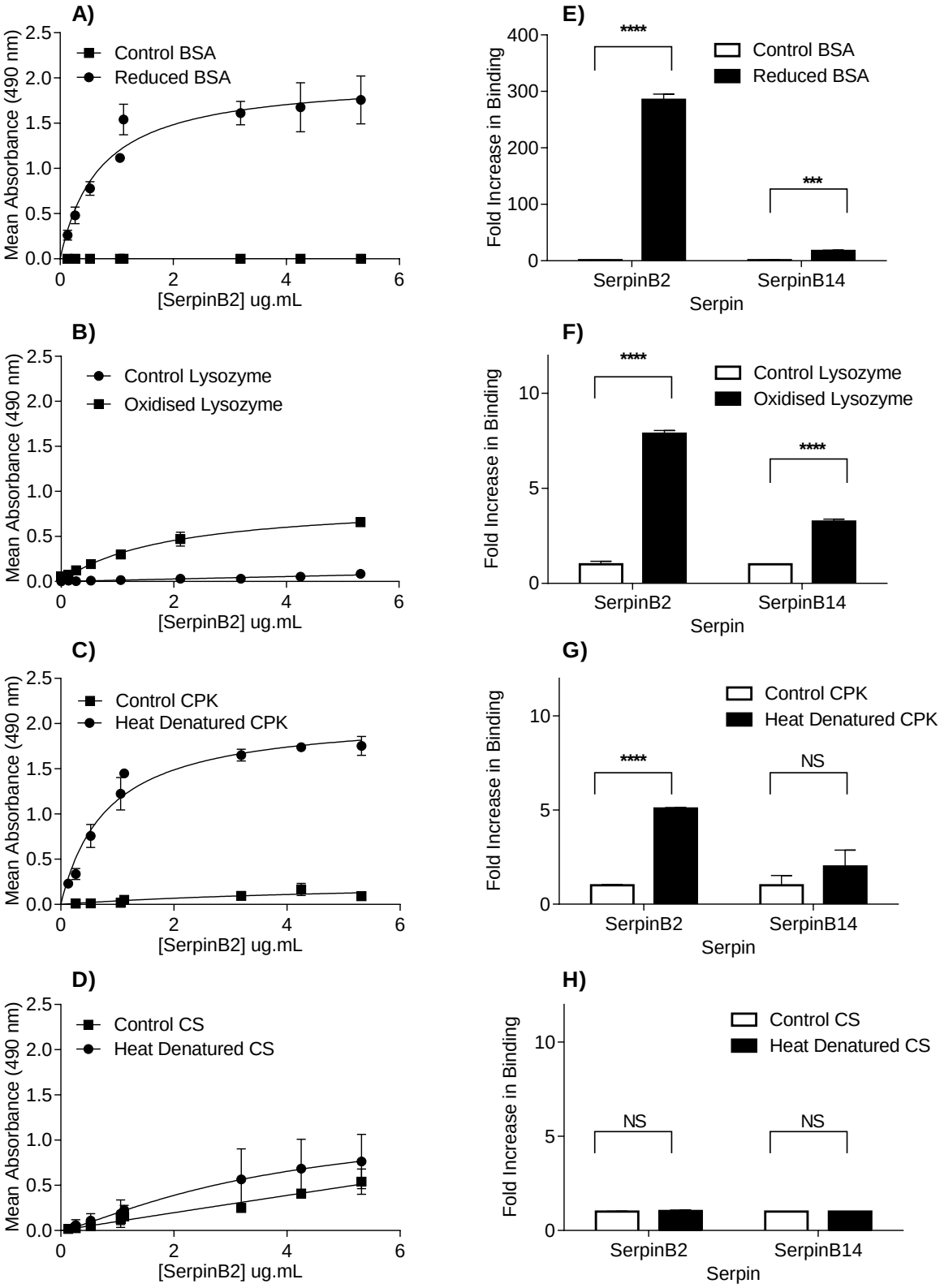
A)
Mean Absorbance (490 nm)
[SerpinB2] ug.mL
Control BSA
Reduced BSA
B)
Control Lysozyme
Oxidised Lysozyme
C)
Control CPK
Heat Denatured CPK
D)
Control CS
Heat Denatured CS
E)
Fold Increase in Binding
****
***
SerpinB2
SerpinB14
Serpin
F)
G)
NS
H)

Figure 4.2: SerpinB2 binds preferentially to misfolded proteins. Left panel: Dose dependent binding of SerpinB2 to native and misfolded proteins was determined using an ELISA system with relevant specific antibodies and controls. **(A)** BSA (1 mg.mL^{-1}) was incubated overnight at 37 °C in the absence (native control) or presence of 20 mM DTT (Reduced BSA) **(B)** Lysozyme (1 mg.mL^{-1}) was incubated overnight at 37 °C in the absence (control) or presence of OSB (100 µM $CuSO_4$ and 4 mM H_2O_2; Oxidised Lysozyme) **(C)** CPK and **(D)** CS (250 µg.mL^{-1}) were incubated overnight at 4 °C (control) or 43 °C (heat misfolded). **Right panel: Fold increase in SerpinB2 or SerpinB14 (control) interaction with misfolded substrates, compared to controls.** ELISA plates containing (**E)** BSA, (**F)** Lysozyme, **(G)** CPK and **(H)** CS were prepared as per (A - D) and specific binding of either SerpinB2 or SerpinB14 (250 µg.mL^{-1}) was determined as above. Data has been normalised to control (native) protein and represents mean fold increase in detectable interactions ± SEM, n=3. Asterisks denote significant differences, ***p<0.001. ****p<0.0001, NS = not significant.

Table 4.1: Kinetic parameters for binding of SerpinB2 to misfolded protein substrates.

Stressed Substrate	$_{app}K_D$ ± SEM (µM)	B_{MAX} ± SEM	DF	R^2
BSA	0.705 (0.131)	2.006 (0.109)	22	0.897
Lysozyme	1.927 (0.323)	0.893 (0.066)	19	0.958
CPK	0.818 (0.115)	2.096 (0.090)	22	0.945
CS	N.D			

Specific binding was analysed by a non-linear fit regression using GraphPad. The data best fit a one site specific binding model. Mean data ± SEM, n=3, from a representative experiment. N.D = not determined.

4.5.2. Real-time protein aggregation

4.5.2.1. Amorphous aggregation models

Given that SerpinB2 binds specifically to some unfolded proteins, we next tested its ability to inhibit the stress-induced aggregation of the same client proteins. When tested at the same w/w ratio to client protein, SerpinB2 (21 µM) inhibited the DTT-induced aggregation of BSA (15 µM) to the same extent as αB-crystallin (50 µM) a well characterised chaperone (positive control) (Fig.4.3.A and B). Interestingly, this level of aggregation inhibition was only observed when the real-time light scattering assay was conducted within a 96 well microplate (Fig.4.3.A). When the assay was conducted within a 384 well plate, under the same conditions, SerpinB2 was found to be less efficient (Fig.4.3.C). The variability in chaperone activity observed between the two plate formats may be related to aggregation dynamics, whereby loss of chaperone function is correlated with increasing rate of substrate aggregation (Lindner et al. 2001). This is supported by the finding that a 1 $mg.mL^{-1}$ solution of BSA/DTT aggregated faster and to a greater extent within the 384 well plate (Fig.4.3.C), compared to that within a 96 well plate (Fig.4.3.A) as is shown by the A360 trace over time. Regardless, in both assay formats SerpinB2 was able to at least partially inhibit BSA aggregation suggesting potential chaperone activity for this serpin under reducing conditions. In comparison, SerpinB14 (22 µM) enhanced aggregation of BSA within the 96 well plate based assay, when used at the same w/w ratio as SerpinB2 (Fig.4.3.A). Furthermore,

when incubated alone under the same conditions, the serpins and αB-crystallin did not aggregate (Fig.4.3B).

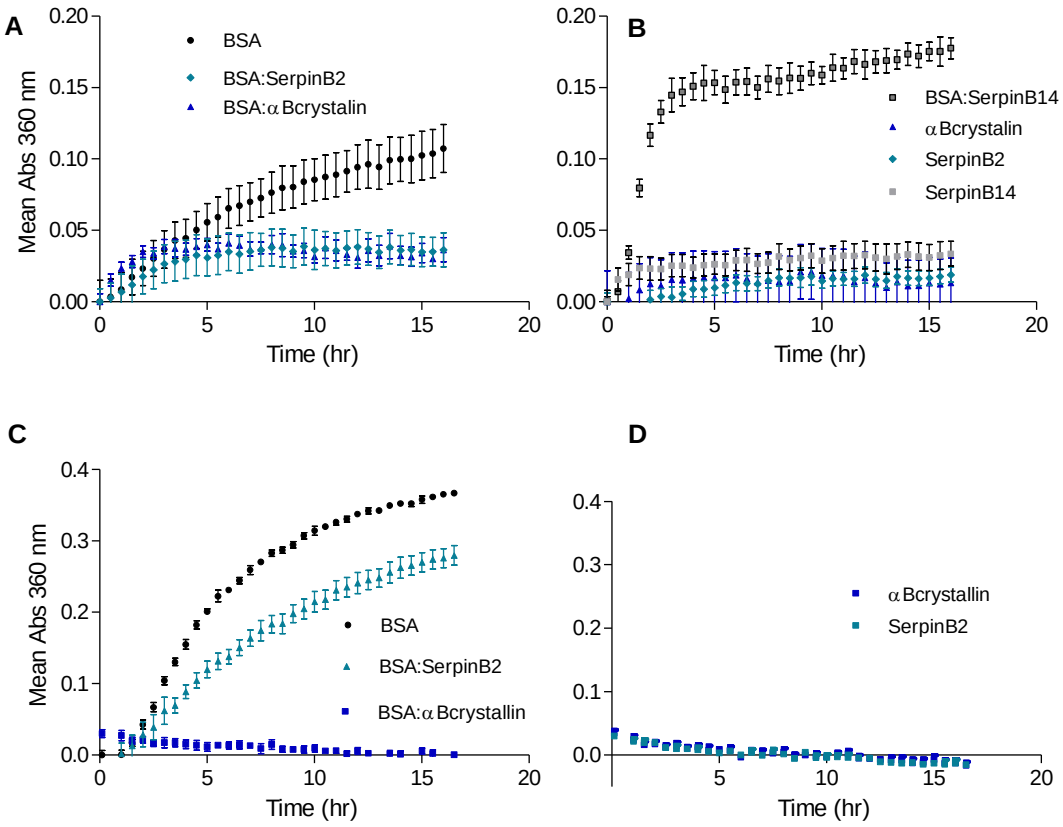

Figure 4.3. SerpinB2 inhibits aggregation of BSA under reducing stress. BSA (1 mg.mL^{-1}) was incubated for 15 h at 37 °C in the presence of 20 mM DTT in the absence or presence of SerpinB2, αB-crystallin or SerpinB14 (1:1 w/w) within either a **(A)** 96 or **(C)** 384 well plate. Controls are shown in panel **(B and D)** for each experiment respectively. In all assays, aggregation was determined in real time by assessing changes in turbidity (A360 nm). Data = mean ± SEM with appropriate background controls subtracted, n=3.

We next investigated the chaperone activity of SerpinB2 under oxidative stress using the substrate lysozyme, as previously described (French et al. 2008). SerpinB2 is known to polymerise under these conditions (Wilczynska et al. 2003;

Lobov et al. 2004), however the physiological function of this property is unknown. SerpinB2 enhanced aggregation of lysozyme incubated at 37 °C in oxidative stress buffer (OSB) at a molar ratio of 20:1 (Lysozyme:SerpinB2) (Fig. 4.4.A). SerpinB14 (negative control) used at the same molar ratio (20:1) also enhanced aggregation of lysozyme, however the affect was greater than that seen for SerpinB2 (Fig. 4.4.B). It is important to note that incubation of SerpinB2 or SerpinB14 only in the presence of OSB did not result in detectable protein aggregation (Fig. 4.4.B.).

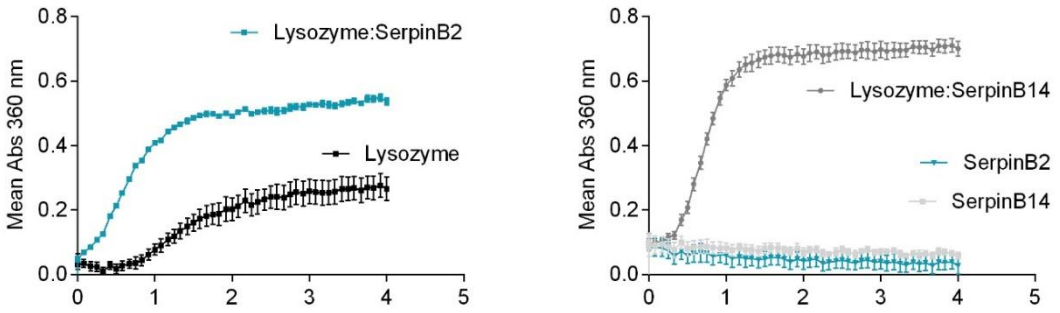

Figure 4.4: SerpinB2 enhances amorphous aggregation of Lysozyme under oxidative stress. Lysozyme (70 µM) was incubated at 37 °C for 4 h under oxidative stress conditions in the absence or presence of **(A)** SerpinB2 or **(B)** SerpinB14 (20:1 molar ratio). In all assays, aggregation was determined in real time by assessing changes in turbidity (A360). Data represents mean ± SEM with appropriate background controls subtracted, n=3.

We next investigated SerpinB2 chaperone activity in the presence of CS, under heat denaturing conditions (Fig. 4.5). SerpinB2 had no effect on CS aggregation at a 1:1 molar ratio and was indistinguishable to SOD1 (negative control), which was not surprising given that there was no specific binding to the misfolded CS

within the end-point binding assays (refer to Fig.4.1), whilst αB crystallin reduced CS precipitation by approximately 50% (Fig.4.6).

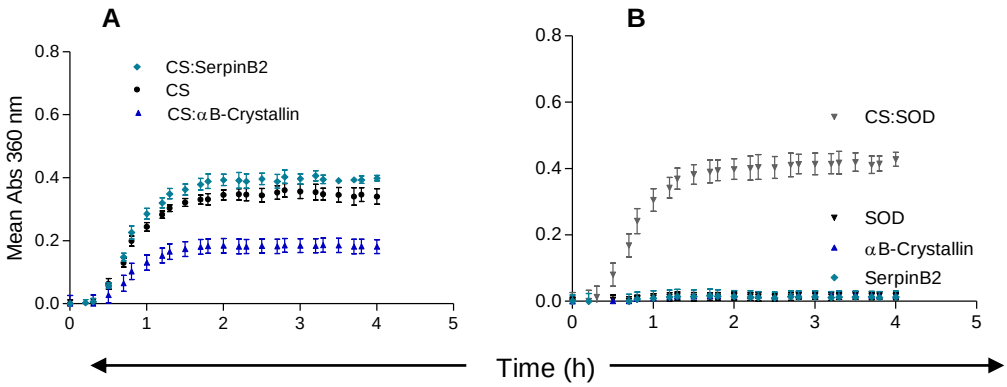

Figure 4.5: SerpinB2 does not inhibit amorphous aggregation of Citrate Synthase (CS) under heat stress. CS was incubated in the absence or presence of **(A)** SerpinB2, αB-crystallin or (**B)** SOD1 at 1:1 molar ratio for 4 h at 43 °C. Also shown in **(B)** are protein only controls. In all assays, aggregation was determined in real time by assessing changes in turbidity (A360). Data represents mean ± SEM with appropriate background controls subtracted, n=3.

4.5.2.2. Amyloid-β peptide Fibril formation

Given the co-localisation of SerpinB2 with microglial aggregates, in association with senile plaques of Alzheimer's patients (Akiyama et al. 1993), up-regulation of SerpinB2 by microglia following activation by incubation with amyloid-β 1-42 peptide for 24 h (Walker et al. 2006) and other published works showing interactions between amyloid-β and other Serpin family members (Schubert 1997; Janciauskiene et al. 1998; Kinghorn et al. 2006; Chiou et al. 2009) we also investigated the potential for SerpinB2 to inhibit fibril formation of amyloid-β peptide (Aβ) using a standard thio-T fluorescence assay. SerpinB2 was able to completely

inhibit $A\beta_{1-40}$ peptide from aggregating at a 10:1 molar ratio of $A\beta_{1-40}$:SerpinB2 (Fig.4.6.A). The efficiency was comparable to that of αB-crystallin used at similar molar ratios (Fig.4.6.A). SerpinB2 was not as efficient as αB-crystallin at inhibiting the faster aggregating $A\beta_{1-42}$ peptide (Fig.4.6.B). SerpinB2 was able to inhibit fibril formation by $A\beta_{1-42}$ peptide during the first 5 h of incubation as seen by the extended lag phase, but this was not sustained as a substantial increase in thio-T fluorescence was observed in the latter part of the real-time assay (Fig.4.6.B). In comparison, αB-crystallin completely inhibited $A\beta_{1-42}$ fibril formation for the duration of the assay (Fig 4.6.B), whilst SOD1 (negative control) had minimal effect.

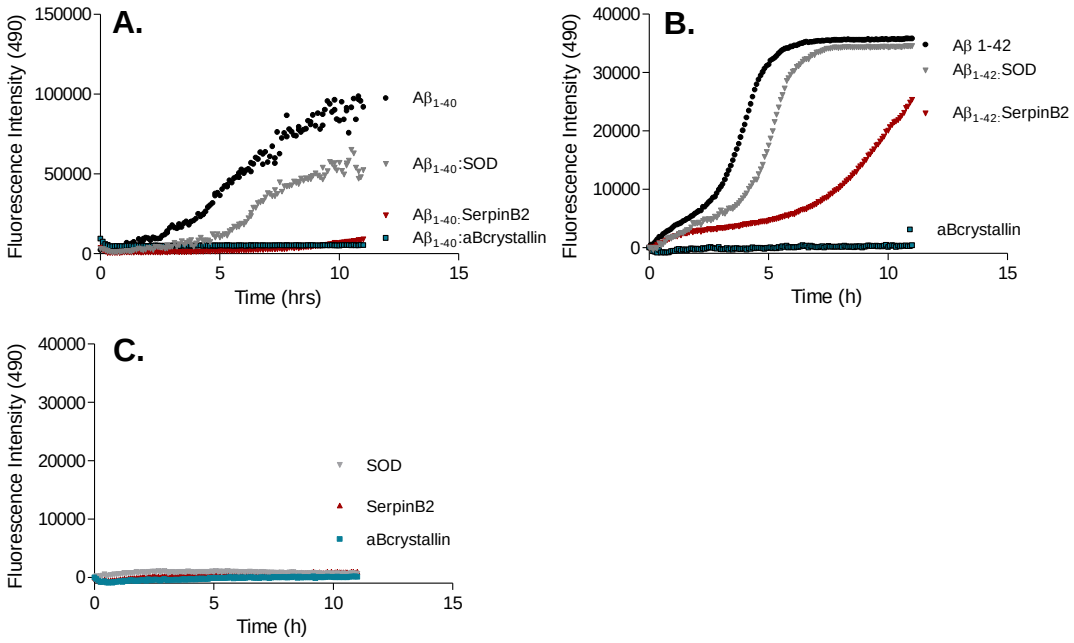

Figure 4.6: SerpinB2 inhibits the formation of amyloid fibrils *in vitro*. Amyloid peptide **(A)** $A\beta_{1-40}$ or **(B)** $A\beta_{1-42}$ were incubated at 37ºC in the absence or presence of SerpinB2, αB-crystallin or SOD1 (negative control) at 10:1 Aβ:protein molar ratio for 11 h. **(C)** No fibril formation was observed in protein samples alone. Fibril formation was determined using Thioflavin-T (25 µM) and change in relative fluorescence (490 nm) over time. Data represents mean fluorescence intensity with background controls subtracted, n=2.

As a complementary approach to analyse the ability of SerpinB2 to inhibit Aβ peptide fibril formation, samples taken from $A\beta_{1-42}$ solutions supplemented (or not) with SerpinB2, αB-crystallin or SOD1, and incubated for 12 h at 37ºC were analysed by scanning electron microscopy (SEM). As expected under these conditions we observed the formation of fibrillar structures within both the $A\beta_{1-42}$ (Fig.4.7.A) and $A\beta_{1-42}$:SOD1 (negative control) (Fig.4.7.B) solutions, indicating that SOD1 was unable to prevent fibril formation and this was consistent with results

obtained within the thio-T assays (Fig.4.6). Importantly, $A\beta_{1-42}$ fibrilar structures were absent from the $A\beta_{1-42}$:SerpinB2 (Fig.4.7.C) or $A\beta_{1-42}$:αB-crystallin (Fig.4.7.D) solutions, which is indicative of inhibited fibril formation.

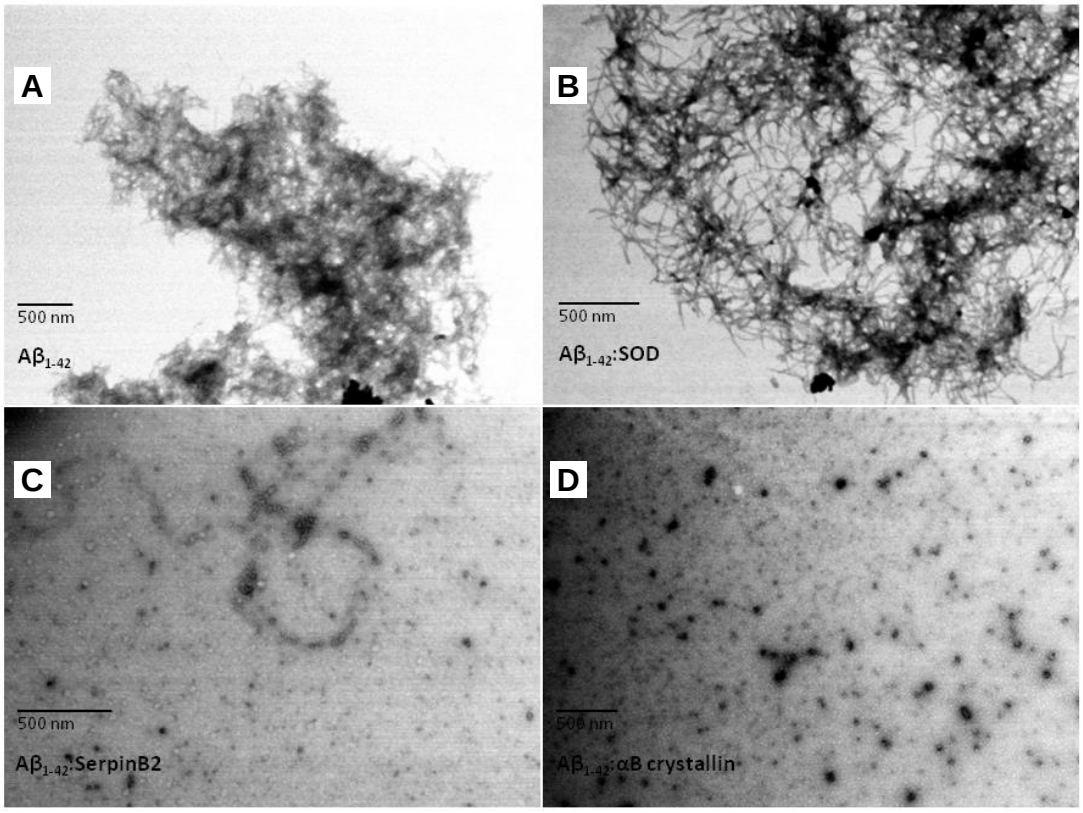

Figure 4.7: Scanning Electron Micrographs of $A\beta_{1-42}$ (25 μM) fibril formation in the absence **(A)** or presence of either (2.5 μM) SOD1 **(B)** (negative control), SerpinB2 **(C)** or αB-crystallin **(D)**. Samples were incubated at 37ºC of 12 h prior to mounting onto carbon coated nickel 400 mesh grids covered in formvar resin and visualised using a JSM7500FA cold Field Emission Gun Scanning Electron Microscope (JEOL) with an acceleration voltage of 20.0 kV and a working distance of 8 mm (spot size setting of 8).

Previous work investigating the interactions between Aβ peptide and SerpinA1 (alpha1-antichymotrypsin) (Janciauskiene et al. 1998) or SerpinI1 (neuroserpin) (Kinghorn et al. 2006) suggests that Aβ binding occurs within the β-sheet A of serpins, which in turn, obstructs complete RCL insertion upon protease inhibition and results in loss of inhibitory function (ref Fig. 1.1). To investigate this potential interaction between SerpinB2 and Aβ peptide we used end-point samples taken from the real-time assay shown in Fig. 4.6.B, and assessed SerpinB2 inhibitory activity by formation of uPA-SerpinB2 complexes using a gel-shift assay and western blotting. Samples were resolved and membranes probed for SerpinB2 (Fig. 4.8). As expected, SerpinB2 only (positive control) (Fig. 4.8, Lane i) consisted of monomer and high molecular weight species indicative of polymerised SerpinB2 (Wilczynska et al. 2003; Lobov et al. 2004). In the absence of $A\beta_{1-42}$, SerpinB2 was able to form a high molecular weight complex with uPA (Fig. 4.8, Lane ii orange arrows). A small amount of cleaved SerpinB2 was present in this sample (Fig. 4.8, Lane ii; blue arrow), which is indicative of SerpinB2 acting as a uPA substrate (Silverman et al. 2001). Importantly, the bands corresponding to uPA:SerpinB2 complex formation are diminished in the presence of $A\beta_{1-42}$ peptide (Fig.4.8 lane iii; orange arrows). Furthermore, the loss of signal intensity for complex formation coincided with an increased signal intensity for cleaved SerpinB2 (Fig. 4.8, Lane ii; blue arrow), indicating that the inhibitory activity of SerpinB2 is compromised in the presence of $A\beta_{1-42}$ peptide.

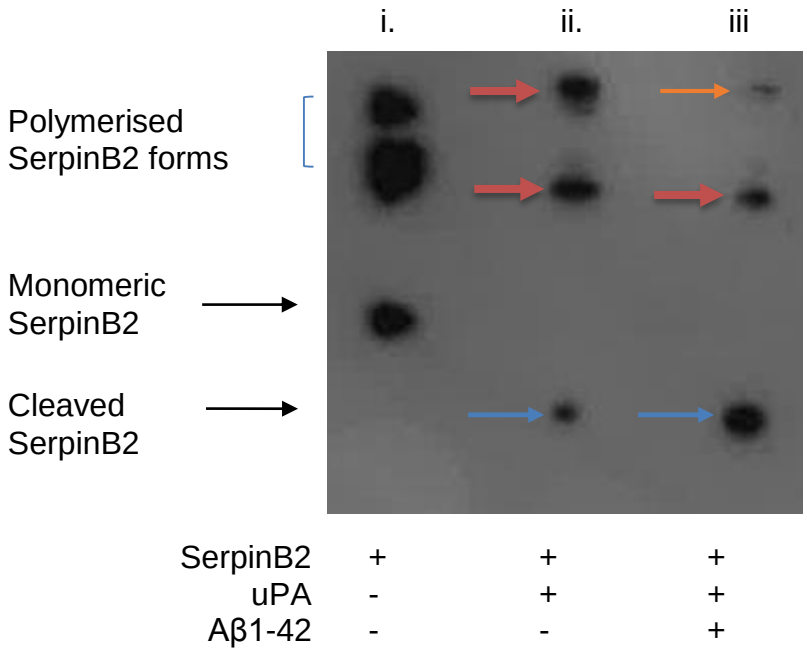

Figure 4.8. $A\beta_{1-42}$:SerpinB2 complex formation inhibits Serpin activity. SerpinB2 was incubated for 11 h at 37 ^{o}C in the absence or presence of 10 molar excess $A\beta_{1-42}$ peptide. SerpinB2 (2.5µM) activity was then assessed by complex formation with uPA (1.25 µM) at a 2:1 Serpin:protease molar ratio. Samples (15 µL) were fractionated under non-reducing conditions by SDS PAGE and analysed by western blot. Detection of SerpinB2 was conducted with relevant primary and HRP-conjugated secondary antibodies as stated in the methods. Orange arrows indicate uPA:SerpinB2 complexes. Blue arrows indicate cleaved SerpinB2.

4.6. Discussion

Disruption of normal protein homeostasis (proteotoxic stress) is integral to the pathophysiology of both acute injury associated inflammation, neuronal dysfunction and age related neurodegeneration (Hipp et al. 2014). As described in section 4.2, recent research has shown that SerpinB2 expression is massively upregulated in neurons and immune cells after stress. These observations, and the role of other serpin molecules in modulating proteostasis through chaperone-like activities, such SerpinH1/H2 (Gettins 2002; Sauk et al. 2005), SerpinA1 (Zsila 2010), SerpinA6 (Westphal 1986; Hammond et al. 1987; Pemberton et al. 1988; Hammond 1990) and SerpinA7 (Pemberton et al. 1988), led us to assess SerpinB2 for chaperone activity, as a potential mechanism for the putative cytoprotective role described for SerpinB2.

A defining characteristic of chaperones is their ability to bind to misfolded or unfolded proteins (substrates), via exposed hydrophobic residues which are normally buried within the three-dimensional structure of the native protein (Tompa and Csermely 2004; Schroder and Kaufman 2005). We show here that SerpinB2 also binds preferentially to misfolded-stressed BSA, CPK and lysozyme, compared to their respective native-conformation controls and to either native or misfolded conformations of CS. This shows that SerpinB2, like known chaperones such as αB-crystallin (Carver and Lindner 1998) and clusterin (Humphreys et al. 1999), is able to identify misfolded proteins. Whether the association of SerpinB2 with misfolded substrates occurs via hydrophobic interaction remains to be

investigated. Of note however, 44% of the amino acid residues within the highly mobile C-D loop of SerpinB2 are hydrophobic. Furthermore, the finding by (Wilczynska et al. 2003) that SerpinB2 undergoes redox sensitive conformational rearrangements via disulphide bond formation between C79, located within the C-D loop, and C161 at the bottom of helix F, is of interest. Disruption of this bond by site directed mutagenesis (C79S), was shown to significantly increase the surface hydrophobicity of SerpinB2, as determined by an observed increase in the 4,4′-Dianilino-1,1′-binaphthyl-5,5′-disulfonic acid dipotassium salt (*bis*-ANS) binding, a common dye used to identify or block pockets of hydrophobicity (Musci and Berliner 1985). It is tempting therefore, to speculate that these hydrophobic characteristics described for SerpinB2 contribute to the preferential binding of SerpinB2 to misfolded proteins and as such warrant further investigation. Interestingly, SerpinB14, used here as a negative control, also bound, preferentially, to misfolded-stressed BSA and lysozyme, compared to their relative controls, but not CPK or CS. Importantly, the fold increase in binding of SerpinB2 to misfolded substrate, relative to controls, was consistently higher in magnitude than that seen for SerpinB14. Given the sequence identity of 36% (Benarafa and Remold-O'Donnell 2005) and sequence similarity of 33% between SerpinB2 and SerpinB14, it is possible that SerpinB14 contains exposed regions of hydrophobicity, which contribute to these observed binding interactions.

Importantly, the ability of molecular chaperones to identify and interact with misfolded substrates typically corresponds with protection of the substrate from

aggregation (Hartl et al. 2011). In this respect, we show here that SerpinB2 significantly inhibited the formation of amorphously structured BSA aggregates under reducing conditions and that this protective effect was indistinguishable from that of a classical chaperone, αB-crystallin at the same BSA:chaperone (1:1 w/w) ratio. It was therefore surprising to find that under oxidative conditions lysozyme aggregation was enhanced by SerpinB2. However, this observation is supportive of the increased hydrophobicity of SerpinB2 upon disruption of the C79-C161 disulfide bond, described by Wilczynska et al. (2003), which would also occur under reducing conditions. In the presence of oxidative stress, formation of the C79-C161 disulfide bond would be favourable, potentially not allowing the increase in hydrophobicity and disrupting chaperone activity by decreasing hydrophobic interactions. The loss or gain of chaperone activity in response to changes in redox states, pH or temperature is well documented, for example, Hsp33 is a redox sensitive chaperone found in bacteria and is activated under oxidative conditions (Graumann et al. 2001) (Kumsta and Jakob 2009). Furthermore, the chaperone activity of clusterin was found to been enhanced by reduction in pH (Poon et al. 2002), whilst that of αA-crystallin is enhanced by increased temperature (Bova et al. 1997). Interestingly, the increased chaperone activity described for αA-crystallin coincided with increased hydrophobicity, as determined by BIS-ANS binding assays (Das and Surewicz 1995). Of note, SerpinB2 alone did not aggregate in the presence of oxidative stress, therefore it seems most likely that SerpinB2 interaction with lysozyme, possibly through disulphide bond formation, enhances the rate of aggregation. Therefore it is possible that the substrate model used for

investigation of SerpinB2 chaperone activity, under oxidative stress conditions may not be suitable and further experiments are required to characterise the efficiency of SerpinB2 to inhibit aggregation undergoing oxidative stress.

SerpinB14 was found to enhance aggregation of BSA and lysozyme under the same experimental conditions for SerpinB2. Interactions between lysozyme and SerpinB14, undergoing heat-stress have been reported previously (Matsudomi 1986; Matsudomi 1987) and thought to occur via electrostatic attraction and sulfhydryl-disulfide interchange. Recent investigation of the interaction between heat-stressed lysozyme and ovalbumin shows incorporation of both molecules into amyloid like fibril formations (Sugimoto et al. 2011). Whether fibril aggregation occurred between lysozyme and SerpinB14, or indeed SerpinB2 in the presence of oxidative stress is unknown however, the increase in relative turbidity suggests that SerpinB14 is interacting with both BSA and lysozyme, and therefore is contributing to amorphous aggregation through an unknown mechanism. In contrast, αB-crystallin completely inhibited BSA and lysosome aggregation under these assay conditions. Importantly, the preferential binding of SerpinB14 to either BSA or lysozyme in the plate based assays did not correlate with chaperone activity within the amorphous aggregation models investigated. Neither SerpinB2 or SerpinB14 were effective inhibitors of amorphous aggregation by citrate synthase under heat denaturing conditions, whilst αB-crystallin reduced aggregation by approximately 50%.

Whilst rapid aggregation is largely driven by hydrophobic forces and primarily results in amorphous aggregates, the formation of fibrillar aggregate structures is slower and gives rise to neurodegenerative diseases (Chiti and Dobson 2006). Interestingly, Serpins A1, A3 (Eriksson et al. 1995) (Aksenova et al. 1996) and I1 (neuroserpin) (Kinghorn et al. 2006) have previously been shown to inhibit fibril formation by the Aβ peptides, associated with Alzheimer's disease. Therefore, we next investigated the potential chaperone activity of SerpinB2, using Aβ peptides within fibril formation assays. Importantly, SerpinB2 was able to inhibit fibril formation by $A\beta_{1-40}$ peptide at a molar ratio of 10:1 Aβ:SerpinB2 and this was indistinguishable from the inhibitory efficiency of αB-crystallin, at the same molar ratio. The inhibition of $A\beta_{1-40}$ fibril formation by αB-crystallin, under similar assay conditions used herein, has been previously described (Dehle et al. 2010) and is consistent with our findings.

In similar experiments, SerpinB2 was found to inhibit $A\beta_{1-42}$ fibril formation over a 5 h period, however this effect was not sustainable and an increase in fibril formation as assessed by Thio-T fluorescence was observed between the 5 and 10 h time periods. Conversely, no $A\beta_{1-42}$ fibrillar forms were observed, by SEM, within an alternate experiment, in the presence of SerpinB2 or αB-crystallin. Fibrillar aggregation follows a classical sigmoidal trajectory whereby the initial phase (lag phase) of the time course consists of dimer and trimer formations, increasing in subunit association until nuclei form, at which point rapid polymerisation/elongation (growth phase) occurs until the reaction reaches

equilibrium and plateaus (Jarrett and Lansbury 1993). In this context it is possible that SerpinB2 interacts directly with the monomeric form of $A\beta_{1-42}$ peptide, either blocking initial nucleation, as is suggested by the lack of fibril formation observed within the SEM experiment, or by reducing the rate of elongation of pre-existing nuclei (seeds) by sequestering soluble monomers.

Interestingly, early experiments conducted by Fraser et al. (1993) reported the association of Aβ peptide with SerpinA3, via 10 amino acid residues within the N-terminal region of the peptide. It has since been shown that $A\beta_{1-42}$ peptide interacts directly with SerpinA3 via either the carboxyl-terminal segment (peptide) and β-sheet C of the serpin or the amino-terminal segment (peptide) and β-sheet A (Janciauskiene et al. 1998). Furthermore, Kinghorn et al., (2006) reported a direct interaction between SerpinI1 (neuroserpin) and $A\beta_{1-42}$ which was shown to obstruct serpin function and inhibited SerpinI1 polymer formation. As both conformational rearrangements of SerpinI1 require RCL insertion into β-sheet A, this work corroborates $A\beta_{1-42}$-Serpin (β-sheet A) interactions previously described for SerpinA3 (Janciauskiene et al. 1998). Therefore, we have utilised a similar gel-shift assay to that described by Kinghorn et al. (2006) and shown that Aβ peptide interactions with SerpinB2 result in the same reduction of serpin function as described for SerpinI1 (Kinghorn et al. 2006). Whilst a reduction in serpin-protease complex formation was observed, experiment confirmation of the proposed β-amyloid binding site within β-sheet A of SerpinB2 is required. Nonetheless, we have shown that SerpinB2 interacts with both forms of Aβ peptide

and the binding interaction is consistent with those recently described for other serpin members. Importantly, the loss of serpin function supports the observation that SerpinB2 may bind to monomeric Aβ peptide, thereby limiting nucleation or the rate of polymerisation by reducing the concentration of peptide in solution.

Taken together the work presented here provides preliminary evidence that SerpinB2 may function within proteostasis networks, as a chaperone-like protein. In this context we show that SerpinB2 identifies and binds preferentially to misfolded proteins and displays holdase-like chaperone activity towards amorphous aggregations within a reducing, but not oxidative or heat stressed environment. Whether this variation in chaperone-activity is related to functional conformational rearrangement and activation, is not clear, but warrants further investigation. SerpinB2 also exhibits efficient chaperone-like activity towards Aβ peptide, consistent with previous works for other serpins. Further investigation of the proposed function of SerpinB2, within proteostasis networks is required at a cellular level. Therefore, experiments investigating the cytoprotective characteristics of SerpinB2 within a cell based, protein aggregation model are described in chapter 5.

5. SerpinB2 protects cells from proteotoxic stress through modulation of protein degradation pathways.

5.1. Abstract

Up-regulation of SerpinB2 in response to cellular stress is well-established, the intracellular pathways in which SerpinB2 may function, however, are poorly defined. Key to cell survival are protein quality control systems which maintain proteostasis through the chaperone and protein degradation pathways. SerpinB2 has been implicated within these networks via identification of potential intracellular binding partners, such as proteasome subunit beta type 1 (PSMB1, a component of the proteasome) (Fan et al. 2004) and the ubiquitin-like interferon stimulated gene-15 (ISG15) (Giannakopoulos et al. 2005), which are functional components of the ubiquitin-proteasome degradation pathway. In this context, the mutant Htt_{exn-1} model of protein aggregation and proteotoxicity (Olshina et al. 2010) was utilised to investigate the cellular processing of misfolded protein by SerpinB2 null mouse embryonic fibroblasts and provides evidence of impaired inclusion body (IB) formation and proteasome activity in the absence of SerpinB2. Furthermore, this work suggests that SerpinB2 may exert its cytoprotective characteristics through regulation of autophagy.

5.2. Introduction

SerpinB2 is a member of the Serine Protease Inhibitor super family that has been localised to both the extracellular and intracellular environment of numerous cell types including keratinocytes, endothelial, epithelial, monocytic and neuronal cells (Lee et al. 2011). Secreted as a 47 kDa or glycosylated 60 kDa protein,

extracellular SerpinB2 is thought to function as an inhibitor of the urokinase plasminogen activator and to a lesser extent, tissue-type plasminogen activator (Kruithof et al. 1995). The majority of SerpinB2 is, however, retained within the intracellular environment as a 47 kDa protein (Lee et al. 2011). The main producers of SerpinB2 are cells of the myeloid lineage which up regulate SerpinB2 expression during cell developmental phases, such as proliferation and differentiation, or in response to pathology, especially inflammation and cellular stress (Schroder et al. 2010; Lee et al. 2011). As yet an intracellular protease target for this serpin has not been defined which suggests a role independent of the classical inhibitory mechanisms characteristic of serpins (Law et al. 2006).

Of interest are the intracellular networks upregulated in response to cellular stress and the role SerpinB2 may pay within these pathways. We have previously shown that SerpinB2 binds preferentially to unfolded proteins following reductive, oxidative or heat stress (Chapter 4). Furthermore, SerpinB2 was found to inhibit amorphous aggregation of reduction-stressed BSA, but not other models, and fibril formation of both amyloid-β 1-40 or 1-42 peptides (Chapter 4). These chaperone-like characteristics of SerpinB2 suggest a role within quality control systems that maintain proteostasis. The isolation or removal of deleterious proteins from the intracellular compartment is key to cell survival and is facilitated through either the ubiquitin/proteasome degradation pathways or autophagy and the lysosomal degradation pathway (Tyedmers et al. 2010).

The 26S proteasome is an ATP-dependent proteolytic macro-complex that is found within the cytoplasm and nucleus (Peters et al. 1993; Brooks et al. 2000). Comprising of a proteolytic core (20S complex), the proteasome forms a cylindrical structure, which incorporates 28 protein subunits arranged into 4 rings (Gallastegui and Groll 2010). The proteolytic component of the proteasome is made up of seven β-subunits (β_1 to β_7) that are buried within the core of the complex. Proteasome activity is tightly regulated with assembly and disassembly of the macro-complexes facilitated by proteasome assembly chaperones; and access to the enzymatic core - via the 19S regulatory subunits, which cap the 20S complex - is mediated by a tightly regulated network of deubiquitinating enzymes (DUBs), shuttling factors and unfoldase chaperones (reviewed in (Adams 2004; Nalepa et al. 2006; Herrmann et al. 2007). Proteins are targeted to the proteasome for degradation through modification with ubiquitin or ubiquitin-like adapter proteins, such as SUMO, Nedd8 and interferon stimulated gene-15 (ISG15) (Kerscher et al. 2006). In the context of proteostasis, the proteasome system functions to recycle functional proteins that are no longer required by the cell or to protect cells through the clearance of soluble, misfolded proteins, thereby preventing protein aggregation (Tyedmers et al. 2010). However, the proteasome does not function in the clearance of insoluble protein aggregates (Bence et al. 2001; Verhoef et al. 2002). Therefore, alternative quality control mechanisms, such as the autophagy-lysosomal degradation pathway, are required to maintain cellular proteostasis, in complementation with the proteasome.

Macro-autophagy (herein referred to as autophagy) involves the complex cascade of steps that give rise to the formation of double-membrane structures, which incorporate substrates such as protein aggregates and damaged organelles, for degradation via the lysosome (He and Klionsky 2009; Nakatogawa et al. 2009). The class III phosphatidylinositol 3-kinase (PtdIns3K) complex mediates initiation of the pathway through formation of the phagophore membrane. Recruitment of autophagy specific (Atg) proteins into the phagophore, facilitates elongation of the membrane and encapsulation of target substrates (Suzuki et al. 2007; Kawamata et al. 2008), resulting in the formation of a complete vesicular compartment, known as the autophagosome. This vesicle is transported along the microtubule network via dynein and microtubule-associated proteins, such as the HDAC6 (Iwata et al. 2005), to the lysosome where autophagosome-lysosome fusion results in formation of the autolysosome and cargo degradation by lysosomal proteases occurs. Basal levels of autophagy activity within cells (under normal physiological conditions) are low and regulation (positive or negative) of the pathway is tightly controlled throughout each phase from phagophore initiation to neutralisation of the autolysosome (He and Klionsky 2009). Interestingly, the initial seeding of the phagophore is negatively regulated by B-cell lymphoma-2 (Bcl-2) inhibitory interaction with Beclin-1 (Liang et al. 1998; Pattingre et al. 2005), a component of the PtdIns3K complex.

SerpinB2 expression was recently shown to stabilise Beclin-1 and promote autophagy (Chuang et al. 2013). Furthermore, SerpinB2 was found to interact with the β-subunit type-1 component of the proteasome 20S core chamber, following GST-pulldown experiments (Fan et al. 2004), and SerpinB2 was identified as a target for the ubiquitin-like adapter protein, ISG15, following mass spectrometric analysis of anti-ISG15 immunoprecipitates (Giannakopoulos et al. 2005). Taken together, these findings provide evidence for a possible role of SerpinB2 within proteostasis pathways which warrants further investigation.

5.2.1. Rationale and Aims

Given the *in vitro* chaperone-like activity of SerpinB2 (Chapter 4) and evidence in the literature implicating SerpinB2 within autophagy and the ubiquitin/proteasome pathways, we hypothesise that SerpinB2 may function in cellular stress response pathways that involve binding to misfolded proteins. Therefore, using mouse embryonic fibroblasts (MEF) from control (wild-type) mice or the SERPINB2 null mouse model (Dougherty et al. 1999) we investigated the potential role of intracellular SerpinB2 in proteostasis. To this end we employed an intracellular aggregation model to investigate the processing of aberrant proteins and the affect SerpinB2 may have on i) Cell viability ii) Inclusion body formation and iii) Protein degradation pathways.

5.3. Materials and Methods

5.3.1. Materials

Recombinant human SerpinB2 (47 kDa) was purified from *E. coli* (M15) using the pREP4/PQE-9 expression system as described in section 4.3.2. ISOLATE RNA Mini Kit and BioScript One-Step RT-PCR kit were from Bioline. 20 µm filter caps were from Millipore and Polyfect was from Qiagen Pty Ltd, RPMI1640, tissue culture flasks, Lipofectamine2000, fetal calf serum (FCS), trypsin EDTA. Sytox-red was obtained from Invitrogen. Polybrene, gelatin, MG-132 and propidium iodine were from Sigma Aldrich.

5.3.2. Generation of Mouse Embryonic Fibroblast primary cell lines.

MEFs were isolated from wild-type and SerpinB2$^{-/-}$mice as previously described (Dougherty et al. 1999; Schroder et al. 2010). Briefly, a pregnant female C57/Black-6 mouse was euthanised at day 13.5 post coitus by CO_2 asphyxiation. The uterine horns containing the embryos were dissected from the mouse and placed in sterile PBS on ice. The uterine wall was cut and each embryo removed and separated from its amniotic sac. A scalpel blade was used to remove the head and liver and the remaining tissue was resuspended in 10 ml of trypsin-EDTA. The embryos were finely minced with a scalpel blade for approximately 1 min and then incubated at 37 ºC for 5 min. The tissue was homogenised by passing gently through an 18 gauge needle several times and allowed to settle for 5 min at room temperature. The supernatant (cell suspension) was transferred to a tube containing 20 mL of pre-warmed RPMI + 10% FCS and centrifuged for 5 min at

300 x *g*. The cell pellet was resuspended in RPMI1640 + 10% FCS and plated on 0.1% gelatin (passage 0). Primary cultures were then continually passaged until spontaneous immortality was obtained. This work was conducted by Dr Wayne Schroder, Queensland Institute of Medical Research (QIMR).

Mouse embryonic fibroblasts were maintained in RPMI-1640 containing 10% FCS and cultured at 37 °C with 5% CO_2.

5.3.3. Generation of stable MEF cell lines expressing human SerpinB2.

Human WT SerpinB2 cDNA was cloned into the *Xho*1 restriction sites of a murine stem cell virus (MSCV)-based retroviral vector (pMIG) (Szymczak et al. 2004; Brummer et al. 2006; Brummer et al. 2008), giving rise to $pMIG^{SerpinB2}$ constructs (Fig 5.1). Control plasmids ($pMIG^{GFP}$) were also generated.

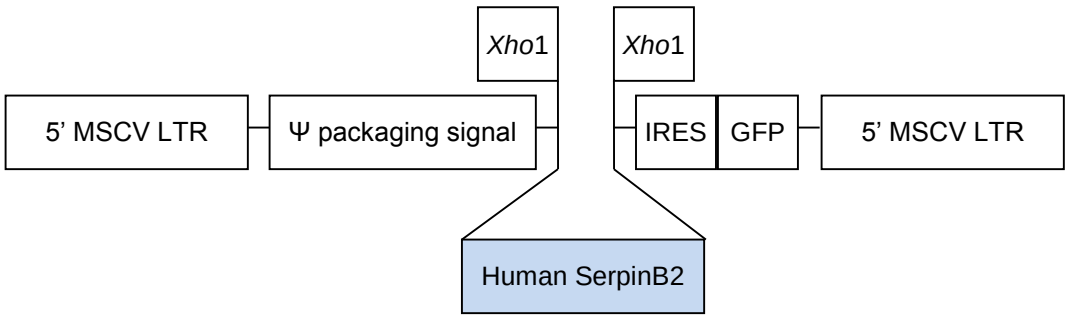

Figure 5.1: Schematic representation of pMIG retroviral construct containing *SerpinB2* cDNA. This vector contains an internal ribosome entry site (IRES) between the SerpinB2 open reading frame (1.2 kb) and a Green Fluorescent Protein (GFP) reporter, driving expression of both from a single promoter. Correct insertion of human SerpinB2 cDNA was confirmed by DNA sequencing of constructs Dr S Lobov, University of Wollongong NSW.

For the production of stable cell lines, retrovirus packaging cell line, PlatE cells (Jomar Biosciences Pty Ltd, Welland, South Australia), were transfected with the pMIG constructs using Polyfect, according to the manufacturer's instructions. Viral supernatants were collected 48 h later, filtered through 20 µm filter caps, 8 µg/mL of polybrene was added and supernatant was added to MEFs. Positive cells were selected by cell sorting on a FACS Vantage (Becton Dickinson), based on the bicistronic expression of GFP. Cell genotype was verified by rt-PCR and SerpinB2 expression within SerpinB2$^{-/-}$ (WT rescue) MEF cells was observed by western blot detection system.

5.3.4. Reverse-transcription PCR

Extraction of total RNA from cell lines and subsequent rt-PCR was conducted using the ISOLATE RNA Mini Kit and BioScript One-Step rt-PCR kit (both from Bioline), as per the manufacturer's instructions. The concentration and purity of RNA obtained using this kit was then assessed by absorbance at 260 nm and 260/280 ratio using a NanoDrop 2000c Spectrophotometer (Thermo Fischer Scientific, VIC, Australia) (Table 5.1).

Table 5.1: Characterisation of total RNA samples extracted from various untransduced and pMIG transduced Mouse Embryonic Fibroblast lines.

Cell Line*	Conc. mRNA sample ($ng.\mu L^{-1}$)	260/280 nm Ratio	Volume used in PCR (µL)
WT MEF	307.2	2.10	4.0
WT(vector) MEF	523.5	2.18	2.5
$SerpinB2^{-/-}$ MEF	371.2	2.12	3.4
$SerpinB2^{-/-}$ (Vector) MEF	636.3	2.16	2.0
$SerpinB2^{-/-}$ (WT rescue) MEF	791.2	2.16	1.6
U-937**	256.9	2.08	5.0

*Refer to Results section 5.4.1 for a description of the various MEF cell lines
**Human histocytic lymphoma cell line, used as a positive control for SerpinB2 expression (Kruithof et al. 1986)

rt-PCR was performed using a Eppendorf, (Mastercycler Pro S) thermal cycler and conducted in 25 µL reaction volumes containing 1.3 µg mRNA (Tab. 5.1), 12.5 µL 2 x One-step RT-PCR Buffer, 1 µL One-step enzyme mix, forward 5′-CTGCTACCCGAAGGTTCTG-3′ and reverse 5′-GGAAGCAACAGGAGCATGC-3′

murine *SERPINB2* primers, 0.5 µL RNAse sample and 8 µL DEPC-treated water. Cycling conditions were as previously described (Schroder et al. 2010) with one cycle of 50 °C for 2 min and one cycle of 95 °C for 2 min, followed by 45 cycles of 94 °C for 5 s, 60 °C for 10 s, and 72 °C for 40 s. The resulting PCR products were analysed by 2% agarose gel electrophoresis and ethidum bromide staining.

5.3.5. Whole cell Lysis

MEF cells were harvested from confluent 25 cm^2 tissue culture flasks using standard trypsinisation methods, washed twice with ice cold PSB then incubated on ice with 500 µL RIPA mammalian cell lysis buffer (65 mM Tris-base, 150 mM NaCl, 8.5 mM MgCl, 10% v/v Gycerol, 0.1% v/v Triton-X100, 12 mM Na-deoxycholate, 5 mM Ethylenediaminetetraacetic acid (EDTA), 1 mM α-phenylmethylsulfonyl fluoride (PMSF)). Samples were then used for protein detection via Western Blot.

5.3.6. Western Blot Development

Proteins fractionated by SDS PAGE were blotted onto Immobilom^{TM}-P PVDF (Millipore, USA) membrane using a Bio-Rad Mini Trans-Blot system as per manufacturer's instructions. After transfer, the PVDF membranes were blocked with 10% skim milk powder in Tris-buffered saline (TBS) with 0.05% (v/v) Tween-20 (TBST) overnight at 4^{o}C. After washing in TBST the primary antibody (α-SerpinB2 MAb (ADI#3750)) was applied at a final concentration of 1:500 in 2% milk/TBST and blots were incubated for 2 hs at RT on a shaker. The membrane

was extensively washed with TBST then re-blocked with 6% milk/TBST for 30 min at RT followed by one wash with TBST for 5 min. Detection of bound primary antibody was conducted using the appropriate horseradish peroxidise (HRP) labelled secondary antibody, which was applied at a final concentration of 1:5000 in 2% milk/TBST for 1 h at RT. Three 5 min washes with TBST were conducted to remove unbound secondary antibody followed by three 5 min washes with TBS.

Protein detection was visualised by an enhanced chemiluminescence (ECL) reaction using SuperSignal® Substrate for Western Blotting (Progen, Australia) as per manufacturer's instructions. The membranes were exposed to X-ray film and developed for analysis.

5.3.7. Mammalian Transfection using the Huntingtin exon1 polyglutamine (polyQ) expansion cell model.

Huntington's disease is caused by autosomal dominant mutations in the *HTT* gene resulting in expansion of a polyQ sequence near the amino-terminus of the huntingtin (Htt) protein that promotes its aggregation (Hatters 2008). Wild type alleles of the *HTT* gene encode polyQ sequences that range between 7 and 36 contiguous glutamine residues and mutant Htt is considered to contain >36 and up to 250 contiguous glutamine residues (Hatters 2008). In the current work we used a well-established Htt aggregation model comprising an exon 1 fragment fused to either 25 polyQ or 46 polyQ sequences (Olshina et al. 2010; Ramdzan et al. 2010; Polling et al. 2014). While longer expansions are more pathogenic, it has been previously demonstrated that aggregation of the 46 polyQ Htt exon 1 fusion protein

occurs in an experimentally tractable timeframe in a process that is well characterised (Olshina et al. 2010).

Untransduced or pMIG construct transduced MEFs were seeded into 6-well plates (in triplicate) containing 19 mm coverslips ($2x10^5$ cells per well) 24 h before transfection with 200 ng of pcDNA3.1-mCherry (control) or pcDNA3.1-Huntingtin exon1-polyglutamine variants fused C-terminally to mCherry (Htt_{ex1}25Q-mCherry or Htt_{ex1}46Q-mCherry) expression vectors (Ramdzan et al. 2010; Polling et al. 2014), using Lipofectamine2000 (Invitrogen) as per manufacturer's instructions. At 24, 36 and 48 h post-transfection, coverslips were removed prior to harvesting the remaining cells for analysis of cell viability by flow cytometry (described below). Cells grown on coverslips were then fixed by incubation in freshly prepared ice cold PBS containing 4% paraformaldehyde (PFA) for 10 min prior to mounting on microscopy slides using mounting solution (1 x PBS containing 50% glycerol). The fixed cells were then visualised using a Nikon Eclipse TE2000-E (Nikon Instruments) with FITC (ex 470-490, em 520-560) and Cy3 (ex 510 – 560 nm, em 565 - 625 nm) filter sets and 60x Plan Apo ∞/0.10-0.22 WD 0.13 oil emersion lens. For analysis of cell viability, cells were harvested by brief trypsinisation, washed in phosphate buffered saline (PBS), incubated on ice with 5 nM Sytox-red in PBS and then analysed by flow cytometry (Becton Dickinson). All data obtained was analysed using FLOJO software version 7.1 (Treestar, Inc).

5.3.8. Huntingtin aggregation assay

Monomeric Htt_{ex1}-46Q-Cerulean-MBP fusion protein was aggregated as previously described (Ramdzan et al. 2010). Briefly, recombinant Htt_{ex1}-46Q-Cerulean-MBP was thawed from frozen stocks, diluted to 9 μM, and rapidly mixed with a 1:20 stock of TEV protease. After 10 min Htt_{ex1}-46Q-Cerulean was diluted, with or without SerpinB2, to a final concentration of 2 μM and at a 1:1 final molar ratio of SerpinB2: Htt_{ex1}-46Q-Cerulean. Duplicate samples were taken at intervals and total protein was determined by cerulean fluorescence (43,000 M-1.cm-1 at 434 nm). Samples were then centrifuged at 13,000 x g for 30 min and supernatant collected as soluble fraction.

5.3.9. Ligand binding assay

Aggregate ligand blots were performed as previously described (Yerbury et al. 2007). Htt_{ex1}-46Q-Cerulean (1 μg) was spotted on nitrocellulose membrane and then blocked with 1% (w/v) heat denatured casein in PBS buffer. SerpinB2 (10 μg/ml solution) or control proteins SerpinB14 (10 μg/ml solution) and clusterin (10 μg/ml solution) were then incubated with separate membranes for 2 h, at RT. Bound interactors were detected using antibodies to either SerpinB2 (1:1000; Abcam, UK; ab137588), SerpinB14 (1:30000; Sigma-Aldrich, C6534), or α-clusterin (neat hybridoma culture supernatant) and subsequent HRP conjugated secondary antibodies (1:2000) all diluted in 1% (w/v) heat denatured casein in PBS buffer.

5.3.10. SerpinB2 Immunostaining

WT MEF cell lines were transiently transfected with Htt_{ex1}46Q:mCherry expression vector as described above, fixed with 4% paraformaldehyde (PFA), permeabilized with 0.1% triton X-100 and then blocked using 5% FCS, 1% BSA 0.1% triton-X100 in PBS. Cells were then incubated in the presence of either rabbit anti-mouse SerpinB2 polyclonal antibody (2 $\mu g.ml^{-1}$; diluted in 1% BSA, 0.1% TX-100 in PBS) (Lee et al. 2015) or matched isotype control rabbit IgG antibody (2 $\mu g.ml^{-1}$; ABCAM; ab171870), followed by wash steps and binding detected using goat anti-rabbit IgG Alexa Fluor®488-conjugated secondary antibody (ABCAM; ab181448 1:500 dilution). Cells were then imaged using laser scanning confocal microscopy. Imaging of SerpinB2 immunofluorescence was kindly conducted by Natalie Farrawell, University of Wollongong.

5.3.11. GFPu Ubiquitin-Proteasome System (UPS) reporter assay

To quantify UPS activity we used the fluorescent UPS reporter GFPu, which relies on a 16 amino acid degron (ACKNWFSSLSHFVIHL) (CL1) fused to the carboxyl terminus of GFP (Gilon et al. 1998; Bence et al. 2001; Bence et al. 2005). Degradation of polypeptides containing the degron is specific to the proteasome, therefore loss of GFP signal is indicative of ubiquitin dependent proteasome activity. GFPu was transfected into MEF cell lines as previously described (section. 5.3.5) and the level of GFP fluorescence in the absence or presence of 250 nM MG-132 was determined using flow cytometry (Becton Dickinson), 48 h post transfection. Data represents viable cells only, as determined by propidium iodide

exclusion and was normalised to MG-132 treated cells after removal of background autofluorescence.

5.3.12. Autophagy reporter assay

Autophagy dysfunction was assessed using the Lyso-ID autophagy reporter (Enzo Life Sciences) as previously described (Francois et al. 2013). WT and SerpinB2$^{-/-}$ MEF cell lines were seeded into a 96-well plate 24 h before addition of an autophagy inhibitor, 3-methyladenine (3-MA, 0-5 mM; Adipogen) or an autophagy inducer, verapamil (0-100 µM; Enzo Life Sciences). MEF cells were then cultured overnight and autophagy quantified using Lyso-ID kit (ENZO), as per manufacturer's instructions. Briefly cells were washed and incubated with the Lyso-ID red dye for 30 min at RT before measuring the level of red fluorescence per cell on the IncucyteZoom automated imaging system (ESSEN Bioscience). Data shown is corrected for background fluorescence. This experiment was conducted by Natalie Farrawell, University of Wollongong.

5.3.13. Statistical Analysis

Statistical analysis was conducted using GraphPad Prism 5. Comparison of growth curves was conducted using nonlinear fit, exponential growth equation (`Y=Y0*exp(k*X)`) to generate doubling times of respective cell lines. Corresponding K values (rate constant) obtained from the analysis were compared by One-way anova, applying the Tukey-Kramer multiple comparison test. Cell

viability assays were analysed by 2-way anova with Bonferroni's multiple comparisons test for significant differences.

5.4. Results

5.4.1. Generation of stable MEF cell lines expressing human SerpinB2 of Mouse Embryonic Fibroblast Cell Lines.

To investigate the role of SerpinB2 as a stress protein we used spontaneously immortalised WT and SerpinB2$^{-/-}$ MEFs that had been retrovirally transduced with either pMIG^{GFP} or pMIG^{SerpinB2} vectors. Using this method three new cell lines were made, consisting of two empty vector control lines, MEF^{WTpMIG} [WT(vector)], MEF$^{SERPINB2-/-}$:pMIG [SerpinB2$^{-/-}$(vector)] and a SerpinB2 knock-in line, MEF^{SERPINB2KI}:pMIG [SerpinB2$^{-/-}$(WT rescue)]. Efficiency of gene introduction was assessed by flow cytometry, with the GFP positive population for each cell line found to represent 93.8%, 92.4% and 80% of total viable cells, respectively (Fig.5.2).

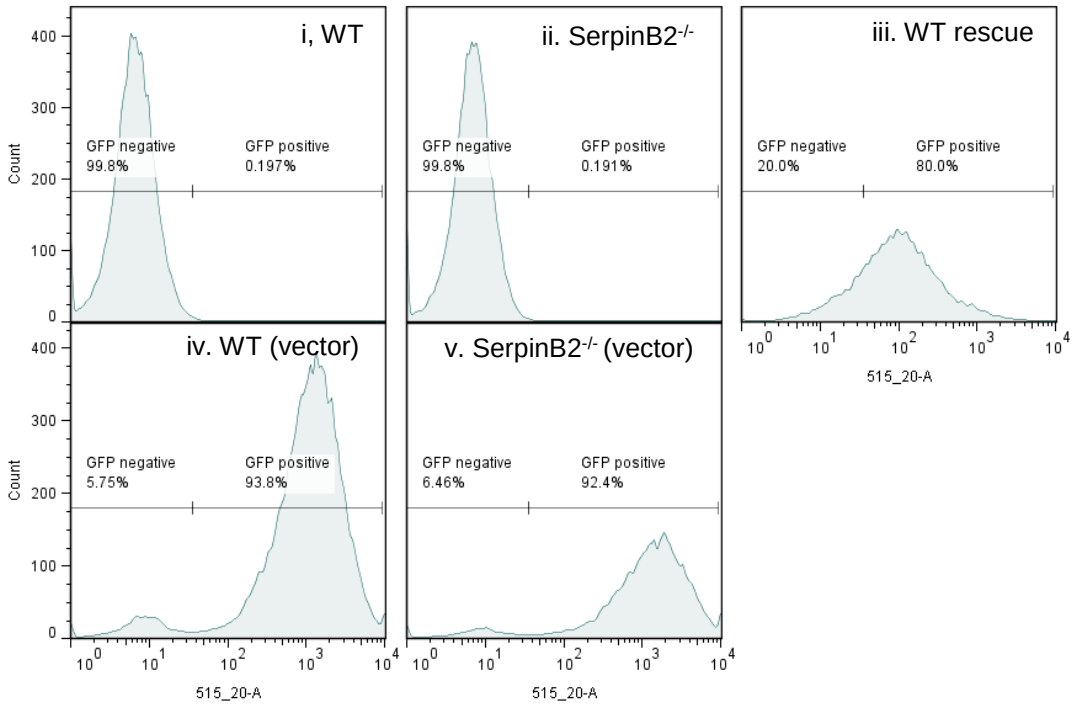

Figure 5.2: Generation of *SERPINB2*$^{-/-}$ WT rescue cell line. Spontaneously immortalised MEF cell lines established from control (WT) and *SerpinB2*$^{-/-}$ mice were transduced with mouse stem cell retroviral pMIG^{GFP}. Transduction efficiency of the parental lines was determined by GFP expression within the transduction control cell lines (empty vector), WT (vector) and SerpinB2$^{-/-}$ (vector) and the human SerpinB2 knock in (SerpinB2$^{-/-}$ WT rescue) cell line using flow cytometry. Cells were gated as GFP negative or positive based on parental lineage **i)** WT, **ii)** SerpinB2$^{-/-}$, **iii)** SerpinB2$^{-/-}$ (WT rescue); **iv)** WT (vector) **v)** SerpinB2$^{-/-}$ (vector). Data represents a minimum of 5000 viable cells as determined by PI exclusion.

To confirm SerpinB2$^{+/+}$, SerpinB2$^{-/-}$ status of the parental lines and transduced cell lines we next conducted RT-PCR amplification of murine *SERPINB2* transcripts using fresh RNA extracts from all MEF cell lines (Fig.5.3A). As expected, the WT and WT (vector) cell lines screened positive for the presence of murine *SERPINB2* gene transcript as is evident by the 270 bp band within lanes 2 and 4 (Fig. 5.3A).

Importantly, no corresponding band was observed for the SerpinB2$^{-/-}$, SerpinB2$^{-/-}$ (vector) and SerpinB2$^{-/-}$(WT rescue) cell lines, (lanes 6, 8 and 10 respectively, Fig.5.3A) confirming their murine SerpinB2 null genotype. Comparable banding intensity was observed for all cell lines corresponding to GAPDH amplification (250 bp) thus confirming the presence of equal template within rt-PCR starting sample and equal loading of the sample onto the visualisation gel. Given the sequence homology between human and murine *SerpinB2* and the potential for non-specific amplification of the human gene using the PCR primers designed to target the murine gene, we also included mRNA extracted from the human U-937 monocytic cell line as a negative control.

We next confirmed expression of SerpinB2 protein via western blot analysis of whole cell lysates. We were unable to detect protein expression within the WT and WT(vector) cell lines due to the lack of a sufficient antibody specific for murine SerpinB2 detection via western blot analysis, at the time these experiments were conducted. Importantly, clear expression of human SerpinB2 was detectable within the whole cell lysates of the SerpinB2$^{-/-}$(WT rescue) cell line, confirming transduction via the pMIG vector system (Fig.5.3B).

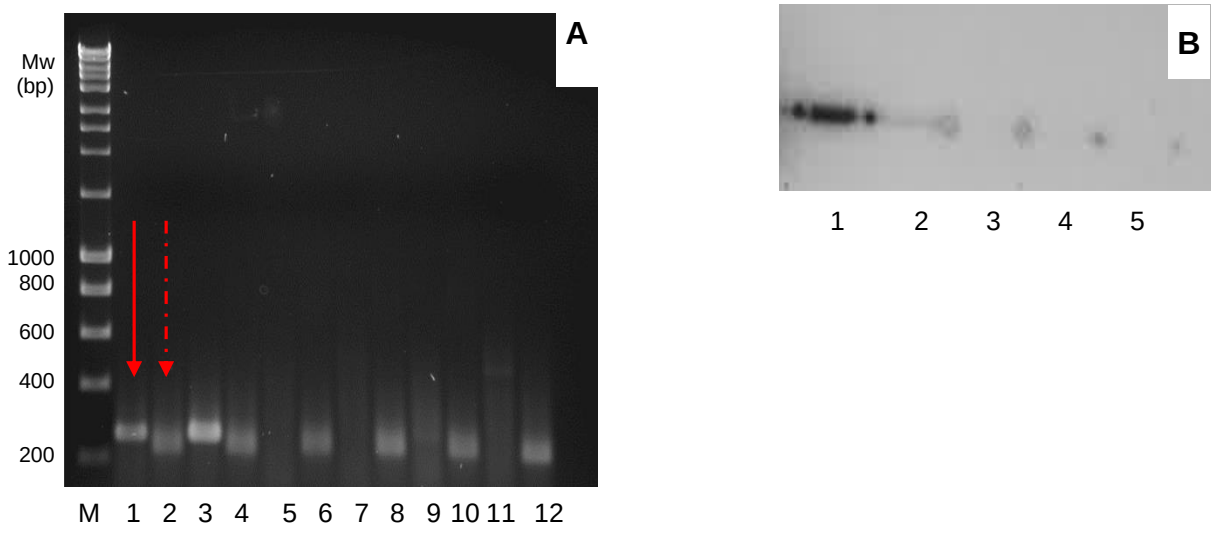

Figure 5. 3: SERPINB2 gene and protein expression in mouse embryonic cell lines (MEF). **A) Reverse transcription-PCR** screening for murine SERPINB2 gene. Fresh mRNA extracts were prepared and equal quantities of template (1.3 µg) used for rt-PCR amplification by BioScript One-Step RT-PCR kit. Predicted Murine SERPINB2 product size is 270 bp (red arrow). Rt-PCR product was visualised by electrophoresis on a 2% Agrose gel. **Lanes: 2**. WT **4**. WT(vector) **6**. SerpinB2$^{-/-}$ **8**. SerpinB2$^{-/-}$(vector) **10.** SerpinB2$^{-/-}$(WT rescue) and **12.** U937 cell line (negative control) show samples containing primers specific for murine SERPINB2. Amplification of GAPDH (positive control) for each cell line can be seen in adjacent odd numbered lanes. **B) Western blot analysis** of MEF whole cell lysates for detection of human-SerpinB2 epression. **Lanes: 1** SerpinB2$^{-/-}$(WT rescue). **2.** SerpinB2$^{-/-}$(vector). **3.** SerpinB2$^{-/-}$. **4.** WT(vector). **5.** WT. Detection of human SerpinB2 was conducted using anti-human SerpinB2 MAb (ADI ##3750) and relevant HRP conjugated secondary antibody

We next assessed the effect, if any, the pMIG transduction had on the growth rates of the respective MEF cell lines relative to parental (non-transduced) cells. Growth curves were constructed from a 72 h time course with measurements taken every 12 h. Non-linear curves were fitted and analysed by application of the exponential growth equation with least squares (ordinary) fit (Fig. 5.4.A). Using this method of analysis it was possible to calculate the mean doubling times for each cell line, being 57.57 h (WT), 61.4 h (WT(vector)), 53.58 h (SerpinB2$^{-/-}$), 53.17 h (SerpinB2$^{-/-}$(vector)) and 71.11 h (SerpinB2$^{-/-}$(WT rescue)) (Fig. 5.4.B). The overall growth trend observed across cell lines was comparable as can be seen by the spread in the calculated doubling times (Fig. 5.4.B) however, the mean doubling time of 71.11 h for the SerpinB2-/-(WT rescue) cell line was 10 to 20 h longer than the time required for population doubling by all other cell lines. We therefore conducted a one way anova analysis using the rate constants (K) obtained from the exponential growth fit, and found that there was a significant difference in growth rates between cell lines ($p=0.0052$, $n=5$). Further comparison using the Tukey-Kramer post test (CI = 95%) ascertained that this difference was only present between SerpinB2$^{-/-}$(WT rescue) and SerpinB2$^{-/-}$ or SerpinB2$^{-/-}$(vector) cell lines (Tab. 5.2). Importantly, the pMIG transduction did not significantly alter the growth rates of the cells relative to their parental lineage, with respect to the control cell

lines. There was no difference observed between the WT and SerpinB2$^{-/-}$ parental lines, indicating that the cell models did not contain metabolic biases. Therefore we concluded that adjustment was not required within future experiments.

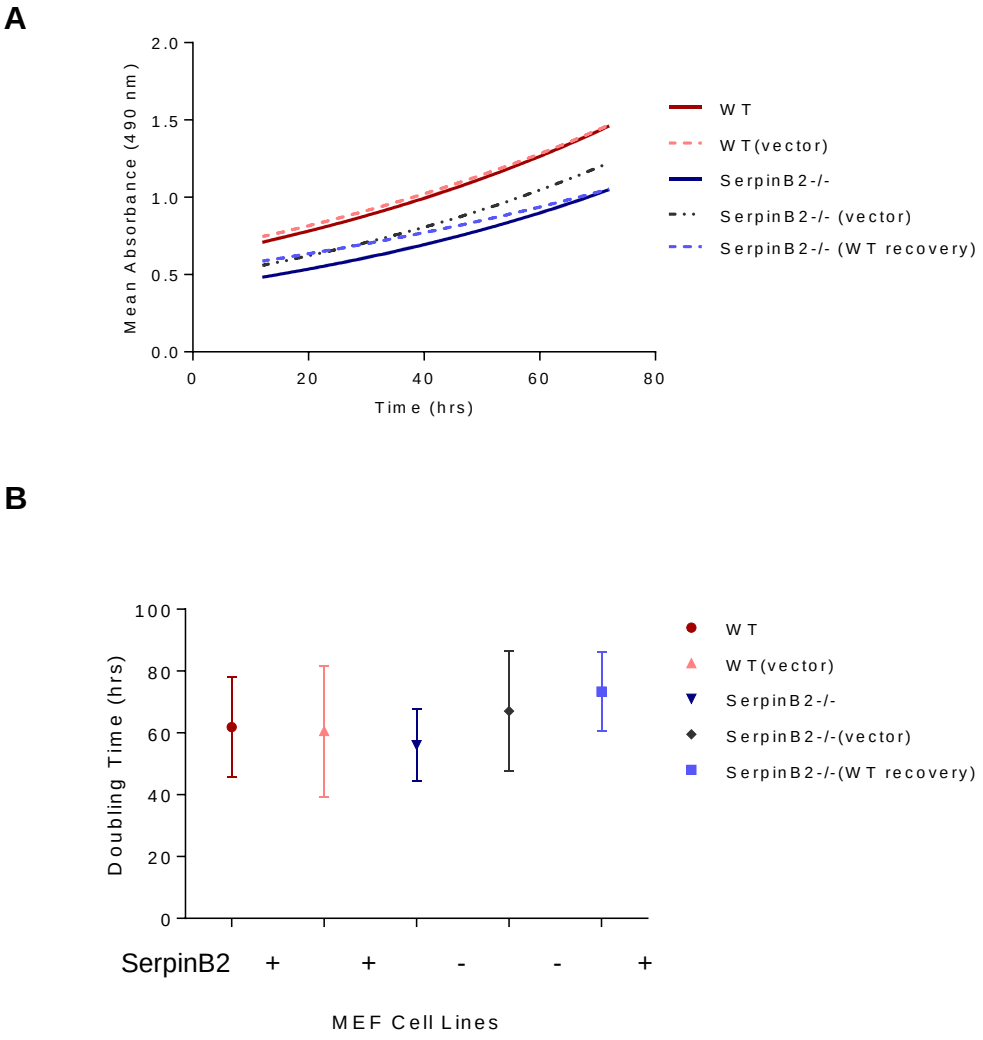

Figure 5.4: MEF growth rates. Parental and pMIG transduced MEF cell lines were cultured for 72 h and growth rates determined every 12 h by relative change in absorbance at 490 nm using MTS reagent. **A)** Non-linear curves were fitted to data points and **B)** mean doubling times (symbols) calculated using the exponential growth equation. Bars indicate the variance in mean doubling times. Plots represent mean data, n=3, with relevant background controls subtracted.

Table 5.2: Multiple comparisons of growth rate constants for MEF cell lines. One way ANOVA Tukey-Kramer post-test (CI = 95%).

	WT	WT (vector)	SerpinB2 $^{-/-}$	SerpinB2 $^{-/-}$(vector)	SerpinB2 $^{-/-}$ (WT rescue)
WT	-	NS	NS	NS	NS
WT(vector)	NS	-	NS	NS	NS
SerpinB2$^{-/-}$	NS	NS	-	NS	NS
SerpinB2$^{-/-}$(vector)	NS	NS	NS	-	NS
SerpinB2$^{-/-}$(WT rescue)	NS	NS	**	**	-

ns = not significant, ** = significantly different ($p<0.05$).

5.4.2. SerpinB2 protects MEFs from proteotoxic stress of Huntingtin protein expression/aggregation.

In order to test the hypothesis that SerpinB2 is involved in proteostasis pathways within the intracellular environment we utilised wild type (Htt_{ex1}25Q-mCherry) and mutant (Htt_{ex1}46Q-mCherry) huntingtin-mCherry mammalian expression vectors as an intracellular protein aggregation model. Htt polyQ expansion is characterized by the aggregation of Htt and decreased cell survival in a polyQ-expansion dependent manner within neuronal models (Arrasate et al. 2004). Therefore we conducted transient transfection experiments using the MEF cell lines to investigate Htt_{ex1} aggregation and processing in the absence or presence of SerpinB2, relative to controls. Initially, proteotoxic stress was determined by quantification of cell viability using flow cytometry and SytoxRed staining at 24, 36 and 48 hs post transfection. Using flow cytometry, cells were firstly gated based on forward and side scatter (Fig. 5.6.A.i) to remove debris from the analysis. This

population was then gated based on mCherry (660_20, green laser 561 nm) and GFP (515_20, blue laser 488 nm) expression (Fig. 5.6.A.ii). Analysis of cell viability by SytoxRed (660_20, red laser 633 nm) exclusion (Fig. 5.6.A.iii) was then conducted on mCherry and GFP positive cells only (Q2 of Fig. 5.6.A.ii) within the pMIG transduced cell lines or mCherry positive cells (Q1 of Fig. 5.6.A.ii) within the parental lines. The percentage of viable cells determined by this gating method was then normalised against the relevant mCherry control populations to allow for potential bias arising from the transfection process or possible differences in transfection efficiency and vector expression between cell lines.

Using this model, a significant difference in cell viability between SerpinB2 null and SerpinB2 expressing cell lines was observed and this was most obvious 48 h post transfection (Fig 5.5.B). Cell viability was reduced to 60% and 45% at this time point for Htt_{ex1}25Q-mCherry (Fig. 5.5.B.i) and Htt_{ex1}46Q-mCherry (Fig. 5.5.B.ii) expressing SerpinB2$^{-/-}$(vector) cells compared to 100% viability observed for the WT (vector) cell line respectively. The latter observation [WT(vector)] is consistent with previous work using wild-type MEFs that showed no difference in toxicity responses between cells expressing Htt_{ex1}25Q and Htt_{ex1}97Q (King et al. 2008). Importantly, cell viability was partially recovered with the reintroduction of SerpinB2 by pMIG transduction, SerpinB2$^{-/-}$(WT rescue), showing normalised cell viability of 89% and 84% for Htt_{ex1}25Q-mCherry (Fig. 5.5.B.i) and Htt_{ex1}46Q-mCherry (Fig. 5.5.B.ii) expressing cells which was significantly different to the SerpinB$^{-/-}$ (vector) cell line ($p<0.001$).

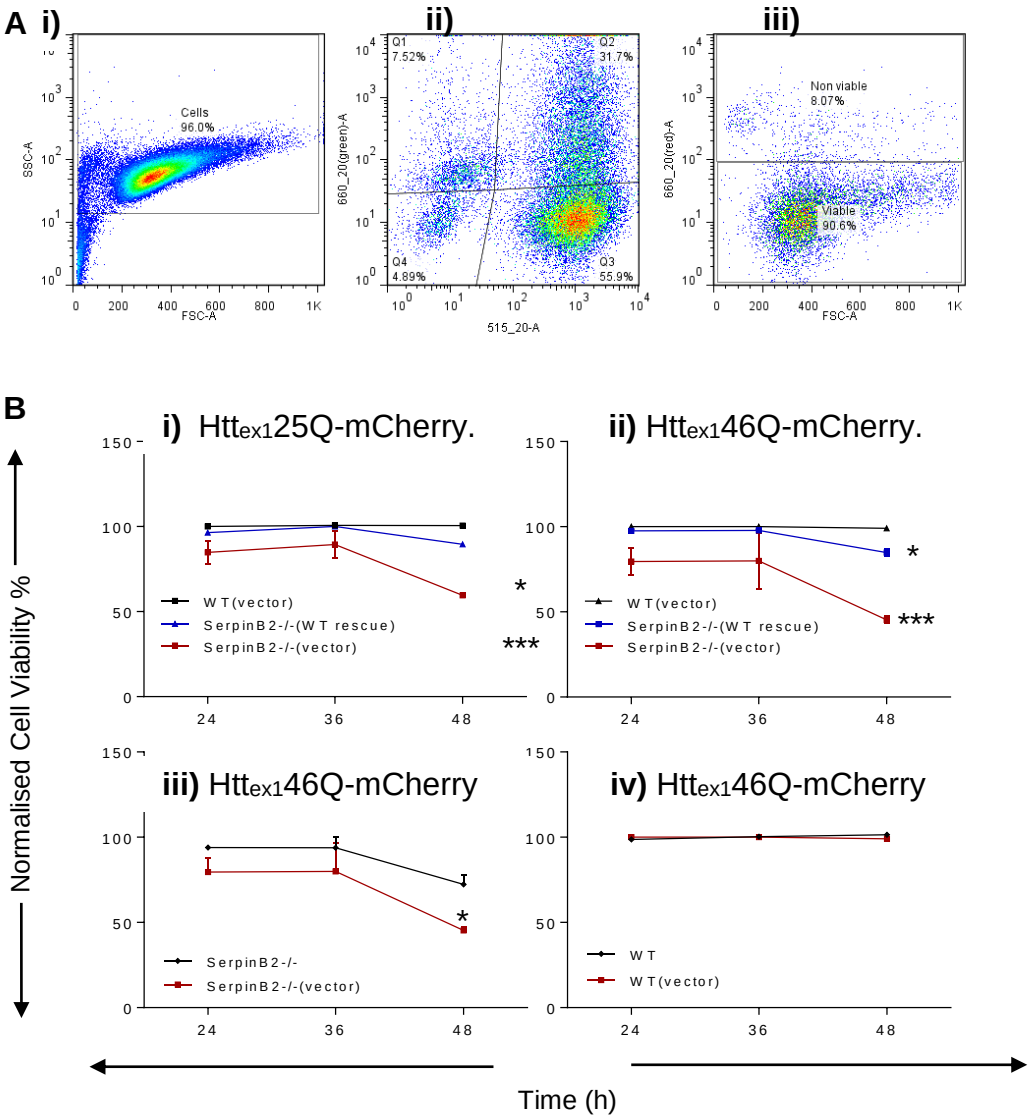

Figure 5.5: SerpinB2 protects MEFs from Huntingtin protein toxicity. Parental and pMIG transduced MEF cell lines were transiently transfected with either Htt$_{ex1}$25Q-mCherry (WT), Httex146Q-mCherry (mutant) or mCherry (control) expression vectors and cell viability assessed at 24, 36 and 48 h post transfection using flow cytometry. **A)** Representative gating of data; **(i)** initial removal of debris **(ii)** mCherry$_{(660_20\ green)}$/GFP$_{(515_20\ blue)}$ positive cells were selected for analysis of **(iii)** cell viability using SytoxRed$_{(660_20\ red)}$ exclusion. **B)** Comparison of cell viability in the absence (SerpinB2-/-(vector)) or presence (WT(vector)) and (SerpinB2-/-(WT rescue)) of SerpinB2 following transfection with either **(i)** Htt$_{ex1}$25Q-mCherry or **(ii)** Htt$_{ex1}$46Q-mCherry. Effects of pMIG transduction on cell viability following transfection with Htt$_{ex1}$46Q-mCherry was assessed by comparison to parental lines; **iii)** SerpinB2$^{-/-}$ and **iv)** WT. Data represents mean percentage of viable cells normalised to mCherry only controls, n=3, ± SEM. Significant difference to WT(vector) (i) and (ii) or parent line (iii) denoted as *p<0.05. ***p<0.001.

Comparison of the MEF parental cell lines and their respective pMIG transduction control cell lines, 48 h post transfection with Htt_{ex1}46Q-mCherry was also conducted to assess the effects if any of the mouse stem cell virus (MSCV - pMIG transduction) on cell viability. Interestingly there was a significant difference between the percentage of viable cells determined for SerpinB2$^{-/-}$(vector) compared to the SerpinB2$^{-/-}$ parental cell line ($p<0.05$) (Fig. 5.5.B.iii), whilst no difference was observed between the WT (vector) and WT cell lines (Fig. 5.5.B.iv). Suggesting that pMIG transduction is impacting on the cell viability of SerpinB2$^{-/-}$ cell lines, however given that there was no significant difference in doubling times for these cell lines (Fig. 5.4), it seems they are more sensitive to the accumulative effect of GFP and Htt_{ex1}46Q-mCherry expression. This sensitivity may be attributed to by the constitutive expression of GFP, which has previously been shown to have a cytotoxic effect within some cell models (Liu et al. 1999). The cell viability of Htt_{ex1}46Q-mCherry expressing SerpinB2$^{-/-}$ MEF cells (parental line, no GFP) at 48 h post transfection was also found to be significantly reduced compared to the WT ($p<0.001$) and WT (vector) ($p<0.001$) cell lines, confirming the cytotoxic effect of Htt expression in the absence of SerpinB2. Importantly, WT rescue of the SerpinB2$^{-/-}$ cell line (WT rescue) was shown to significantly increase cell viability ($p<0.05$), indicating that reintroduction of SerpinB2 into the SerpinB2$^{-/-}$ cells not only facilitated recovery of cell viability due to the pMIG transduction process but also that resulting from the proteotoxicity of Htt_{ex1}46Q-mCherry expression. Altogether, this supports a potential role for SerpinB2 in cellular protection against

proteotoxicity. It was not possible, however, to identify within these experiments, potential protein aggregation pathways associated with this observation.

Therefore, Htt_{ex1}46Q:mCherry aggregation and processing was visualised by microscopy at 24 and 48 h post transfection. Expression of Htt_{ex1}46Q-mCherry or mCherry only (data not shown) was clearly visible after 24 h in all cell lines with mCherry fluorescence appearing evenly dispersed throughout the cytosol (Fig.5.6). At this time point, inclusion bodies (IB) were observed within the WT (Fig.5.6A) and SerpinB2$^{-/-}$ (WT rescue) (Fig.5.6C) cell lines, transfected with the mutant huntingtin expression vector (Htt_{ex1}46Q-mCherry). However, negligible inclusion formation was observed within the SerpinB2$^{-/-}$ cell lines (Fig.5.6B). This subtle difference in IB profile became more distinct 48 h post transfection, whereby a clear difference in phenotype between cell lines with respect to formation of IB in the absence or presence of SerpinB2 was observed (Fig. 5.6). Importantly, the WT rescue cell line showed clear recovery of wild-type phenotype verifying that the difference observed between the WT (vector) and SerpinB2$^{-/-}$ (vector) cell lines was due to absence or presence of SerpinB2. As expected, no observable IBs formed within cells transfected with the mCherry control vector during the course of the experiment (data not shown).

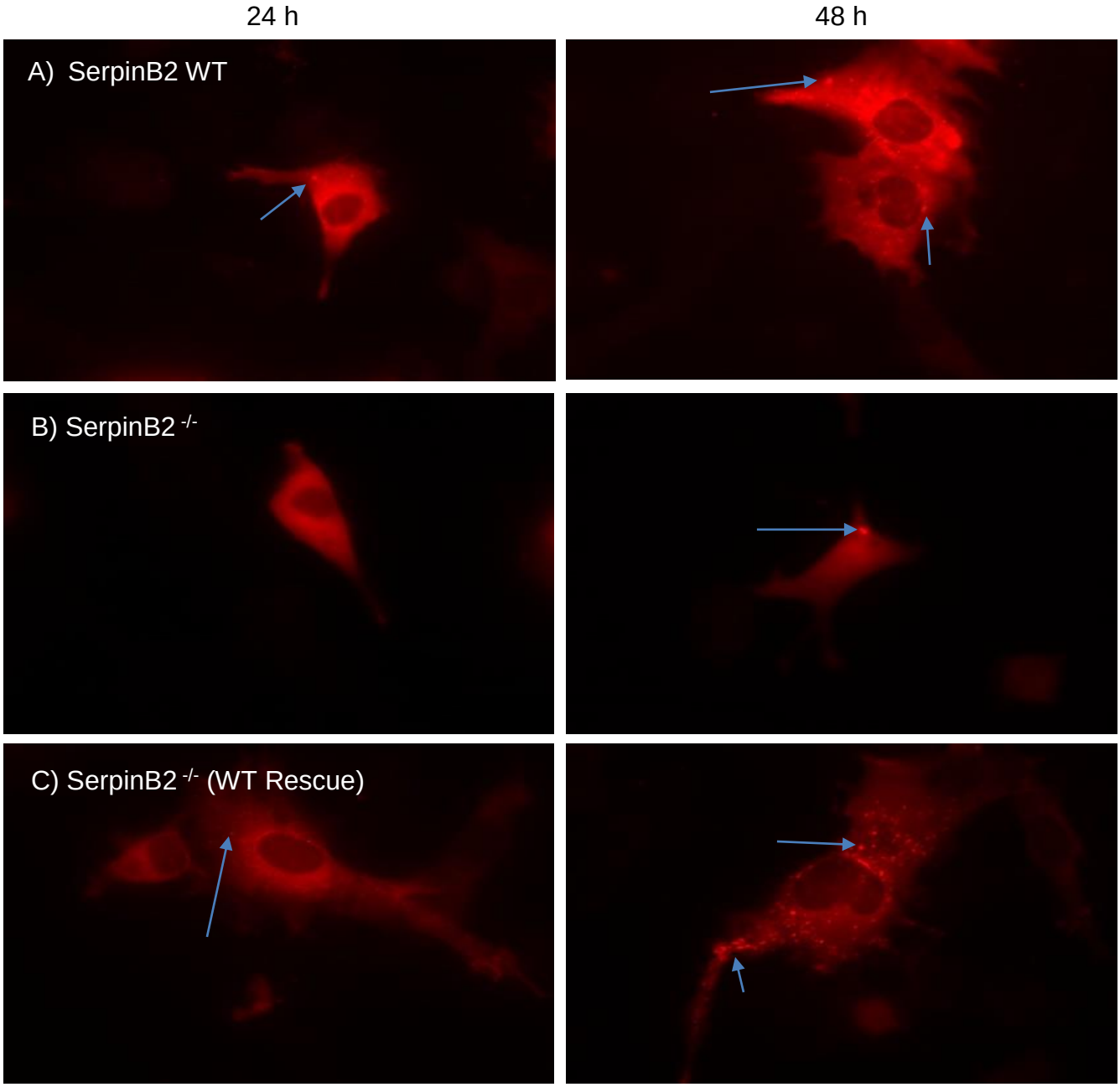

Figure 5.6: Photomicrographs showing expression and cellular processing of Htt_{exn1}46Q:mCherry by Mouse Embryonic Fibroblasts (MEF). Inclusion body formation (blue arrows) within **(A)** WT (vector), **(B)** SerpinB2$^{-/-}$ (vector) or **(C)** SerpinB2$^{-/-}$ WT rescue MEFs, 24 or 48 h post transfection with Htt_{ex1}46Q-mCherry using Lipofectamine2000. Cells were visualised using a Nikon Eclipse TE2000-E (Nikon Instruments) with FITC (ex 470-490, em 520-560) and Cy3 (ex 510 – 560 nm, em 565 - 625 nm) filter sets and 60x Plan Apo ∞ /0.10-0.22 WD 0.13 oil emersion lens.

We next compared the partitioning of Htt in wild-type and SerpinB2$^{-/-}$ MEFs. Previous work has established that overexpression of Htt$_{ex1}$ containing expanded polyQ repeats (including 46Q used in this study) produces a dense round inclusion in the cytoplasm or nucleus (Kaganovich et al. 2008; Polling et al. 2014), while wild-type or 25Q expansion does not. Following expression of Htt$_{ex1}$25Q-mCherry in wild-type MEFs we observed small, Htt-positive foci in ~15% of cells (Fig. 5.7A). These foci were < 2 µm in diameter and were counted separately to inclusions (Fig. 5.7B).

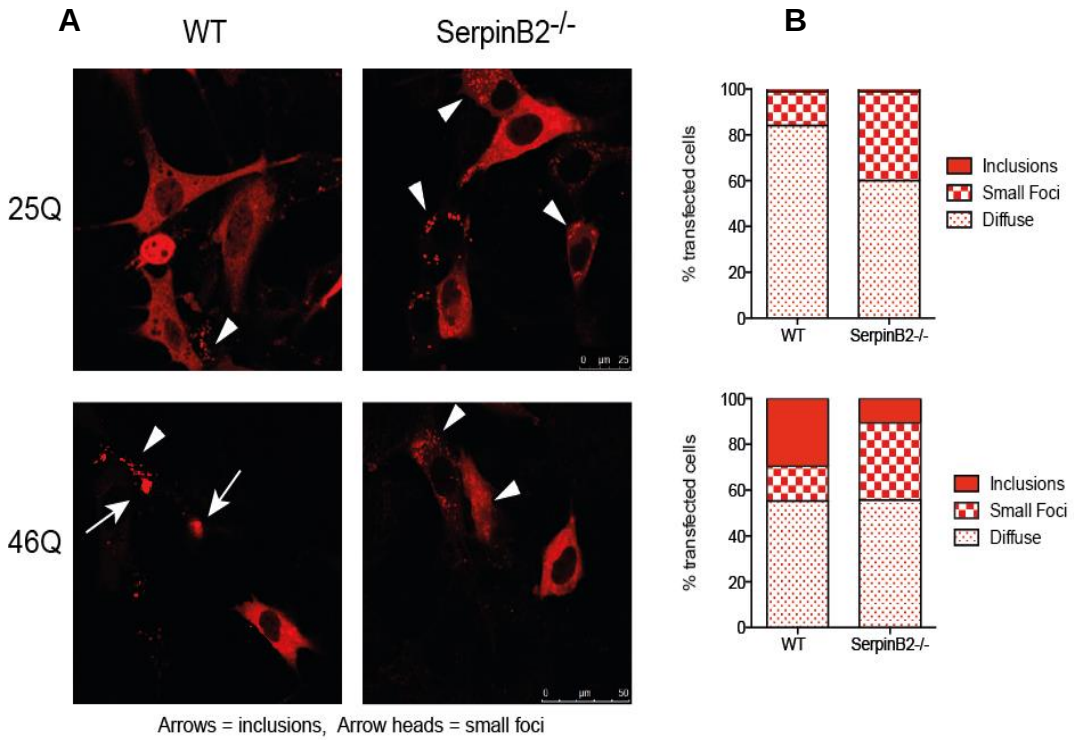

Figure 5.7: Differential partitioning of Htt$_{exn1}$ in WT vs SerpinB2$^{-/-}$ MEF A. Inclusion formation in wild-type versus SerpinB2$^{-/-}$ MEFs 48 h post transfection with either Htt$_{ex1}$25Q-mCherry or Htt$_{ex1}$46Q-mCherry. Two types of Htt foci were observed, small (< 2um; white arrow heads) and large (> 2 um; white arrows); **B.** Distribution of Htt in MEFs was quantified as diffuse, small foci, or inclusion in each cell. Images were taken by Natalie Farrawell, University of Wollongong.

There was an increase in the proportion of cells containing these small foci (from ~ 15% to ~ 40%) in the absence of SerpinB2 (Fig. 5.7B), indicating a significant shift in localisation of Htt_{ex1}25Q in SerpinB2$^{-/-}$ cells. Following expression of Htt_{ex1}46Q in wild-type MEFs we observed a large proportion of cells containing inclusions (~ 30%) that were not present in 25Q-expressing cells (Fig. 5.7A and 5.7B). However, ~ 15% of cells still contained small Htt foci in 46Q-expressing wild-type cells. In contrast, the proportion of cells containing inclusions was reduced and the number of cells containing smaller fluorescent foci increased following expression of Htt_{ex1}46Q-mCherry in SerpinB2$^{-/-}$MEFs (Fig.5.7A and 5.7B).

Given that the expression of SerpinB2 modulated cellular inclusion formation and cell viability we tested the ability of recombinant SerpinB2 to supress the *in vitro* fibril formation of Htt_{ex1}46Q fused to the monomeric cyan fluorescent protein, Cerulean. As previously reported (Olshina et al. 2010), activation of purified recombinant Htt_{ex1}46Q-Cerulean through cleavage of the protective mannose binding protein (MBP) with TEV protease, resulted in the formation of insoluble Htt_{ex1}46Q-Cerulean fibrillar aggregates over 72 h (Fig. 5.8A). Whilst the presence of SerpinB2 modestly attenuated the formation of insoluble Htt_{ex1}46Q-Cerulean aggregates within this assay, there were no apparent changes in morphology of the Htt_{ex1}46Q-Cerulean insoluble fibrils formed, in the absence or presence of SerpinB2 (Fig. 5.8B). We next investigated the potential for SerpinB2 to interact directly with Htt_{ex1}46Q-Cerulean using a solid phase ligand blotting assay and

immunodetection, as previously described (Yerbury et al. 2007). Interestingly, SerpinB2 was found to interact with non-aggregated Htt_{ex1}46Q-Cerulean, but not to aggregated material (Fig. 5.8C-D). Only negligible binding of SerpinB14 (negative control) to non-aggregated Htt_{ex1}46Q-Cerulean could be detected, whilst no interaction between SerpinB14 and aggregated Htt_{ex1}46Q-Cerulean was observed. Conversely, clusterin (positive chaperone control) bound both soluble and insoluble Htt_{ex1}46Q-Cerulean (Fig. 5.8C-D), which is consistent with previous work using clusterin within this assay format (Yerbury et al. 2007).

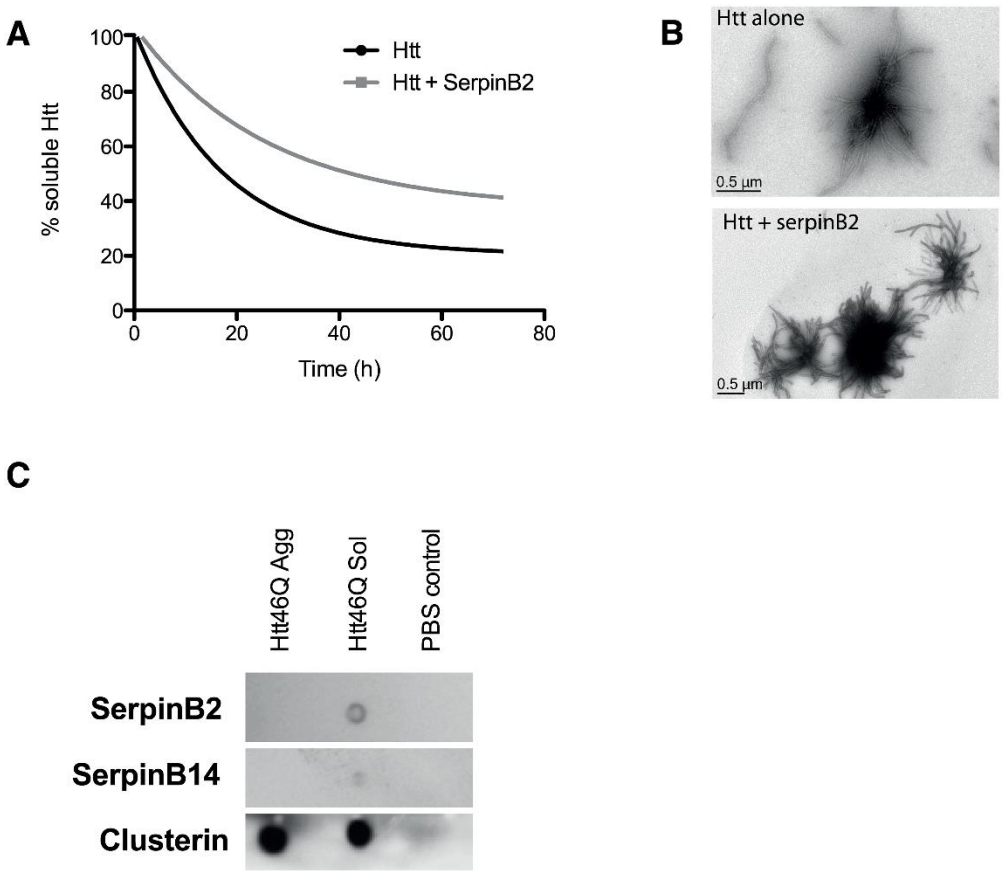

Figure 5.8: SerpinB2 attenuates Htt42q fibril formation *in vitro*. A. Soluble Htt remaining in Htt_{ex1}46Q-Cerulean aggregation reactions in the absence or presence of SerpinB2 (equimolar ratio); **B.** TEM images of fibril formation at 72 h; **C.**Representative ligand blot (n = 3) showing differences in binding of SerpinB2 to soluble and aggregated Htt_{ex1}46Q. Binding was determined by immunoassay. SerpinB14 or clusterin binding to soluble and aggregated Htt_{ex1}46Q are also shown. Data was kindly provided by Natalie Farrawell, University of Wollongong.

As SerpinB2 was found to interact with soluble Htt_{ex1}46Q-Cerulean and inhibit aggregation, albeit at modest amounts, we next examined a possible interaction between SerpinB2 and aggregated Htt_{exn1}46Q-mCherry within the WT cell line, by immuno-staining. Using this method there was no evidence of SerpinB2 co-localisation with Htt_{exn1}46Q-mCherry, indicating that SerpinB2 is not sequestered into IBs containing Htt_{exn1}46Q-mCherry aggregates (Fig.5.7). However, it is

possible that SerpinB2 interacts, transiently, with the soluble oligomeric form of Htt_{exn1}46Q-mCherry, which would not be detectable within this system. Of note, these experiments confirmed the presence of detectable amounts of endogenous SerpinB2 protein within the WT cell line (Fig. 5.7.B).

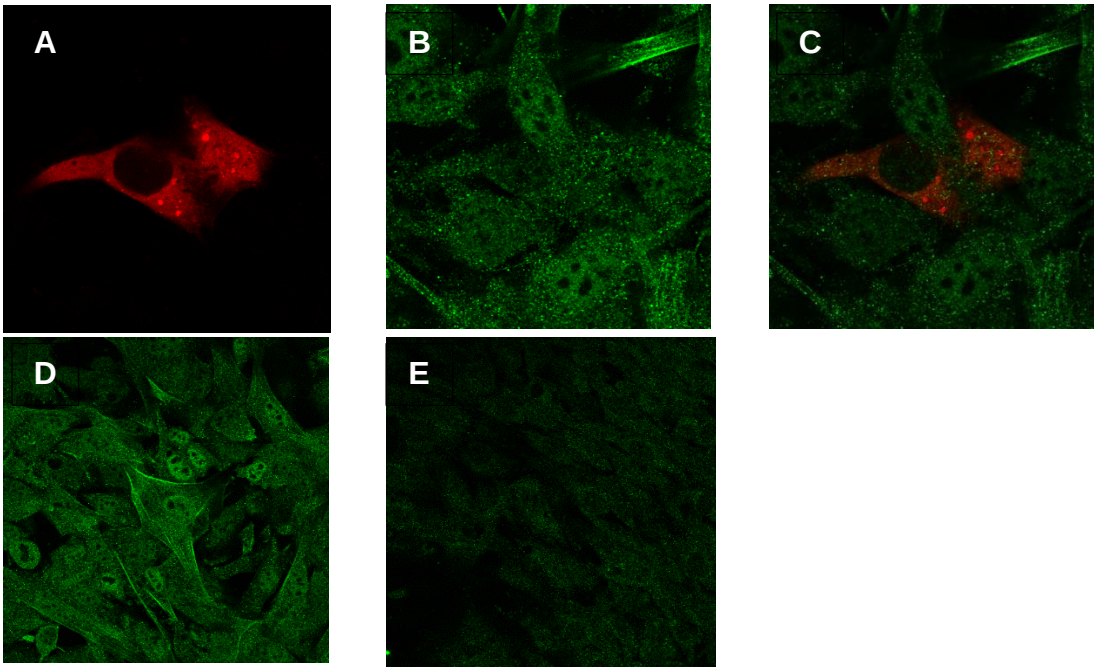

Fig. 5.9: Huntingtin does not co-localize with SerpinB2. Photomicrographs showing **(A)** expression of Htt_{ex1}46Q:mCherry in WT MEFs following transient transfection for 48 – 72 h and **(B)** SerpinB2, detected using rabbit anti-mouse serpinB2 polyclonal antibody and goat anti-rabbit IgG Alexa Fluor®488-conjugated secondary antibody immunostaining. **(C)** Image overlay showing cellular distribution of Htt_{ex1}46Q:mCherry and SerpinB2. Control staining was conducted on non-transfected WT MEFs for **(D)** SerpinB2 and **(E)** Rabbit IgG antibody used as an isotype control. Cells were imaged using laser scanning confocal microscopy. Imaging kindly performed by Natalie Farrawell, University of Wollongong.

SerpinB2 has previously been shown to interact with the β-subunit of the proteasome proteolytic core (Fan et al. 2004) and recent work has shown that SerpinB2 co-localises with Beclin-1 and promotes the degradation of the NOD-like

receptor-3 (NLR3) via the autophagy-lysosomal degradation pathway (Chuang et al. 2013). Taken together these works suggest SerpinB2 may function within protein degradation pathways, which led us to investigate if SerpinB2 influences proteasomal or autophagy-lysosomal degradation pathways. To investigate this, we conducted cellular based assays to compare proteasomal degradation activity in the absence or presence of SerpinB2 utilising a proteasome reporter GFPμ (Bence et al. 2001; Bence et al. 2005).

5.4.3. SerpinB2 null MEFs have impaired proteasome activity compared to wild-type MEFs.

SerpinB2 has previously been shown to interact with the β-subunit of the proteasome proteolytic core (Fan et al. 2004) and recent work has shown that SerpinB2 co-localises with Beclin-1 and promotes the degradation of the NOD-like receptor-3 (NLR3) via the autophagy-lysosomal degradation pathway (Chuang et al. 2013). Taken together these works suggest SerpinB2 may function within protein degradation pathways, which led us to investigate if SerpinB2 influences proteasomal or autophagy-lysosomal degradation pathways.

We thus first conducted cellular based assays to compare proteasomal degradation activity in the absence or presence of SerpinB2 utilising a proteasome reporter. In these assays, WT and MEF$^{SerpinB2-/-}$ cell lines were transiently transfected with the proteasome reporter expression vector containing GFPμ, which relies on a 16 amino acid degron (ACKNWFSSLSHFVIHL) (CL1) fused to the carboxyl terminus of GFP (Gilon et al. 1998; Bence et al. 2001; Bence et al.

2005). Degradation of the degron is specific to the proteasome, therefore changes in GFP signal is indicative of proteasome activity. Cells were analysed by flow cytometry 48 h post transfection, following an overnight incubation in the absence or presence of proteasome inhibitor, MG-132. Normalisation of the GFP signal against MG-132 treated cells (100% inhibition) provides a basis to compare relative levels of proteasome activity. Larger relative loss of GFP signal in the absence of MG132 suggests a more efficient UPS. Interestingly, the loss of GFP signal within the WT cell line was 70% compared to 40% loss, observed in the SerpinB2$^{-/-}$ cell line (Fig.5.10.A), indicating that the proteasomal degradation pathway is impaired in the absence of SerpinB2.

Whilst the GFP signal following MG132 treatment was normalised in order to quantitate GFP degradation, it is important to note that the histograms showing GFP signal intensity is comparable between cell lines (Fig.5.10.B). Therefore indicating that the difference observed in GFP degradation was not due to variability in transfection or expression efficiency between cell lines and that basal levels of proteasome activity appears to be comparable between the two cell lines. Furthermore, a dose response analysis of cell viability after 48 h treatment with MG132 revealed half maximal inhibitory concentration values of ~10 μM for both cell lines (data not shown), indicating that toxicity issues were not responsible for this difference. These data suggest that the absence of SerpinB2 in cells places stress on the UPS.

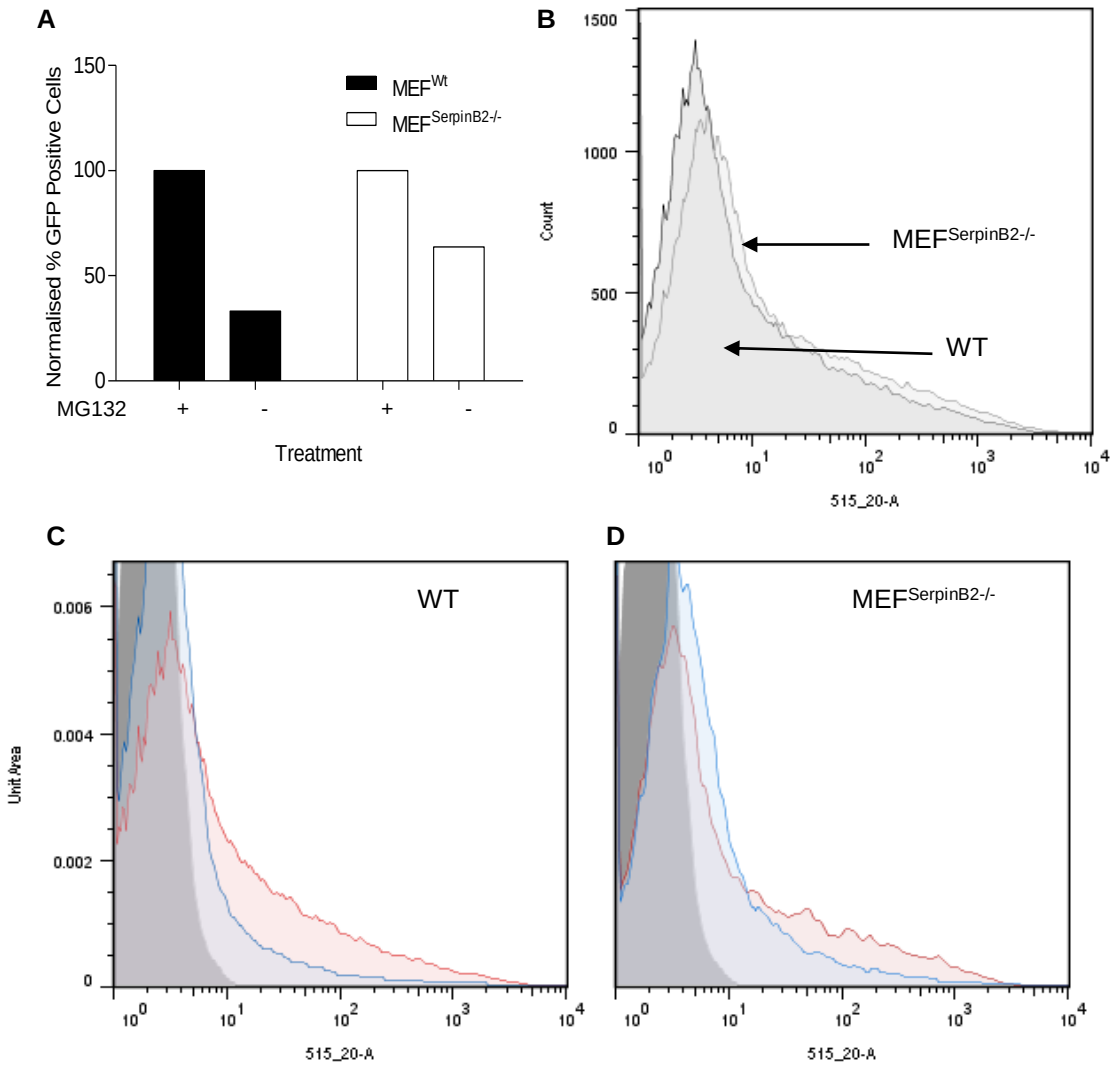

Figure 5.10: **SerpinB2$^{-/-}$ exhibit impaired proteasome activity. (A)** Wild-type and SerpinB2$^{-/-}$ Mouse Embryonic Fibroblast cell lines were transiently transfected with proteasome reporter GFPμ then incubated overnight in the absence or presence of [250 nM] MG-132, where indicated. Data has been normalised to geometric mean GFP (515/20A) signal of MG132 viable cells only, as determined by propidium iodide exclusion (695/40). **(B)** Overlay of MG132 treated MEF cell lines showing maximum GFPμ signal following inhibition of p26 proteasome. Representative histograms for **(C)** WT or **(D)** SerpinB2-/- showing GFP signal intensities in the absence (Blue histogram) or presence (Red histogram) of MG132, grey histograms represent MEF autofluorescence controls (non-transfected).

5.4.4. Autophagy-lysosomal degradation pathway dysregulation in SerpinB2 null MEFs.

We next investigated a potential role for SerpinB2 within the autophagy-lysosomal degradation pathway. WT and SerpinB2-/- MEF cell lines were cultured overnight in the absence or presence of either an autophagy promoter (Verapamil) or inhibitor (3-Methyladenine (3-MA)), then the number of acidic (autolysosome and lysomsomal) vesicles quantified using the Lyso-ID kit as previously described (Francois et al. 2013). Interestingly, basal level autophagy (indicated by cellular fluorescence) was significantly increased in SerpinB2$^{-/-}$ MEFs compared to WT cells (Fig. 5.11). Addition of verapamil, a known Ca^{2+} channel antagonist which induces autophagy through the Ca^{2+}-calpain–$G\alpha_s$ pathway (Williams et al. 2008), resulted in a dose dependent increase in fluorescence in both cell lines, however fluorescent signal was significantly increased within SerpinB2$^{-/-}$ MEFs compared to WT MEFs (Fig. 5.11A), suggesting dysregulation of autophagy pathways.

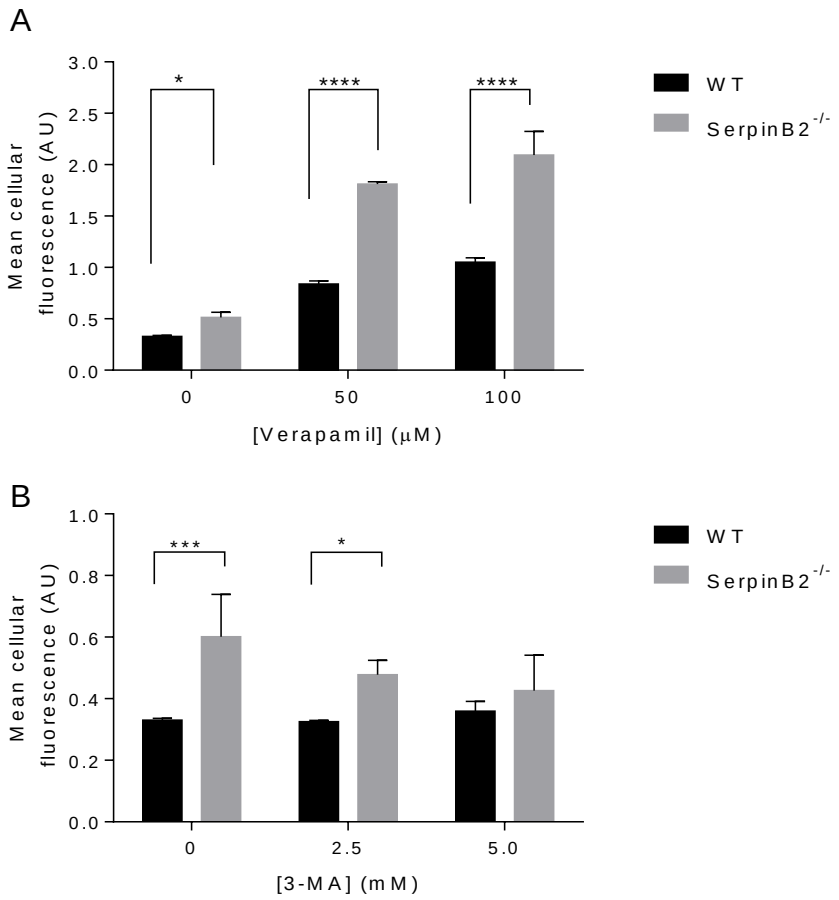

Figure 5.11: Autophagy is dysregulated in SerpinB2$^{-/-}$ MEF. Wild-type and SerpinB2$^{-/-}$ Mouse Embryonic Fibroblast cell lines were incubated in the absence or presence of either **(A)** verapamil (activator) or **(B)** 3-MA (inhibitor) overnight and autophagy function quantified by addition of Lyso-ID red dye. Data shown represents mean (± SEM) fluorescence intensity per cell as determined by IncucyteZoom automated imaging system with background subtracted. Data kindly provided by Natalie Farrawell, University of Wollongong.

In the presence of 3-MA, an inhibitor of class III phosphoinositide 3-kinases (PI3K) (Seglen and Gordon 1982), a small increase in fluorescence was observed in WT cells at the highest concentration (5 mM) (Fig. 5.9B). In contrast, while there was a dose-dependent decrease in fluorescence in SerpinB2$^{-/-}$ MEFs with increasing

3-MA concentration (likely due to the stress placed on the cells under these inhibitory conditions), compared to WT cells the level of fluorescence was significantly higher in the presence of 2.5 mM 3-MA.

5.5. Discussion

Up-regulation of SerpinB2 in response to cellular stress is well-established, the intracellular pathways in which SerpinB2 may function however, are poorly defined. Key to cell survival are protein quality control systems which maintain proteostasis through the chaperone and protein degradation pathways. SerpinB2 has been implicated within these networks via identification of potential intracellular binding partners, such as proteasome subunit beta type 1 (PSMB1, a component of the proteasome) (Fan et al. 2004), the ubiquitin-like adapter protein, interferon stimulated gene-15 (ISG15) (Giannakopoulos et al. 2005) and autophagy regulator, Beclin-1 (Chuang et al. 2013). In this context, this work utilises the mutant Htt_{exn-1} model (Olshina et al. 2010; Ramdzan et al. 2010) to investigate the cellular processing of protein aggregates by WT and SerpinB2$^{-/-}$ cell lines, and provides evidence of impaired inclusion formation, proteasome activity and dysregulation of autophagy-lysosomal degradation pathways in the absence of SerpinB2.

Huntington Disease (HD) is characterised by the accumulation of soluble and insoluble fibrillar protein species, resulting from polyglutamine (polyQ) expansion, in the N-terminus of the Huntingtin protein (MacDonald 1993) and represents one of nine neurodegenerative disorders termed polyQ diseases. In normal, healthy

humans the polyQ expansion may contain up to 35 repeats, whilst 36 upwards has been shown to cause cell death through classic loss and gain of function associated with protein aggregation, similar to those described for other neurodegenerative disorders, such as Alzheimer's and Parkinson's Disease (Bano et al. 2011). Here we have utilised the highly aggregation prone region of Huntingtin protein, exon-1 fused to a poly-Q expansion, as a model for intracellular protein aggregation and found that SerpinB2 protects against the cytotoxic effect of Htt_{exn-1}-46Q-mCherry expression 48 h post transfection (Fig. 5.5), as determined by cell viabilty.

Visualisation of MEFs, 24 and 48 h post transfection with either Htt_{exn1}-25Q or Htt_{exn-1}-46Q-mCherry, revealed morphological differences in Htt processing between SerpinB2$^{-/-}$ (vector) and WT (vector) cells lines. Clear inclusion formation was visible in WT (vector) cells within 24 h, becoming more pronounced by 48 h post transfection (Fig. 5.6.A). This was in stark contrast to the SerpinB2$^{-/-}$ (vector) cells, which exhibited diffused cellular distribution of Htt_{exn-1}-46Q-mCherry at 24 hs and minimal inclusion formation at 48 hs post-transfection (Fig. 5.6.B). It should be noted however, that visualisation of Htt_{exn-1}-46Q-mCherry processing within the SerpinB2$^{-/-}$ (vector) cell line was problematic, given the high cell loss due to the sensitivity of these cells to the transfection process and Htt_{exn-1}-46Q-mCherry expression. Importantly, recovery of WT phenotype was observed within the SerpinB2$^{-/-}$ (WT rescue) cell line (Fig.5.6.C). This return of inclusion formation coincided with recovery of cell viability, and supports recent research indicating that inclusion formation - traditionally thought to be cytotoxic and concomitant with

cell death - is a protective mechanism through which, cells are able to isolate the cytotoxic, soluble oligomeric, forms of Htt_{exn-1} and other pernicious protein species (Waelter et al. 2001; Bucciantini et al. 2002; Arrasate et al. 2004; Takahashi et al. 2008).

Of interest is the finding that ubiquitinated, soluble substrates destined for degradation are typically deposited within juxtanuclear compartments – termed juxtanuclear quality control (JUNQ), whilst insoluble protein aggregates, characteristic of amyloid-like fibril structures are preferentially directed to perivascular compartments, or insoluble protein deposits (IPODs) (Kaganovich et al. 2008). Furthermore, it is becoming apparent that misdirection of substrates between these distinct quality control compartments, or delayed downstream processing results in increased cytotoxicity (Weisberg et al. 2012; Amen and Kaganovich 2015), as would be expected with the breakdown of a protein quality control network. Importantly, JUNQ clearance is predominantly facilitated by proteasomal degradation pathway (Weisberg et al. 2012; Ogrodnik et al. 2014) whilst IPODs are processed through the autophagy-lysosomal degradation pathways (Kaganovich et al. 2008). Whether SerpinB2 functions directly within these compartmentalisation networks either in the formation of inclusions or to sequester Htt_{exn1}46Q-mCherry is unclear. However, our observations of decreased numbers of large IPOD inclusions (Fig.5.7) and increased cell death in SerpinB2-null cells (Fig. 5.5) are consistent with a role for SerpinB2 in mediating the formation of cellular inclusions. SerpinB2 binds soluble Htt_{exn1}46Q (Fig. 5.8), but has a modest effect on Htt_{ex1}46Q-Cerulean aggregation, nor does SerpinB2

co-localisation with Htt IPOD structures, but this does not preclude an indirect role in inclusion formation. An RNAi genome wide screen in in *C. elegans* identified RNA synthesis, protein synthesis, protein folding, protein transport and protein degradation as vital classes of genes that control polyQ protein aggregation (Nollen et al. 2004). This study implicated all aspects of the proteostasis network as modulators of protein aggregation *in vivo*. Hence, our data showing reduced numbers of large Htt46Q inclusions in the absence of SerpinB2 suggests SerpinB2 is part of the cellular proteostasis regulation network.

Given that the formation of quality control compartments are thought to appear as a result of protein degradation pathway overload (Hipp et al. 2014), we compared proteasome and autophagy function. Interestingly, the proteasomal degradation pathway was impaired within SerpinB2$^{-/-}$ null cell lines, suggesting a role within this protein degradation pathway. Surprisingly, the absence of SerpinB2 was found to negatively impact on GFPμ degradation. Given the reported interaction between SerpinB2 and PSMB1 by Fan et al. 2004 and the chymotrypsin-like specificity of this enzymatic subunit (Baldovino et al. 2006), it is plausible to hypothesise that SerpinB2 inhibits PSMB1 and therefore proteasome activity. This does not appear to be the case given that depletion of SerpinB2 reduced proteasomal activity, rather than enhanced it. Furthermore, it is unlikely that SerpinB2 is interacting with PSMB1 within the intact proteasome as this would require direct access into the proteasome which is tightly controlled by ubiquitin, unfoldases and an entrance as narrow as 13 Aº, necessitating the linearization of proteins to allow spatial placement within the proteolytic 20S core. It is tempting to speculate that SerpinB2

may interact with PSMB1 during assembly and disassembly of the 26S proteasome, functioning to help shuttle the subunit into place, either as a substrate or as a non-inhibitory adapter protein.

Cellular mutant Htt is known to form insoluble aggregate deposits and degradation has been reported to be predominantly autophagy-lysosomal degradation pathway dependent (Martin et al. 2015). Here we show that the autophagy-lysosomal degradation pathway becomes dysregulated in the absence of SerpinB2, which is in keeping with recent work describing co-localisation of SerpinB2 with Beclin-1 and Hsp90, within the membrane of autophagosomes (Chuang et al. 2013). Whilst it is not possible to elucidate the functional mechanism behind SerpinB2 regulation of autophagy, given the dynamic nature of the pathway, dissociation of Bcl-2 from Beclin-1 initiates seeding of the phagophore, which can wrap around aggregates such as those found in iPODs and gives rise to autophagosomes. Our finding that loss of SerpinB2 results in decreased numbers of large IPOD inclusions and dysregulation of the autophagy-lysosomal degradation pathway suggests a possible role for SerpinB2 within this initial seeding stage of the pathway.

Taken together this work indicates that SerpinB2 is a prominent component of the cells proteostasis networks, which exerts its cytoprotective effects through modulation of the protein degradation pathways. Intriguingly, loss of SerpinB2 results in attenuation of both the proteasome and autophagy-lysosomal degradation pathways. Whether SerpinB2 functions within both systems or has an indirect effect on one, through loss of the other, remains to be shown. It is clear

however that SerpinB2 interacts with misfolded proteins, inhibits aggregation and facilitates downstream processing of these deleterious protein species.

6. Conclusions and Future Directions.

6.1. Overview.

The specific aims of this thesis were to examine; 1) the role of SerpinB2 within the extracellular environment as a plasminogen activator inhibitor in monocytes and 2) the role of SerpinB2 within the intracellular environment as a potential stress response protein. Accordingly, the conclusions drawn and future directions suggested below have been divided into two sections centred on these distinct cellular distribution and functions of SerpinB2.

6.2. The role of Extracellular SerpinB2 as a plasminogen activator inhibitor.

There have been many biochemical studies conducted which have defined and supported the role of SerpinB2 as a classical inhibitory serpin. *In vivo*, SerpinB2 can be detected at very high concentrations under specific patho/physiological conditions in the circulation, seminal fluid, tears, gingival crevicular fluid and saliva (Croucher et al. 2010). SerpinB2 has also been shown to be efficiently externalised on the surface of macrophage and cancer cell-derived microparticles (Schroder et al. 2014). Thus SerpinB2 is present in the extracellular milieu, where it is available to inhibit uPA or tPA. Moreover, SerpinB2 facilitates the rapid endocytosis of uPA:uPAR complexes from the surface of prostate cancer (PC-3) (Croucher et al. 2006) and breast cancer (MCF-7) (Croucher et al. 2007; Cochran et al. 2011) cell lines, via members of the Low Density Lipoprotein Receptor (LDLR) family. Clarification of the inhibition and possible subsequent endocytosis of uPA:SerpinB2 complexes by monocytic cells was of interest with respect to i) understanding the role of SerpinB2 in modulating plasminogen activation on

monocytic cells in a patho/physiological context, and ii) the possible future development of SerpinB2 directed therapeutics for the treatment of hematopoietic disorders such as acute myeloid leukaemias. We confirmed (Chapter 2) that SerpinB2 inhibits monocytic cell surface uPA and the uPA:serpin complex is subsequently cleared via LRP and VLDR, showing a consistent endocytosis pathway to that previously described for prostate (Croucher et al. 2006) and breast cancer (Croucher et al. 2007) cell lines.

Indeed, this work supports the development of ligand targeted therapy by Vine et al. (2012), which shows the selective targeting of receptor bound uPA at the cell surface of U937 and THP-1 cell lines, with prodrug, 5,7-dibromo-N-(p-hydroxymethylbenzyl)isatin (N-AI) conjugated via an esterase-labile linker (N-AIE) to SerpinB2. The cytotoxicity of the activated (endocytosed) drug was found to correlate with uPA levels, whereby the THP-1 cell line (high uPA expression profile (Fig. 2.1)) was found to be more susceptible to the cytotoxic effects of SerpinB2-*N*-AIE, compared to the U-937 cell line (low uPA expression profile (Fig. 2.1)). Early work investigating the expression patterns for components of the uPA system clearly indicate a correlation between differentiation towards macrophage phenotype and uPAR expression (Lanza et al. 1998; Scherrer et al. 1999). Importantly, uPA is the predominant plasminogen activator in leukaemic marrow, a characteristic not found in healthy marrow (McWilliam et al. 1998; Scherrer et al. 1999), therefore SerpinB2 targeted therapeutics may prove successful in

eradicating multiple drug resistant leukemic blasts and stem cells within the marrow of patients and warrants further detailed preclinical investigation.

As such, a thorough understanding of the role SerpinB2 plays in the inhibition of plasminogen activation at the cell surface of monocytes was required. SerpinB2 is able to inhibit other cell type surface bound tc-tPA *in vitro* (Lobov et al. 2008). Therefore, we next examined the inhibition and fate of cell surface tPA by SerpinB2 on freshly isolated peripheral blood monocytes (PBMs). We not only confirmed that SerpinB2 inhibits monocyte-bound tPA but show for the first time that these tPA:Serpin inhibitory complexes are subsequently endocytosed, predominantly via an LDLR dependent pathway, thus clearing cell surface tPA activity. Definitive proof for SerpinB2 as a physiological inhibitor of tPA *in vivo* requires experimentation in appropriate animal models. However, co-expression of tPA and SerpinB2 has been shown in normal bone marrow (McWilliam et al. 1998), skin (Chen et al. 1993), saliva and salivary gland tissue (Virtanen et al. 2006), gingival fluid (Brown et al. 1995; Kinnby 2002), as well during pregnancy (Astedt et al. 1998). Enhanced co-expression of both tPA and SerpinB2 by epithelial cells is indicative of some disease states, e.g. periodontal disease (Kinnby 2002), psoriasis and pre/eclampsia (Kruithof et al. 1995). Furthermore, in inflamed gingiva the local concentration of SerpinB2 and tPA in gingival fliud can reach up to 5 µg/ml (~100 nM) and 1.5 µg/ml (~20 nM), respectively (Brown et al. 1995; Kinnby 2002). Therefore, SerpinB2 may dampen tPA mediated proteolysis, which is thought to compromise epithelial integrity in these tissues. Taken together, these previous

works suggest that extracellular SerpinB2 is localized in significant concentrations where it may be a physiological inhibitor of cell surface tPA.

Definitive identification of uPA:serpin or tPA:serpin complexes within human tissue or animal models has not been forthcoming, most likely due to the rapid clearance of PAs complexed with SerpinB2 and their subsequent degradation via the lysosomes. Furthermore, knock-out animal models may not offer conclusive phenotypes to indicate where SerpinB2 and uPA or tPA may interact. For example, the SerpinB2$^{-/-}$ murine model by (Dougherty et al. 1999) did not identify any clear phenotype for SerpinB2-deficient mice. However, subtle phenotypes related to viral infection (Schroder et al. 2010), adipose development (Lijnen et al. 2007) and enhanced thrombus resolution attributable to enhanced uPA activity (Siefert et al. 2014) have since been reported in SerpinB2 null mice. This suggests that development of knock-in models may offer further insight into the specific nature of the PA systems and their inhibitors, SerpinB2 and SerpinE1. The development of dual fluorescent expressing mice offers the opportunity to knock in fluorescently labelled tPA/uPA and SerpinB2/SerpinE1, which will identify specific organs and systems where co-localisation occurs. Recently the bimolecular fluorescence complementation (BiFC) system, which enables direct visualisation (in live cells), of protein interactions (Kerppola 2008), has been shown to work within a Drosophila model (Hudry et al. 2011). This system utilises two complementary fragments of the venus yellow fluorescent protein, which when brought into close proximity by an interaction between proteins fused to these fragments, refold to form a fluorescent protein (Kerppola 2008). Development of a murine models using

this system with uPA/tPA and SerpinB2/E1 will open up many new areas of interest and contribute immensely to establishing physiological context to both SerpinB2 and SerpinE1, as mediators of proteolysis within the pericellular environment.

Importantly, expression of both tPA and SerpinB2 by monocytes, macrophages and myeloid progenitors within normal bone marrow, has been reported (McWilliam et al. 1998) and is consistent with the cell surface profile analysis conducted here, showing very low levels of uPA compared to the U937 or THP-1 cell line and some detectable cell surface tPA, which was absent on the malignant cell lines. The up-regulation of the uPA system within hematopoietic and solid mass tumours is well characterised and is the basis for the development of ligand targeted therapeutics, using SerpinB2 (Stutchbury et al. 2007; Ranson et al. 2012; Vine et al. 2012). In this respect, whilst SerpinB2 clearly inhibits cell surface tPA (Lobov et al. 2008) and is subsequently endocytosed via LRP or VLDLR (Lee et al. 2010), the modest levels of endogenous tPA present on freshly isolated monocytes suggests that minimal, non-specific drug delivery to these cell types may occur. This is essential when considering the use of SerpinB2 targeted therapeutics for the eradication of multiple drug resistant leukemic blasts and stem cells within the marrow of patients, as it may tip the balance in prognostic outcome through increased protection of healthy tissue whilst efficiently targeting aberrant cell types. In conclusion, this body of work contributes towards the proof of concept foundations for the development of SerpinB2 directed therapeutics for the treatment of haematological disorders and lymphomas.

6.3. Intracellular SerpinB2 – The proteostasis moderator.

Up-regulation of intracellular SerpinB2 in response to acute and chronic homeostatic imbalances is consistent with a potential function within cellular stress response pathways. Molecular chaperones tightly regulate proteostasis within cells under normal and stress conditions. The results within this thesis show for the first time that SerpinB2 exhibits chaperone-like activity, whereby SerpinB2 binds preferentially to misfolded stressed proteins, inhibits amorphous aggregation of DTT-reduced BSA and fibril formation of $A\beta_{1-40}$ and $A\beta_{1-42}$. Chaperones have been shown to interact with target substrates via hydrophobic interactions, whether the binding characteristics described here for SerpinB2 are also via hydrophobic interactions requires further experimentation. Surface modelling reveals the presence of a hydrophobic cluster, within a cavity on the surface of SerpinB2, which is in close proximity to the CD-loop (Fig. 6.1 B). The CD-loop itself also contains hydrophobic residues, contributing to 44% of the loop sequence (Fig. 6.1C). Early work by Wilczynska et al. (2003) showed significant changes in surface hydrophobicity which were dependent on the formation of C79-C161 disulfide bond, involving the C-D loop of SerpinB2 (Fig. 6.1B). Intriguingly, formation of this di-sulfide bond is thought to stabilize the opening of β-sheet-A and promote polymersiation, however disruption of the bond, is thought to close the β-sheet-A, whilst resulting in a 3 fold increase in the binding of a known hydrophobic probe, *bis*-ANS (Musci and Berliner 1985). It is possible that release of the CD-loop from the di-sulfide bond, allows interaction between the target

protein and hydrophobic regions of the loop itself, whilst also opening up the region of hydrophobicity along helix-D (Fig 6.1B).

In this context, future experiments investigating the effect of these hydrophobic pockets, if any, on the ability of SerpinB2 to interact with native or misfolded client proteins should be conducted using *bis*-ANS within the ELISA based end-point binding assays (see section 4.3.4). Pretreatment of plate bound substrates with *bis*-ANS, prior to the addition of SerpinB2, also in the presence of *bis*-ANS, should block hydrophobicity (Poon et al. 2002) and reduce detectable bound SerpinB2. Once established, site directed mutagenesis studies can be used to validate the specific residues which function within these hydrophobic pockets. Furthermore, the role of the CD-loop should be considered utilizing the ΔCD-loop mutant form of SerpinB2 (Cochran et al. 2009). Given that SerpinB2 was shown to inhibit the amorphous aggregation of BSA under reducing conditions, mild reduction of SerpinB2 prior to use within either end-point binding or real-time aggregation assays may improve the chaperone efficiency of the molecule. Of note however, the redox sensitive conformational changes proposed by Wilczynska et al. (2003) are thought to open the breach region of the serpin, when the C79-C161 di-sulfide bond is formed. This may open a functional region of the molecule for interaction with binding partners and is worth consideration in future experimentation exploring SerpinB2 chaperone-like activity. This is of particular interest in the context of fibril formation.

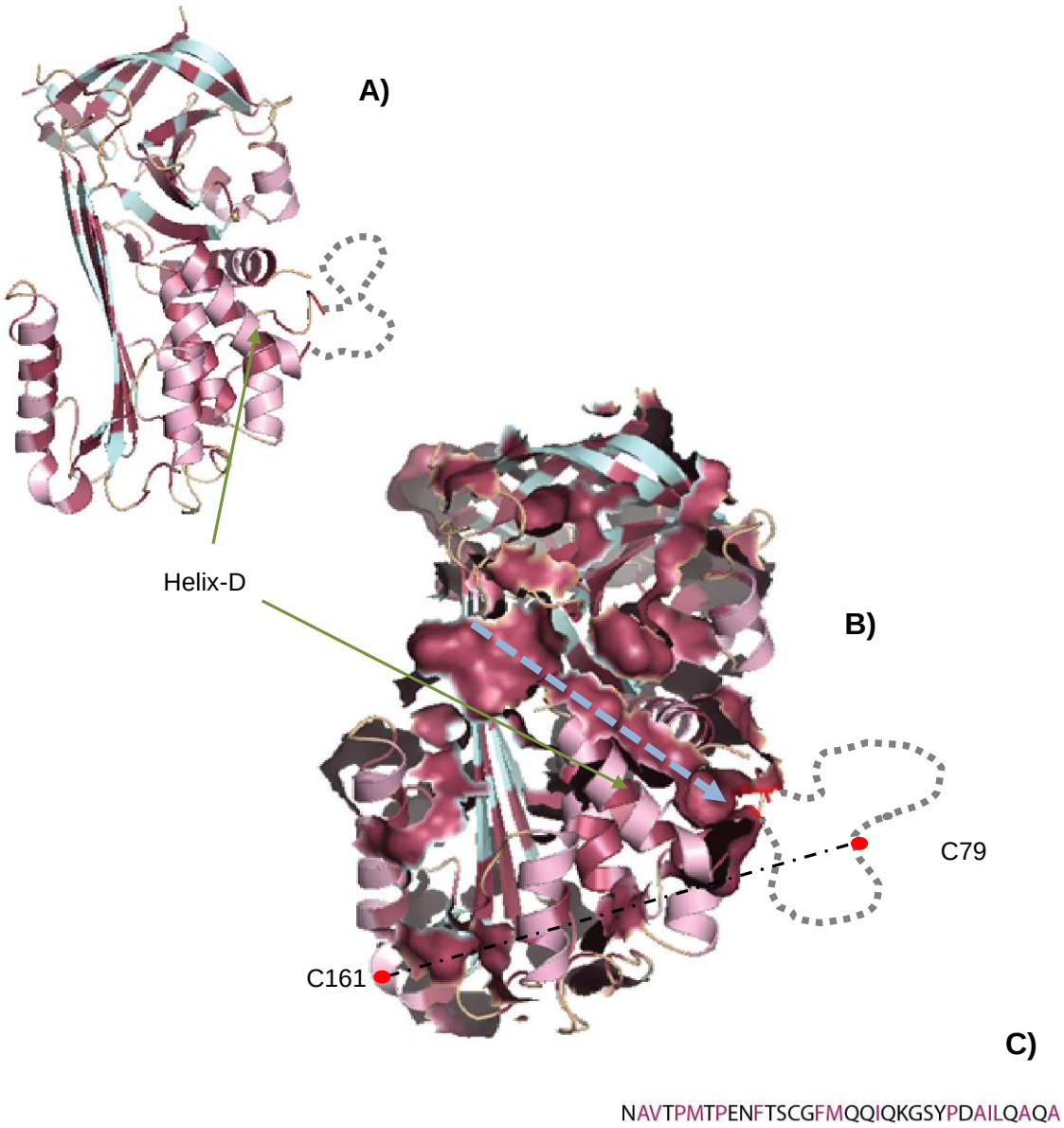

Figure 6.1: SerpinB2 molecule contains a hydrophobic cluster located along Helix D. A) Ribbon structure of SerpinB2 showing helices (light pink), β-sheets (pale cyan) and hydrophobic residues (raspberry). C-D inter-helical loop is located between residues 66-98 (grey dotted line). Helix D is labeled for visual orientation. **B)** Hydrophobic surface residues (raspberry) reveals a cluster (blue dotted arrow) within proximity of the C-D loop. Cysteine residues (C79-C161) (red circles) essential for proposed redox sensitive conformational rearrangement (Wilczynska et al. 2003) **C)** Amino acid sequence of the C-D loop with hydrophobic residues (raspberry). Modelling was conducted with crystal structure by (Harrop et al. 1999), 1BY7, using PyMOL Molecular Graphics System, Version 1.7.4.4 Schrödinger, LLC.

We show here that inhibition of $A\beta_{1-42}$ peptide fibril formation by SerpinB2 impairs its classic serpin inhibitory mechanism, suggesting that $A\beta_{1-42}$ peptide binds within the β-sheet-A region of SerpinB2. Whether the interaction occurs as a direct insertion of the peptide, into the breach or shutter regions of the serpin is unknown. However, further characterisation of this binding interaction may be obtained experimentally using small synthetic peptides which mimic the RCL sequence (Saunders et al. 2001). Such peptides will mimic insertion of the endogenous RCL into β-sheet-A region of SerpinB2 and block Aβ peptide insertion, which would be expected to abolish chaperone activity, thus confirming this particular mode of action.

Interestingly, the association of Serpins with Aβ peptides (within the extracellular environment) appears to be widespread in that Serpins A1 (α1-antitrypsin (AAT)), A3 (α1-antichymotrypsin (ACT)) (Abraham et al. 1988; Rozemuller et al. 1991), B2 (Akiyama et al. 1993) and I1 (Neuroserpin) (Kinghorn et al. 2006) have all been shown to co-localise with senile plaques associated with Alzheimer's Disease (AD). By means of *in vitro* studies SerpinA3 was reported to inhibit fibril formation by $A\beta_{1-40}$ (Eriksson et al. 1995; Aksenova et al. 1996) but not $A\beta_{1-42}$ (Aksenov et al. 1996) peptide, yet SerpinA3 reduced the cytotoxicity of $A\beta_{1-42}$ but not $A\beta_{1-40}$ peptide against rat hippocampal cell cultures (Aksenov et al. 1996; Aksenova et al. 1996). Furthermore, Serpins A1, A3, C1 and F2 were all found to inhibit the cytotoxicity of Aβ peptide added to rat pancreatic islet cell tumour line, subclone (I5) (Schubert 1997). Whether SerpinB2 in the extracellular space also buffers

against the cytotoxicity of Aβ-peptide requires investigation. Future cell based experiments utilising inactive (RCL blocked) SerpinB2 as a control would be useful in determining whether SerpinB2 interrupts endocytosis of toxic amyloid species. The exact role serpins play in AD progression is unclear, therefore gaining an understanding of how SerpinB2 inhibits Aβ-peptide fibril formation and determining if SerpinB2 is able to protect against the cytotoxicity of Aβ-peptide, may clarify whether serpins, in general, are actively involved within extracellular proteostasis pathways or are themselves sequestered by Aβ-peptide.

Molecular chaperones are classically defined as proteins that participate in *de novo* folding, facilitate the formation of functional tertiary conformations and re-folding of stress-denatured proteins (Jakob and Buchner 1994; Netzer and Hartl 1998; Hartl and Hayer-Hartl 2009). These chaperones are active within the “on-folding” pathway (Fig. 6.2A) and belong to the family of heat shock proteins (HSP) (Hartl et al. 2011). Alternatively, some molecular chaperones function to stabilise stressed proteins but do not work within the folding pathway to re-conform misfolded substrates into their functional native tertiary structures (Jakob and Buchner 1994; Ehrnsperger et al. 1997). These chaperones are functional within the “off-folding” pathway (Fig. 6.2B) and belong to the small heat shock protein (sHSP) family (Hartl et al. 2011). Importantly, molecular chaperones within either system bind preferentially to misfolded proteins, as does SerpinB2. Whether SerpinB2 functions within the “on” folding pathway is not known. Of interest, sHsp47 (SerpinH1) interacts transiently with pro-collagen during its folding,

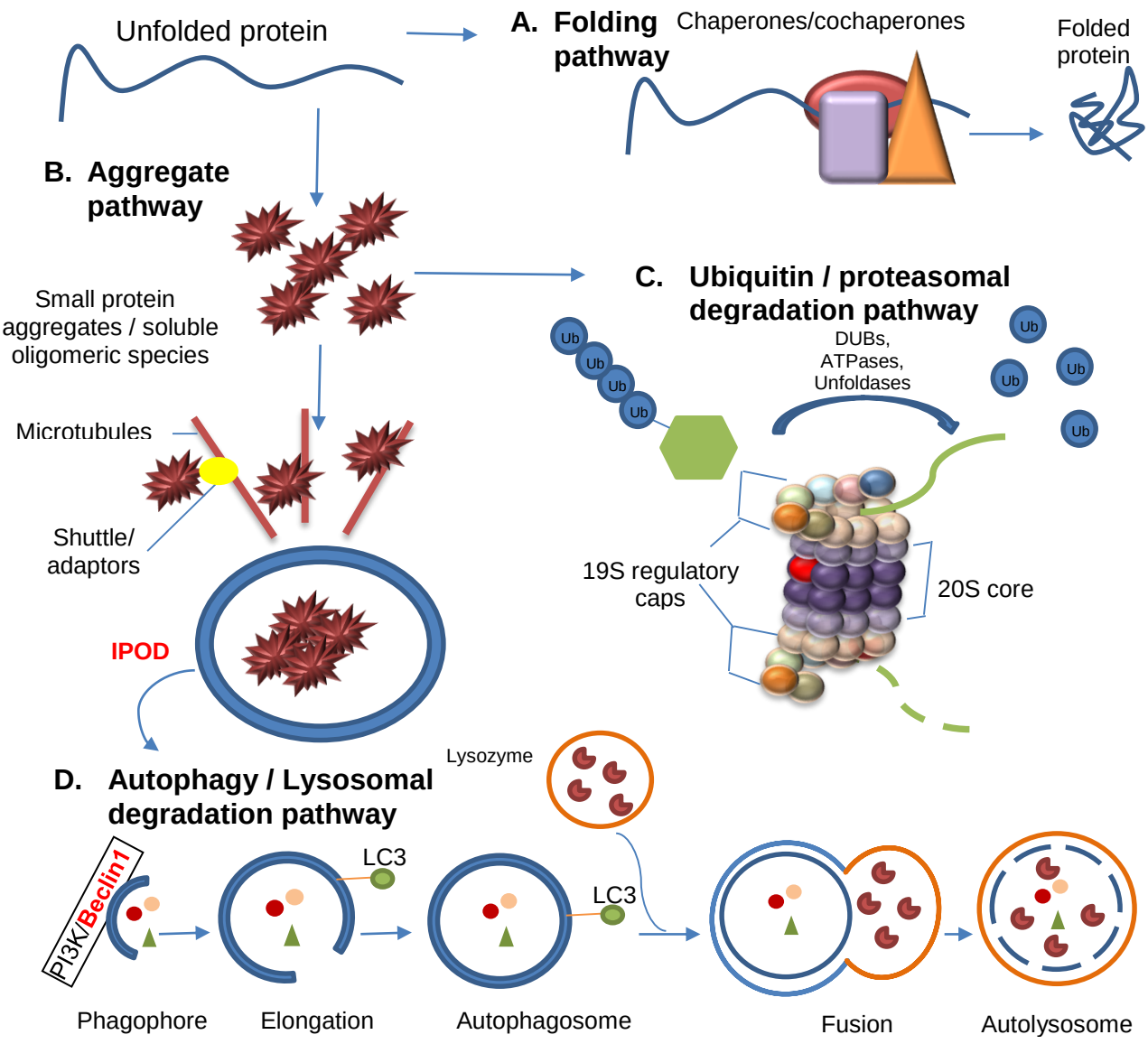

Figure 6.2. SerpinB2 identified as a potential player in cellular proteostasis networks. Unfolded proteins are re/folded into their correct tertiary structure by chaperones and co-chaperones within the **folding pathway (A)** or enter the **aggregate pathway (B)** where they form small protein aggregates, which are either degraded via the **ubiquitin/proteasomal degradation pathway (C)** or sequestered into inclusion bodies such as the insoluble protein deposits (IPOD) for degradation via the **autophagy/lysosomal degradation pathway (D).** SerpinB2 binds to misfolded protein and influences IPOD formation (Lee et al. 2015) (pathway B). SerpinB2 influences proteasome activity (pathway C) (Lee et al. 2015) possibly through interaction with proteasome subunit-β1 (red) (Fan et al. 2004). SerpinB2 deletion results in dysregulation of the autophagy/lysosomal degradation (pathway D). Possibly through protective interaction with Beclin-1 (Chuang et al. 2013).

assembly and transport from the endoplasmic reticulum (Tasab et al. 2000). Given that SerpinB2 protein has been shown localized within the nucleus and cytosol it is plausible to consider a potential role within the on-folding pathway.

The work presented within this thesis provides novel evidence that SerpinB2 may function within proteostasis networks, as a chaperone-like protein. SerpinB2 identifies and binds preferentially to misfolded proteins suggesting it may interact with soluble oligomers and small aggregates (Fig 6.2B) and facilitate their trafficking into inclusion bodies or the proteasomal degradation pathway (Fig 6.2C). Indeed, our finding that loss of SerpinB2 results in decreased numbers of large IPOD inclusions (Fig. 6.2B) is consistent with a role for SerpinB2 in mediating the formation of cellular inclusions, which requires rearrangement of the cytoskeleton. In this context, investigation of potential cytoskeleton interactions for SerpinB2 are warranted. Intriguingly, loss of SerpinB2 also results in attenuation of both the proteasome (Fig 6.2D) and autophagy-lysosomal degradation pathways (Fig 6.2D). Whether SerpinB2 functions within both systems or has an indirect effect on one, through loss of the other, remains to be shown. The reported interaction of SerpinB2 with proteasome subunit beta type 1 (Fan et al. 2004) (Fig 6.2C) and autophagy regulator, Beclin-1 (Chuang et al. 2013) (Fig 6.2D) suggests a role within both pathways. It is tempting to speculate that SerpinB2 may interact with PSMB1 during assembly and disassembly of the 26S proteasome, functioning to help shuttle the subunit into place, either as a substrate or an adapter protein.

We also show dysregulation of the autophagy-lysosomal degradation pathway suggesting a possible role for SerpinB2 within this initial seeding stage (phagosome formation) of the pathway (Fig. 6.2D), possibly through cytoskeleton rearrangement. Also of interest, dissociation of Bcl-2 from Beclin-1 initiates seeding of the phagophore. Interestingly, Bcl-2 interacts with Beclin-1 through hydrophobic interactions so it is plausible to consider that SerpinB2 may also bind in a similar way, potentially obscuring the Bcl-2 binding site on Beclin-1, thus promoting autophagy. Of interest, SerpinB2 expression was recently shown by Chuang et al. (2013) to protect Beclin-1 degradation via the proteasome. Furthermore, Chuang et al. (2013) found that SerpinB2 associated with and enhanced the binding of Hsp90 and Beclin-90, suggesting a functional multi-protein complex arrangement for SerpinB2.

In this context, the role Hsp90 plays within the phagophore, in relation the SerpinB2 is also of interest. Hsp90 is an essential mediator of proteostasis networks and co-localises with co-chaperones to form macro-complexes (Hipp et al. 2014). Investigation of the interaction between Beclin-1, SerpinB2 and Hsp90 is required to better understand how SerpinB2 influences autophagy. It is possible that the chaperone-like biochemical properties described for SerpinB2 within this thesis contribute to a co-chaperone like function for SerpinB2 within the Hsp90 complex systems. Previous work has shown that the co-chaperone and ubiquitin ligase, CHIP, binds to Hsp70 and Hsp90, mediating ubiquitylation of target proteins and transporting them to the proteasome (Kettern et al. 2010). The hypothesis that

SerpinB2 may act as a co-chaperone or adapter protein is supported by the finding that SerpinB2 interacts with ubiquitin in a non-covalent manner (Lee et al. 2015). Furthermore, SerpinB2 has also been shown to interact with the ubiquitin-like adapter protein, interferon stimulated gene-15 (ISG15) (Giannakopoulos et al. 2005) which has also been implicated in autophagy and proteosomal degradation pathways (Nakashima et al. 2015).

Of interest then is the finding that SerpinB2 structure is unique whereby the highly conserved Thr203 residue, found in all other serpins, is replaced by an asparagine residue, resulting in the loss of a helical turn and the extension of a chain, at the top of the molecule near the RCL (Fig. 6.3) (Harrop et al. 1999). Importantly, this results in a more flexible region than that of the body of the protein. The lack of an intracellular protease target for SerpinB2 has confounded progression of SerpinB2 research, particularly given numerous studies which report the characterization of cleaved SerpinB2, post induction of cellular stress. Intriguingly recent work by (Chuang et al. 2013), describing Hsp90 interaction with SerpinB2, showed that the pro-autophagy and Beclin-1 protective mechanisms are dependent on an active serpin. The authors report loss of function when using the R380A mutant of SerpinB2, once again suggesting a protease target. If however, SerpinB2 forms a functional multiprotein complex with Hsp90, or other proteins, in its proposed role as a co-chaperone, it is hypothesized that cleavage of the RCL by protease/s releases the serpin and/or its cargo.

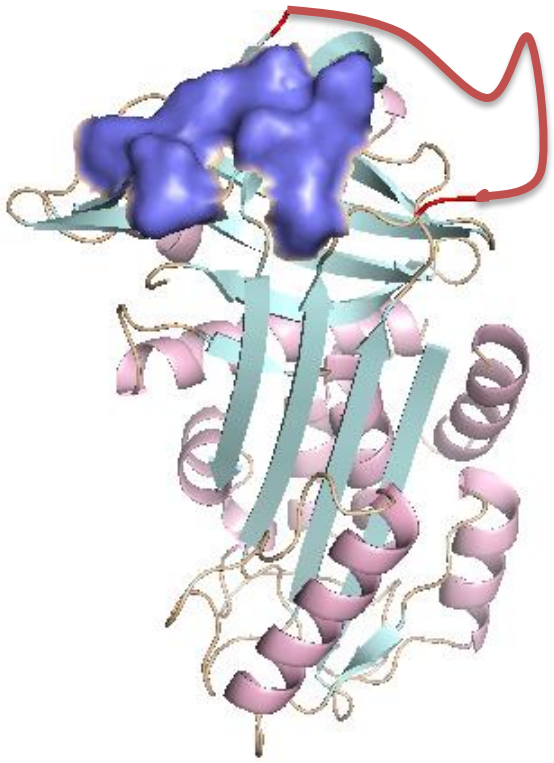

Figure 6.3: SerpinB2 contains a unique region of increased flexibility. Ribbon structure of SerpinB2 showing helices (light pink) and β-sheets (pale cyan). Region containing residues Glu213 to Tyr220 (blue) forms a unique region of flexibility within SerpinB2. RCL superimposed (red line). Modelling was conducted with crystal structure by (Harrop et al. 1999), 1BY7, using PyMOL Molecular Graphics System, Version 1.7.4.4 Schrödinger, LLC

In conclusion, this work opens up an exciting new focus of research for intracellular SerpinB2 biology, in that SerpinB2 has chaperone-like characteristics and clearly influences autophagy-lysosomal and proteasomal degradation pathways. The cytoprotective role of intracellular SerpinB2 has remained elusive given it's everywhere whilst nowhere expression profile, within many cell types under many varied conditions. Early work focused on an anti-apoptotic role for SerpinB2 (discussed section 1.14.1) with confounding results. Interestingly, BCL-2 has been shown to inhibit both apoptosis and autophagy, furthermore over activation of the autophagy pathway has a pro-apoptotic effect (Pattingre et al. 2005). This raises the question then, if SerpinB2 is pro-autophagic and over-activation of the pathway results in activation of apoptosis, then how may this have influenced the early studies, using SerpinB2 overexpressing cell lines. Given the role of serpinB2 in cytoprotection it is likely that further research will uncover therapeutic targets for neurodegenerative disorders, as well as in cancer.

7. Reference List

Abraham, C. R., D. J. Selkoe, et al. (1988). "Immunochemical identification of the serine protease inhibitor alpha 1-antichymotrypsin in the brain amyloid deposits of Alzheimer's disease." Cell **52**(4): 487-501.

Adams, J. (2004). "The proteasome: a suitable antineoplastic target." Nat Rev Cancer **4**(5): 349-360.

Ahn, N. S., H. Hu, et al. (2005). "Molecular mechanisms of the 2,3,7,8-tetrachlorodibenzo-p-dioxin-induced inverted U-shaped dose responsiveness in anchorage independent growth and cell proliferation of human breast epithelial cells with stem cell characteristics." Mutat Res **579**(1-2): 189-199.

Akiyama, H., K. Ikeda, et al. (1993). "Microglia express the type 2 plasminogen activator inhibitor in the brain of control subjects and patients with Alzheimer's disease." Neurosci Lett **164**(1-2): 233-235.

Aksenov, M. Y., M. V. Aksenova, et al. (1996). "Alpha 1-antichymotrypsin interaction with A beta (1-42) does not inhibit fibril formation but attenuates the peptide toxicity." Neurosci Lett **217**(2-3): 117-120.

Aksenova, M. V., M. Y. Aksenov, et al. (1996). "alpha-1-antichymotrypsin interaction with A beta (1-40) inhibits fibril formation but does not affect the peptide toxicity." Neurosci Lett **211**(1): 45-48.

Al-Ejeh, F., D. Croucher, et al. (2004). "Kinetic analysis of plasminogen activator inhibitor type-2: urokinase complex formation and subsequent internalisation by carcinoma cell lines." Exp Cell Res **297**(1): 259-271.

Allen, B. J., Z. Tian, et al. (2003). "Preclinical studies of targeted alpha therapy for breast cancer using 213Bi-labelled-plasminogen activator inhibitor type 2." Br J Cancer **88**(6): 944-950.

Almeida-Vega, S., K. Catlow, et al. (2009). "Gastrin activates paracrine networks leading to induction of PAI-2 via MAZ and ASC-1." Am J Physiol Gastrointest Liver Physiol **296**(2): G414-423.

Amen, T. and D. Kaganovich (2015). "Dynamic droplets: the role of cytoplasmic inclusions in stress, function, and disease." Cell Mol Life Sci **72**(3): 401-415.

Andreasen, P. A., R. Egelund, et al. (2000). "The plasminogen activation system in tumor growth, invasion, and metastasis." Cell Mol Life Sci **57**(1): 25-40.

Andreasen, P. A., L. Kjoller, et al. (1997). "The urokinase-type plasminogen activator system in cancer metastasis: a review." Int J Cancer **72**(1): 1-22.

Antalis, T. M., M. A. Clark, et al. (1988). "Cloning and expression of a cDNA coding for a human monocyte-derived plasminogen activator inhibitor." Proc Natl Acad Sci U S A **85**(4): 985-989.

Antalis, T. M., E. Costelloe, et al. (1996). "Regulation of the plasminogen activator inhibitor type-2 gene in monocytes: localization of an upstream transcriptional silencer." Blood **88**(10): 3686-3697.

Antalis, T. M., M. La Linn, et al. (1998). "The serine proteinase inhibitor (serpin) plasminogen activation inhibitor type 2 protects against viral cytopathic

effects by constitutive interferon alpha/beta priming." J Exp Med **187**(11): 1799-1811.
Arrasate, M., S. Mitra, et al. (2004). "Inclusion body formation reduces levels of mutant huntingtin and the risk of neuronal death." Nature **431**(7010): 805-810.
Askew, D. J., S. Cataltepe, et al. (2007). "SERPINB11 is a new noninhibitory intracellular serpin. Common single nucleotide polymorphisms in the scaffold impair conformational change." J Biol Chem **282**(34): 24948-24960.
Askew, Y. S., S. C. Pak, et al. (2001). "SERPINB12 is a novel member of the human ov-serpin family that is widely expressed and inhibits trypsin-like serine proteinases." J Biol Chem **276**(52): 49320-49330.
Astedt, B., B. Bladh, et al. (1985). "Different inhibition of one and two chain tissue plasminogen activator by a placental inhibitor studied with two tripeptide-p-nitroanilide substrates." Scand J Clin Lab Invest **45**(5): 429-435.
Astedt, B., I. Lecander, et al. (1985). "Purification of a specific placental plasminogen activator inhibitor by monoclonal antibody and its complex formation with plasminogen activator." Thromb Haemost **53**(1): 122-125.
Astedt, B., C. Lindoff, et al. (1998). "Significance of the plasminogen activator inhibitor of placental type (PAI-2) in pregnancy." Semin Thromb Hemost **24**(5): 431-435.
Bailey, C. M., Z. Khalkhali-Ellis, et al. (2005). "Mammary serine protease inhibitor (Maspin) binds directly to interferon regulatory factor 6: identification of a novel serpin partnership." J Biol Chem **280**(40): 34210-34217.
Baldovino, S., M. Piccinini, et al. (2006). "Structural and functional properties of proteasomes purified from the human kidney." J Nephrol **19**(6): 710-716.
Bano, D., F. Zanetti, et al. (2011). "Neurodegenerative processes in Huntington's disease." Cell Death Dis **2**: e228.
Behrendt, N., K. List, et al. (2003). "The pro-urokinase plasminogen-activation system in the presence of serpin-type inhibitors and the urokinase receptor: rescue of activity through reciprocal pro-enzyme activation." Biochem J **371**(Pt 2): 277-287.
Behrendt, N. and R. Stephens (1998). "The Urokinanse Receptor." Fibrinolysis & Proteolysis **12**(4): 191-204.
Belorgey, D., P. Hagglof, et al. (2007). "Protein misfolding and the serpinopathies." Prion **1**(1): 15-20.
Benarafa, C. and E. Remold-O'Donnell (2005). "The ovalbumin serpins revisited: perspective from the chicken genome of clade B serpin evolution in vertebrates." Proc Natl Acad Sci U S A **102**(32): 11367-11372.
Bence, N. F., E. J. Bennett, et al. (2005). "Application and analysis of the GFPu family of ubiquitin-proteasome system reporters." Methods Enzymol **399**: 481-490.
Bence, N. F., R. M. Sampat, et al. (2001). "Impairment of the ubiquitin-proteasome system by protein aggregation." Science **292**(5521): 1552-1555.

Bird, C. H., E. J. Blink, et al. (2001). "Nucleocytoplasmic distribution of the ovalbumin serpin PI-9 requires a nonconventional nuclear import pathway and the export factor Crm1." Mol Cell Biol **21**(16): 5396-5407.
Bird, C. H., V. R. Sutton, et al. (1998). "Selective regulation of apoptosis: the cytotoxic lymphocyte serpin proteinase inhibitor 9 protects against granzyme B-mediated apoptosis without perturbing the Fas cell death pathway." Mol Cell Biol **18**(11): 6387-6398.
Bolognesi, B., J. R. Kumita, et al. (2010). "ANS binding reveals common features of cytotoxic amyloid species." ACS Chem Biol **5**(8): 735-740.
Boncela, J., P. Przygodzka, et al. (2013). "Secretion of SerpinB2 from endothelial cells activated with inflammatory stimuli." Exp Cell Res **319**(8): 1213-1219.
Boutahar, N., A. Wierinckx, et al. (2011). "Differential effect of oxidative or excitotoxic stress on the transcriptional profile of amyotrophic lateral sclerosis-linked mutant SOD1 cultured neurons." J Neurosci Res **89**(9): 1439-1450.
Bova, M. P., L. L. Ding, et al. (1997). "Subunit exchange of alphaA-crystallin." J Biol Chem **272**(47): 29511-29517.
Boyer, S. N., D. E. Wazer, et al. (1996). "E7 protein of human papilloma virus-16 induces degradation of retinoblastoma protein through the ubiquitin-proteasome pathway." Cancer Res **56**(20): 4620-4624.
Braungart, E., V. Magdolen, et al. (2001). "Retinoic acid upregulates the plasminogen activator system in human epidermal keratinocytes." J Invest Dermatol **116**(5): 778-784.
Brooks, P., G. Fuertes, et al. (2000). "Subcellular localization of proteasomes and their regulatory complexes in mammalian cells." Biochem J **346 Pt 1**: 155-161.
Brown, J. M., K. Watanabe, et al. (1995). "Molecular characterization of plasminogen activators in human gingival crevicular fluid." Arch Oral Biol **40**(9): 839-845.
Brownstein, C., A. B. Deora, et al. (2004). "Annexin II mediates plasminogen-dependent matrix invasion by human monocytes: enhanced expression by macrophages." Blood **103**(1): 317-324.
Brummer, T., M. Larance, et al. (2008). "Phosphorylation-dependent binding of 14-3-3 terminates signalling by the Gab2 docking protein." EMBO J **27**(17): 2305-2316.
Brummer, T., D. Schramek, et al. (2006). "Increased proliferation and altered growth factor dependence of human mammary epithelial cells overexpressing the Gab2 docking protein." J Biol Chem **281**(1): 626-637.
Bu, G., S. Williams, et al. (1992). "Low density lipoprotein receptor-related protein/alpha 2-macroglobulin receptor is an hepatic receptor for tissue-type plasminogen activator." Proc Natl Acad Sci U S A **89**(16): 7427-7431.
Bucciantini, M., E. Giannoni, et al. (2002). "Inherent toxicity of aggregates implies a common mechanism for protein misfolding diseases." Nature **416**(6880): 507-511.

Buechler, C., H. Ullrich, et al. (2001). "Lipoprotein (a) up-regulates the expression of the plasminogen activator inhibitor 2 in human blood monocytes." Blood **97**(4): 981-986.

Buyru, N., J. Altinisik, et al. (2003). "PCR-RFLP detection of PAI-2 variants in myocardial infarction." Clin Appl Thromb Hemost **9**(4): 333-336.

Bystrom, J., T. A. Wynn, et al. (2004). "Gene microarray analysis reveals interleukin-5-dependent transcriptional targets in mouse bone marrow." Blood **103**(3): 868-877.

Camani, C., F. Bachmann, et al. (1994). "The role of plasminogen activator inhibitor type 1 in the clearance of tissue-type plasminogen activator by rat hepatoma cells." J Biol Chem **269**(8): 5770-5775.

Camani, C., O. Gavin, et al. (2000). "Cellular degradation of free and inhibitor-bound tissue-type plasminogen activator--requirement for a co-receptor?" Thromb Haemost **83**(2): 290-296.

Camerer, E., E. Gjernes, et al. (2000). "Binding of factor VIIa to tissue factor on keratinocytes induces gene expression." J Biol Chem **275**(9): 6580-6585.

Cao, C., D. A. Lawrence, et al. (2006). "Endocytic receptor LRP together with tPA and PAI-1 coordinates Mac-1-dependent macrophage migration." Embo J **25**(9): 1860-1870.

Carrell, R. W. and D. A. Lomas (1997). "Conformational disease." Lancet **350**(9071): 134-138.

Carver, J. A. and R. A. Lindner (1998). "NMR spectroscopy of alpha-crystallin. Insights into the structure, interactions and chaperone action of small heat-shock proteins." Int J Biol Macromol **22**(3-4): 197-209.

Cesarman, G. M., C. A. Guevara, et al. (1994). "An endothelial cell receptor for plasminogen/tissue plasminogen activator (t-PA). II. Annexin II-mediated enhancement of t-PA-dependent plasminogen activation." J Biol Chem **269**(33): 21198-21203.

Champelovier, P., A. Simon, et al. (2003). "Is interferon gamma one key of metastatic potential increase in human bladder carcinoma?" Clin Cancer Res **9**(12): 4562-4569.

Chen, C. S., B. Lyons-Giordano, et al. (1993). "Differential expression of plasminogen activators and their inhibitors in an organotypic skin coculture system." J Cell Sci **106 (Pt 1)**: 45-53.

Chiou, A., P. Hagglof, et al. (2009). "Probing neuroserpin polymerization and interaction with amyloid-beta peptides using single molecule fluorescence." Biophys J **97**(8): 2306-2315.

Chiti, F. and C. M. Dobson (2006). "Protein misfolding, functional amyloid, and human disease." Annu Rev Biochem **75**: 333-366.

Chuang, S. Y., C. H. Yang, et al. (2013). "TLR-induced PAI-2 expression suppresses IL-1beta processing via increasing autophagy and NLRP3 degradation." Proc Natl Acad Sci U S A **110**(40): 16079-16084.

Chuang, T. L. and R. R. Schleef (1999). "Identification of a nuclear targeting domain in the insertion between helices C and D in protease inhibitor-10." J Biol Chem **274**(16): 11194-11198.

Cochran, B. J., D. R. Croucher, et al. (2011). "Dependence on endocytic receptor binding via a minimal binding motif underlies the differential prognostic profiles of SerpinE1 and SerpinB2 in cancer." J Biol Chem **286**(27): 24467-24475.

Cochran, B. J., L. P. Gunawardhana, et al. (2009). "The CD-loop of PAI-2 (SERPINB2) is redundant in the targeting, inhibition and clearance of cell surface uPA activity." BMC Biotechnol **9**(1): 43.

Collen, D. and H. R. Lijnen (2004). "Tissue-type plasminogen activator: a historical perspective and personal account." J Thromb Haemost **2**(4): 541-546.

Corsetti, J. P., P. Salzman, et al. (2013). "Plasminogen activator inhibitor-2 polymorphism associates with recurrent coronary event risk in patients with high HDL and C-reactive protein levels." PLoS One **8**(7): e68920.

Costelloe, E. O., K. J. Stacey, et al. (1999). "Regulation of the plasminogen activator inhibitor-2 (PAI-2) gene in murine macrophages. Demonstration of a novel pattern of responsiveness to bacterial endotoxin." J Leukoc Biol **66**(1): 172-182.

Cousin, E., R. L. Medcalf, et al. (1991). "Regulatory elements involved in constitutive and phorbol ester-inducible expression of the plasminogen activator inhibitor type 2 gene promoter." Nucleic Acids Res **19**(14): 3881-3886.

Croucher, D., D. N. Saunders, et al. (2006). "The urokinase/PAI-2 complex: a new high affinity ligand for the endocytosis receptor low density lipoprotein receptor-related protein." J Biol Chem **281**(15): 10206-10213.

Croucher, D. R., M. Ranson, et al. (2010). "SerpinB2." UCSD-Nature Molecules Page.

Croucher, D. R., D. N. Saunders, et al. (2008). "Revisiting the biological roles of PAI2 (SERPINB2) in cancer." Nat Rev Cancer.

Croucher, D. R., D. N. Saunders, et al. (2007). "A structural basis for differential cell signaling by PAI-1 and PAI-2 in breast cancer cells." Biochem J **408**(2): 203-210.

Czekay, R. P., T. A. Kuemmel, et al. (2001). "Direct binding of occupied urokinase receptor (uPAR) to LDL receptor-related protein is required for endocytosis of uPAR and regulation of cell surface urokinase activity." Mol Biol Cell **12**(5): 1467-1479.

Dahlen, J. R., F. Jean, et al. (1998). "Inhibition of soluble recombinant furin by human proteinase inhibitor 8." J Biol Chem **273**(4): 1851-1854.

Dano, K., P. Andreasen, et al. (1985). "Plasminogen Activators, Tissue Degradation and Cancer." Advances in Cancer Research **44**: 139 - 266.

Dano, K., N. Behrendt, et al. (2005). "Plasminogen activation and cancer." Thromb Haemost **93**(4): 676-681.

Darnell, G. A., T. M. Antalis, et al. (2003). "Inhibition of retinoblastoma protein degradation by interaction with the serpin plasminogen activator inhibitor 2 via a novel consensus motif." Mol Cell Biol **23**(18): 6520-6532.

Darnell, G. A., T. M. Antalis, et al. (2005). "Silencing of integrated human papillomavirus type 18 oncogene transcription in cells expressing SerpinB2." J Virol **79**(7): 4246-4256.

Das, K. P. and W. K. Surewicz (1995). "Temperature-induced exposure of hydrophobic surfaces and its effect on the chaperone activity of alpha-crystallin." FEBS Lett **369**(2-3): 321-325.
Davis, R. L., A. E. Shrimpton, et al. (1999). "Familial dementia caused by polymerization of mutant neuroserpin." Nature **401**(6751): 376-379.
Dear, A. E. and R. L. Medcalf (2000). "The novel anti-tumour agent oxamflatin differentially regulates urokinase and plasminogen activator inhibitor type 2 expression and inhibits urokinase-mediated proteolytic activity." Biochim Biophys Acta **1492**(1): 15-22.
Dear, A. E., Y. Shen, et al. (1996). "Molecular mechanisms governing tumor-necrosis-factor-mediated regulation of plasminogen-activator inhibitor type-2 gene expression." Eur J Biochem **241**(1): 93-100.
Degryse, B., J. G. Neels, et al. (2004). "The low density lipoprotein receptor-related protein is a motogenic receptor for plasminogen activator inhibitor-1." J Biol Chem **279**(21): 22595-22604.
Dehle, F. C., H. Ecroyd, et al. (2010). "alphaB-Crystallin inhibits the cell toxicity associated with amyloid fibril formation by kappa-casein and the amyloid-beta peptide." Cell Stress Chaperones **15**(6): 1013-1026.
Di Bernardo, M. C., A. Matakidou, et al. (2009). "Plasminogen activator inhibitor variants PAI-1 A15T and PAI-2 S413C influence lung cancer prognosis." Lung Cancer **65**(2): 237-241.
Dickinson, J. L., E. J. Bates, et al. (1995). "Plasminogen activator inhibitor type 2 inhibits tumor necrosis factor alpha-induced apoptosis. Evidence for an alternate biological function." J Biol Chem **270**(46): 27894-27904.
Dickinson, J. L., B. J. Norris, et al. (1998). "The C-D interhelical domain of the serpin plasminogen activator inhibitor-type 2 is required for protection from TNF-alpha induced apoptosis." Cell Death Differ **5**(2): 163-171.
Dietzmann, K., P. von Bossanyi, et al. (2000). "Expression of the plasminogen activator system and the inhibitors PAI-1 and PAI-2 in posttraumatic lesions of the CNS and brain injuries following dramatic circulatory arrests: an immunohistochemical study." Pathol Res Pract **196**(1): 15-21.
Dougherty, K. M., J. M. Pearson, et al. (1999). "The plasminogen activator inhibitor-2 gene is not required for normal murine development or survival." Proc Natl Acad Sci U S A **96**(2): 686-691.
Duffy, M. J. (2004). "The urokinase plasminogen activator system: role in malignancy." Curr Pharm Des **10**(1): 39-49.
Ehrnsperger, M., S. Graber, et al. (1997). "Binding of non-native protein to Hsp25 during heat shock creates a reservoir of folding intermediates for reactivation." Embo j **16**(2): 221-229.
Eichner, T., A. P. Kalverda, et al. (2011). "Conformational conversion during amyloid formation at atomic resolution." Mol Cell **41**(2): 161-172.
Elliott, P. R., D. A. Lomas, et al. (1996). "Inhibitory conformation of the reactive loop of alpha 1-antitrypsin." Nat Struct Biol **3**(8): 676-681.
Ellis, V., M. F. Scully, et al. (1989). "Plasminogen activation initiated by single-chain urokinase-type plasminogen activator. Potentiation by U937 monocytes." J Biol Chem **264**(4): 2185-2188.

Ellis, V., T. C. Wun, et al. (1990). "Inhibition of receptor-bound urokinase by plasminogen-activator inhibitors." J Biol Chem **265**(17): 9904-9908.
Eriksson, S., S. Janciauskiene, et al. (1995). "Alpha 1-antichymotrypsin regulates Alzheimer beta-amyloid peptide fibril formation." Proc Natl Acad Sci U S A **92**(6): 2313-2317.
Estelles, A., J. Gilabert, et al. (1989). "Changes in the plasma levels of type 1 and type 2 plasminogen activator inhibitors in normal pregnancy and in patients with severe preeclampsia." Blood **74**(4): 1332-1338.
Fan, J., Y. Q. Zhang, et al. (2004). "Interaction of plasminogen activator inhibitor-2 and proteasome subunit, beta type 1." Acta Biochim Biophys Sin (Shanghai) **36**(1): 42-46.
Feder, M. E. and G. E. Hofmann (1999). "Heat-shock proteins, molecular chaperones, and the stress response: evolutionary and ecological physiology." Annu Rev Physiol **61**: 243-282.
Feener, E. P., J. M. Northrup, et al. (1995). "Angiotensin II induces plasminogen activator inhibitor-1 and -2 expression in vascular endothelial and smooth muscle cells." J Clin Invest **95**(3): 1353-1362.
Felez, J., C. J. Chanquia, et al. (1991). "Binding of tissue plasminogen activator to human monocytes and monocytoid cells." Blood **78**(9): 2318-2327.
Felez, J., L. A. Miles, et al. (1996). "Characterization of cellular binding sites and interactive regions within reactants required for enhancement of plasminogen activation by tPA on the surface of leukocytic cells." Thromb Haemost **76**(4): 577-584.
Finno, C. J., C. Stevens, et al. (2015). "SERPINB11 Frameshift Variant Associated with Novel Hoof Specific Phenotype in Connemara Ponies." PLoS Genet **11**(4): e1005122.
Fish, R. J. and E. K. Kruithof (2006). "Evidence for serpinB2-independent protection from TNF-alpha-induced apoptosis." Exp Cell Res **312**(3): 350-361.
Foy, C. A. and P. J. Grant (1997). "PCR-RFLP detection of PAI-2 gene variants: prevalence in ethnic groups and disease relationship in patients undergoing coronary angiography." Thromb Haemost **77**(5): 955-958.
Francois, A., F. Terro, et al. (2013). "Involvement of interleukin-1beta in the autophagic process of microglia: relevance to Alzheimer's disease." J Neuroinflammation **10**: 151.
Fraser, P. E., J. T. Nguyen, et al. (1993). "Alpha 1-antichymotrypsin binding to Alzheimer A beta peptides is sequence specific and induces fibril disaggregation in vitro." J Neurochem **61**(1): 298-305.
French, K., J. J. Yerbury, et al. (2008). "Protease activation of alpha2-macroglobulin modulates a chaperone-like action with broad specificity." Biochemistry **47**(4): 1176-1185.
Gallastegui, N. and M. Groll (2010). "The 26S proteasome: assembly and function of a destructive machine." Trends Biochem Sci **35**(11): 634-642.
Gan, H., J. Lee, et al. (2008). "Mycobacterium tuberculosis blocks crosslinking of annexin-1 and apoptotic envelope formation on infected macrophages to maintain virulence." Nat Immunol **9**(10): 1189-1197.

Gan, H., G. W. Newman, et al. (1995). "Plasminogen activator inhibitor type 2 prevents programmed cell death of human macrophages infected with Mycobacterium avium, serovar 4." J Immunol **155**(3): 1304-1315.
Genton, C., E. K. Kruithof, et al. (1987). "Phorbol ester induces the biosynthesis of glycosylated and nonglycosylated plasminogen activator inhibitor 2 in high excess over urokinase-type plasminogen activator in human U-937 lymphoma cells." J Cell Biol **104**(3): 705-712.
George, F., N. Pourreau-Schneider, et al. (1990). "Modulation of tPA, PAI-1 and PAI-2 antigen and mRNA levels by EGF in the A431 cell line." Blood Coagul Fibrinolysis **1**(6): 689-693.
Gettins, P. G. W. (2002). "Serpin structure, mechanism, and function." Chemical Reviews **102**: 4751-4803.
Giannakopoulos, N. V., J. K. Luo, et al. (2005). "Proteomic identification of proteins conjugated to ISG15 in mouse and human cells." Biochem Biophys Res Commun **336**(2): 496-506.
Gibson, C. S., A. H. MacLennan, et al. (2007). "Genetic polymorphisms and spontaneous preterm birth." Obstet Gynecol **109**(2 Pt 1): 384-391.
Gilon, T., O. Chomsky, et al. (1998). "Degradation signals for ubiquitin system proteolysis in Saccharomyces cerevisiae." EMBO J **17**(10): 2759-2766.
Gliemann, J., G. Hermey, et al. (2004). "The mosaic receptor sorLA/LR11 binds components of the plasminogen-activating system and platelet-derived growth factor-BB similarly to LRP1 (low-density lipoprotein receptor-related protein), but mediates slow internalization of bound ligand." Biochem J **381**(Pt 1): 203-212.
Graf, M., S. Reif, et al. (2005). "High expression of urokinase plasminogen activator receptor (UPA-R) in acute myeloid leukemia (AML) is associated with worse prognosis." Am J Hematol **79**(1): 26-35.
Graumann, J., H. Lilie, et al. (2001). "Activation of the redox-regulated molecular chaperone Hsp33--a two-step mechanism." Structure **9**(5): 377-387.
Greten, F. R., M. C. Arkan, et al. (2007). "NF-kappaB is a negative regulator of IL-1beta secretion as revealed by genetic and pharmacological inhibition of IKKbeta." Cell **130**(5): 918-931.
Gross, T. J. and R. G. Sitrin (1990). "The THP-1 cell line is a urokinase-secreting mononuclear phagocyte with a novel defect in the production of plasminogen activator inhibitor-2." J Immunol **144**(5): 1873-1879.
Gyetko, M. R., S. B. Shollenberger, et al. (1992). "Urokinase expression in mononuclear phagocytes: cytokine-specific modulation by interferon-gamma and tumor necrosis factor-alpha." J Leukoc Biol **51**(3): 256-263.
Gyetko, M. R., C. C. Wilkinson, et al. (1993). "Monocyte urokinase expression: modulation by interleukins." J Leukoc Biol **53**(5): 598-601.
Haile, W. B., J. L. Coleman, et al. (2006). "Reciprocal upregulation of urokinase plasminogen activator and its inhibitor, PAI-2, by Borrelia burgdorferi affects bacterial penetration and host-inflammatory response." Cell Microbiol **8**(8): 1349-1360.

Hajjar, K. A. (1993). "Homocysteine-induced modulation of tissue plasminogen activator binding to its endothelial cell membrane receptor." J Clin Invest **91**(6): 2873-2879.
Hajjar, K. A. and N. M. Hamel (1990). "Identification and characterization of human endothelial cell membrane binding sites for tissue plasminogen activator and urokinase." J Biol Chem **265**(5): 2908-2916.
Hajjar, K. A., A. T. Jacovina, et al. (1994). "An endothelial cell receptor for plasminogen/tissue plasminogen activator. I. Identity with annexin II." J Biol Chem **269**(33): 21191-21197.
Hamaguchi, M., Y. Morishita, et al. (1991). "FDP D-dimer induces the secretion of interleukin-1, urokinase-type plasminogen activator, and plasminogen activator inhibitor-2 in a human promonocytic leukemia cell line." Blood **77**(1): 94-100.
Hamilton, J. A., G. A. Whitty, et al. (1993). "Macrophage colony-stimulating factor and granulocyte-macrophage colony-stimulating factor stimulate the synthesis of plasminogen-activator inhibitors by human monocytes." Blood **82**(12): 3616-3621.
Hamilton, J. A., J. Wojta, et al. (1993). "Contrasting effects of transforming growth factor-beta and IL-1 on the regulation of plasminogen activator inhibitors in human synovial fibroblasts." J Immunol **151**(10): 5154-5161.
Hammond, G. L. (1990). "Molecular properties of corticosteroid binding globulin and the sex-steroid binding proteins." Endocr Rev **11**(1): 65-79.
Hammond, G. L., C. L. Smith, et al. (1987). "Primary structure of human corticosteroid binding globulin, deduced from hepatic and pulmonary cDNAs, exhibits homology with serine protease inhibitors." Proc Natl Acad Sci U S A **84**(15): 5153-5157.
Hannocks, M. J., L. Oliver, et al. (1992). "Regulation of proteolytic activity in human bone marrow stromal cells by basic fibroblast growth factor, interleukin-1, and transforming growth factor beta." Blood **79**(5): 1178-1184.
Hardy, M. M., J. Feder, et al. (1997). "Low density lipoprotein receptor-related protein modulates the expression of tissue-type plasminogen activator in human colon fibroblasts." J Biol Chem **272**(10): 6812-6817.
Harrop, S. J., L. Jankova, et al. (1999). "The crystal structure of plasminogen activator inhibitor 2 at 2.0 A resolution: implications for serpin function." Structure **7**(1): 43-54.
Hart, P. H., D. R. Burgess, et al. (1989). "Interleukin-4 stimulates human monocytes to produce tissue-type plasminogen activator." Blood **74**(4): 1222-1225.
Hart, P. H., G. F. Vitti, et al. (1989). "Human monocytes can produce tissue-type plasminogen activator." J Exp Med **169**(4): 1509-1514.
Hartl, F. U., A. Bracher, et al. (2011). "Molecular chaperones in protein folding and proteostasis." Nature **475**(7356): 324-332.
Hartl, F. U. and M. Hayer-Hartl (2009). "Converging concepts of protein folding in vitro and in vivo." Nat Struct Mol Biol **16**(6): 574-581.
Hatters, D. M. (2008). "Protein misfolding inside cells: the case of huntingtin and Huntington's disease." IUBMB Life **60**(11): 724-728.

He, C. and D. J. Klionsky (2009). "Regulation mechanisms and signaling pathways of autophagy." Annu Rev Genet **43**: 67-93.
Herrmann, J., L. O. Lerman, et al. (2007). "Ubiquitin and ubiquitin-like proteins in protein regulation." Circ Res **100**(9): 1276-1291.
Hibino, T., S. Izaki, et al. (1988). "Epidermal plasminogen activator inhibitor (PAI) is immunologically identical to placental-type PAI-2." FEBS Lett **231**(1): 202-206.
Hibino, T., Y. Matsuda, et al. (1999). "Suppression of keratinocyte proliferation by plasminogen activator inhibitor-2." J Invest Dermatol **112**(1): 85-90.
Higgins, W. J., D. M. Fox, et al. (2010). "Heparin enhances serpin inhibition of the cysteine protease cathepsin L." J Biol Chem **285**(6): 3722-3729.
Hildenbrand, R., G. Wolf, et al. (1999). "Urokinase plasminogen activator receptor (CD87) expression of tumor-associated macrophages in ductal carcinoma in situ, breast cancer, and resident macrophages of normal breast tissue." J Leukoc Biol **66**(1): 40-49.
Hipp, M. S., S. H. Park, et al. (2014). "Proteostasis impairment in protein-misfolding and -aggregation diseases." Trends Cell Biol **24**(9): 506-514.
Hirst, C. E., M. S. Buzza, et al. (2003). "The intracellular granzyme B inhibitor, proteinase inhibitor 9, is up-regulated during accessory cell maturation and effector cell degranulation, and its overexpression enhances CTL potency." J Immunol **170**(2): 805-815.
Hook, V. Y., R. T. Purviance, et al. (1993). "Purification and characterization of alpha 1-antichymotrypsin-like protease inhibitor that regulates prohormone thiol protease involved in enkephalin precursor processing." J Biol Chem **268**(27): 20570-20577.
Horn, I. R., B. M. van den Berg, et al. (1998). "Plasminogen activator inhibitor 1 contains a cryptic high affinity receptor binding site that is exposed upon complex formation with tissue-type plasminogen activator." Thromb Haemost **80**(5): 822-828.
Horwitz, J., Q. L. Huang, et al. (1998). "Lens alpha-crystallin: chaperone-like properties." Methods Enzymol **290**: 365-383.
Hoyer-Hansen, G., U. Pessara, et al. (2001). "Urokinase-catalysed cleavage of the urokinase receptor requires an intact glycolipid anchor." Biochem J **358**(Pt 3): 673-679.
Hoylaerts, M., D. C. Rijken, et al. (1982). "Kinetics of the activation of plasminogen by human tissue plasminogen activator. Role of fibrin." J Biol Chem **257**(6): 2912-2919.
Hu, K., C. Wu, et al. (2007). "Tissue-type plasminogen activator promotes murine myofibroblast activation through LDL receptor-related protein 1-mediated integrin signaling." J Clin Invest **117**(12): 3821-3832.
Huai, Q., A. P. Mazar, et al. (2006). "Structure of human urokinase plasminogen activator in complex with its receptor." Science **311**(5761): 656-659.
Hudry, B., S. Viala, et al. (2011). "Visualization of protein interactions in living Drosophila embryos by the bimolecular fluorescence complementation assay." BMC Biol **9**: 5.

Humphreys, D. T., J. A. Carver, et al. (1999). "Clusterin has chaperone-like activity similar to that of small heat shock proteins." J Biol Chem **274**(11): 6875-6881.
Hunt, B. J., H. Missfelder-Lobos, et al. (2009). "Pregnancy outcome and fibrinolytic, endothelial markers and coagulation markers in women undergoing uterine artery Doppler screening at 23 weeks." J Thromb Haemost.
Hunt, L. T. and M. O. Dayhoff (1980). "A surprising new protein superfamily containing ovalbumin, antithrombin-III, and alpha 1-proteinase inhibitor." Biochem Biophys Res Commun **95**(2): 864-871.
Huntington, J. A., R. J. Read, et al. (2000). "Structure of a serpin-protease complex shows inhibition by deformation." Nature **407**(6806): 923-926.
Irving, J. A., R. N. Pike, et al. (2000). "Phylogeny of the serpin superfamily: implications of patterns of amino acid conservation for structure and function." Genome Res **10**(12): 1845-1864.
Ivarsson, M. L., L. Holmdahl, et al. (1998). "Characterization and fibrinolytic properties of mesothelial cells isolated from peritoneal lavage." Scand J Clin Lab Invest **58**(3): 195-203.
Iwata, A., B. E. Riley, et al. (2005). "HDAC6 and microtubules are required for autophagic degradation of aggregated huntingtin." J Biol Chem **280**(48): 40282-40292.
Jakob, U. and J. Buchner (1994). "Assisting spontaneity: the role of Hsp90 and small Hsps as molecular chaperones." Trends Biochem Sci **19**(5): 205-211.
Janciauskiene, S., H. Rubin, et al. (1998). "Alzheimer's peptide Abeta1-42 binds to two beta-sheets of alpha1-antichymotrypsin and transforms it from inhibitor to substrate." J Biol Chem **273**(43): 28360-28364.
Jang, W. G., H. S. Kim, et al. (2004). "Analysis of proteome and transcriptome of tumor necrosis factor alpha stimulated vascular smooth muscle cells with or without alpha lipoic acid." Proteomics **4**(11): 3383-3393.
Jankova, L., S. J. Harrop, et al. (2001). "Crystal structure of the complex of plasminogen activator inhibitor 2 with a peptide mimicking the reactive center loop." J Biol Chem **276**(46): 43374-43382.
Jarrett, J. T. and P. T. Lansbury, Jr. (1993). "Seeding "one-dimensional crystallization" of amyloid: a pathogenic mechanism in Alzheimer's disease and scrapie?" Cell **73**(6): 1055-1058.
Jayakumar, A., Y. Kang, et al. (2003). "Inhibition of the cysteine proteinases cathepsins K and L by the serpin headpin (SERPINB13): a kinetic analysis." Arch Biochem Biophys **409**(2): 367-374.
Jensen, P. H., L. I. Cressey, et al. (1994). "Cleaved intracellular plasminogen activator inhibitor 2 in human myeloleukaemia cells is a marker of apoptosis." Br J Cancer **70**(5): 834-840.
Jensen, P. H., K. E. Fladmark, et al. (1999). "Caspase I-related protease inhibition retards the execution of okadaic acid- and camptothecin-induced apoptosis and PAI-2 cleavage, but not commitment to cell death in HL-60 cells." Br J Cancer **79**(11-12): 1685-1691.

Jensen, P. H., T. G. Jensen, et al. (1996). "The exon 3 encoded sequence of the intracellular serine proteinase inhibitor plasminogen activator inhibitor 2 is a protein binding domain." J Biol Chem **271**(43): 26892-26899.

Jensen, P. H., E. Schuler, et al. (1994). "A unique interhelical insertion in plasminogen activator inhibitor-2 contains three glutamines, Gln83, Gln84, Gln86, essential for transglutaminase-mediated cross-linking." J Biol Chem **269**(21): 15394-15398.

Jensen, P. J., Q. Wu, et al. (1995). "Plasminogen activator inhibitor type 2: an intracellular keratinocyte differentiation product that is incorporated into the cornified envelope." Exp Cell Res **217**(1): 65-71.

Jorgensen, M., M. Philips, et al. (1987). "Plasminogen activator inhibitor-1 is the primary inhibitor of tissue-type plasminogen activator in pregnancy plasma." Thromb Haemost **58**(3): 872-878.

Kaczmarek, E., M. H. Lee, et al. (1993). "Initial interaction between fibrin and tissue plasminogen activator (t-PA). The Gly-Pro-Arg-Pro binding site on fibrin(ogen) is important for t-PA activity." J Biol Chem **268**(4): 2474-2479.

Kaganovich, D., R. Kopito, et al. (2008). "Misfolded proteins partition between two distinct quality control compartments." Nature **454**(7208): 1088-1095.

Kantyka, T., K. Plaza, et al. (2011). "Inhibition of Staphylococcus aureus cysteine proteases by human serpin potentially limits staphylococcal virulence." Biol Chem **392**(5): 483-489.

Katic, J., G. Loers, et al. (2014). "Interaction of the cell adhesion molecule CHL1 with vitronectin, integrins, and the plasminogen activator inhibitor-2 promotes CHL1-induced neurite outgrowth and neuronal migration." J Neurosci **34**(44): 14606-14623.

Katsikis, J., F. Maurer, et al. (2000). "The molecular basis for the aberrant production of plasminogen activator inhibitor type 2 in THP-1 monocytes." Thromb Haemost **84**: 468-473.

Kawamata, T., Y. Kamada, et al. (2008). "Organization of the pre-autophagosomal structure responsible for autophagosome formation." Mol Biol Cell **19**(5): 2039-2050.

Kawano, T., K. Morimoto, et al. (1968). "Urokinase inhibitor in human placenta." Nature **217**(5125): 253-254.

Kawano, T., K. Morimoto, et al. (1970). "Partial purification and properties of urokinase inhibitor from human placenta." J Biochem **67**(3): 333-342.

Kerppola, T. K. (2008). "Bimolecular fluorescence complementation (BiFC) analysis as a probe of protein interactions in living cells." Annu Rev Biophys **37**: 465-487.

Kerscher, O., R. Felberbaum, et al. (2006). "Modification of proteins by ubiquitin and ubiquitin-like proteins." Annu Rev Cell Dev Biol **22**: 159-180.

Kettern, N., M. Dreiseidler, et al. (2010). "Chaperone-assisted degradation: multiple paths to destruction." Biol Chem **391**(5): 481-489.

King, M. A., S. Hands, et al. (2008). "Rapamycin inhibits polyglutamine aggregation independently of autophagy by reducing protein synthesis." Mol Pharmacol **73**(4): 1052-1063.

Kinghorn, K. J., D. C. Crowther, et al. (2006). "Neuroserpin binds Abeta and is a neuroprotective component of amyloid plaques in Alzheimer disease." J Biol Chem **281**(39): 29268-29277.
Kinnby, B. (2002). "The plasminogen activating system in periodontal health and disease." Biol Chem **383**(1): 85-92.
Kiso, U., H. Kaudewitz, et al. (1988). "Determination of intermediates, products and cleavage site in the reaction between plasminogen activator inhibitor type-2 and urokinases." FEBS Lett **230**(1-2): 51-56.
Komiyama, T., C. A. Ray, et al. (1994). "Inhibition of interleukin-1 beta converting enzyme by the cowpox virus serpin CrmA. An example of cross-class inhibition." J Biol Chem **269**(30): 19331-19337.
Korcsmaros, T., I. A. Kovacs, et al. (2007). "Molecular chaperones: the modular evolution of cellular networks." J Biosci **32**(3): 441-446.
Krishnamurti, C. and B. Alving (1989). "Effect of dengue virus on procoagulant and fibrinolytic activities of monocytes." Rev Infect Dis **11 Suppl 4**: S843-846.
Krishnamurti, C., L. M. Wahl, et al. (1989). "Stimulation of plasminogen activator inhibitor activity in human monocytes infected with dengue virus." Am J Trop Med Hyg **40**(1): 102-107.
Kruithof, E. K., M. S. Baker, et al. (1995). "Biological and clinical aspects of plasminogen activator inhibitor type 2." Blood **86**(11): 4007-4024.
Kruithof, E. K. and E. Cousin (1988). "Plasminogen activator inhibitor 2. Isolation and characterization of the promoter region of the gene." Biochem Biophys Res Commun **156**(1): 383-388.
Kruithof, E. K., C. Tran-Thang, et al. (1987). "Fibrinolysis in pregnancy: a study of plasminogen activator inhibitors." Blood **69**(2): 460-466.
Kruithof, E. K., C. Tran-Thang, et al. (1984). "Demonstration of a fast-acting inhibitor of plasminogen activators in human plasma." Blood **64**(4): 907-913.
Kruithof, E. K., J. D. Vassalli, et al. (1986). "Purification and characterization of a plasminogen activator inhibitor from the histiocytic lymphoma cell line U-937." J Biol Chem **261**(24): 11207-11213.
Kuiper, J., M. Otter, et al. (1988). "Characterization of the interaction in vivo of tissue-type plasminogen activator with liver cells." J Biol Chem **263**(34): 18220-18224.
Kumar, S. and C. Baglioni (1991). "Protection from tumor necrosis factor-mediated cytolysis by overexpression of plasminogen activator inhibitor type-2." J Biol Chem **266**(31): 20960-20964.
Kumsta, C. and U. Jakob (2009). "Redox-regulated chaperones." Biochemistry **48**(22): 4666-4676.
Lanza, F., G. L. Castoldi, et al. (1998). "Expression and functional role of urokinase-type plasminogen activator receptor in normal and acute leukaemic cells." Br J Haematol **103**(1): 110-123.
Larsson, A. and B. Astedt (1985). "Immunohistochemical localisation of tissue plasminogen activator and urokinase in the vessel wall." J Clin Pathol **38**(2): 140-145.

Latha, K., W. Zhang, et al. (2005). "Maspin mediates increased tumor cell apoptosis upon induction of the mitochondrial permeability transition." Mol Cell Biol **25**(5): 1737-1748.
Law, R. H., Q. Zhang, et al. (2006). "An overview of the serpin superfamily." Genome Biol **7**(5): 216.
Leblond, J., M. H. Laprise, et al. (2006). "The serpin proteinase inhibitor 8: an endogenous furin inhibitor released from human platelets." Thromb Haemost **95**(2): 243-252.
Lee, J. A., B. J. Cochran, et al. (2011). "Forty years later and the role of plasminogen activator inhibitor type 2/SERPINB2 is still an enigma." Semin Thromb Hemost **37**(4): 395-407.
Lee, J. A., B. J. Cochran, et al. (2011). "Forty years on and the role of Plasminogen Activator Inhibitor Type–2/SERPINB2 is still an enigma. ." Seminars in Thrombosis and Haemostasis **In press**.
Lee, J. A., D. R. Croucher, et al. (2010). "Differential endocytosis of tissue plasminogen activator by serpins PAI-1 and PAI-2 on human peripheral blood monocytes." Thromb Haemost **104**(6): 1133-1142.
Lee, J. A., J. J. Yerbury, et al. (2015). "SerpinB2 (PAI-2) Modulates Proteostasis via Binding Misfolded Proteins and Promotion of Cytoprotective Inclusion Formation." PLoS One **10**(6): e0130136.
Leung, K. C., J. A. Byatt, et al. (1987). "Poly-D-lysine dependent inactivation of tissue plasminogen activator by a class PAI-2 inhibitor (minactivin)." Thromb Res **46**(6): 767-777.
Leung, K. C., J. A. Byatt, et al. (1987). "The resistance of fibrin-stimulated tissue plasminogen activator to inactivation by a class PAI-2 inhibitor (minactivin)." Thromb Res **46**(6): 755-766.
Li, J., L. Yu, et al. (2013). "Tissue plasminogen activator regulates Purkinje neuron development and survival." Proc Natl Acad Sci U S A **110**(26): E2410-2419.
Liang, X. H., L. K. Kleeman, et al. (1998). "Protection against fatal Sindbis virus encephalitis by beclin, a novel Bcl-2-interacting protein." J Virol **72**(11): 8586-8596.
Lijnen, H. R., L. Frederix, et al. (2007). "Deficiency of plasminogen activator inhibitor-2 impairs nutritionally induced murine adipose tissue development." J Thromb Haemost **5**(11): 2259-2265.
Lim, W., J. H. Kim, et al. (2011). "Avian SERPINB11 gene: characteristics, tissue-specific expression, and regulation of expression by estrogen." Biol Reprod **85**(6): 1260-1268.
Lindner, R. A., T. M. Treweek, et al. (2001). "The molecular chaperone alpha-crystallin is in kinetic competition with aggregation to stabilize a monomeric molten-globule form of alpha-lactalbumin." Biochem J **354**(Pt 1): 79-87.
Ling, Q., A. T. Jacovina, et al. (2004). "Annexin II regulates fibrin homeostasis and neoangiogenesis in vivo." J Clin Invest **113**(1): 38-48.
Liu, H. S., M. S. Jan, et al. (1999). "Is green fluorescent protein toxic to the living cells?" Biochem Biophys Res Commun **260**(3): 712-717.
Liu, J., S. Yin, et al. (2004). "Bax mediates the apoptosis-sensitizing effect of maspin." Cancer Res **64**(5): 1703-1711.

Ljungner, H., L. Holmberg, et al. (1983). "Immunological characterisation of plasminogen activators in the human vessel wall." J Clin Pathol **36**(9): 1046-1049.
Lobov, S., D. R. Croucher, et al. (2008). "Plasminogen activator inhibitor type 2 inhibits cell surface associated tissue plasminogen activator in vitro: potential receptor interactions." Thromb Haemost **100**(2): 319-329.
Lobov, S., M. Wilczynska, et al. (2004). "Structural bases of the redox-dependent conformational switch in the serpin PAI-2." J Mol Biol **344**(5): 1359-1368.
Loebermann, H., R. Tokuoka, et al. (1984). "Human alpha 1-proteinase inhibitor. Crystal structure analysis of two crystal modifications, molecular model and preliminary analysis of the implications for function." J Mol Biol **177**(3): 531-557.
Loeffler, J., Z. Haddad, et al. (2009). "Interaction analyses of human monocytes co-cultured with different forms of Aspergillus fumigatus." J Med Microbiol **58**(Pt 1): 49-58.
Losick, V. P. and R. R. Isberg (2006). "NF-kappaB translocation prevents host cell death after low-dose challenge by Legionella pneumophila." J Exp Med **203**(9): 2177-2189.
Loskutoff, D. J. and T. E. Edgington (1977). "Synthesis of a fibrinolytic activator and inhibitor by endothelial cells." Proc Natl Acad Sci U S A **74**(9): 3903-3907.
Lundgren, C. H., H. Sawa, et al. (1994). "Modulation of expression of monocyte/macrophage plasminogen activator activity and its implications for attenuation of vasculopathy." Circulation **90**(4): 1927-1934.
MacDonald, M., Ambrose, CM., Duyao, MP., Myers, RH., Lin, C., Srinidhi, L., Barnes, G., Taylor, SA., James, M., Groot N., et al (1993). "A novel gene containing a trinucleotide repeat that is expanded and unstable on Huntington's disease chromosomes. The Huntington's Disease Collaborative Research Group." Cell **72**(6): 971-983.
Mahony, D., B. Kalionis, et al. (1999). "Plasminogen activator inhibitor type-2 (PAI-2) gene transcription requires a novel NF-kappaB-like transcriptional regulatory motif." Eur J Biochem **263**(3): 765-772.
Martin, D. D., S. Ladha, et al. (2015). "Autophagy in Huntington disease and huntingtin in autophagy." Trends Neurosci **38**(1): 26-35.
Matsudomi, N. Y., Y. and Kobayashi, K. (1986). "Heat-induced Aggregation between Ovalbumin and Lysozyme." Agric. Biol. Chem. **50**(6): 1389-1395.
Matsudomi, N. Y., Y. and Kobayashi, K. (1987). "Aggregation between Lysozyme and Heat-denatured Ovalbumin." Agric. Biol. Chem. **51**(7): 1811-1817.
Maurer, F. and R. L. Medcalf (1996). "Plasminogen activator inhibitor type 2 gene induction by tumor necrosis factor and phorbol ester involves transcriptional and post-transcriptional events. Identification of a functional nonameric AU-rich motif in the 3'-untranslated region." J Biol Chem **271**(42): 26074-26080.
Maurer, F., M. Tierney, et al. (1999). "An AU-rich sequence in the 3'-UTR of plasminogen activator inhibitor type 2 (PAI-2) mRNA promotes PAI-2 mRNA decay and provides a binding site for nuclear HuR." Nucleic Acids Res **27**(7): 1664-1673.

McCarthy, J. J., A. Parker, et al. (2004). "Large scale association analysis for identification of genes underlying premature coronary heart disease: cumulative perspective from analysis of 111 candidate genes." J Med Genet **41**(5): 334-341.
McGeer, P. L. and E. G. McGeer (2002). "Innate immunity, local inflammation, and degenerative disease." Sci Aging Knowledge Environ **2002**(29): re3.
McWilliam, N., L. Robbie, et al. (1998). "Plasminogen activator in acute myeloid leukaemic marrows: u-PA in contrast to t-PA in normal marrow." Br J Haematol **101**(4): 626-631.
Medcalf, R. L. (1992). "Cell- and gene-specific interactions between signal transduction pathways revealed by okadaic acid. Studies on the plasminogen activating system." J Biol Chem **267**(17): 12220-12226.
Medcalf, R. L. (2011). "Plasminogen activator inhibitor type 2: still an enigmatic serpin but a model for gene regulation." Methods Enzymol **499**: 105-134.
Medcalf, R. L., E. K. Kruithof, et al. (1988). "Plasminogen activator inhibitor 1 and 2 are tumor necrosis factor/cachectin-responsive genes." J Exp Med **168**(2): 751-759.
Medcalf, R. L., E. Van den Berg, et al. (1988). "Glucocorticoid-modulated gene expression of tissue- and urinary-type plasminogen activator and plasminogen activator inhibitor 1 and 2." J Cell Biol **106**(3): 971-978.
Melchor, J. P., R. Pawlak, et al. (2003). "The tissue plasminogen activator-plasminogen proteolytic cascade accelerates amyloid-beta (Abeta) degradation and inhibits Abeta-induced neurodegeneration." J Neurosci **23**(26): 8867-8871.
Melchor, J. P. and S. Strickland (2005). "Tissue plasminogen activator in central nervous system physiology and pathology." Thromb Haemost **93**(4): 655-660.
Meshinchi, S. and R. J. Arceci (2007). "Prognostic factors and risk-based therapy in pediatric acute myeloid leukemia." Oncologist **12**(3): 341-355.
Mikus, P. and T. Ny (1996). "Intracellular polymerization of the serpin plasminogen activator inhibitor type 2." J Biol Chem **271**(17): 10048-10053.
Mikus, P., T. Urano, et al. (1993). "Plasminogen-activator inhibitor type 2 (PAI-2) is a spontaneously polymerising SERPIN. Biochemical characterisation of the recombinant intracellular and extracellular forms." Eur J Biochem **218**(3): 1071-1082.
Missen, M. A., D. Haylock, et al. (2006). "Stage specific gene expression of serpins and their cognate proteases during myeloid differentiation." Br J Haematol **135**(5): 715-724.
Miyata, T., R. Inagi, et al. (2002). "Overexpression of the serpin megsin induces progressive mesangial cell proliferation and expansion." J Clin Invest **109**(5): 585-593.
Miyata, T., M. Nangaku, et al. (1998). "A mesangium-predominant gene, megsin, is a new serpin upregulated in IgA nephropathy." J Clin Invest **102**(4): 828-836.
Montemurro, P., G. Barbuti, et al. (1999). "Retinoic acid stimulates plasminogen activator inhibitor 2 production by blood mononuclear cells and inhibits

urokinase-induced extracellular proteolysis." Br J Haematol **107**(2): 294-299.
Morimoto, R. I. (2008). "Proteotoxic stress and inducible chaperone networks in neurodegenerative disease and aging." Genes Dev **22**(11): 1427-1438.
Muchowski, P. J. and J. L. Wacker (2005). "Modulation of neurodegeneration by molecular chaperones." Nat Rev Neurosci **6**(1): 11-22.
Mulder, M., U. Kohnert, et al. (1997). "The interaction of recombinant tissue type plasminogen activator and recombinant plasminogen activator (r-PA/BM 06.022) with human endothelial cells." Blood Coagul Fibrinolysis **8**(2): 124-133.
Musci, G. and L. J. Berliner (1985). "Probing different conformational states of bovine alpha-lactalbumin: fluorescence studies with 4,4'-bis[1-(phenylamino)-8-naphthalenesulfonate]." Biochemistry **24**(15): 3852-3856.
Nakashima, H., T. Nguyen, et al. (2015). "Interferon-stimulated gene 15 (ISG15) and ISG15-linked proteins can associate with members of the selective autophagic process, histone deacetylase 6 (HDAC6) and SQSTM1/p62." J Biol Chem **290**(3): 1485-1495.
Nakatogawa, H., K. Suzuki, et al. (2009). "Dynamics and diversity in autophagy mechanisms: lessons from yeast." Nat Rev Mol Cell Biol **10**(7): 458-467.
Nalepa, G., M. Rolfe, et al. (2006). "Drug discovery in the ubiquitin-proteasome system." Nat Rev Drug Discov **5**(7): 596-613.
Nardai, G., E. M. Vegh, et al. (2006). "Chaperone-related immune dysfunction: an emergent property of distorted chaperone networks." Trends Immunol **27**(2): 74-79.
Netzer, W. J. and F. U. Hartl (1998). "Protein folding in the cytosol: chaperonin-dependent and -independent mechanisms." Trends Biochem Sci **23**(2): 68-73.
Nguyen, G., S. J. Self, et al. (1992). "Demonstration of a specific clearance receptor for tissue-type plasminogen activator on rat Novikoff hepatoma cells." J Biol Chem **267**(9): 6249-6256.
Niiya, K., T. Taniguchi, et al. (1994). "Different regulation of plasminogen activator inhibitor 2 gene expression by phorbol ester and cAMP in human myeloid leukemia cell line PL-21." Thromb Haemost **72**(1): 92-97.
Nollen, E. A., S. M. Garcia, et al. (2004). "Genome-wide RNA interference screen identifies previously undescribed regulators of polyglutamine aggregation." Proc Natl Acad Sci U S A **101**(17): 6403-6408.
Noorman, F., E. A. Braat, et al. (1995). "Degradation of tissue-type plasminogen activator by human monocyte-derived macrophages is mediated by the mannose receptor and by the low-density lipoprotein receptor-related protein." Blood **86**(9): 3421-3427.
Norris, E. H. and S. Strickland (2007). "Modulation of NR2B-regulated contextual fear in the hippocampus by the tissue plasminogen activator system." Proc Natl Acad Sci U S A **104**(33): 13473-13478.
O'Hara, A., A. Howarth, et al. (2013). "The role of proteasome beta subunits in gastrin-mediated transcription of plasminogen activator inhibitor-2 and regenerating protein1." PLoS One **8**(3): e59913.

Obiang, P., R. Macrez, et al. (2012). "GluN2D subunit-containing NMDA receptors control tissue plasminogen activator-mediated spatial memory." J Neurosci **32**(37): 12726-12734.
Odero-Marah, V. A., Z. Khalkhali-Ellis, et al. (2003). "Maspin regulates different signaling pathways for motility and adhesion in aggressive breast cancer cells." Cancer Biol Ther **2**(4): 398-403.
Ogbourne, S. M. and T. M. Antalis (2001). "Characterisation of PAUSE-1, a powerful silencer in the human plasminogen activator inhibitor type 2 gene promoter." Nucleic Acids Res **29**(19): 3919-3927.
Ogrodnik, M., H. Salmonowicz, et al. (2014). "Dynamic JUNQ inclusion bodies are asymmetrically inherited in mammalian cell lines through the asymmetric partitioning of vimentin." Proc Natl Acad Sci U S A **111**(22): 8049-8054.
Oh, S. B., C. J. Byun, et al. (2014). "Tissue plasminogen activator arrests Alzheimer's disease pathogenesis." Neurobiol Aging **35**(3): 511-519.
Ohba, K., Y. Miyata, et al. (2005). "Expression of urokinase-type plasminogen activator, urokinase-type plasminogen activator receptor and plasminogen activator inhibitors in patients with renal cell carcinoma: correlation with tumor associated macrophage and prognosis." J Urol **174**(2): 461-465.
Ohtomo, S., M. Nangaku, et al. (2008). "The role of megsin, a serine protease inhibitor, in diabetic mesangial matrix accumulation." Kidney Int **74**(6): 768-774.
Olshina, M. A., L. M. Angley, et al. (2010). "Tracking mutant huntingtin aggregation kinetics in cells reveals three major populations that include an invariant oligomer pool." J Biol Chem **285**(28): 21807-21816.
Ong, K., W. Horsfall, et al. (2000). "Early embryonic expression of murine coagulation system components." Thromb Haemost **84**(6): 1023-1030.
Orth, K., E. L. Madison, et al. (1992). "Complexes of tissue-type plasminogen activator and its serpin inhibitor plasminogen-activator inhibitor type 1 are internalized by means of the low density lipoprotein receptor-related protein/alpha 2-macroglobulin receptor." Proc Natl Acad Sci U S A **89**(16): 7422-7426.
Otter, M., M. M. Barrett-Bergshoeff, et al. (1991). "Binding of tissue-type plasminogen activator by the mannose receptor." J Biol Chem **266**(21): 13931-13935.
Palafox-Sanchez, C. A., M. Vazquez-Del Mercado, et al. (2009). "A functional Ser(413)/Ser(413) PAI-2 polymorphism is associated with susceptibility and damage index score in systemic lupus erythematosus." Clin Appl Thromb Hemost **15**(2): 233-238.
Park, J. M., F. R. Greten, et al. (2005). "Signaling pathways and genes that inhibit pathogen-induced macrophage apoptosis--CREB and NF-kappaB as key regulators." Immunity **23**(3): 319-329.
Pattingre, S., A. Tassa, et al. (2005). "Bcl-2 antiapoptotic proteins inhibit Beclin 1-dependent autophagy." Cell **122**(6): 927-939.
Pemberton, P. A., P. E. Stein, et al. (1988). "Hormone binding globulins undergo serpin conformational change in inflammation." Nature **336**(6196): 257-258.

Pennica, D., W. E. Holmes, et al. (1983). "Cloning and expression of human tissue-type plasminogen activator cDNA in E. coli." Nature **301**(5897): 214-221.
Peters, J. M., Z. Cejka, et al. (1993). "Structural features of the 26 S proteasome complex." J Mol Biol **234**(4): 932-937.
Piquette, G. N., M. E. Crabtree, et al. (1993). "Regulation of plasminogen activator inhibitor-1 and -2 messenger ribonucleic acid levels in human cumulus and granulosa-luteal cells." J Clin Endocrinol Metab **76**(2): 518-523.
Plesner, T., N. Behrendt, et al. (1997). "Structure, function and expression on blood and bone marrow cells of the urokinase-type plasminogen activator receptor, uPAR." Stem Cells **15**(6): 398-408.
Polling, S., Y. F. Mok, et al. (2014). "Misfolded polyglutamine, polyalanine, and superoxide dismutase 1 aggregate via distinct pathways in the cell." J Biol Chem **289**(10): 6669-6680.
Poon, S., M. S. Rybchyn, et al. (2002). "Mildly acidic pH activates the extracellular molecular chaperone clusterin." J Biol Chem **277**(42): 39532-39540.
Przygodzka, P., B. Ramstedt, et al. (2010). "Bomapin is a redox-sensitive nuclear serpin that affects responsiveness of myeloid progenitor cells to growth environment." BMC Cell Biol **11**: 30.
Pytel, B. A., K. Peppel, et al. (1990). "Plasminogen activator inhibitor type-2 is a major protein induced in human fibroblasts and SK-MEL-109 melanoma cells by tumor necrosis factor." J Cell Physiol **144**(3): 416-422.
Ragno, P., N. Montuori, et al. (1995). "Urokinase-type plasminogen activator/type-2 plasminogen-activator inhibitor complexes are not internalized upon binding to the urokinase-type-plasminogen-activator receptor in THP-1 cells. Interaction of urokinase-type plasminogen activator/type-2 plasminogen-activator inhibitor complexes with the cell surface." Eur J Biochem **233**(2): 514-519.
Ramdzan, Y. M., R. M. Nisbet, et al. (2010). "Conformation sensors that distinguish monomeric proteins from oligomers in live cells." Chem Biol **17**(4): 371-379.
Ranson, M. and N. M. Andronicos (2003). "Plasminogen binding and cancer: promises and pitfalls." Front Biosci **8**: s294-304.
Ranson, M., N. M. Andronicos, et al. (1998). "Increased Plasminogen binding is associated with metastatic breast cancer cells: differential expression of plasminogen binding proteins." Br J Cancer **77**(10): 1586-1597.
Ranson, M., P. Berghofer, et al. (2012). "Different radiolabelling methods alter the pharmacokinetic and biodistribution properties of plasminogen activator inhibitor type 2 (PAI-2) forms." Nucl Med Biol **39**(6): 833-839.
Rasch, M. G., I. K. Lund, et al. (2008). "Intact and cleaved uPAR forms: diagnostic and prognostic value in cancer." Front Biosci **13**: 6752-6762.
Reijerkerk, A., G. Kooij, et al. (2008). "Tissue-type plasminogen activator is a regulator of monocyte diapedesis through the brain endothelial barrier." J Immunol **181**(5): 3567-3574.
Remold-O'Donnell, E. (1993). "The ovalbumin family of serpin proteins." FEBS Lett **315**(2): 105-108.

Remold-O'Donnell, E., J. Chin, et al. (1992). "Sequence and molecular characterization of human monocyte/neutrophil elastase inhibitor." Proc Natl Acad Sci U S A **89**(12): 5635-5639.

Riewald, M., T. Chuang, et al. (1998). "Expression of bomapin, a novel human serpin, in normal/malignant hematopoiesis and in the monocytic cell lines THP-1 and AML-193." Blood **91**(4): 1256-1262.

Rijken, D. C. and D. Collen (1981). "Purification and characterization of the plasminogen activator secreted by human melanoma cells in culture." J Biol Chem **256**(13): 7035-7041.

Ritchie, H. and N. A. Booth (1998). "The distribution of the secreted and intracellular forms of plasminogen activator inhibitor 2 (PAI-2) in human peripheral blood monocytes is modulated by serum." Thromb Haemost **79**(4): 813-817.

Ritchie, H., A. Jamieson, et al. (1995). "Thrombin modulates synthesis of plasminogen activator inhibitor type 2 by human peripheral blood monocytes." Blood **86**(9): 3428-3435.

Ritchie, H., A. Jamieson, et al. (1997). "Regulation, location and activity of plasminogen activator inhibitor 2 (PAI-2) in peripheral blood monocytes, macrophages and foam cells." Thromb Haemost **77**(6): 1168-1173.

Ritchie, H., L. C. Lawrie, et al. (2001). "Characterization of crosslinking sites in fibrinogen for plasminogen activator inhibitor 2 (PAI-2)." Ann N Y Acad Sci **936**: 215-218.

Ritchie, H., L. A. Robbie, et al. (1999). "Monocyte plasminogen activator inhibitor 2 (PAI-2) inhibits u-PA-mediated fibrin clot lysis and is cross-linked to fibrin." Thromb Haemost **81**(1): 96-103.

Romani, A. A., P. Soliani, et al. (2006). "The associated expression of Maspin and Bax proteins as a potential prognostic factor in intrahepatic cholangiocarcinoma." BMC Cancer **6**: 255.

Rozemuller, J. M., J. J. Abbink, et al. (1991). "Distribution pattern and functional state of alpha 1-antichymotrypsin in plaques and vascular amyloid in Alzheimer's disease. A immunohistochemical study with monoclonal antibodies against native and inactivated alpha 1-antichymotrypsin." Acta Neuropathol **82**(3): 200-207.

Ruiz, J., D. Kouiavskaia, et al. (2005). "The apoE isoform binding properties of the VLDL receptor reveal marked differences from LRP and the LDL receptor." J Lipid Res **46**(8): 1721-1731.

Sauk, J. J., N. Nikitakis, et al. (2005). "Hsp47 a novel collagen binding serpin chaperone, autoantigen and therapeutic target." Front Biosci **10**: 107-118.

Saunders, D. N., L. Jankova, et al. (2001). "Interaction between the P14 residue and strand 2 of beta-sheet B is critical for reactive center loop insertion in plasminogen activator inhibitor-2." J Biol Chem **276**(46): 43383-43389.

Scarff, K. L., K. S. Ung, et al. (2004). "Targeted disruption of SPI3/Serpinb6 does not result in developmental or growth defects, leukocyte dysfunction, or susceptibility to stroke." Mol Cell Biol **24**(9): 4075-4082.

Scheffner, M., K. Munger, et al. (1992). "Targeted degradation of the retinoblastoma protein by human papillomavirus E7-E6 fusion proteins." EMBO J **11**(7): 2425-2431.
Scherrer, A., A. Wohlwend, et al. (1999). "Plasminogen activation in human acute leukaemias." Br J Haematol **105**(4): 920-927.
Schick, C., D. Bromme, et al. (1998). "The reactive site loop of the serpin SCCA1 is essential for cysteine proteinase inhibition." Proc Natl Acad Sci U S A **95**(23): 13465-13470.
Schick, C., Y. Kamachi, et al. (1997). "Squamous cell carcinoma antigen 2 is a novel serpin that inhibits the chymotrypsin-like proteinases cathepsin G and mast cell chymase." J Biol Chem **272**(3): 1849-1855.
Schick, C., P. A. Pemberton, et al. (1998). "Cross-class inhibition of the cysteine proteinases cathepsins K, L, and S by the serpin squamous cell carcinoma antigen 1: a kinetic analysis." Biochemistry **37**(15): 5258-5266.
Schleuning, W. D., R. L. Medcalf, et al. (1987). "Plasminogen activator inhibitor 2: regulation of gene transcription during phorbol ester-mediated differentiation of U-937 human histiocytic lymphoma cells." Mol Cell Biol **7**(12): 4564-4567.
Schroder, M. and R. J. Kaufman (2005). "The mammalian unfolded protein response." Annu Rev Biochem **74**: 739-789.
Schroder, W. A., J. Gardner, et al. (2010). "SerpinB2 deficiency modulates Th1Th2 responses after schistosome infection." Parasite Immunol **32**(11-12): 764-768.
Schroder, W. A., T. T. Le, et al. (2010). "A Physiological Function of Inflammation-Associated SerpinB2 Is Regulation of Adaptive Immunity." J Immunol **184**(5): 2663-2670.
Schroder, W. A., L. D. Major, et al. (2014). "Tumor cell-expressed SerpinB2 is present on microparticles and inhibits metastasis." Cancer Med **3**(3): 500-513.
Schubert, D. (1997). "Serpins inhibit the toxicity of amyloid peptides." Eur J Neurosci **9**(4): 770-777.
Schuster, W. A., R. L. Medcalf, et al. (1993). "Retinoic acid potentiates phorbol ester-mediated induction of urokinase and plasminogen activator inhibitor type 2 in human myeloid leukemic cell lines." Endocrinology **133**(4): 1724-1730.
Schuster, W. A., R. L. Medcalf, et al. (1994). "Localization and characterisation of a retinoic acid response-like element in the plasminogen activator inhibitor-2 gene promoter." Fibrinolysis **8**: 113-119.
Schwartz, B. S. (1994). "Differential inhibition of soluble and cell surface receptor-bound single-chain urokinase by plasminogen activator inhibitor type 2. A potential regulatory mechanism." J Biol Chem **269**(11): 8319-8323.
Schwartz, B. S. and J. D. Bradshaw (1992). "Regulation of plasminogen activator inhibitor mRNA levels in lipopolysaccharide-stimulated human monocytes. Correlation with production of the protein." J Biol Chem **267**(10): 7089-7094.
Scott, F. L., H. J. Eyre, et al. (1999). "Human ovalbumin serpin evolution: phylogenic analysis, gene organization, and identification of new PI8-

related genes suggest that two interchromosomal and several intrachromosomal duplications generated the gene clusters at 18q21-q23 and 6p25." Genomics **62**(3): 490-499.
Scott, F. L., C. E. Hirst, et al. (1999). "The intracellular serpin proteinase inhibitor 6 is expressed in monocytes and granulocytes and is a potent inhibitor of the azurophilic granule protease, cathepsin G." Blood **93**(6): 2089-2097.
Seeds, N. W., M. E. Basham, et al. (2003). "Absence of tissue plasminogen activator gene or activity impairs mouse cerebellar motor learning." J Neurosci **23**(19): 7368-7375.
Seglen, P. O. and P. B. Gordon (1982). "3-Methyladenine: specific inhibitor of autophagic/lysosomal protein degradation in isolated rat hepatocytes." Proc Natl Acad Sci U S A **79**(6): 1889-1892.
Sekine, H., J. Mimura, et al. (2009). "Hypersensitivity of aryl hydrocarbon receptor-deficient mice to lipopolysaccharide-induced septic shock." Mol Cell Biol **29**(24): 6391-6400.
Seo, E. Y., Y. J. Piao, et al. (2002). "Identification of calcium-induced genes in HaCaT keratinocytes by polymerase chain reaction-based subtractive hybridization." Arch Dermatol Res **294**(9): 411-418.
Sharon, R., R. Abramovitz, et al. (2002). "Plasminogen mRNA induction in the mouse brain after kainate excitation: codistribution with plasminogen activator inhibitor-2 (PAI-2) mRNA." Brain Res Mol Brain Res **104**(2): 170-175.
Shea-Donohue, T., A. Zhao, et al. (2014). "SerpinB2 mediated regulation of macrophage function during enteric infection." Gut Microbes **5**(2): 254-258.
Shi, H. Y., L. J. Stafford, et al. (2007). "Maspin controls mammary tumor cell migration through inhibiting Rac1 and Cdc42, but not the RhoA GTPase." Cell Motil Cytoskeleton **64**(5): 338-346.
Shioji, G., Y. Ezura, et al. (2005). "Nucleotide variations in genes encoding plasminogen activator inhibitor-2 and serine proteinase inhibitor B10 associated with prostate cancer." J Hum Genet **50**(10): 507-515.
Siefert, S. A., C. Chabasse, et al. (2014). "Enhanced venous thrombus resolution in plasminogen activator inhibitor type-2 deficient mice." J Thromb Haemost **12**(10): 1706-1716.
Silverman, G. A., P. I. Bird, et al. (2001). "The serpins are an expanding superfamily of structurally similar but functionally diverse proteins. Evolution, mechanism of inhibition, novel functions, and a revised nomenclature." J Biol Chem **276**(36): 33293-33296.
Silverman, G. A., J. I. Jockel, et al. (1991). "Yeast artificial chromosome cloning of a two-megabase-size contig within chromosomal band 18q21 establishes physical linkage between BCL2 and plasminogen activator inhibitor type-2." Genomics **9**(2): 219-228.
Silverman, G. A., J. C. Whisstock, et al. (2010). "Serpins flex their muscle: I. Putting the clamps on proteolysis in diverse biological systems." J Biol Chem **285**(32): 24299-24305.
Simon, D. I., H. Xu, et al. (1995). "Cathepsin D-like aspartyl protease activity mediates the degradation of tissue-type plasminogen

activator/plasminogen activator inhibitor-1 complexes in human monocytes." Biochim Biophys Acta **1268**(2): 143-151.
Sirmaci, A., S. Erbek, et al. (2010). "A truncating mutation in SERPINB6 is associated with autosomal-recessive nonsyndromic sensorineural hearing loss." Am J Hum Genet **86**(5): 797-804.
Skeldal, S., J. V. Larsen, et al. (2006). "Binding areas of urokinase-type plasminogen activator-plasminogen activator inhibitor-1 complex for endocytosis receptors of the low-density lipoprotein receptor family, determined by site-directed mutagenesis." Febs J **273**(22): 5143-5159.
Soo, K. S., A. D. Northeast, et al. (1996). "Tissue plasminogen activator production by monocytes in venous thrombolysis." J Pathol **178**(2): 190-194.
Springhetti, E. M., N. E. Istomina, et al. (2003). "Role of the M-loop and reactive center loop domains in the folding and bridging of nucleosome arrays by MENT." J Biol Chem **278**(44): 43384-43393.
Stefansson, S., S. Muhammad, et al. (1998). "Plasminogen activator inhibitor-1 contains a cryptic high affinity binding site for the low density lipoprotein receptor-related protein." J Biol Chem **273**(11): 6358-6366.
Stein, P. E. and R. W. Carrell (1995). "What do dysfunctional serpins tell us about molecular mobility and disease?" Nat Struct Biol **2**(2): 96-113.
Strickland, D. K., S. L. Gonias, et al. (2002). "Diverse roles for the LDL receptor family." Trends Endocrinol Metab **13**(2): 66-74.
Strik, M. C., B. A. Bladergroen, et al. (2002). "Distribution of the human intracellular serpin protease inhibitor 8 in human tissues." J Histochem Cytochem **50**(11): 1443-1454.
Stringer, B., E. A. Udofa, et al. (2012). "Regulation of the human plasminogen activator inhibitor type 2 gene: cooperation of an upstream silencer and transactivator." J Biol Chem **287**(13): 10579-10589.
Stutchbury, T. K., F. Al-Ejeh, et al. (2007). "Preclinical evaluation of 213Bi-labeled plasminogen activator inhibitor type 2 in an orthotopic murine xenogenic model of human breast carcinoma." Mol Cancer Ther **6**(1): 203-212.
Sugimoto, Y., Y. Kamada, et al. (2011). "Aggregates with lysozyme and ovalbumin show features of amyloid-like fibrils." Biochem Cell Biol **89**(6): 533-544.
Sun, J., C. H. Bird, et al. (1996). "A cytosolic granzyme B inhibitor related to the viral apoptotic regulator cytokine response modifier A is present in cytotoxic lymphocytes." J Biol Chem **271**(44): 27802-27809.
Sutter, T. R., K. Guzman, et al. (1991). "Targets for dioxin: genes for plasminogen activator inhibitor-2 and interleukin-1 beta." Science **254**(5030): 415-418.
Suzuki, K., Y. Kubota, et al. (2007). "Hierarchy of Atg proteins in pre-autophagosomal structure organization." Genes Cells **12**(2): 209-218.
Suzuki, T., S. Hashimoto, et al. (2000). "Comprehensive gene expression profile of LPS-stimulated human monocytes by SAGE." Blood **96**(7): 2584-2591.
Swartz, J. M., J. Bystrom, et al. (2004). "Plasminogen activator inhibitor-2 (PAI-2) in eosinophilic leukocytes." J Leukoc Biol **76**(4): 812-819.
Syrjanen, S., P. Naud, et al. (2009). "Up-regulation of plasminogen activator inhibitor-2 is associated with high-risk HPV and grade of cervical lesion at

baseline but does not predict outcomes of high-risk HPV infections or incident CIN." Am J Clin Pathol **132**(6): 883-892.
Szymczak, A. L., C. J. Workman, et al. (2004). "Correction of multi-gene deficiency in vivo using a single 'self-cleaving' 2A peptide-based retroviral vector." Nat Biotechnol **22**(5): 589-594.
Takahashi, T., S. Kikuchi, et al. (2008). "Soluble polyglutamine oligomers formed prior to inclusion body formation are cytotoxic." Hum Mol Genet **17**(3): 345-356.
Takeda, A., T. Yamamoto, et al. (1995). "Squamous cell carcinoma antigen is a potent inhibitor of cysteine proteinase cathepsin L." FEBS Lett **359**(1): 78-80.
Tasab, M., M. R. Batten, et al. (2000). "Hsp47: a molecular chaperone that interacts with and stabilizes correctly-folded procollagen." EMBO J **19**(10): 2204-2211.
Teoh, S. S., J. C. Whisstock, et al. (2010). "Maspin (SERPINB5) is an obligate intracellular serpin." J Biol Chem **285**(14): 10862-10869.
Thorsen, S., M. Philips, et al. (1988). "Kinetics of inhibition of tissue-type and urokinase-type plasminogen activator by plasminogen-activator inhibitor type 1 and type 2." Eur J Biochem **175**(1): 33-39.
Tierney, M. J. and R. L. Medcalf (2001). "Plasminogen activator inhibitor type 2 contains mRNA instability elements within exon 4 of the coding region. Sequence homology to coding region instability determinants in other mRNAs." J Biol Chem **276**(17): 13675-13684.
Tompa, P. and P. Csermely (2004). "The role of structural disorder in the function of RNA and protein chaperones." Faseb j **18**(11): 1169-1175.
Tonnetti, L., S. Netzel-Arnett, et al. (2008). "SerpinB2 protection of retinoblastoma protein from calpain enhances tumor cell survival." Cancer Res **68**(14): 5648-5657.
Tyedmers, J., A. Mogk, et al. (2010). "Cellular strategies for controlling protein aggregation." Nat Rev Mol Cell Biol **11**(11): 777-788.
Udofa, E. A., B. W. Stringer, et al. (2013). "The transcription factor C/EBP-beta mediates constitutive and LPS-inducible transcription of murine SerpinB2." PLoS One **8**(3): e57855.
van den Berg, E. A., E. le Clercq, et al. (1990). "The human gene for plasminogen activator inhibitor 2 (PAI2) exhibits an EcoRI RFLP." Nucleic Acids Res **18**(9): 2837.
van Gent, D., P. Sharp, et al. (2003). "Serpins: structure, function and molecular evolution." Int J Biochem Cell Biol **35**(11): 1536-1547.
van Zonneveld, A. J., H. Veerman, et al. (1986). "On the interaction of the finger and the kringle-2 domain of tissue-type plasminogen activator with fibrin. Inhibition of kringle-2 binding to fibrin by epsilon-amino caproic acid." J Biol Chem **261**(30): 14214-14218.
Varro, A., E. Hemers, et al. (2002). "Identification of plasminogen activator inhibitor-2 as a gastrin-regulated gene: Role of Rho GTPase and menin." Gastroenterology **123**(1): 271-280.

Vassalli, J. D., A. Wohlwend, et al. (1992). "Urokinase-catalyzed plasminogen activation at the monocyte/macrophage cell surface: a localized and regulated proteolytic system." Curr Top Microbiol Immunol **181**: 65-86.

Vazquez-Del Mercado, M., T. A. Garcia-Cobian, et al. (2007). "Genotype Ser413/Ser of PAI-2 polymorphism Ser413/Cys is associated with anti-phospholipid syndrome and systemic lupus erythematosus in a familial case: comparison with healthy controls." Scand J Rheumatol **36**(3): 206-210.

Verhoef, L. G., K. Lindsten, et al. (2002). "Aggregate formation inhibits proteasomal degradation of polyglutamine proteins." Hum Mol Genet **11**(22): 2689-2700.

Vine, K. L., V. I. Chandran, et al. (2012). "Targeting urokinase and the transferrin receptor with novel, anti-mitotic N-alkylisatin cytotoxin conjugates causes selective cancer cell death and reduces tumor growth." Curr Cancer Drug Targets **12**(1): 64-73.

Vine, K. L., V. Indira Chandran, et al. (2012). "Targeting urokinase and the transferrin receptor with novel, anti-mitotic N-alkylisatin cytotoxin conjugates causes selective cancer cell death and reduces tumor growth." Curr Cancer Drug Targets **12**(1): 64-73.

Virtanen, O. J., V. Siren, et al. (2006). "Plasminogen activators and their inhibitors in human saliva and salivary gland tissue." Eur J Oral Sci **114**(1): 22-26.

von Heijne, G., P. Liljestrom, et al. (1991). "The efficiency of the uncleaved secretion signal in the plasminogen activator inhibitor type 2 protein can be enhanced by point mutations that increase its hydrophobicity." J Biol Chem **266**(23): 15240-15243.

Wada, H., T. Kaneko, et al. (1994). "Effect of lipoproteins on tissue factor activity and PAI-II antigen in human monocytes and macrophages." Int J Cardiol **47**(1 Suppl): S21-25.

Wada, H., Y. Kumeda, et al. (1993). "Plasminogen activators and their inhibitors in leukemic cell homogenates." Am J Hematol **42**(2): 166-170.

Waelter, S., A. Boeddrich, et al. (2001). "Accumulation of mutant huntingtin fragments in aggresome-like inclusion bodies as a result of insufficient protein degradation." Mol Biol Cell **12**(5): 1393-1407.

Walker, D. G., J. Link, et al. (2006). "Gene expression changes by amyloid beta peptide-stimulated human postmortem brain microglia identify activation of multiple inflammatory processes." J Leukoc Biol **79**(3): 596-610.

Wang, L., Q. Li, et al. (2013). "Identification of SERPINB1 as a physiological inhibitor of human granzyme H." J Immunol **190**(3): 1319-1330.

Wang, Y. and P. J. Jensen (1998). "Regulation of the level and glycosylation state of plasminogen activator inhibitor type 2 during human keratinocyte differentiation." Differentiation **63**(2): 93-99.

Webb, G., M. S. Baker, et al. (1994). "Chromosomal localization of the human urokinase plasminogen activator receptor and plasminogen activator inhibitor type-2 genes: implications in colorectal cancer." J Gastroenterol Hepatol **9**(4): 340-343.

Weisberg, S. J., R. Lyakhovetsky, et al. (2012). "Compartmentalization of superoxide dismutase 1 (SOD1G93A) aggregates determines their toxicity." Proc Natl Acad Sci U S A **109**(39): 15811-15816.
Welss, T., J. Sun, et al. (2003). "Hurpin is a selective inhibitor of lysosomal cathepsin L and protects keratinocytes from ultraviolet-induced apoptosis." Biochemistry **42**(24): 7381-7389.
Westermark, P., M. D. Benson, et al. (2007). "A primer of amyloid nomenclature." Amyloid **14**(3): 179-183.
Westphal, U. (1986). "Steroid-protein interactions II." Monogr Endocrinol **27**: 1-603.
Whisstock, J. C. and S. P. Bottomley (2008). "Structural biology: Serpins' mystery solved." Nature **455**(7217): 1189-1190.
Whisstock, J. C., G. A. Silverman, et al. (2010). "Serpins flex their muscle: II. Structural insights into target peptidase recognition, polymerization, and transport functions." J Biol Chem **285**(32): 24307-24312.
Wilczynska, M., S. Lobov, et al. (2003). "The spontaneous polymerization of plasminogen activator inhibitor type-2 and Z-antitrypsin are due to different molecular aberrations." FEBS Lett **537**(1-3): 11-16.
Wilczynska, M., S. Lobov, et al. (2003). "A redox-sensitive loop regulates plasminogen activator inhibitor type 2 (PAI-2) polymerization." Embo J **22**(8): 1753-1761.
Williams, A., S. Sarkar, et al. (2008). "Novel targets for Huntington's disease in an mTOR-independent autophagy pathway." Nat Chem Biol **4**(5): 295-305.
Wing, L. R., G. M. Hawksworth, et al. (1991). "Clearance of t-PA, PAI-1, and t-PA-PAI-1 complex in an isolated perfused rat liver system." J Lab Clin Med **117**(2): 109-114.
Wohlwend, A., D. Belin, et al. (1987). "Plasminogen activator-specific inhibitors produced by human monocytes/macrophages." J Exp Med **165**(2): 320-339.
Wojta, J., R. L. Hoover, et al. (1989). "Vascular origin determines plasminogen activator expression in human endothelial cells. Renal endothelial cells produce large amounts of single chain urokinase type plasminogen activator." J Biol Chem **264**(5): 2846-2852.
Woodruff, P. G., H. A. Boushey, et al. (2007). "Genome-wide profiling identifies epithelial cell genes associated with asthma and with treatment response to corticosteroids." Proc Natl Acad Sci U S A **104**(40): 15858-15863.
Xia, Y., Y. Zhang, et al. (2011). "Overexpression of megsin induces mesangial cell proliferation and excretion of type IV collagen in vitro." Cell Immunol **271**(2): 413-417.
Xiao, Y. and P. M. Bartold (2004). "Modulating effect of serum on the stimulation of plasminogen activator inhibitor 2 production in human gingival fibroblasts by lipopolysaccharide and interleukin-1beta." J Int Acad Periodontol **6**(3): 81-88.
Yamanaka, H., K. Obata, et al. (2005). "Induction of plasminogen activator inhibitor-1 and -2 in dorsal root ganglion neurons after peripheral nerve injury." Neuroscience **132**(1): 183-191.

Ye, R. D., T. C. Wun, et al. (1988). "Mammalian protein secretion without signal peptide removal. Biosynthesis of plasminogen activator inhibitor-2 in U-937 cells." J Biol Chem **263**(10): 4869-4875.
Ye, S., A. L. Cech, et al. (2001). "The structure of a Michaelis serpin-protease complex." Nat Struct Biol **8**(11): 979-983.
Yepes, M., M. Sandkvist, et al. (2003). "Tissue-type plasminogen activator induces opening of the blood-brain barrier via the LDL receptor-related protein." J Clin Invest **112**(10): 1533-1540.
Yerbury, J. J., S. Poon, et al. (2007). "The extracellular chaperone clusterin influences amyloid formation and toxicity by interacting with prefibrillar structures." FASEB J **21**(10): 2312-2322.
Yu, H., S. Stasinopoulos, et al. (2003). "Inherent instability of plasminogen activator inhibitor type 2 mRNA is regulated by tristetraprolin." J Biol Chem **278**(16): 13912-13918.
Zhang, M., S. M. Park, et al. (2006). "Serine protease inhibitor 6 protects cytotoxic T cells from self-inflicted injury by ensuring the integrity of cytotoxic granules." Immunity **24**(4): 451-461.
Zhang, S., L. Zou, et al. (2015). "The sGC activator inhibits the proliferation and migration, promotes the apoptosis of human pulmonary arterial smooth muscle cells via the up regulation of plasminogen activator inhibitor-2." Exp Cell Res **332**(2): 278-287.
Zhang, S. J., M. Zou, et al. (2009). "Nuclear calcium signaling controls expression of a large gene pool: identification of a gene program for acquired neuroprotection induced by synaptic activity." PLoS Genet **5**(8): e1000604.
Zhang, Y. Q., P. Li, et al. (2003). "Identification of interaction between PAI-2 and IRF-3." Sheng Wu Hua Xue Yu Sheng Wu Wu Li Xue Bao (Shanghai) **35**(7): 661-665.
Zhao, A., Z. Yang, et al. (2013). "SerpinB2 is critical to Th2 immunity against enteric nematode infection." J Immunol **190**(11): 5779-5787.
Zheng, B., Y. Matoba, et al. (2009). "Crystal structure of SCCA1 and insight about the interaction with JNK1." Biochem Biophys Res Commun **380**(1): 143-147.
Zhou, H. M., I. Bolon, et al. (2001). "Overexpression of plasminogen activator inhibitor type 2 in basal keratinocytes enhances papilloma formation in transgenic mice." Cancer Res **61**(3): 970-976.
Zsila, F. (2010). "Inhibition of heat- and chemical-induced aggregation of various proteins reveals chaperone-like activity of the acute-phase component and serine protease inhibitor human alpha(1)-antitrypsin." Biochem Biophys Res Commun **393**(2): 242-247.

8. Appendix

8.1. Buffers

10x PBS

NaCl	80 $g.L^{-1}$
KCl	2 $g.L^{-1}$
Na_2HPO_4	14.4 $g.L^{-1}$
KH_2PO_4	2.4 $g.L^{-1}$

Adjust pH as required. Dilute 1 in 10 before use.

10x TBS

Tris-Base	500 mM
NaCl	1500 mM

Adjust pH as required. Dilute 1 in 10 before use.

TBST

1x TBS (As above)

Tween 20	500 $\mu L.L^{-1}$

Binding Buffer

Hanks modified buffered salt	9.7 $g.L^{-1}$
4-(2-hydroxyethyl)-1-piperazineethanesulfonic acid (HEPES)	4.8 $g.L^{-1}$
$CaCl_2$	1 mM
$MgCl_2$	1 mM

BSA	1 $g.L^{-1}$

Adjust pH to 7.4.

5x SDS PAGE Sample Buffer (non-reducing)

Tris-HCl	60 mM
Glycerol	10% W/V
SDS	2% W/V
Bromophenol Blue	0.01% W/V

RPMI 1640 Growth Media

RPMI	10.4 $g.L^{-1}$
$NaHCO_3$	2 $g.L^{-1}$
Foetal Calf Serum	10% (v/v)

Coomassie Blue Stain

Methanol	400 $mL.L^{-1}$
Glacial Acetic Acid	100 $mL.L^{-1}$
Distilled Water	500 $mL.L^{-1}$
Coomassie Blue R-250	2 $g.L^{-1}$

Destain

Methanol	400 $mL.L^{-1}$
Glacial Acetic Acid	100 $mL.L^{-1}$

Distilled Water	500 $mL.L^{-1}$

SDS-PAGE

10% Acrylamide Gel

Tris-HCL pH 8.8	0.38 M
SDS	0.1% (w/v)
Acrylamide/Bis	10% (w/v)
Ammonium Persulfate APS	8% (w/v)
NNN'N'-tetramethylethylenediamine (TEMED)	8% (w/v)

4% Acrylamide Gel

Tris-HCL pH 8.8	0.125 M
SDS	0.1% (w/v)
Acrylamide/Bis	5.2% (w/v)
Ammonium Persulfate (APS)	8% (w/v)
NNN'N'-tetramethylethylenediamine TEMED	8% (w/v)

Running Buffer

Tris-base	15 $g.L^{-1}$
Glycine	72 $g.L^{-1}$
Sodium Dodecyl Sulphate (SDS)	5 $g.L^{-1}$
Adjust pH to 8.3	

Western Blotting

Transfer Buffer

Tris-Base	3.03 $g.L^{-1}$
Glycine	14.40 $g.L^{-1}$
Methanol	200 $mL.L^{-1}$
Distilled Water	800 $ml.L^{-1}$